# The Aqueous Dispersion of Carbon Nanotubes

**Lucinda Clarke**

A thesis submitted in partial fulfilment
of the requirements for the degree of
Doctor of Philosophy

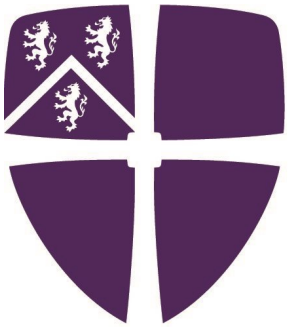

Department of Chemistry
University of Durham
2016

# Contents

Contents

# List of Figures

List of Figures

List of Figures

# List of Tables

# Abstract

This work has focused on the use of biological molecules such as amino acids, glycolic acids, ribonucleosides and simple sugars to improve MWCNT aqueous dispersibility through both covalent and non-covalent functionalisation.

Oxidative treatment of MWCNTs with 6 M nitric acid has been shown to be a mild, yet effective method for introducing carboxylic acid groups, which are known to improve their dispersion, to the surface. The subsequent ionic interactions of these carboxylic acid groups with selected acidic, basic and neutral amino acids was investigated with a view to this further increasing the aqueous dispersibility of the MWCNTs. Of the amino acids considered basic arginine was found to provide the greatest improvement with the MWCNT concentration increasing from 0.35 to 6.79 mg/mL.

The carboxylic acid groups of the oxidised MWCNTs were also used to covalently attach the amino acids through formation of an amide bond. In this instance taurine was found to be the most effective amino acid with dispersibility more than doubling. Non-covalent functionalisation of the MWCNTs was also achieved with taurine functionalised poly(acrylic acid), which resulted in a fivefold increase in the concentration of MWCNTs dispersed when compared with poly(acrylic acid).

Diazonium chemistry is widely used for the functionalisation of CNTs with aryl groups and in this work a diazonium reaction was used to covalently functionalise MWCNTs with pyridine. These pyridine groups were then used as the basis for the covalent attachment of the sugars ribose, fructose and sucrose. Functionalisation with pyridine alone did not improve the aqueous dispersion of the MWCNTs, however the subsequent attachment of the sugars led to enhanced MWCNT dispersibility with sucrose the most effective at 20 $\mu$g/mL.

The effect of functionalisation on MWCNT dispersibility was probed using UV-vis-NIR spectroscopy. The modified MWCNTs were further characterised using TGA, TEM, Raman and FTIR spectroscopy.

# Declaration

The work presented here was undertaken within the Department of Chemistry of the University of Durham between October 2010 and March 2014. I confirm that no part of this work has been submitted for a degree at this or any other institution and, unless otherwise stated is the orginal work of the author.

# Acknowledgements

Firstly I would like to thank my supervisor Prof. Karl Coleman for his guidance throughout my PhD. His extensive knowledge has been invaluable during the course of my studies. I am very grateful to Thomas Swan and Technical Fibre Products for the opportunity to work on such an exciting project. In particular thanks go to Dr Marcelo Motta and Andy Goodwin (TS) and Dr Mike Jeschke and Victoria Wright (TFP) for their support and valuable input.

Thanks to Dr Mustafa Bayazit and Dr Chris Herron for their help during my Masters year and their encouragement towards pursuing a PhD. I would also like to thank Dr David Johnson for all of of his suggestions and advice, Dr Stephen Boothroyd for his assistance with conductivity measurements and Douglas Carswell for his help with TGA. I am thankful to the rest of the group, Ben Dobson, Rob Mora, Mike Tynan and especially Bnar Ahmed for her friendship and helpful discussions about amino acids and peptide synthesis. Thanks as well must go to Stacey Lindsay and Emma Puttock for all the stealthy Zen lunches!

Finally I wish to thank my family and Tom for all their love, encouragement and support.

# Abbreviations and Acronyms

| | |
|---|---|
| AHA | Alpha hydroxy acid |
| CCFs | Carboxylated carbonaceous fragments |
| CNTs | Carbon nanotubes |
| CVD | Chemical vapour deposition |
| DIPEA | *N,N*-Diisopropylethylamine |
| DMEN | *N,N*-Dimethylethylenediamine |
| DMF | *N,N*-Dimethylformamide |
| DWCNTs | Double-walled carbon nanotubes |
| FTIR | Fourier transform infrared |
| HiPco | High pressure carbon monoxide |
| HRTEM | High resolution transmission electron microscopy |
| MWCNTs | Multi-walled carbon nanotubes |
| PAA | Poly(acrylic acid) |
| PEG | Poly(ethylene glycol) |
| RBM | Radial breathing mode |
| SDS | Sodium dodecyl sulfate |
| SWCNTs | Single-walled carbon nanotubes |
| TEM | Transmission electron microscopy |
| TGA | Thermogravimetric analysis |
| UV-vis-NIR | Ultraviolet-visible-near infrared |

# Symbols and Physical Constants

| | |
|---|---|
| $\mathbf{a}_1$, $\mathbf{a}_2$ | Graphene unit vectors |
| A | Absorbance |
| $C_h$ | CNT chiral vector |
| $\epsilon$ | Extinction coefficient |
| $\lambda$ | Wavelength |
| $\theta$ | CNT chiral angle |
| $n$, $m$ | CNT chiral indices |
| pI | Isoelectric point |

# Chapter 1

# Introduction

## 1.1 Overview

This chapter aims to provide an overview of the structure, synthesis, properties, reactivity and possible applications of carbon nanotubes (CNTs). Particular emphasis is placed on their functionalisation and dispersion in water, as these are the areas upon which this thesis is centred.

## 1.2 Structure

Carbon nanotubes are allotropes of carbon that are a member of the fullerene structural family. In general they can be separated into two categories: single-walled (SWCNT) and multi-walled (MWCNT). SWCNTs consist of an individual, one atom thick cylinder of $sp^2$ carbon atoms with a diameter typically between 0.6 and 2 nm[1] and a length that can reach centimeters.[2, 3] MWCNTs are assemblies of multiple such cylinders concentrically arranged and separated by 0.34 nm, slightly larger than the interlayer distance in graphite (0.335 nm).[4] The diameter of MWCNTs usually ranges from 2 to 100 nm[1] and they can grow several cm long.[5] A double-walled carbon nanotube (DWCNT) is composed of exactly two concentric SWCNTs and represents the simplest type of MWCNT.[6]

SWCNTs can be considered as a single layer of graphite (graphene) rolled into a seamless cylinder with the ends either open or capped with a hemisphere of a fullerene.

The properties of nanotubes are dependent on how the graphene sheet is rolled up, as well as on their length and diameter. The graphene sheet can be rolled into a cylinder in a number of ways that are specified by the chiral vector $\mathbf{C}_\mathrm{h}$.[7] $\mathbf{C}_\mathrm{h}$ is defined in terms of the graphene unit vectors $\mathbf{a}_1$ and $\mathbf{a}_2$ and a pair of integers $n$ and $m$ ($0 \leq |m| \leq n$) as in equation 1.1;

$$\mathbf{C}_\mathrm{h} = n\mathbf{a}_1 + m\mathbf{a}_2 \equiv (n, m). \tag{1.1}$$

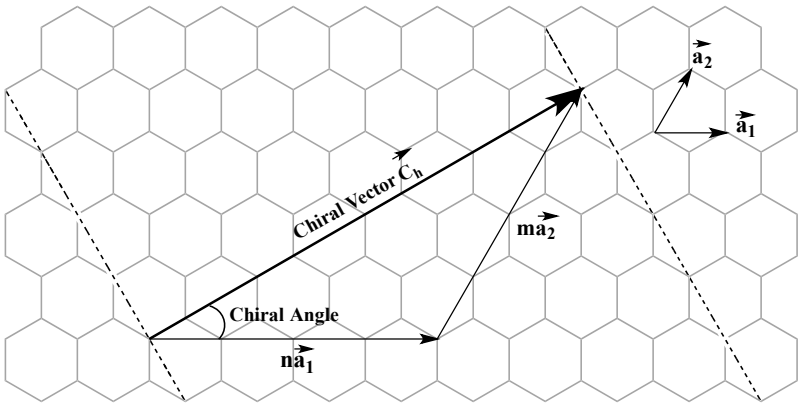


Figure 1.1: Schematic diagram showing how a graphene sheet can be rolled to make a CNT.

Each SWCNT is defined by a distinct set of $n$ and $m$ values, which determines the diameter and chiral angle, $\theta$, of the nanotube. According to the values of n and m SWCNTs can be classified further as having armchair, zigzag or chiral structure based on the arrangement of the carbon bonds around the circumference of the nanotube.[7] If $n = m$ then the circumference of the tube has an armchair pattern and the chiral vector and chiral angle are $(n, n)$ and $\theta = 30^\mathrm{o}$. When $m$ is zero a zigzag outline in the circumference is made and $\mathbf{C}_\mathrm{h} = (n, 0)$ with $\theta = 0^\mathrm{o}$. Chiral tubes are formed in all other cases with $n \neq m \neq 0$ and $0^\mathrm{o} < \theta < 30^\mathrm{o}$ (Figure 1.2).[8]

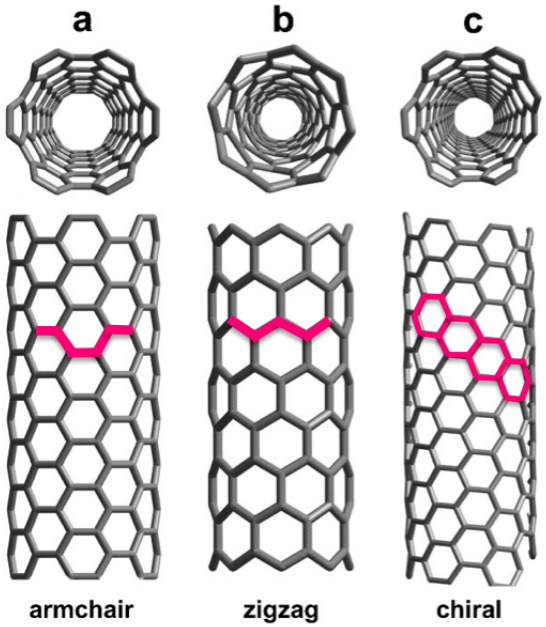


Figure 1.2: The atomic structure of (a) an armchair, (b) a zigzag and (c) a chiral SWCNT. Reprinted with permission from [8].

## 1.3 Synthesis

MWCNTs were first observed in the soot produced from an arc evaporation method originally designed to produce fullerenes.[9] Iijima and Ichihashi[10] and Bethune *et al.*[11] independently reported the discovery of SWCNTs two years later in the product from transition metal catalysed arc evaporation experiments. Techniques such as arc discharge,[12] or laser ablation,[13] were first used to produce CNTs but chemical vapour deposition (CVD) is now the primary method.[14] The CNTs produced are contaminated with a number of impurities such as amorphous carbon, non-tubular fullerenes and metal catalysts so purification procedures are commonly employed after synthesis. Each synthesis method also generates a mixture of metallic and semiconducting CNTs; therefore techniques for the selective preparation and separation of nanotubes with uniform electronic character have been developed.[15]

## 1.4 Purification

Metal and amorphous carbon impurities are present in as-synthesised CNTs. The presence of impurities can interfere with the properties of CNTs and hinder their characterisation and application so a variety of purification techniques, both chemical and physical, have been developed.[16] Small quantities of CNTs have been purified by size exclusion chromatography[17] and microfiltration.[18] Ultrasonically assisted microfiltration has been employed for large-scale purification, however during the process the nanotubes are shortened due to sonication-induced cutting.[19] Gas phase oxidation consists of heating the CNTs in an oxidising atmosphere to oxidise the amorphous carbon and metal present.[20–22] Removal of the metal oxides is then achieved by treatment using an acid such as hydrochloric acid. The most commonly used method however is liquid phase oxidation, which typically involves refluxing the CNTs in nitric acid.[23–25] This method is straightforward and effective, yet it is known that the process can also damage the nanotube structure and introduce oxygen-containing groups, in particular carboxylic functionalities.[26–28] These groups confer aqueous solubility to the nanotube and have been widely used as the basis for the attachment of other functional groups to the CNT.[29–32]

## 1.5 Physical Properties

CNTs possess an array of remarkable physical properties, which make them a very promising material for a range of applications. CNTs can carry a current density of order $10^9$ A/cm$^2$ which is a thousand times better than copper.[33, 34] SWCNTs can exhibit metallic or semiconducting behaviour, depending on their diameter and helicity (the integers $n$ and $m$). SWCNTs are metallic if $n$-$m$=3q, where q is an integer, and semiconductors if $n$-$m$ $\neq$3q. For a uniform distribution of $n$ and $m$ values one third of SWCNTs are metallic and two thirds semiconducting.[35] The sharp peaks in the density of states (DOS) of SWCNTs are known as van Hove singularities, and are believed to reflect the 1D band structure of SWCNTs (Figure 1.3).[36] All armchair SWNTs ($n$, $n$) are metallic with a continuous DOS near the Fermi level. All other metallic SWCNTs have a small band gap, which can be disregarded at room temperature. The DOS of semiconducting SWCNTs have band gaps on the order of $\approx$0.5 eV that scale

inversely with diameter. MWCNTs consist of concentrically arranged SWCNTs, however due to weak coupling between them, only the outermost SWCNT contributes to electron transport and so to their electronic properties.[37]

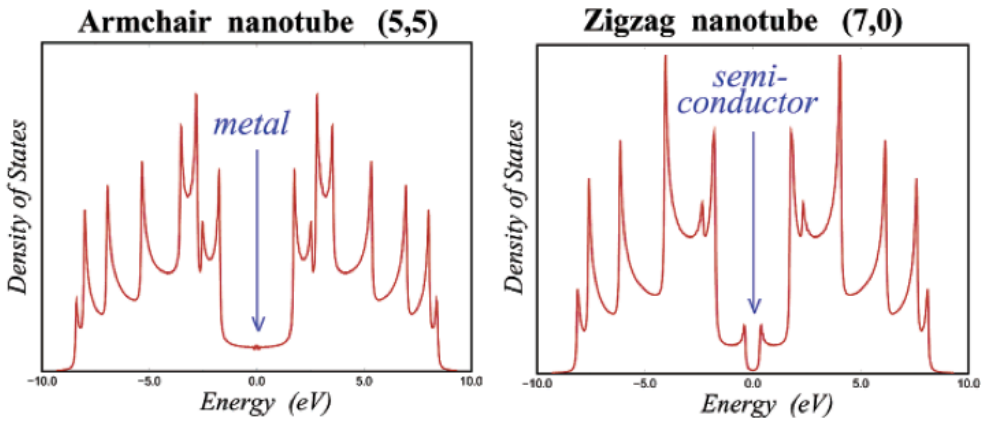


Figure 1.3: Density of states diagrams showing the electronic properties of (l) the metallic armchair (5,5) nanotube and (b) the small gap semiconductor zigzag (7,0) nanotube. Reprinted with permission from [36]. Copyright (2002) American Chemical Society.

Experimental studies on the mechanical properties of CNTs have indicated that CNTs exhibit a Youngs modulus on the order of 1 TPa,[38–42] comparable with that of diamond.[43] The highest measured tensile strength for CNTs is 63 GPa,[42] an order of magnitude stronger than high strength carbon fibers.[44] CNTs are very flexible, with bending shown to be fully reversible up to bending angles of $110^o$.[45] The superior mechanical properties of CNTs mean that they are promising materials for use as fillers in polymer composites[44, 46] and as tips in probe microscopy.[47]

## 1.6 Reactivity

Perfect CNTs consist of a hexagonal framework in which each carbon atom is $sp^2$ hybridised as in graphene. CNTs, however, are more reactive than planar graphene because of the curvature of their structure. Their curvature results in the carbon atoms experiencing strain from pyramidalization and $\pi$ orbital misalignment between adjacent atoms. $\pi$ orbital misalignment is associated with bonds that are at an angle

to the circumference and is principally responsible for the reactivity of their sidewalls. As an example, for an armchair (5,5) SWCNT the $\pi$-orbital misalignment angles $\phi$ of bonds parallel to the circumference and those at an angle to the circumference are $0^o$ and $21.3^o$, respectively (Figure 1.4).[48]

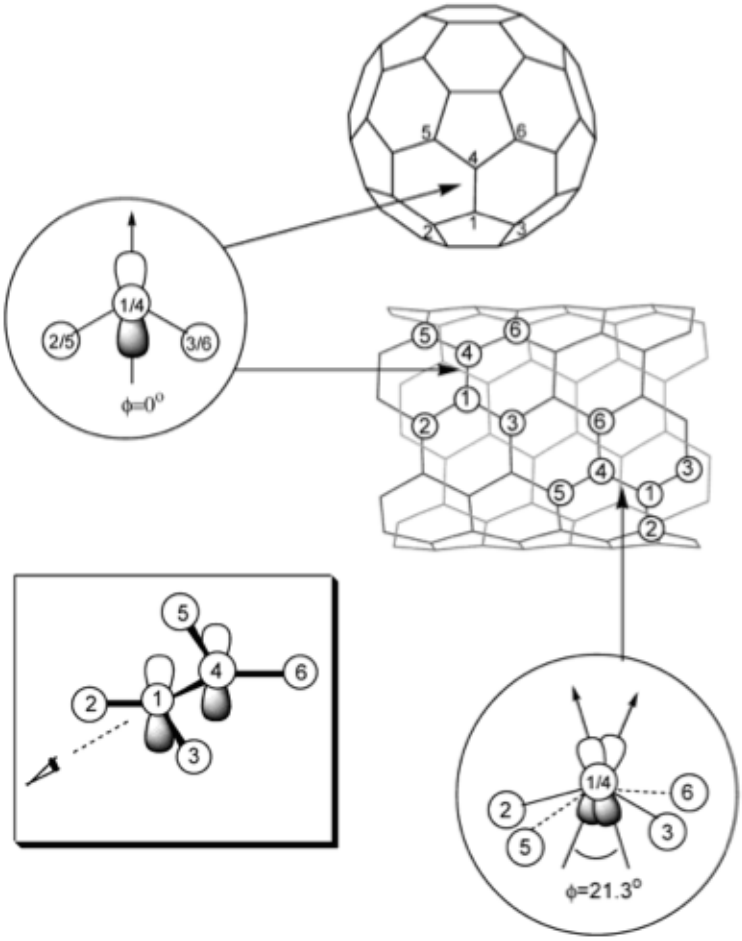


Figure 1.4: The $\pi$-orbital misalignment angles ($\phi$) along the C1-C4 bond in a (5,5) SWCNT and its capping fullerene, $C_{60}$. Reprinted with permission from [48]. Copyright (2002) American Chemical Society.

The end caps of tubes are equivalent to a hemisphere of fullerene and are more reactive than their sidewalls due to the greater strain enforced by their spherical geometry. In contrast to the sidewalls the $\pi$ orbital misalignment in the end caps is almost perfect and so pyramidalization is the main source of strain. Trigonal ($sp^2$ hybridised)

carbon atoms prefer planarity, however, the geometry of fullerenes suits a tetrahedral ($sp^3$ hybridised) arrangement and it is the relief of this strain as $sp^2$ hybridised carbon is converted to $sp^3$ that drives the addition reactions. Pyramidalization and $\pi$ orbital misalignment angles scale inversely with CNT diameter and so smaller diameter tubes are expected to be more reactive than their larger diameter counterparts.

The electronic properties of CNTs have also been noted to influence their reactivity in many different functionalisation reactions.[49] Diazonium compounds are reported to preferentially functionalise metallic CNTs, due to the availability of electrons near the Fermi level.[50, 51] Treatment of SWCNTs with a nitric/sulfuric acid mixture has also shown that the dissolved nitronium ions display a clear selectivity for metallic SWCNTs.[52] The preferential adsorption of the positively charged nitronium ions on metallic SWCNTs was also suggested to be due to more available electron densities at the Fermi level. Evidence for the selective oxidation of semiconducting SWCNTs by hydrogen peroxide has been reported.[53] It was suggested that weak hole-doping of SWCNTs by hydrogen peroxide increased the electron density at the Fermi level of semiconducting SWCNTs relative to metallic SWCNTs, resulting in faster oxidation. The 1,3-dipolar cycloaddition of pyridinium ylides has been shown to be selective for metallic SWCNTs and larger diameter semiconducting SWCNTs.[54] In this case the larger diameter SWCNTs were proposed to be more reactive than those of smaller diameter due the latter having a larger band gap, and so a larger region were the DOS was zero.

### 1.6.1 Defects in Structure

In reality the structure of carbon nanotubes are not ideal and topological defects (incorporation of ring sizes other than hexagons), vacancies and $sp^3$ hybridisation sites can be present in the carbon network. An important topological defect is the Stone-Wales (SW) defect, which consists of a pentagon-heptagon pair (5/7/7/5). The SW defect is formed by the rotation of a C=C bond by $90^o$, transforming four adjacent hexagons into two pentagons and two heptagons (Figure 1.5). The presence of these defects can have a detrimental effect on the physical properties of the CNTs and alter their chemical reactivity. It is commonly accepted that the defect sites are more reactive than the perfect sites in CNTs, however it has been shown that the central C-C

bond of a Stone-Wales defect in an armchair (5,5) SWCNT is less reactive than those in perfect sites.[55]

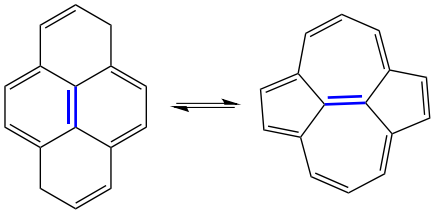

Figure 1.5: Formation of the Stone Wales (5/7/7/5) defect.

Purification by liquid phase oxidation can result in shortened open-ended CNTs decorated with oxygenated functional groups such as carboxylic acids, both at the ends and at sites along the sidewall (Figure 1.6).[56] The inclusion of topologic pentagon-heptagon (5/7) defects in the hexagonal framework can bend the CNT structure,[57] and also form intramolecular junctions between two nanotube segments with different electronic properties.[58]

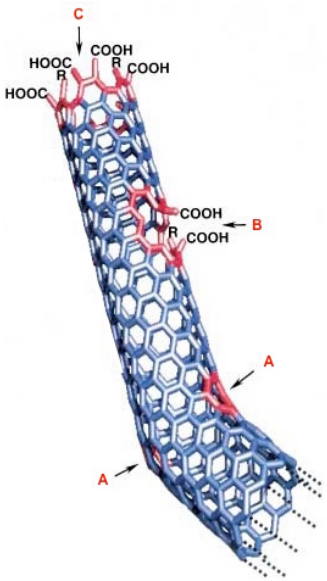


Figure 1.6: Typical defects in a CNT: A) inclusion of five- or seven-membered rings leads to a bend in the tube, B) structure damaged by oxidative conditions which leaves a hole lined with carboxylic acid groups and C) open end of the CNT terminated with carboxylic acid groups. Adapted with permission from [56].

## 1.7 Functionalisation of CNTs

Pristine CNTs tend to aggregate into bundles or ropes due to strong non-covalent interactions between their sidewalls. These substantial intermolecular cohesive forces of 500 eV/$\mu$m that exist between the tubes render them insoluble in most common solvents.[59] This lack of solubility is a major disadvantage as it makes them difficult to process and handle and so has hindered their use in many potential applications. In order to disrupt these strong $\pi$-$\pi$ interactions and facilitate the dispersion of CNTs, mechanical dispersion methods, such as ultrasonication and high shear mixing, and chemical modification of the CNT surface have been employed. Mechanical dispersion methods, although straightforward, result in sedimentation of the CNTs when the applied agitation is removed and can also damage the CNTs.[60] Chemical alteration of the CNT surface by functionalisation is therefore the widely accepted method to enhance their solubility. The key approaches used for the functionalisation of CNTs can be classified as either non-covalent or covalent. Functionalisation of CNTs for the purpose of achieving aqueous solubility is covered in Section 1.8.

### 1.7.1 Covalent

The covalent attachment of functional groups to CNTs occurs either by direct reaction with the $\pi$-conjugated framework or through defect site functionalisation, which takes advantage of the nanotube-bound carboxylic acid groups introduced during oxidative acid treatment. Covalent approaches change the hybridisation of the bonding carbon from $sp^2$ to $sp^3$, which disrupts the extended $\pi$-conjugation of the CNT and so can adversely affect the desirable properties they possess, however the functionalisation is highly stable. The covalent functionalisation of CNTs is possible with a wide range of species and has been extensively reviewed.[61–63]

#### 1.7.1.1 Oxidation

The oxidation of CNTs has been reported using a variety of methods, such as exposure to ozone,[64] potassium permanganate,[65] piranha solution,[66] carbon dioxide,[67] nitric acid vapour[68] and sonication in a sulfuric/nitric acid mixture.[69] Selective oxidation of metallic CNTs has been achieved using halogen oxoanions,[70] while the selec-

tive oxidation of semiconducting CNTs has been realised with hydrogen peroxide.[71] Typically however the procedure used involves reflux in nitric acid or a sulfuric/nitric acid mixture for several hours.[72] These procedures introduce oxygenated functional groups, primarily carboxylic acids, to the CNT surface which improves the dispersibility of the CNTs in water.[27] The number of functional groups introduced is dependent on the oxidative conditions used.[26] An increase in the oxidising agent concentration or oxidation duration will increase the degree of functionalisation however this must be balanced with the accompanying increase in damage inflicted to the CNT structure. The nanotube-bound carboxylic acid groups are commonly used as anchors for the attachment of other functional groups to the surface, usually through esterification or amidation reactions. In most cases the carboxylic functionalities are initially activated by a carbodiimide or converted to the more reactive acyl chloride before undergoing reaction with the required alcohol,[30] or amine.[73]

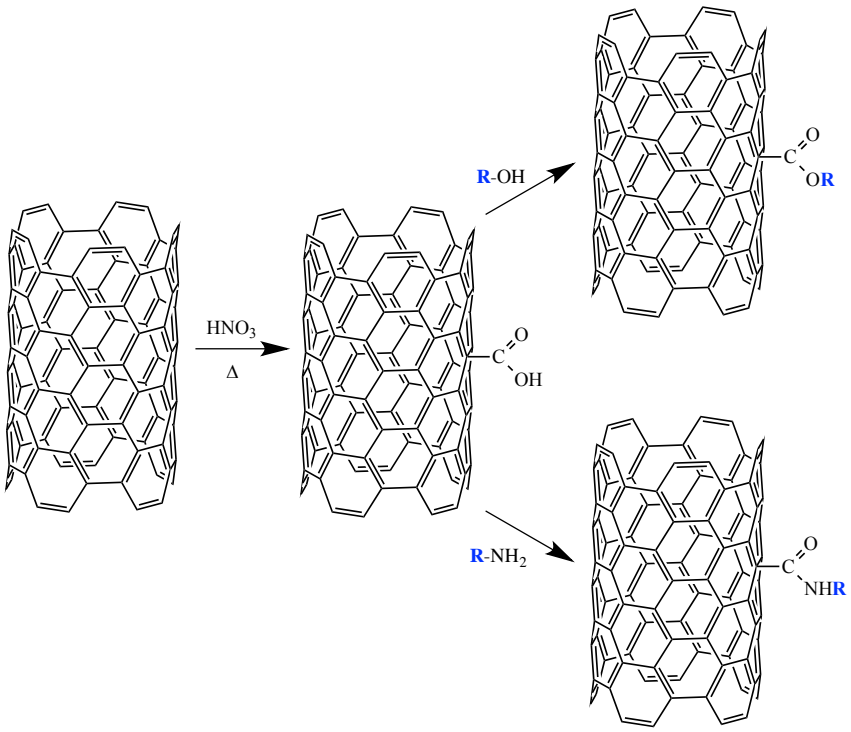


Figure 1.7: Thermal oxidation of CNTs and the subsequent esterification or amidation of the carboxylic acid groups.

It has been proposed that nitric acid treatment of CNTs results in the formation of

oxidation debris or carboxylated carbonaceous fragments (CCFs).[74] Amorphous carbon is the most reactive form of carbon present in as-synthesised CNTs so these CCFs are suggested to act as the major carrier of acid functionality (rather than the CNT walls).[75] Subsequent washing with aqueous base has been reported to remove the CCFs from both MWCNTs and SWCNTs.[74, 76, 77] Haddon *et al.*[78] have demonstrated that even after thorough base washing a sufficient number of acid functionalities are available on the CNTs themselves for further reaction. Purification of CNTs to remove amorphous carbon before treatment with acid has been recommended to greatly reduce the formation of oxidation debris and result in carboxylation primarily on the CNT walls.[75] A more recent report which used a two step purification/oxidation procedure found that in the absence of the base wash step, carboxylic acid groups were introduced to SWCNTs directly, and not just onto carbonaceous material.[79]

#### 1.7.1.2 Diazonium

The reactivity of CNT sidewalls has been compared to that of the basal plane of graphite, therefore highly reactive reagents are required for functionalisation to occur. Due to their high reactivity diazonium compounds, usually generated in situ, have been extensively used for the successful modification of CNTs.[50, 80–83] The reaction has been shown to favour metallic CNTs and is also selective towards larger diameter CNTs.[50, 84, 85] Diazonium salts have been generated in situ by oxidation of an aniline precursor and activated thermally [86, 87] or electrochemically [81] for radical addition to the nanotube surface. The addition of aryl diazonium salts to CNTs has been realised in ionic liquids,[83],urea,[88] non-aqueous solvent,[86] on water,[87] aqueous solution using surfactant coated SWCNTs,[82] and solvent-free conditions.[89] Recently the diazonium reaction has been extended to heterocycles with pyridine functionalised SWCNTs achieved using a diazonium salt generated in situ from 4-aminopyridine (Figure 1.8).[51]

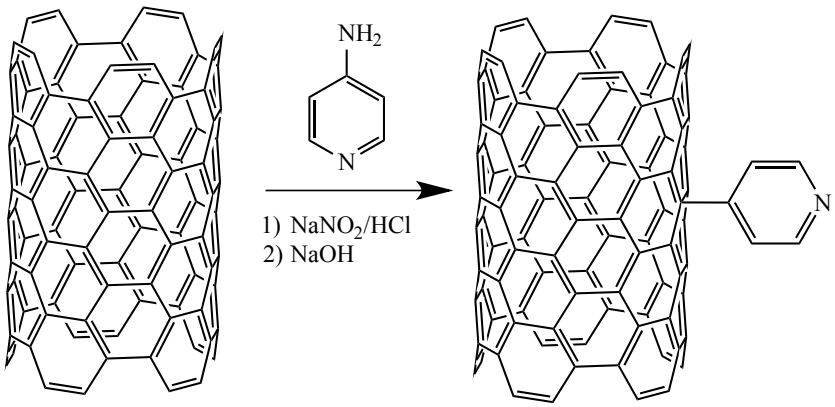


Figure 1.8: Synthesis of pyridine functionalised SWCNTs.

#### 1.7.1.3 Cycloadditions

The 1,3-dipolar cycloaddition of azomethine ylides, created in situ from the condensation of an aldehyde and $\alpha$-amino acid, has produced pyrrolidine functionalised SWCNTs and MWCNTs that are soluble in most organic solvents and water.[90, 91] Microwave conditions are known to increase the rate of the 1,3-dipolar cycloaddition of aziridines,[92] (precursors to azomethine ylides) and pyridinuim ylides[54] to the nanotube surface. The cycloaddition of pyridinuim ylides has been shown to be selective for metallic and large diameter semiconducting SWCNTs, which is consistent with a mechanism involving electron donation from the CNT to the 1,3 dipole. Ozone adds to SWCNTs in a 1,3 dipolar cycloaddition reaction to give a primary ozonide that can be cleaved using specific chemicals to favour a certain oxygenated functional group over another.[93] Alvaro *et al.* have also carried out 1,3-dipolar cycloaddition reactions on SWCNTs using nitrile imine,[94] and nitrile oxide.[95] The [2+1] cycloaddition of nitrene, generated by thermal removal of nitrogen from alkyl azidoformates, has resulted in aziridine functionalised SWCNTs that are soluble in DMSO.[96] The same reaction carried out using di-nitrenes can covalently crosslink two SWCNTs or form loops on the sidewall of one nanotube.[97] The Bingel reaction, a [2+1] cycloaddition, has successfully functionalised SWCNTs with a cyclopropane group.[98]

#### 1.7.1.4 Fluorination

The fluorination of SWCNTs with elemental fluorine has produced stoichiometries of approximately $C_2F$ at 325$^o$C with the majority of the tube structure remaining intact.[99] At higher temperatures complete destruction of the SWCNTs occurs. The pristine SWCNTs could be recovered by using hydrazine as a defluorinating agent. The fluorinated tubes form metastable solutions in DMF, THF and alcohols but are insoluble in water.[100] They can also serve as precursors for the attachment of other functional groups to the CNT surface. Alkyllithium and Grignard reagents have been used to alkylate fluorinated CNTs through displacement of fluorine.[101] The mild fluorinating agent hexafluorophosphoric acid ($HPF_6$) has been used recently to fluorinate MWCNTS.[102] A stoichiometry of $CF_{0.018}$ could be attained, without destruction of the MWCNT structure, when the fluorination procedure was carried out at 150 $^o$C.

### 1.7.2 Non-Covalent

Non-covalent functionalisation is not discussed in depth here as the covalent functionalisation of CNTs was the focus of this work, however there are many reviews that cover this method in detail.[63, 103–105] CNTs may be functionalised non-covalently by species that can form hydrophobic or $\pi$-$\pi$ stacking interactions with the CNT surface. Non-covalent modification preserves the $\pi$-conjugated system, allowing the desirable properties of the nanotube to be retained, however the adsorbed species may obstruct further functionalisation and for some applications, particularly composite materials, a direct bond is necessary.

Aromatic compounds such as pyrene and porphyrin derivatives have functionalised CNTs through $\pi$-$\pi$ stacking interactions.[106–109] Polymer wrapping of CNTs can occur through various non-covalent interactions, such as $\pi$-$\pi$, CH-$\pi$ and cation-$\pi$.[110] Surfactants are small molecules that have a hydrophobic tail and a hydrophilic head group and the former is able to adsorb onto the hydrophobic CNT walls, leaving the head group free to extend into the bulk water phase.[111] Similarly proteins with their hydrophobic and hydrophilic domains have also functionalised CNTs through hydrophobic interactions, in addition to $\pi$-$\pi$ stacking interactions.[112, 113] The non-covalent functionalisation of CNTs with aromatic compounds, surfactants, polymers and biomolecules has been used to improve CNT aqueous dispersibilty and is considered

in detail in Section 1.8.

## 1.8 Aqueous Dispersion of CNTs

The formation of stable and homogenous aqueous CNT dispersions is a crucial development if many of the applications envisioned for CNTs are to be realised. The aqueous dissolution of CNTs via both covalent and non-covalent means has been reported. The aqueous dispersibility of the functionalised CNTs depends on the inherent water solubility of the adsorbed molecule or attached functional group and also on the extent of modification to the CNT surface. Covalent strategies are superior to non-covalent modifications in terms of the stability of the functionalistion, however covalent functionalisation disrupts the CNT structure and affects their desirable intrinsic properties. Non-covalent functionalisation has been an attractive area for investigation due to the ease of the procedure (typically just involves sonicating the desired functionality with the CNTs) and because the nanotube's structure, and therefore properties, are usually preserved. Functionalising agents are needed that not only interact with the CNTs, but also with water to achieve dissolution.

### 1.8.1 Covalent

Microwave assisted oxidation of SWCNTs in a nitric/sulphuric acid mixture has been shown to be a rapid method for producing SWCNT solutions with concentrations as high as 10 mg/mL.[72] Elemental analysis indicated one in three carbon atoms were carboxylated and one in ten sulfonated, accounting for the high aqueous solubility attained. An oleum/nitric acid treatment has simultaneously produced carboxylated, ultra short (<60 nm) SWCNTs that spontaneously dissolved in water up to 2 wt%.[114] Dispersions of carboxylated SWCNTs have been shown to be pH dependent with aggregation observed at pH $\leq$ 3, presumably due to protonation of the carboxylate groups.[115] The combination of oleum and nitric acid has also been used in the selective oxidation of the outer walls of DWCNTs.[116] As expected an improvement in aqueous solubility of the oxidised DWCNTs was observed, but interestingly this was accompanied by the retention of 66% of their electrical conductivity. The preservation of their electrical properties was attributed to the ability of the intact inner tubes to

provide a continuous conductive pathway (Figure 1.9).[116]

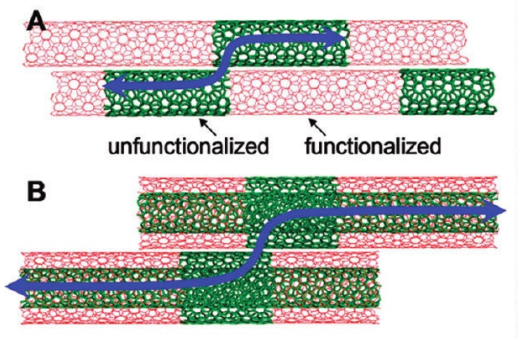


Figure 1.9: Preservation of the electrical properties in an oxidised DWCNT: (A) The broken conductive pathway due to sidewall functionalisation of a SWCNT. (B) Intact inner tubes extend the conductive pathway in a DWCNT. Reprinted with permission from [116]. Copyright (2010) American Chemical Society.

Oxidation of MWCNTs in nitric acid has been shown to better preserve the tube structure than a nitric/sulphuric acid mixture due to its relatively lower acidity,[27] however prolonged oxidation (48 h) in concentrated nitric acid (60%) whilst producing MWCNT dispersions of 40 mg/mL has resulted in the loss of more than 90% of the MWCNTs.[117] Shortened MWCNTs ($\approx$ 1 $\mu$m) have formed stable dispersions in water at a concentration of 0.013 mg/mL.[118] After refluxing in dilute nitric acid the aqueous MWCNT concentration increased to 0.24 mg/mL. The conversion of these carboxylic acid groups to thiols through a carbodiimide activated amidation reaction with cysteamine resulted in a decrease in concentration to 0.17 mg/mL. Phosphoryl choline (PC) has been attached to oxidised MWCNTs via the acyl chloride. The hydrophilic nature of PC enabled the MWCNTs to be dispersed at 10 mg/mL by ultrasonication.[119] Oxidised SWCNTs have formed an ionic bond with the protonated amine group of a water-soluble functionalised crown ether to give a SWCNT concentration of 1.1 mg/mL.[29]

Treatment of SWCNTs with sec-butyllithium to generate a carbanion followed by reaction with carbon dioxide has produced SWCNTs functionalised with alkyl and carboxyl groups that can be individually dispersed at a concentration of 0.5 mg/mL.[120] Hydroxyl functionalised SWCNTs have been prepared from the displacement of fluorine from fluoronanotubes by a selection of diols and glycerol.[121] The glycerol derived

SWCNTs displayed the greatest solubility of 0.04 mg/mL, seemingly due to the greater number of hydroxyl groups present on the SWCNT surface.

Diazonium functionalisation using a range of aniline precursors in the presence of oleum has produced individual water-soluble SWCNTs due to the sulfonation that occurs on the aryl rings under these conditions.[122] An SWCNT concentration of 0.24 mg/mL was achieved using the derivative 4-chloroaniline. Radical addition of phenyl groups to SWCNTs has also been carried out using benzoyl peroxide as the source of phenyl radicals.[123] Subsequent sulfonation in oleum ($H_2SO_4$, 20% free $SO_3$) of the phenylated SWCNTs resulted in a concentration of 0.492 mg/mL. Sulfonation of 4-aminophenyl and phenyl groups covalently bound to the MWCNT surface by reductive arylation produced MWCNT concentrations of 0.03 mg/mL and 0.015 mg/mL respectively.[124]

### 1.8.2 Non-Covalent

$\pi$-$\pi$ stacking of 1-pyrenecarboxylic acid to SWCNTs non-covalently functionalises the surface with carboxylic acid groups and affords their dispersion in water as well as THF.[125] Gas responsive aqueous dispersions of SWCNTs have been produced using a pyrene functionalised with an amidinium cation.[126] Reversible conversion between the amidinium cation and amidine triggered by the addition/removal of carbon dioxide allows the dispersion state of the SWCNTs to be controlled. Water soluble SWCNTs have been achieved using a pyrene-carrying ammonium ion.[106] Confirmation of the importance of the $\pi$-$\pi$ interaction was demonstrated by Nakashima *et al.*[127] The phenanthrene derivative was observed to be much less effective than the pyrene one while phenyl and naphthalene ammonium analogs were unable to solubilise SWCNTs. However, the successful solubilisation of SWCNTs at concentrations between 0.1-0.3 mg/mL through non-covalent functionalisation with various ionic naphthalene and pyrene derivatives has been reported.[128] $\pi$-$\pi$ stacking interactions between a phosphonate functionalised naphthalene derivative and SWCNTs has produced SWCNT solutions of 1 mg/mL.[129] The strong electrostatic repulsion between the phosphonate groups combined with their hydrophilic nature enables the partial debundling of the SWCNTs in aqueous solution.

An aqueous solution (pH 7) containing 0.11 mg/mL SWCNTs has been attained

using a low concentration (0.1 wt%) of a perylene bisimide derivative bearing a hydrophilic dendritic structure containing many carboxylic acid groups.[130] The perylene derivative displayed an enhanced affinity for adsorption to smaller-diameter nanotubes,[131] and was found to disperse the SWCNTs more efficiently at higher pH due to the complete deprotonation of the carboxylic acid functionalities.[132] The alkali metal counterion has also been shown to influence the efficiency of an anionic perylene dye to solubilise SWCNTs under basic conditions.[133]

A synthesised amphiphilic molecule containing a bent triptycene group and a hydrophilic tetra (ethylene glycol) chain (Trp-TEG) has enabled the selective solubilisation of SWCNTs with a diameter of 1.0 nm.[134] An aqueous dispersion of SWCNTs in Trp-TEG was observed to be stable for more than six months and contain a concentration of 0.052 mg/mL SWCNTs.

Liu *et al.*[135] have evaluated the ability of several aromatic dyes to noncovalently functionalise and solubilise MWCNTs. $\pi$-$\pi$ stacking was found to be the most important factor in the MWCNT-dye interaction with the planar dyes Acridine Orange (AO), Xylenol Orange (XO), Orange G (OG) and Alizarin Red (AR) producing stable suspensions of MWCNTs in water. OG has also been used to produce stable suspensions of SWCNTs for the solution fabrication of $NO_2$ sensors.[136] A solubility of 3.5 mg/mL for SWCNTs has been achieved though their $\pi$-stacking interaction with the planar, diazo dye Congo Red (CR).[137]

Graphene oxide (GO) sheets are able to stably disperse larger diameter pristine MWCNTs.[138] The multiple aromatic regions on GO are able to adsorb the MWCNTs through $\pi$ stacking interactions while the hydrophilic oxygenated groups impart aqueous solubility.

### 1.8.3 Biomolecules

#### 1.8.3.1 Amino Acids and Peptides

The FMOC-protected aromatic amino acid tryptophan has dispersed SWCNTs and MWCNTs in phosphate buffer saline solution at concentrations of 0.08 and 0.21 mg/mL respectively through $\pi$-stacking interactions.[139] Remarkably high water concentrations (20 and 12 mg/mL for SWCNTs and MWCNTs respectively) have been attained by the 1,3-dipolar cycloaddition of an N-protected glycine derivative to the

CNT surface.[140] Taurine, a derivative of cysteine, has been covalently linked to oxidised SWCNTs through amide bond formation.[141] As a result the SWCNTs were functionalised with sulfonic acid groups, which enhanced their solubility to 1.3 mg/mL at neutral pH. Amino acids have also been covalently attached to fluorinated SWCNTs by reaction of their amine group with fluorine.[142] This results in the carboxylic acid group of the amino acid being exposed and imparting some aqueous solubility to the SWCNTs. Chain length was shown to have an effect on the SWCNT solubility obtained. 6-aminohexanoic acid (AHA), a derivative of lysine, gave stable dispersions at 3 <pH <11 of 0.5 mg/mL at room temperature. The amidation of oxidised MWCNTs with lysine has produced stable dispersions in the pH range 5-14.[143] Concentrations of MWCNTs as high as 10 mg/mL could be obtained without sonication. pH dependent dispersions of SWCNTs have been produced by non-covalent functionalisation with poly-L-lysine (PLL), a natural polyelectrolyte.[144] In basic environments PLL has a $\alpha$-helix formation however under acidic and neutral conditions PLL adopts an uncoiled conformation and is able to interact with the SWCNTs. Non-covalent functionalisation of MWCNTs with polycystine has produced dispersions close to 7 mg/mL without the aid of sonication.[145]

A designed peptide, termed nano-1, adopts an amphiphilic $\alpha$-helical conformation in the presence of SWCNTs.[146] The hydrophobic face of the peptide noncovalently interacts with the SWCNT surface while the hydrophilic face promotes their dispersion to concentrations of 0.7 mg/mL. Atomic force microscopy (AFM) has showed that nano-1 is able to debundle SWCNTs and disperse them as intact individuals using minimal sonication.[147] An increase in the number of aromatic residues on the hydrophobic face of nano-1 has increased the amount of SWCNTs dispersed, thus demonstrating the importance of $\pi$-$\pi$ stacking interactions in the peptide dispersion of SWCNTs.[148] MWCNTs have been dispersed using anionic and cationic peptide amphiphiles that consist of a hydrophobic alkyl chain covalently attached to an amino acid sequence.[149] As the net ionic charge of the peptides varies with pH so will the ionic repulsion between the nanotubes, allowing the solubility of the MWCNTs to be controlled as a function of pH. Reversible cyclic peptides (RCPs), which can exist in linear or cyclic conformations by the reduction or oxidation of a disulfide bond incorporated into their backbone, have been used as dispersants for SWCNTs.[150] The RCPs noncovalently wrap around the SWCNT circumference and form closed rings through

intramolecular disulfide bonds. This produces very stable dispersions, as the peptide is unable to disassociate from the SWCNTs, while controlling the length of the peptide enables diameter-selective solubilisation.

#### 1.8.3.2 Proteins

Proteins are useful dispersing agents, as they possess both hydrophobic and hydrophilic domains, which allows for simultaneous interaction with the CNTs and water. Their ability to disperse CNTs in aqueous medium is dependent on their amino acid sequence and pH conditions. A variety of enzymes have been covalently attached to acid oxidised SWCNTs and MWCNTs though carbodiimide activation.[151, 152] The enzymes attached to the CNTs display enhanced stability under denaturing environments relative to the free enzyme and retained a high fraction of their native structure and activity. Non-covalent functionalisation with lysozyme (LSZ) has been shown to selectively disperse larger diameter DWCNTs and facilitate the separation of DWCNTs from SWCNT impurities.[153] Additionally the DWCNT-LSZ dispersions displayed a reversible dependence on pH, the optimal pH was found to be pH 3 where the DWCNT concentration was 0.087 mg/mL. Dispersions of SWCNTs non-covalently functionalised with LSZ have also been shown to be pH sensitive as they aggregate between pH 8-11 but remain highly dispersed outside this range.[154] Davis *et al.*[113] have demonstrated the importance of the strength of the interaction between LSZ and SWCNTs on aqueous solubility. LSZ was able to non-covalently functionalise pristine and oxidised SWCNTs to give concentrations of 0.108 and 0.027 mg/mL respectively in water. The lower solubility of the oxidised SWCNTs was attributed to the reduced ability of the oxidised SWCNTs to form hydrophobic interactions with LSZ. $\pi$-$\pi$ stacking between the hydrophobic aromatic amino acid residue tryptophan of LSZ and the SWCNT sidewall has been suggested as the key interaction.[112, 113] Bovine serum albumin (BSA) has also been covalently attached to oxidised CNTs through diimide activated amidation to give water-soluble nanotube-BSA conjugates.[155] pH responsive dispersions of MWCNTs have been produced using a fibrous protein component of silk known as fibroin.[156] The dispersions are stable in basic conditions (pH 12) but sediment under acidic conditions (pH 4) due to conformational changes in the silk fibroin.

#### 1.8.3.3 Sugars

The amino sugar glucosamine has been covalently attached to oxidised SWCNTs through an amide bond.[157] The solubility of SWCNT-glucosamine was found to be temperature dependent with a value of 0.1 mg/mL attained at room temperature, which increased to 0.3 mg/mL at ≈100 $^{o}$C.

A series of sugar dendrons of $\beta$-D-galactopyranosides (Gal) and $\alpha$-D-mannopyranosides (Man) with a terminal amino group have been covalently attached to oxidised SWCNTs through carbodiimide activated amidation reactions.[158] The higher order sugar dendrons were the most effective solubilising agents with SWCNT concentrations of 3.1 and 4.3 mg/mL achieved respectively for $Gal_4$- and $Man_4$-SWCNT. Pristine SWCNTs have been covalently functionalised with three sugar azides based on glucose, galactose and mannose under microwave conditions.[159] These nitrogen linked sugar functionalised SWCNTs formed stable dispersions in water with the galactopyranosyl functionalised SWCNTs soluble at 1.3 mg/mL and the gluco- and mannopyranosyl at 0.6 mg/mL.

12-membered cyclodextrins (CDs) have been used to solubilise SWCNTs in water and enable their partial separation by diameter.[160] Oxidised SWCNTs have formed complexes with CDs by using a mechanochemical high-speed vibration milling technique (HSVM).[161] The solubility in aqueous media of these SWCNT-CD complexes increased with the CDs ring size with the $\alpha$, $\beta$, and $\gamma$ complexes giving SWCNT solubilities of 0.44, 0.73 and 1.15 mg/mL respectively. The increase in solubility was attributed to the increasing number of hydroxyl groups on the CDs that could hydrogen bond with the carboxylic acid groups on the SWCNTs. Under the milder conditions of sonication SWCNTs are insoluble in water with only CDs present, however physical adsorption of a host-guest inclusion complex between $\beta$-CD and the guest compound sodium adamantanecarboxylate (AdCNa) has rendered the SWCNTs soluble at a concentration of 0.83 mg/mL.[162, 163] Decreasing the pH of the solution from 7 to 3 resulted in protonation of the carboxylate of AdCNa and aggregation of the SWCNTs, indicating electrostatic repulsive forces between the anionic carboxylate groups are necessary for dispersion.

A glycoconjugate polymer (0.5 mg/mL) with pendant sugar groups has helically wrapped around SWCNTs through hydrophobic interactions to give a maximum

SWCNT solubility of 0.2 mg/mL.[164]

#### 1.8.3.4 Polysaccharides

Cellulose is insoluble in water due to its hydrogen bonded supramolecular structure. The disruption of these intramolecular hydrogen bonds by hydroxyl groups present on SWCNTs and the subsequent formation of intermolecular hydrogen bonds between the SWCNTs and cellulose however has resulted in the dispersion of SWCNTs in water.[165] Stable dispersions were achieved within the pH range 6-10 with a maximum concentration of SWCNTs between 0.2-0.3 mg/mL. Pyrene-labelled hydroxypropyl cellulose has dispersed MWCNTs in water (0.05 mg/mL) and many organic solvents through $\pi$-$\pi$ stacking interactions.[166] Takahashi *et al.*[167] used the anionic cellulose derivative, carboxymethylcellulose (CMC) to disperse SWCNTs using sonication. The SWCNT-CMC aqueous dispersions were found to be stable for a few months. Electrostatic repulsion between the anionic CMC chains was suggested to be responsible for this. Sodium carboxymethylcellulose (Na-CMC), an etherified form of cellulose was found to be more effective at dispersing SWCNTs than the surfactant sodium dodecyl sulfate with concentrations of 1.2 and 0.5 mg/mL achieved respectively.[168]

Chitosan contains both hydrophobic acetyl groups and hydrophilic amino groups. The concentration of MWCNTs dispersed by non-covalent adsorption of chitosan has been improved by using chitosan with a lower degree of deacetylation.[169] This was attributed to increased hydrophobic interactions between MWCNTs and chitosan, afforded by the presence of more acetyl groups. Non-covalent wrapping with chitosan is known to result in the selective dispersion of SWCNTs of smaller diameter, allowing for separation of SWCNTs by size.[170] Chitosan is insoluble in aqueous solutions at pH>6 and therefore is only effective at dispersing SWCNTs under acidic conditions.[171] $\pi$-$\pi$ stacking of pyrene labelled chitosan,[172] and covalent grafting of chitosan to MWCNTs through nucleophilic substitution,[173, 174] has produced MWCNTs soluble in aqueous acetic acid solution. The chitosan derivatives O-carboxymethylchitosan (OC) and OC modified with poly(ethylene glycol) (OPEG) however are soluble in aqueous media at neutral pH and are thought to adsorb on SWCNTs through a donor-acceptor interaction between the free electron pair in the primary amine group of OC/OPEG and the nanotube.[175] The solubility of SWCNTs in water for OC and OPEG are 0.021 and

0.032 mg/mL respectively, which is comparable to that achieved with chitosan in acetic acid (0.038 mg/mL). Recently another neutral pH water-soluble derivative chitosan-hydroxyphenyl acetamide with phenyl side chains was found to strongly adsorb onto nanotubes resulting in individually dispersed SWCNTs at 0.033 mg/mL.

Three isomers of the sulfated glycosaminoglycan chondroitin sulfate, CS-A, CS-B and CS-C have produced aqueous SWCNT concentrations of 0.029, 0.027 and 0.041 mg/mL respectively.[176] The greater dispersing ability of CS-A and CS-C was attributed to their extended conformations, which allows them to helically wrap around the SWCNTs. Hyaluronic acid, an anionic, nonsulfated glycosaminoglycan, has also been used to produce stable dispersion of SWCNTs through noncovalent wrapping.[177]

Alginic acid, an anionic polysaccharide found in brown algae, has been used to wrap MWCNTs to give a concentration of 3.2 mg/mL.[178] Mild sonication of SWCNTs or MWCNTs in an aqueous solution of Gum Arabic, a polysaccharide found in Acacia trees, results in stable dispersions that consist of individual and structurally intact CNTs.[179] Schizophyllan (SPG), a polysaccharide produced by a fungus, can wrap around and dissolve SWCNTs to a maximum concentration of 2.5 mg/mL.[180] The addition of DMSO or aqueous alkaline solution dissociates the SPG resulting in precipitation of the SWCNTs and enabling their recovery from solution.

SWCNTs are soluble to a concentration of 3 mg/mL in an aqueous solution of a starch-iodine complex.[181] The use of the iodine complex was suggested to be necessary to ensure the initial preorganisation of the amylose present in starch into a helical conformation. The SWCNTs were speculated to displace the iodine molecules from the amylose helix via a pea-shooting mechanism, driven by a favourable change in entropy (Figure 1.10).

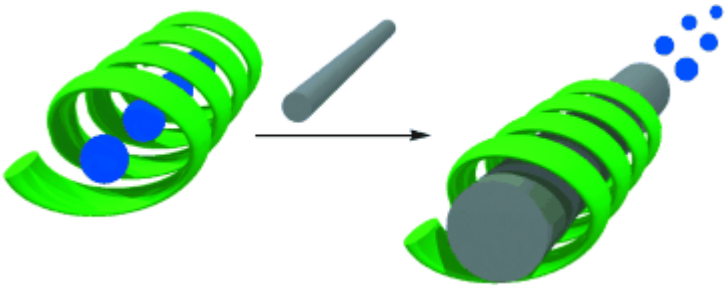

Figure 1.10: Schematic representation of the pea-shooting mechanism whereby carbon nanotubes displace iodine molecules from the amylose helix. Reprinted with permission from [181].

#### 1.8.3.5 Nucleotides/Polynucleotides

A mechanochemical high-speed vibration milling technique (HSVM) has been employed to non-covalently functionalise pristine SWCNTs with various phosphate nucleotides.[182] A maximum SWCNT solubility of 0.78 mg/mL was achieved through $\pi$-$\pi$ stacking of the SWCNTs with guanosine 5-monophosphate (GMP). Deoxyribonucleic acid (DNA) is an effective solubilising agent for CNTs in aqueous solution.[183, 184] Sonication in the presence of singlestranded DNA (ssDNA) has proven to be more successful than double-stranded DNA at dispersing SWCNTs.[184] It was considered that the ssDNA wraps around the nanotube surface through -stacking interactions between the aromatic nucleotide bases and the nanotube sidewall. The exposure of the negatively charged sugar-phosphate backbone of ssDNA to water resulted in SWCNT concentrations of 4 mg/mL. Further research found the wrapping of ssDNA to CNTs to be dependent on the specific sequence of the DNA strand.[185] Investigations with MWCNTs showed that the presence of defect sites in the CNT sidewall improved dispersion in aqueous DNA solutions.[186]

### 1.8.4 Polymers

Polymers can be covalently attached to the CNT surface by grafting to or grafting from methods.[187] The grafting to approach involves reacting the end group of the desired polymer with functional groups that are already attached to the CNT surface. Grafting from relies on the covalent functionalisation of the CNT with an initiator followed by in-situ polymerisation from these sites. Non-covalent functionalisation with polymers

involves the physical adsorption and/or wrapping of the polymer to the CNT surface. The use of stimuli-responsive polymers, which undergo conformational changes when an external stimulus such as temperature or pH is applied, allows the dispersion state of the CNTs to be controlled.

#### 1.8.4.1 Sulfonation

In situ polymerisation of aniline, followed by sulfonation with chlorosulfonic acid resulted in MWCNTs functionalised with sulfonated polyaniline that are dispersible at concentrations of 1.9 mg/mL.[188] Soluble SWCNTs have been prepared via in situ radical polymerisation of sodium 4-styrenesulfonate.[189] The poly(sodium 4-styrenesulfonate) is covalently bound to the SWCNTs and forms an indefinitely stable dispersion. SWCNTs grafted with polyacrylonitrile through the in situ polymerisation of acrylonitrile have been hydrolysed to give polyacrylic acid (PAA) functionalised SWCNTs.[190] PAA is a weak polyanion, which undergoes conformational changes in response to pH. The solubility of SWCNT-PAA was observed to be pH dependent as stable solutions were observed at pH >5, below which precipitation occurred. Sulfonation of polystyrene chains grafted to SWCNTs resulted in water-soluble derivatives.[191] The degree of sulfonation was shown to be directly proportional to the aqueous solubility achieved. The highest sulfonation level attained (34 mol%) gave a stable solution with a SWCNT concentration of 0.24 mg/mL. The solution exhibited pH responsive behaviour, remaining soluble between pH 3-13, but completely insoluble outside this range.

#### 1.8.4.2 Defect Site Functionalisation

A commonly employed tactic to covalently attach polymers to CNTs takes advantage of the nanotube-bound carboxylic acid groups introduced during oxidative acid treatment. Sun *et al.*[192] have attached a hydrophilic dendron species terminated with oligomeric poly(ethylene glycol) (PEG) chains to MWCNTs by an acylation-esterification reaction. The resulting functionalised MWCNTs are soluble in water as well as chloroform and DMSO. Direct thermal, carbodiimide activated amidation and acylation-amidation reactions have been employed for the functionalisation of oxidised SWCNTs using diamine terminated PEG (average molecular weight ∼1500).[193, 194]

Direct thermal reaction was the most effective for PEG functionalisation and gave a nanotube concentration of >87 mg/mL (the viscosity of the solution hindered the determination of the exact solubility). Monoamine terminated PEG has also been attached to SWCNTs via the acylation-amidation route to give SWCNTs soluble in water and organic solvents.[195] An alternative method to achieve carboxylic acid functionalised SWCNTs involved treatment with lithium followed by reaction with $\omega$-bromocarboxylic acids.[196] These SWCNTs were subsequently PEGylated with monoamine terminated PEG ($H_2N$-mPEG-OMe) to give water-soluble SWCNTs. Poly(aminobenzene sulfonic acid) (PABS) and PEG have been covalently attached to SWCNTs by amidation or esterification of nanotube bound carboxylic acids by means of an acyl chloride intermediate.[197, 198] The PABS and PEG functionalised SWCNTs are soluble in water at 5.8 and 5.9 mg/mL respectively. The covalent attachment of poly(vinyl alcohol) (PVA) (average molecular weight ~20,000) by carbodiimide activated amidation produced an SWCNT concentration of 7 mg/mL.[194] Carboxyl functionalised SWCNTs have been functionalised with phosphoryl choline and sugar based polymers through atom transfer radical polymerisation to give maximum concentrations of 7 and 5 mg/mL respectively.[199]

#### 1.8.4.3 Stimuli Responsive

Poly(acrylamide) (PAM) has been grafted from the surface of SWCNTs via reversible addition-fragmentation chain transfer (RAFT) polymerisation to give a stable 5 mg/mL aqueous dispersion of SWCNT-PAM.[144] A diazonium reaction attached the RAFT agents to the SWCNTs from which the PAM chains grew. RAFT polymerisation has also been employed to functionalise MWCNTs with the thermoresponsive polymer poly(N-isopropylacrylamide) (PNIPAM).[200] This allowed the exfoliation and precipitation of MWCNTs in aqueous solution to be controlled through the temperature-induced changes in conformation of PNIPAM. Temperature responsive dispersions of SWCNTs have also been produced by non-covalent functionalisation with PNIPAM.[144] A unique double stimuli-responsive copolymer based on PNIPAM has non-covalently functionalised MWCNTS to produce an aqueous dispersion of MWCNTs sensitive to both temperature and ionic strength.[201] Copolymers of PNIPAM or poly(N-cyclopropylacrylamide) (PNCPA) with pyrene side groups have been

used to produce stable temperature controlled dispersions through $\pi$-$\pi$ interactions with CNTs.[202, 203] PAA, PNIPAM and PAM have all been grafted from hydroxyl functionalised MWCNTs by Ce(IV) induced redox radical polymerisation.[204] These polymer functionalised MWCNTs were all highly soluble in water and once again the MWCNT-PAA and MWCNT-PNIPAM dispersions displayed reversible responses to changes in pH and temperature respectively.

#### 1.8.4.4 Non-Covalent Wrapping

The water-soluble polymers poly(vinyl pyrrolidine) (PVP) and poly(styrene sulfonate) (PSS) have solubilised SWCNTs in aqueous solution by helical wrapping of the tubes.[205] A uniform dispersion of 1.4 mg/mL was possible with SWCNTs non-covalently functionalised with PVP, while with PSS 4.1 mg/mL could be realized. Poly(p-phenyleneethynylene) has also been shown to wrap the SWCNT surface in a helical manner to give mostly individual water-soluble SWCNTs.[206]

Non-covalent association with PAA within the pH range 3-8 dissolves MWCNTs in water to give a homogeneous solution that contains 1 mg/mL MWCNTs.[207] These findings were supported by Zakri *et a*l.[208] who also established the optimum pH for dispersion was pH 5, close to the pKa of PAA.[208] A SWCNT concentration of 1.1 mg/mL has been reported upon mild sonication of the tubes in a 1 wt% PAA solution.[209] Grunlan *et al.*[210] have investigated the ability of several polyelectrolytes to disperse SWCNTs and found that polyanions are able to stabilise SWCNTs more effectively than polycations.

Non-covalent functionalisation with poly(N-(2-(dimethylamino) ethyl)-methacrylate) (PDMAEMA) has resulted in the dispersion of MWCNTs at pH 3 while at pH 11 complete precipitation of the MWCNTs was observed.[211] These observations were attributed to the protonation of the amine groups in the polymer side chain that occurs under acidic conditions, affording good solubility in water.

Low concentrations (0.15 mg/mL) of the natural polyelectrolytes (NPs) sodium lignosulfonate (SLS) and humic acid (HA) have dispersed SWCNTs at 0.068 and 0.053 mg/mL respectively.[212] The NPs contain aromatic groups that interact with the CNTs through $\pi$-$\pi$ interactions while the sulfonate groups present in SLS and carboxylic acid groups in HA allow for aqueous solubility.

Individual SWCNTs have been non-covalently encapsulated within a polyethylene glycol-polyacrylic acid-polystyrene (PEG-PAA-PS) block copolymer.[213] This structure, which contains the SWCNT within the hydrophobic core of a PAA-crosslinked PEGylated micelle, was termed a PEG-egg. These SWCNT PEG-eggs displayed aqueous solubility while near-infrared fluorescence confirmed that the SWCNTs retained their electronic structure. Oligothiophene-terminated PEG (TN-PEG) has dispersed SWCNTs as individuals or small bundles to give very stable solutions.[214] The long-term stability of the dispersions was attributed to the strong $\pi$-$\pi$ interactions between the SWCNT and the thiophene unit.

MWCNTs wrapped with hydrolyzed poly(styrene-co-maleic anhydride) (HPSMA) are soluble in water within the pH range 3-13 to a maximum concentration of 8.7 mg/mL.[215] The benzene ring of the styrene moiety on HPSMA adsorbs on MWCNTs while the hydrophilic maleic acid group allows for dissolution in water. Functionalisation of MWCNTs with the pyrene carrying form of HPSMA resulted in the spontaneous dissolution of MWCNTs to a concentration of 7.4 mg/mL.[216] The pyrene moiety was shown to improve the interactions between the polymer and MWCNTs as the polymer was attached irreversibly to the tube surface.

### 1.8.5 Surfactants

Surfactants are amphiphilic molecules that have been extensively used to solubilise CNTs in water.[82, 217, 218] Typically dispersions are prepared by the addition of the CNTs to an aqueous solution of the selected surfactant followed by bath or tip sonication. The mechanism for dispersion is believed to involve the non-covalent absorption of their hydrophobic tail to the CNT sidewall, which exposes a hydrophilic surface to the aqueous solution for dissolution.[219] Exactly how the surfactant molecules adsorb has been debated. The most common methods suggested involve encapsulation within a cylindrical micelle,[220] the formation of hemispherical micelles on the surface,[221, 222] or random adsorption (Figure 1.11).[223]

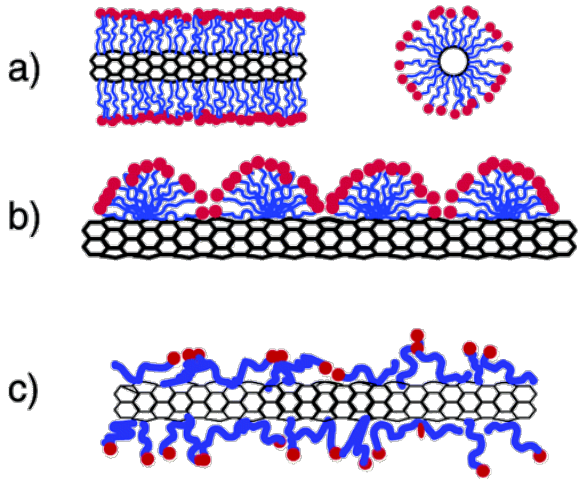


Figure 1.11: Illustrations of the possible conformations of surfactants on the CNT surface (a) cylindrical micelle, side (l) and cross-section (r) views, (b) hemimicelle (c) random adsorption. The hydrophilic head is shown in red, the hydrophobic tail in blue. Reprinted with permission from [223]. Copyright (2004) American Chemical Society.

Surfactants can be classified as anionic, cationic, non-ionic or zwitterionic according to the charge on their head group. Ionic surfactants are able to prevent CNTs aggregating through Columbic repulsion. The ability of non-ionic surfactants to suspend CNTs is due the size of the hydrophilic group, with the efficiency of the surfactant increasing with molecular weight due to enhanced steric repulsion.[224] It has been suggested that non-ionic surfactants are preferable for dispersing CNTs in organic solvents while ionic surfactants are favoured for producing aqueous CNT dispersions.[103] Islam *et al.*[222] however, have shown that the non-ionic surfactant Triton X-100 (TX100) is a better dispersant for SWCNTs in water than the anionic surfactant sodium dodecyl sulfate (SDS) with concentrations of $\leq$0.5 and $\leq$0.1 mg/mL achieved respectively. Another anionic surfactant, sodium dodecylbenzene sulfonate (NaDDBS), however was shown to be a substantially better dispersant for SWCNTs than TX100 with SWCNT concentrations of 20 mg/mL possible.[222] The observed difference between TX100 and NaDDBS was attributed to headgroup size; the larger poly(ethylene oxide) headgroup of TX100 lowered its packing density compared to NaDDBS (Figure 1.12). NaDDBS and TX100 were believed to disperse SWCNTs better than SDS because they contain a benzene ring, which allows for a greater interaction with the SWCNTs. NaDDBS has also been shown to be capable of producing dispersions consisting of long, individual

SWCNTs.[225]

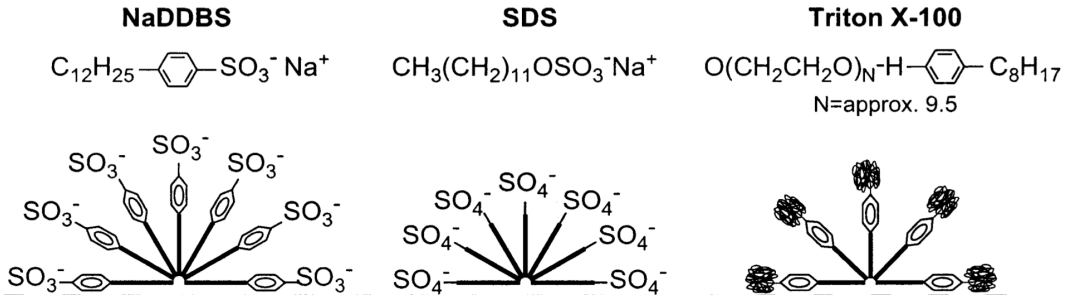


Figure 1.12: Structure of the surfactants NaDDBS, SDS and TX100 (l-r). Reprinted with permission from [222]. Copyright (2003) American Chemical Society.

The significance of a benzene ring was further confirmed by Rastogi *et al.*[226] who evaluated the effectiveness of the non-ionic surfactants, TX100, Tween 20, Tween 80 and SDS to disperse MWCNTs. TX100 displayed the highest dispersing power of the four which was again attributed it to its ability to adsorb more strongly than the others to the MWCNTs through $\pi$-$\pi$ stacking. Tween 80 was the next best because of its longer tail while Tween 20 was more effective than SDS due to its bulkier head group which provided greater steric stabilisation.

The effects of pH on the dispersion of MWCNTs has been compared for the surfactants NaDDBS, hexadecyl(trimethyl)azanium bromide (CTAB), Pluronic F68 and Pluronic F127.[227] Under neutral pH conditions the cationic CTAB was the most efficient surfactant. Variations in pH had a negligible effect on the dispersing ability of the non-ionic Pluronic surfactants. NaDDBS however was found to be a poor dispersing aid at both pH extremes, while CTAB dispersions remained nearly pH independent only under basic conditions. A stimuli responsive azobenzene based surfactant with a third generation glycerol dendron and alkyl chain has been used to solubilise SWCNTs as individuals.[228] The trans to cis isomerisation of the azobenzene group that occurs upon irradiation with light has resulted in the reversible precipitation of the tubes.

## 1.9 Applications of CNTs

A wide range of potential applications for CNTs have been suggested as a result of the remarkable properties they possess, however due to their poor solubility the application

of the material is limited.[229–231] Approaches towards the solubilisation of CNTs in water are important for fields such as polymer composites, biomedicine and conducting thin films.

The excellent mechanical properties of CNTs make them an ideal material for use in the reinforcement of polymer composites, but to be effective in this regard the CNTs must be uniformly dispersed within the matrix to achieve efficient load transfer to the nanotube network.[44] Solution casting is the most common method for fabricating CNT polymer composites. In the case of water-soluble polymers such as poly(vinyl alcohol) (PVA),[232, 233] this involves dispersing the functionalised CNTs in water, mixing the CNT dispersion with the polymer solution and then evaporating off the solvent to give a composite film.[234].

Hydrogels are physically or chemically crosslinked networks of hydrophilic polymer chains that are able to absorb large quantities of water without dissolving.[235] They are useful materials for biomedical applications such as drug delivery and tissue engineering,[236] however their poor mechanical and electrical properties can limit their practical application. To attempt to improve these properties CNTs have been incorporated into the hydrogel matrix. As a uniform dispersion of the CNTs is essential, hydrogels have used water-dispersible CNTs functionalised with pyrene modified cyclodextrin,[237] pluronic copolymer,[238] hyaluronic acid,[239] and polysaccharides.[240]

### 1.9.1 Thin Films

Transparent electronic materials are of interest for many applications, such as antistatic coatings, touch display panels, solar cells and flat panel displays.[241] The metal oxide indium tin oxide (ITO) is the most widely used material for such applications however due to its brittleness, high cost and limited supply of indium suitable alternatives are being investigated.[242] CNTs are a promising potential replacement due to their inherent electronic properties and mechanical flexibility. The fabrication of transparent and conductive CNT films to replace ITO in certain applications has been achieved using drop casting from solvents,[243] inkjet printing,[244] and the Langmuir-Blodgett technique,[245] but vacuum filtration is the most commonly used method. In this process the CNTs are dispersed in aqueous solution, usually through interaction with

a surfactant,[246, 247] and vacuum filtered to form a homogenous film on the membrane (Figure 1.13). The resulting film can then either be transferred to another substrate or the membrane dissolved to give a freestanding film. As is the case in the production of all transparent conducting films a compromise between transparency and conductivity must be made, as an increase in CNT concentration will increase the conductivity but result in a decrease in transparency of the film.

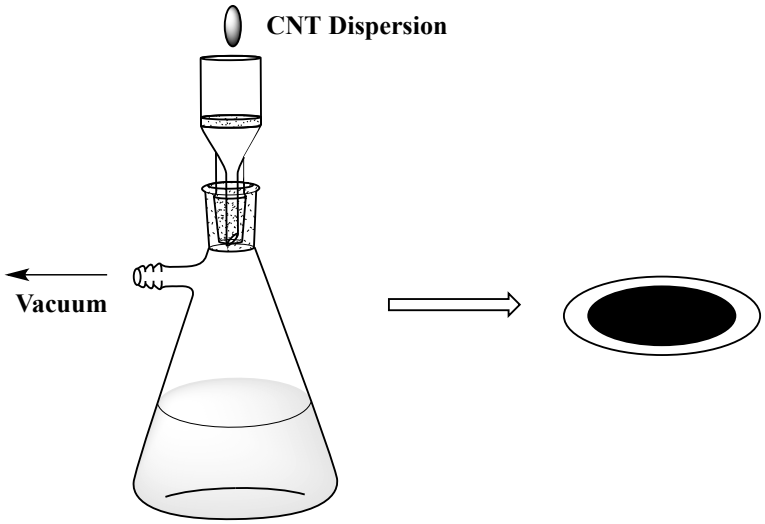


Figure 1.13: Schematic representation of the vacuum filtration method for the preparation of CNT thin films.

Vacuum filtration of SDS dispersed CNTs onto a membrane followed by poly(dimethylsiloxane) based transfer printing to various substrates has produced highly conducting CNT films with performance characteristics comparable to those of ITO films on plastic substrates.[246] SDS dispersed SWCNTs have also been employed to produce thin films on poly(ethylene terephthalate) (PET) using a spray method.[248] Subsequent treatment of these films with nitric acid to remove residual SDS was found to significantly improve their conductivity. TX100 dispersed SWCNTs have been deposited onto PET coated with an adhesion promoter via a dip-coating technique, which allowed the transparency and sheet resistance to be controlled by the number of coatings.[249] Post-deposition treatment with nitric acid was again observed to cause a decrease in the sheet resistance of the films. Thin films fabricated on PET using SWCNTs dispersed in TX100 have been shown to be more optically

transparent and flexible than commercial films of ITO on PET.[250] Thin films of nitric acid oxidised SWCNTs, prepared by vacuum filtration, have displayed improved mechanical properties but decreased electrical conductivity with increasing nitric acid concentration.[251]

# Chapter 2

# Characterisation of CNTs

## 2.1 Overview

This chapter summarises the analytical techniques that have been employed in this thesis to characterise CNTs. A detailed background of the techniques is not provided; the focus is on how these techniques can be used to analyse CNTs. Evidence can be gained on the extent of functionalisation, the nature of the functionalising group and the effect of functionalisation on CNT dispersibility. There are limitations however to the information that can be gained from each characterisation technique, so it is common that several are used and the results correlated before reliable conclusions about the material are drawn.

## 2.2 Thermogravimetric Analysis (TGA)

TGA is a destructive technique that is used to monitor the thermal stability of both as-synthesised and functionalised CNTs. This straightforward method records the change in mass that occurs when the CNTs are heated under a controlled atmosphere, which can be inert (nitrogen or helium) or oxidative (air or pure oxygen).

When performed in an oxidising atmosphere TGA is a useful tool for purity analysis of CNTs.[21, 22] CNT oxidation occurs between 400-600 $^{o}$C (Figure 2.1) with the temperature depending on a number of factors, such as CNT diameter, the number of structural defects and the amount of metal impurity.[252, 253] Nevertheless thermal

stability is commonly used as a measure of the quality of a CNT sample because usually a higher oxidation temperature is indicative of a purer material containing less defects.[254]

In an inert atmosphere CNTs are stable up to 800 $^{o}$C (Figure 2.1) and so the mass loss observed at lower temperatures can be attributed to the loss of functional groups attached to the CNT surface. Covalently attached functionalities will be removed at appreciably higher temperatures than adsorbed groups.[255] By assuming that all the mass loss is due to functionalisation, an estimation of the degree of functionalisation and the number of functional groups per carbon atom can be made by comparison with the starting CNT material. A drawback of TGA is that it does not identify the fragments that are removed from the CNT surface during heating. As a result TGA is often combined with gas phase mass spectrometry (TGA-MS).[51, 54, 255, 256]

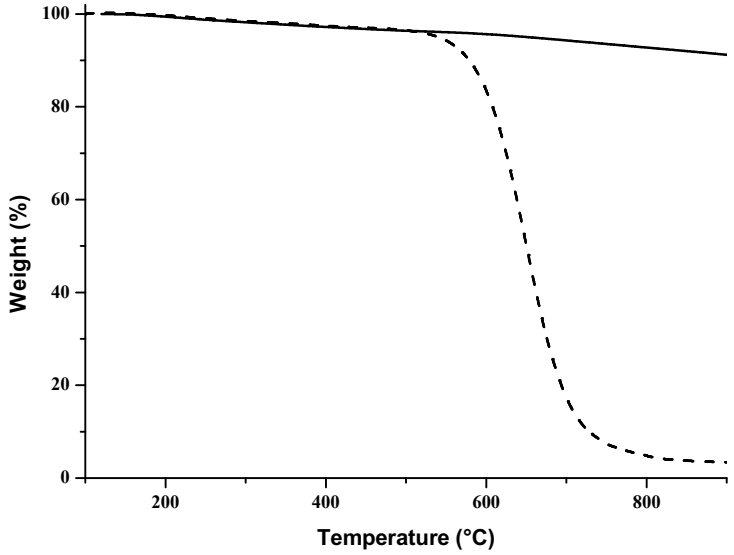


Figure 2.1: TGA of CNTs heated in helium (solid) and in air (dashed) to 900 $^{o}$C.

## 2.3 Ultraviolet-Visible-Near Infrared (UV-vis-NIR) Spectroscopy

The optical properties of CNTs arise from transitions within a one-dimensional density of states (DOS).[257] Three-dimensional materials have a continuous DOS but due to the one dimensional structure of CNTs their DOS is not continuous but features a series of spikes known as van Hove singularities (Figure 2.2).[258] The optical absorption spectra in the UV-vis-NIR range of pristine SWCNTs originates from transitions between the first and the second van Hove singularities and are denoted as $S_{11}$ and $S_{22}$ in the case of semiconducting SWCNTs and $M_{11}$ in the instance of metallic SWCNTs.

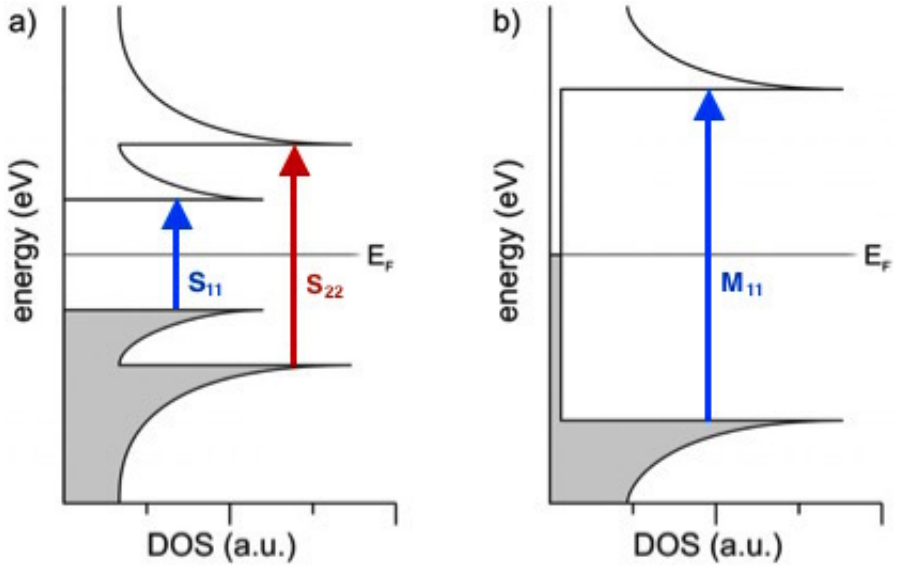


Figure 2.2: Schematic representation of the electronic density of states of a semiconducting (left) and metallic (right) SWCNT and the possible transitions between the van Hove singularities. The valence bands are grey and the conduction bands are white. Adapted from [258] by permission of The Royal Society of Chemistry.

The absorption bands seen in the visible range from 440 to 645 nm are associated with the $M_{11}$ transitions and those in the near infra-red between 830-1600 nm and 600-800 nm are assigned to the $S_{11}$ and $S_{22}$ transitions, respectively (Figure 2.3).[259]

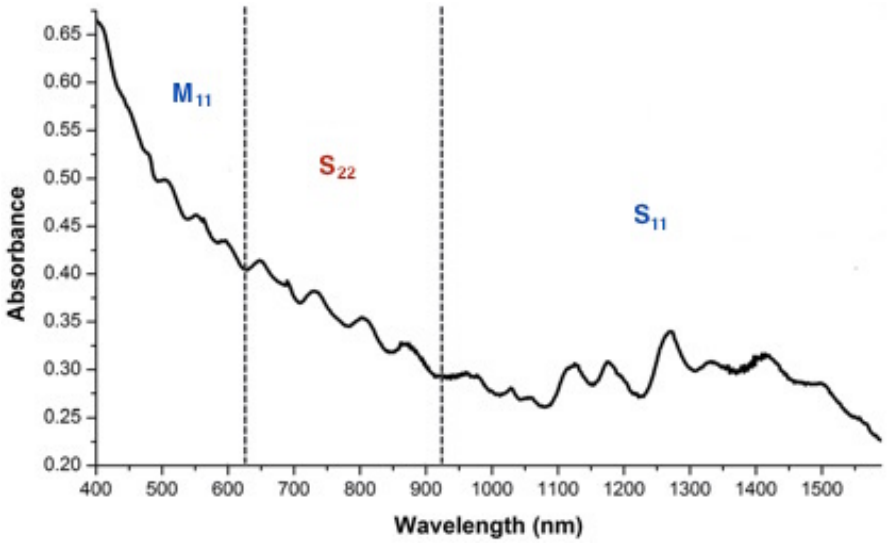


Figure 2.3: A typical UV-vis-NIR absorption spectrum of SWCNTs showing the $M_{11}$, $S_{11}$ and $S_{22}$ regions. Adapted from [260] by permission of The Royal Society of Chemistry.

Covalent modification of SWCNTs disrupts $\pi$ conjugation and induces changes in the electronic structure that results in the suppression of the $S_{11}$, $S_{22}$ and $M_{11}$ features, therefore this technique can be used for further confirmation functionalisation has occurred (Figure 2.4).[64, 81, 86] Unfortunately the ability to detect covalent functionalisation in this manner is limited to SWCNTs because for MWCNTs the different contributions from each tube overlap and so their spectra does not have the well-defined features of SWCNTs.

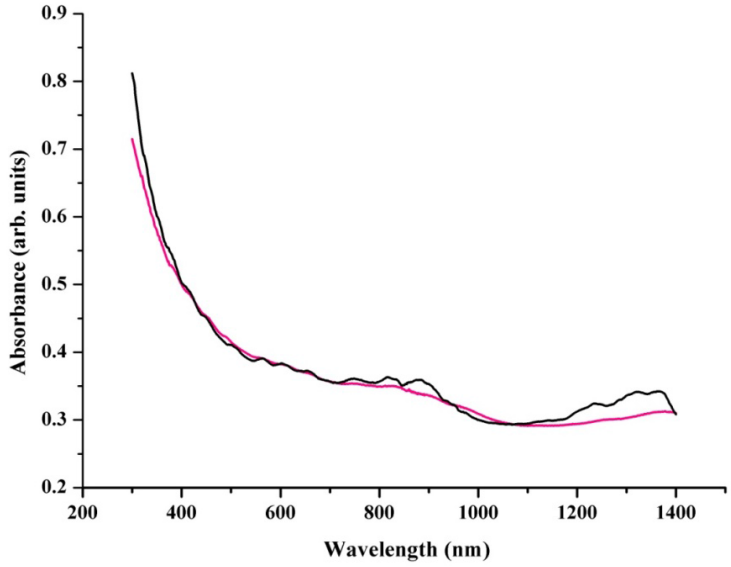


Figure 2.4: UV-Vis-NIR spectrum of pristine (black) and covalently functionalised (magenta) SWCNTs.

UV-vis-NIR spectroscopy is also widely used to determine the dispersibility of CNTs. The non-covalent or covalent modification of CNTs can result in a change in their dispersibility, so in this respect this technique can be used as added proof of either SWCNT or MWCNT functionalisation.[64, 261] The characterisation of CNT dispersions by UV-vis-NIR spectroscopy allows a calculation of the CNT concentration to be made through application of the Beer-Lambert Law (Equation 2.1) which states that the absorbance, A, of a sample is dependent on the light pathlength, l, the concentration, c, of the species and the extinction coefficient, $\varepsilon$.[262, 263] It is therefore possible to determine the concentration of CNTs in a particular solvent from its UV-vis-NIR spectrum if the extinction coefficient is known.

$$A(\lambda) = \varepsilon cl = \varepsilon c, \qquad \text{when;} \qquad l = 1\text{cm}, \tag{2.1}$$

## 2.4 Raman Spectroscopy

Raman spectroscopy is a non-destructive vibrational spectroscopy technique that relies on the inelastic scattering of light. Generally a sample is irradiated with monochromatic light from a laser source in either the visible or near-infrared range. The incident photons excite the molecule into a virtual energy state and when the molecule relaxes the photon is either elastically or inelastically scattered. If the emitted photon is of the same frequency as that of the incident photon then this is an elastic process and is referred to as Rayleigh scattering. Raman scattering occurs when there is a change in frequency of the photon. If the frequency of the emitted photon is lower than that of the incident photon this is termed Stokes scattering, but if it is higher it is known as Anti-Stokes scattering. Molecules in the ground vibrational state give rise to Stokes scattering, while molecules initially in a vibrational excited state give rise to anti-Stokes scattering. An energy level diagram is shown in Figure 2.5, which illustrates Rayleigh and Raman scattering.

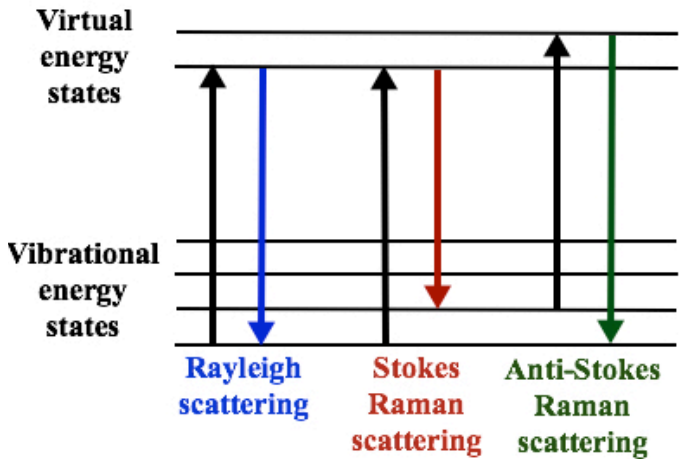


Figure 2.5: Energy-level diagram showing Rayleigh scattering and Stokes and Anti-Stokes Raman scattering.

Raman spectroscopy allows an evaluation of the purity or the extent of covalent functionalisation of CNTs to be made. Information can also be gained on the selectivity of certain functionalisation reactions towards SWCNTs of specific diameters or chirality. A representative Raman spectrum of SWCNTs excited at 632 nm is shown

in Figure 2.6. The Raman spectra of SWCNTs typically have four main features; the radial breathing mode (RBM) between 100-300 $cm^{-1}$, the disorder mode (D band) between 1200-1400 $cm^{-1}$, the tangential mode (G band) between 1500-1600 $cm^{-1}$ and the D-band overtone (G' band) between 2400-2800 $cm^{-1}$. MWCNTs display a very similar spectrum to SWCNTs, the primary difference being the lack of RBM bands which are absent as the RBM signal from large diameter tubes is too weak to be seen.[264].

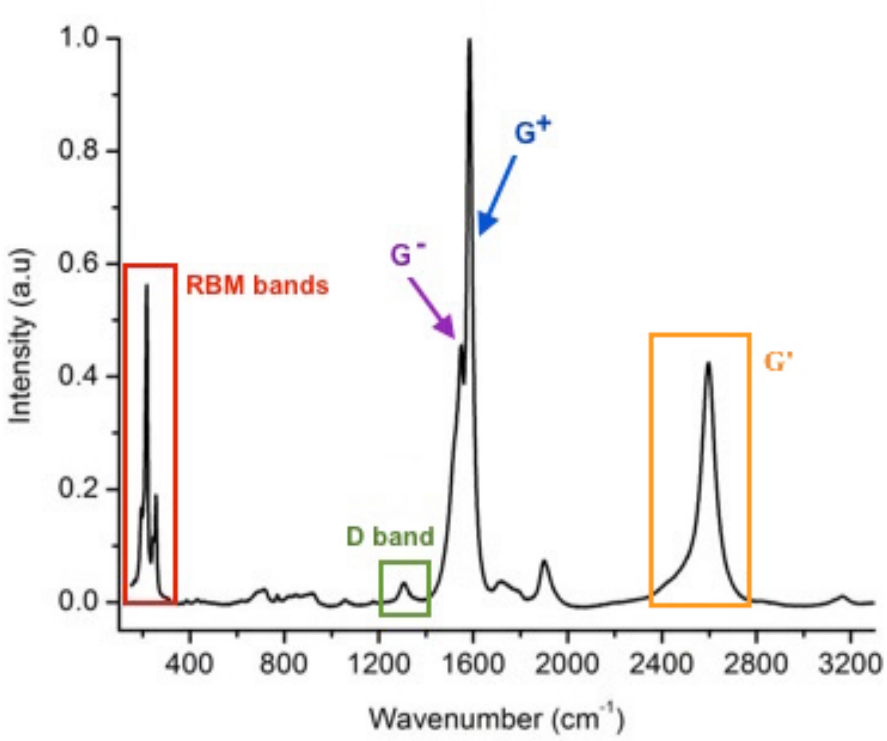


Figure 2.6: A Raman spectrum of pristine SWCNTs showing the most characteristic features: radial breathing mode (RBM), the D, G and G' bands.

The RBM corresponds to the atomic vibration of the carbon atoms in the radial direction and its frequency is directly linked to the reciprocal of the nanotube diameter. The RBM mode can thus be used to determine the selectivity of certain functionalisation reactions towards particular SWCNTs.[50, 258] The D band arises due to the presence of amorphous carbon impurities or because of the formation of defect sites on the CNT as a result of covalent functionalisation. The G' band feature arises from a two-phonon second-order Raman scattering process,[264] and is generally more intense

than the D-band because the second-order G'-band is symmetry allowed by momentum conservation requirements, while the D-band only appears when there is a breakdown in the in-plane translational symmetry.[265, 266] The G band consists of two components; the $G^-$ which is attributed to vibrations along the circumferential direction and the $G^+$ which is associated with vibrations along the tube axis. G band splitting is large for small diameter SWCNTs, however for MWCNTs the splitting is small and smeared out because of the diameter distribution within MWCNTs and the G band usually exhibits a weakly asymmetric lineshape.[267]

The ratio of the D to the G band is conventionally used in nanotube chemistry to evaluate the purity or the extent of covalent functionalisation of CNTs.[22, 80, 268, 269] An enhancement in the intensity of the D band relative to the G band is associated with successful functionalisation of CNTs, while a decrease is associated with a reduction in structural defects.

## 2.5 Fourier-Transform Infrared (FTIR) Spectroscopy

FTIR spectroscopy does not provide direct confirmation of covalent functionalisation or information on the degree of functionalisation but it can indicate the nature of the functional groups present on the CNT surface and has been employed after CNT oxidation to identify the presence of oxygen containing groups, such as carboxyl groups.[25, 28, 65, 270, 271] This technique has also been used in the characterisation of other functionalised CNTs and detection of a variety of functional groups including amine,[32, 272] amide,[32, 273] hydroxyl,[272], ester,[30] dichlorocarbene[274] and indolizine,[54] has been reported. The spectra of CNTs can be recorded using the ATR or potassium bromide disc method. The FTIR spectrum of "as-received" CNTs has been reported to have a strong and broad peak around 3430 $cm^{-1}$, which is assigned to the stretching vibrations of OH groups of adsorbed water and a peak at 1630 $cm^{-1}$ that is due to the C=C stretching (Figure 2.7).[25, 275, 276]

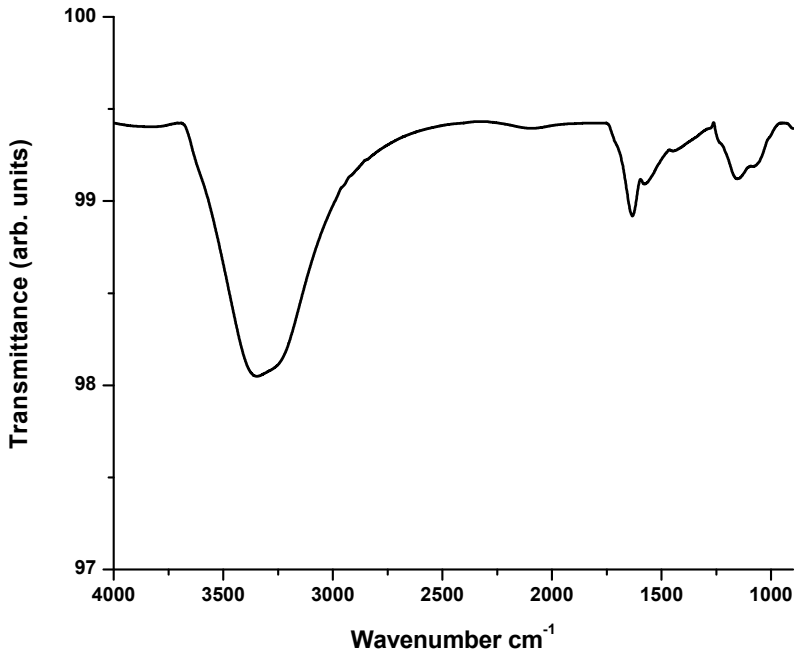


Figure 2.7: FTIR spectrum of "as-received" CNTs recorded using the ATR method.

## 2.6 Transmission Electron Microscopy (TEM)

TEM is a microscopy technique that produces high-resolution, two-dimensional images. Images are produced by illuminating an ultra-thin sample with an electron beam under vacuum and detecting the electrons that are transmitted through the sample. The use of electrons allows for imaging at a significantly higher resolution than light microscopes due to the small wavelength of electrons. TEM therefore allows users to examine detail on the nanoscale and as a result of this has become a important tool for the morphological characterisation of nanomaterials. At low magnification, TEM of a CNT sample can be used to measure CNT length and provide a crude assessment of their purity,[277, 278], while at high magnification it is possible to measure their diameter,[279] and to count the number of walls in MWCNTs and the distance between them.[280] TEM is also capable of identifying sidewall damage that could be caused by functionalisation (Figure 2.8),[281] however the electrons used for imaging can also

cause sidewall damage.[282]

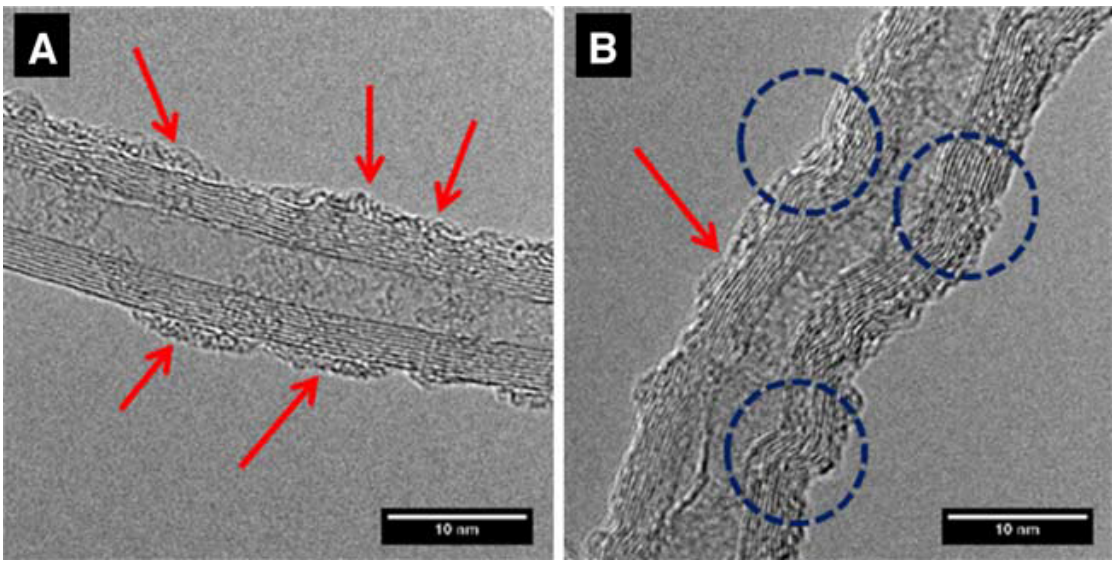


Figure 2.8: High resolution TEM images of a (A) pristine MWCNT and (B) MWCNT oxidised with sulphuric/nitric acid. The presence of amorphous carbon is indicated by arrows and sidewall damage highlighted with circles. Reprinted from [281] with kind permission from Springer Science and Business Media.

# Chapter 3

# The Ionic Interaction of Functionalised MWCNTs with Amino Acids

## 3.1 Introduction

The functionalisation of carbon nanotubes as described in Chapter 1 is considered an effective method to improve their dispersibility in water. In this chapter the MWCNTs were covalently functionalised with both negatively and positively charged functional groups through oxidation and diazonium reactions. Treatment of CNTs with nitric acid has been widely reported as a straightforward method to simultaneously purify and functionalise CNTs with primarily carboxylic acid groups.[26, 283, 284] The use of these carboxylic acid groups as a basis for subsequent attachment or interaction with other functionalising agents has been extensively exploited in nanotube chemistry.[30, 32, 285, 286] Diazonium chemistry, used for the attachment of aryl groups to the CNTs has also been widely used as a functionalisation method due to the high reactivity of the diazonium compounds.[86, 87, 287]

The subsequent ionic interactions of these functionalised MWCNTs with selected amino acids in water was then investigated with a view to this further increasing the aqueous dispersibility of the MWCNTs. This method has the advantage of potentially improving MWCNT dispersibility without causing further disruption of the $sp^2$ net-

work. The amino acid arginine in particular has previously been shown to enhance the aqueous solubility of alkyl gallates,[288, 289] and small aromatic compounds [290, 291] and to suppress the aggregation of proteins by binding to the protein through its guanidino group.[292, 293]

Amino acids are composed of a basic amine and acidic carboxylic acid group as well as a side chain unique to each one. They can be classified as acidic, neutral or basic according to the charge on their side chain at neutral pH. Arginine and lysine are basic amino acids with a guanidinium and amine group present in their side chain, respectively. The structure of the amino acids and the pKa values of the $\alpha$-carboxylic acid, $\alpha$-amine and side chain group are given in Figure 3.1.[294]

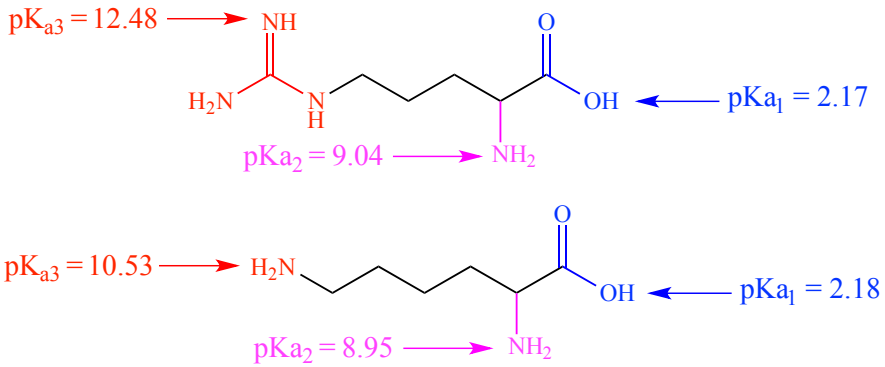


Figure 3.1: Structure and pKa values of arginine (top) and lysine (bottom).

At low pH ($<$p$K$a$_1$) both these amino acids are fully protonated and carry a positive charge of +2. Between p$K$a$_1$$<$pH$<$p$K$a$_2$ the $\alpha$-carboxylic acid loses its proton, so the amino acid has a +1 positive charge. At p$K$a$_2$$<$pH$<$p$K$a$_3$ the $\alpha$-amine loses its proton and the zwitterion form is dominant (no net charge). The pH where an amino acid has zero net charge is known as the isoelectric point (pI). The pI is an average of p$K$a$_2$ and p$K$a$_3$, hence the pI of arginine is 10.76 and lysine is 9.74.[294] Above p$K$a$_3$ the amino acids are completely deprotonated and carry a negative charge of -1.

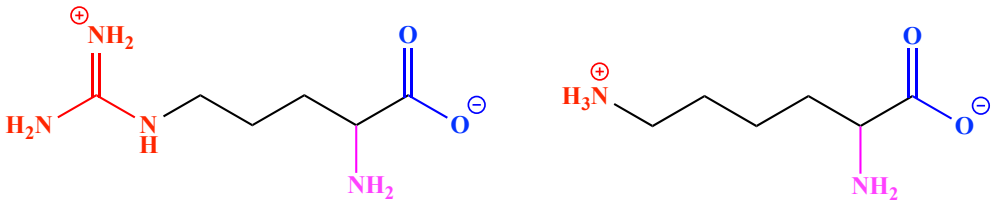


Figure 3.2: Structures of arginine (l) and lysine (r) at their isoelectric points.

Glycine is the smallest and simplest amino acid, having only a hydrogen substituent in its side chain. Taurine is an acid containing an amino group, however it has a sulfonic acid group instead of a carboxyl group and is therefore termed an amino sulfonic acid. The structure of the amino acids and the pKa values of the acid and amine groups are given in Figure 3.3.[294]

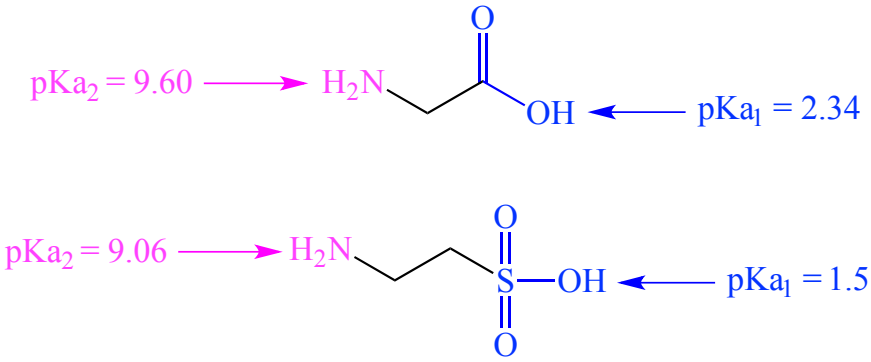


Figure 3.3: Structure and pKa values of glycine (top) and taurine (bottom).

As a result of their neutral side chains these amino acids are characterised by just two p$K$a values; p$K$a$_1$ for the carboxylic acid and p$K$a$_2$ for the amine. The average of these p$K$a values gives a pI of 5.97 for glycine and 5.28 for taurine. The structures of gylcine and taurine at their respective isoelectric points are shown in Figure 3.4.

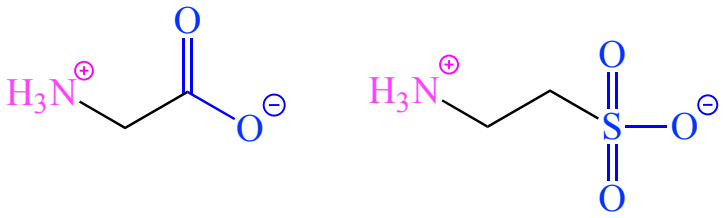


Figure 3.4: Structures of glycine (l) and taurine (r) at their isoelectric points.

Glutamic acid is an acidic amino acid as a carboxylic acid group is present in its side chain. The structure of glutamic acid and the pKa values of the $\alpha$-carboxylic acid, $\alpha$-amine and side chain carboxylic acid are given in Figure 3.5.[294]

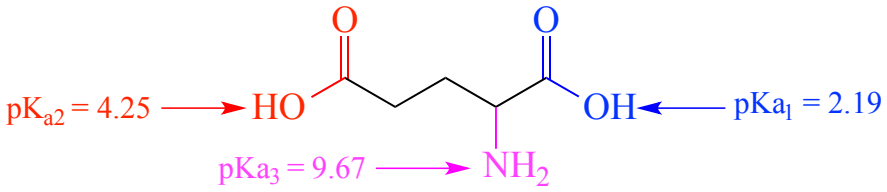


Figure 3.5: Structure and pKa values of glutamic acid.

At low pH (<2.19) glutamic acid is fully protonated and carries a net positive charge. Between 2.19 <pH <4.25 the $\alpha$-carboxylic acid loses its proton giving no net charge and the zwitterion form is dominant. The average of p$K$a$_1$ and p$K$a$_2$ gives glutamic acid a pI of 3.22. At 4.25 <pH <9.67 the carboxylic acid group in the side chain loses its proton and the amino acid carries a net negative charge. Above pH 9.67 the amino acid is completely deprotonated and carries a negative charge of -2.

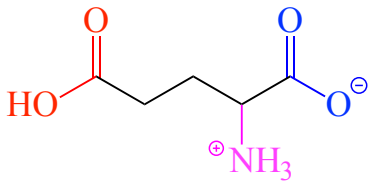


Figure 3.6: Structure of glutamic acid at its isoelectric point.

The functionalised MWCNTs were characterised by TGA, TEM, FTIR and Raman spectroscopy and their dispersions in amino acid solution by UV-vis-NIR spectroscopy.

## 3.2 Oxidation of MWCNTs

The MWCNTs used in this procedure did not undergo any purification beforehand and so were used "as received" (AR). The introduction of carboxylic acid groups to the surface of the AR-MWCNTs was achieved by reflux in 6 M nitric acid in a similar method to that reported previously (Figure 3.7).[26] The oxidative treatment was carried out for 4, 8 and 16 h.

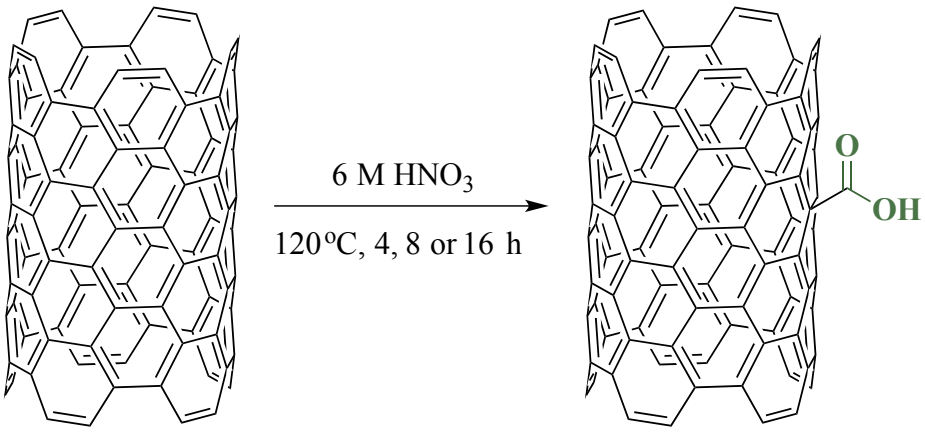


Figure 3.7: Schematic representation of the generation of the carboxylic acid functionalised MWCNTs.

As described in Section 1.7.1 some of the carboxylic acid functionalities generated by treatment of MWCNTs with nitric acid are suggested to be present on oxidation debris that is adsorbed onto the MWCNTs. For this reason dilute base washing at room temperature followed by an acid wash, as outlined in Section 6.3.3, has been employed throughout this thesis for all MWCNT samples after oxidation to remove this debris prior to further functionalisation. Base washing of the oxidised MWCNTs produced a yellow/brown filtrate as has been reported previously (Figure 3.8).[76, 77]

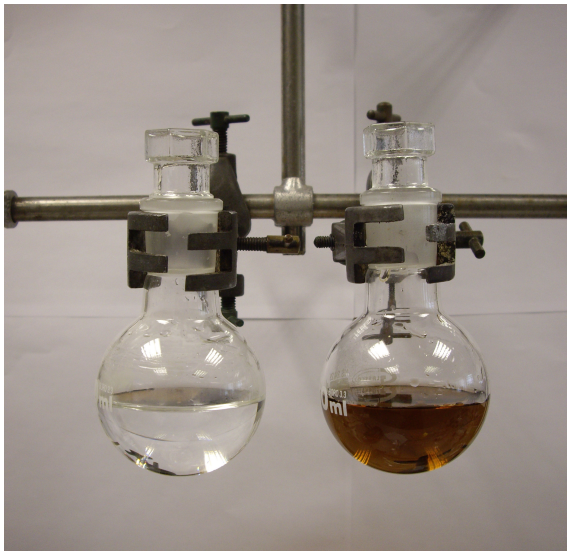

Figure 3.8: Photograph of the filtrate after washing oxidsed MWCNTs with water (l) and aqueous base (r).

### 3.2.1 Thermal Analysis

The degree of functionalisation of the oxidised MWCNTs was estimated by thermogravimetric analysis (TGA) in an inert helium atmosphere. The TGA results of the oxidised MWCNTs for each reflux time are overlaid with that of the AR-MWCNTs for comparison in Figure 3.9.

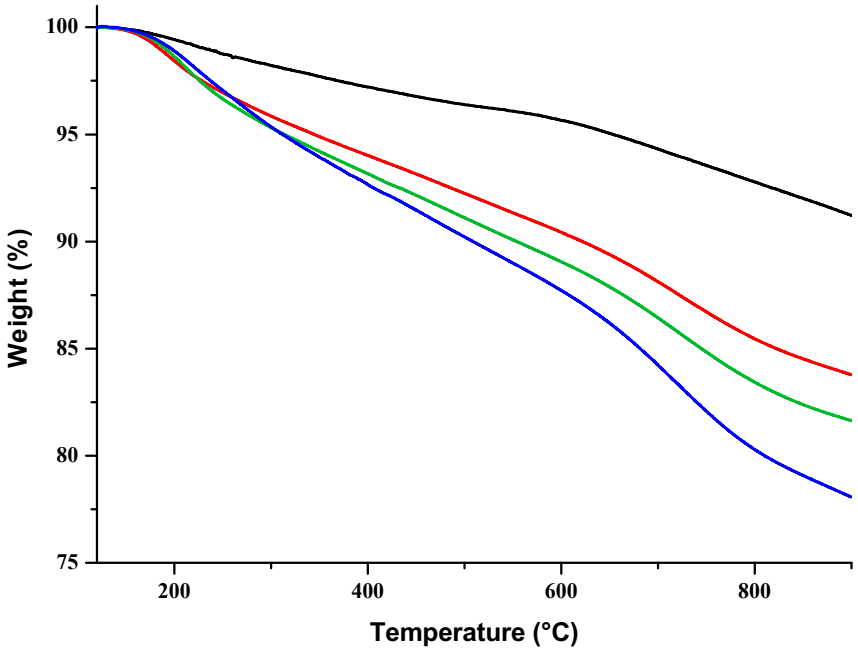


Figure 3.9: TGA results of AR-MWCNTs (black) and MWCNTs oxidised for 4 (red), 8 (green) and 16 hours (blue). All the samples were held at 120$^o$C for 30 minutes and then heated at a rate of 10$^o$C min$^{-1}$ to 900$^o$C.

The MWCNTs that had been oxidised for 4, 8 and 16 h displayed a weight loss of 5.0, 6.5 and 8.0 % respectively at 600 $^o$C when compared to the AR-MWCNTs. The successive increase in mass loss with increasing oxidation duration indicates that greater functionalisation is achieved with prolonged acid treatment.

### 3.2.2 TEM

TEM images of the acid treated MWCNTs after base washing are shown in Figure 3.10. These images show that tube-like structures remain, indicating that the oxidation/base washing procedure preserves the MWCNT structure.

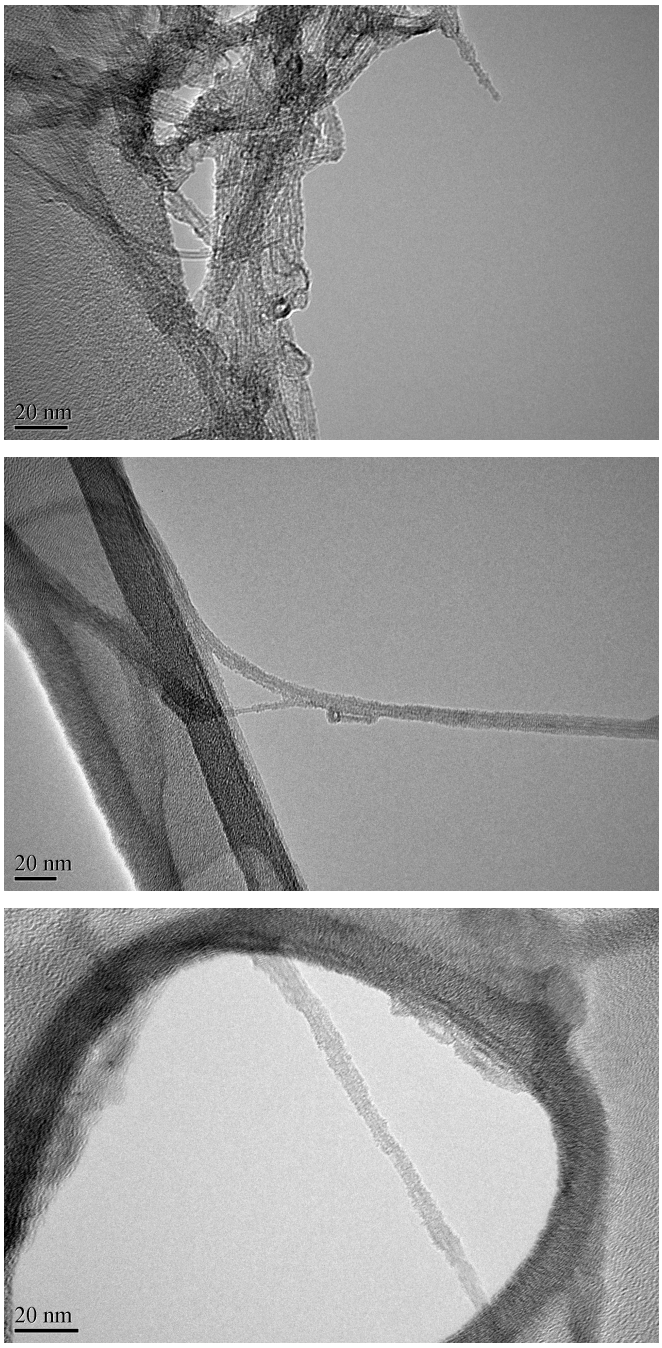


Figure 3.10: TEM images of MWCNTs that have been oxidised in 6 M $HNO_3$ for 4 (top), 8 (middle) and 16 (bottom) h and subsequently base washed.

### 3.2.3 UV-vis-NIR Spectroscopy

The oxidation of MWCNTs and so the introduction of carboxylic acid groups to the surface would be expected to increase their dispersibility in water. To establish the effect of reflux time on the dispersibility of the MWCNTs, the UV-vis-NIR spectra of the stable aqueous dispersions achieved before and after oxidation were recorded (Figure 3.11).

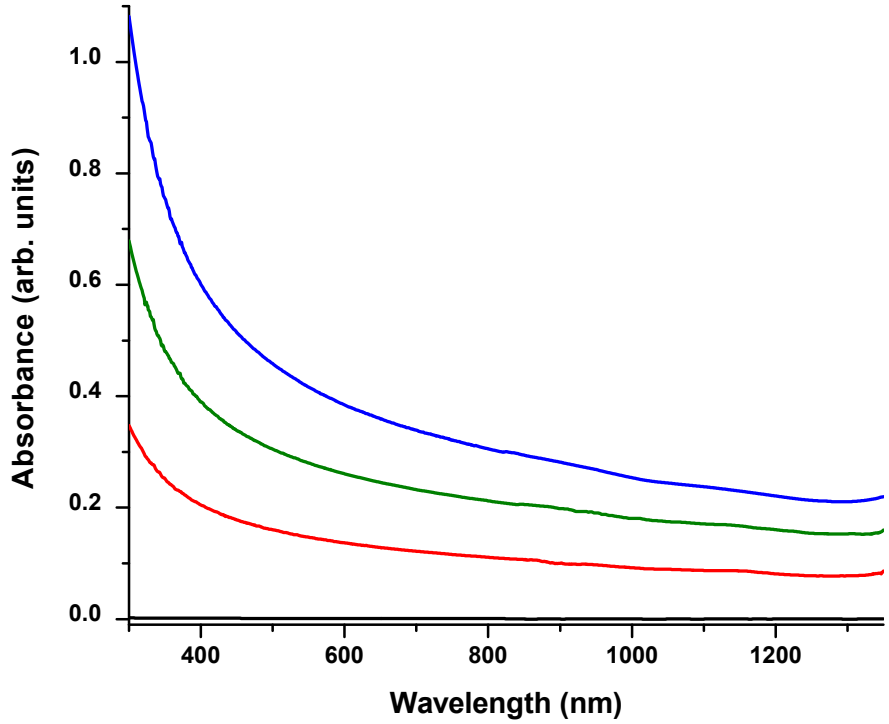


Figure 3.11: UV-vis-NIR spectra in aqueous solution of AR-MWCNTs (black) and MWCNTs oxidised in 6 M $HNO_3$ for 4 (red), 8 (green) and 16 h (blue) (diluted by a factor of 30).

As stated in Section 2.3 absorption spectroscopy has been used to determine the concentration of CNTs in a dispersion through the Beer Lambert law (Equation 2.1). The extinction coefficient is firstly determined from the absorption values at a chosen wavelength ($\lambda$) of dispersions of known CNT concentrations. In this work the wave-

length 700 nm was used, as this value of $\lambda$ has been used previously to calculate the extinction coefficient of CNTs.[51, 263] As the AR-MWCNTs are insoluble in water the molar extinction coefficient was calculated by plotting the absorbance values at $\lambda$=700 nm for ten different known concentrations of AR-MWCNTs in a 1% SDS aqueous solution to give a straight line graph as shown in Figure 3.12. The gradient from the graph, and therefore the extinction coefficient, is equal to 28.9 mL $mg^{-1}$ $cm^{-1}$ and this extinction coefficient was used throughout this thesis when determining the concentration of MWCNTs in solution.

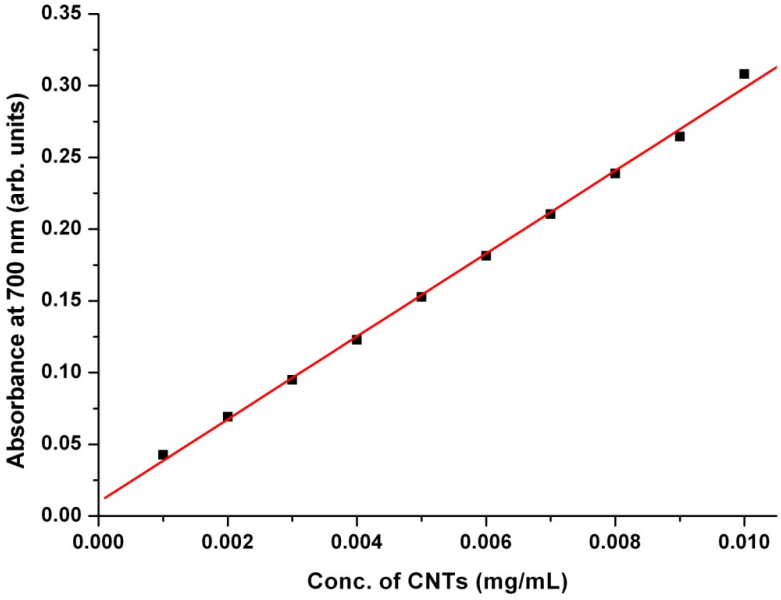


Figure 3.12: The recorded absorbance value at 700 nm versus MWCNT concentration in a 1% SDS aqueous solution.

The dispersibility of the oxidised MWCNTs was therefore calculated from their UV-vis NIR spectra (Figure 3.11) by using their respective absorbance values at $\lambda$=700 nm and the molar extinction coefficient of 28.9 mL $mg^{-1}$ $cm^{-1}$, and the results are given in Table 3.1. As expected, the AR material was completely insoluble, and the oxidation procedure resulted in a considerable improvement in MWCNT dispersibility. The MWCNTs that had undergone acid treatment for the greatest length of time (16 h) produced the most concentrated dispersion at 0.35 mg/mL, presumably due to the

greater number of functional groups present.

| Oxidation Duration (h) | MWCNT Concentration (mg/mL) |
|---|---|
| 0 | 0 |
| 4 | 0.11 |
| 8 | 0.23 |
| 16 | 0.35 |

Table 3.1: Concentration (mg/mL) of AR and oxidised MWCNTs in water.

The significant increase in dispersibility of the MWCNTs after oxidation is clearly demonstrated in Figure 3.13 and is indicative of the successful functionalisation of the MWCNTs.

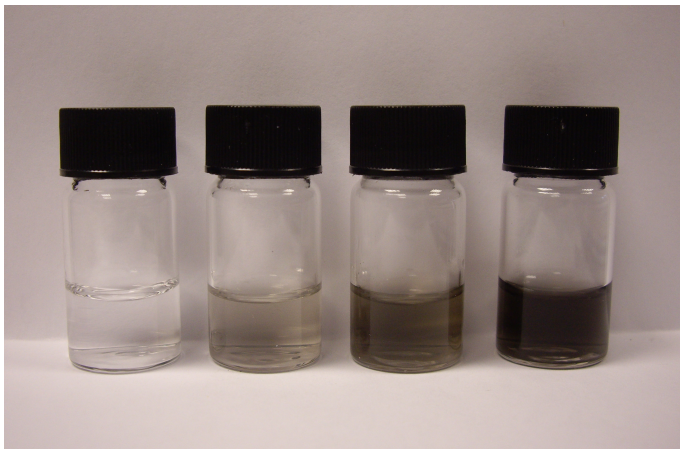

Figure 3.13: Photograph of the stable dispersions of AR-MWCNTs and MWCNTs oxidised in 6 M $HNO_3$ for 4, 8 and 16 h in water (diluted by a factor of 30) (l-r).

### 3.2.4 FTIR Spectroscopy

FTIR spectroscopy was employed to further characterise the nature of the functional groups attached to the oxidised MWCNTs. The FTIR spectra of the AR and oxidised MWCNTs are compared in Figure 3.14. The spectra of all the oxidised MWCNTs show the OH (3200-2800 $cm^{-1}$), C=O (1730 $cm^{-1}$) and C-O (1220 $cm^{-1}$) stretches and O-H (1390 $cm^{-1}$) bend that are characteristic of carboxylic acid groups. These peaks

are all absent in the spectrum of the AR-MWCNTs, which indicates that oxidation has introduced carboxylic acid groups to the MWCNTs.

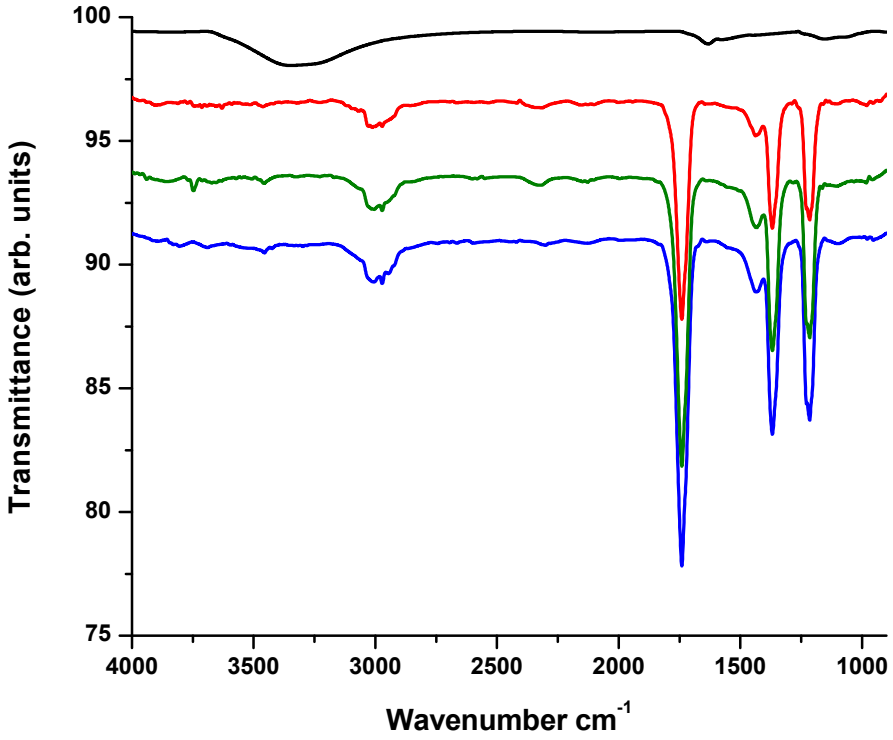


Figure 3.14: FTIR spectra of AR-MWCNTs (black) and MWCNTs oxidised in 6 M $HNO_3$ for 4 (red), 8 (green) and 16h (blue).

### 3.2.5 Raman Spectroscopy

Evidence for the successful covalent functionalisation of CNTs is provided by Raman spectroscopy. Raman spectra (excited at 532 nm) of the AR and oxidised MWCNTs, normalised to the G band at ca. 1600 $cm^{-1}$, are shown in Figure 3.15 for comparison.

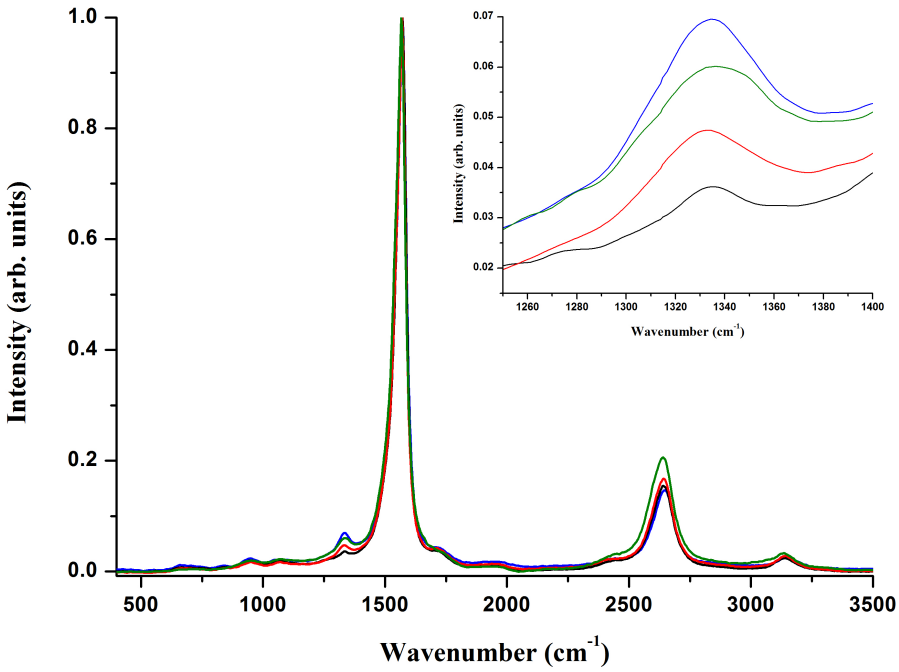


Figure 3.15: Raman spectra (532 nm, 2.33 eV) of AR-MWCNTs (black) and MWCNTs oxidised in 6 M $HNO_3$ for 4 (red), 8 (green) and 16 h (blue) normalised at the G band. Inset: the D band.

The calculated $I_D/I_G$ ratios for the AR and oxidised MWCNTs from the Raman spectra in Figure 3.15 are given in Table 3.2. As expected the oxidised MWCNTs display an increased $I_D/I_G$ when compared to the AR-MWCNTs, which suggests the covalent attachment of functional groups to the nanotube surface has occurred. The successive increase in $I_D/I_G$ with oxidation duration is consistent with prolonged acid treatment introducing a greater number of functional groups.

| Oxidation Duration (h) | $I_D/I_G$ Ratio |
|---|---|
| 0 | $0.036 \pm 2.1 \times 10^{-3}$ |
| 4 | $0.047 \pm 2.5 \times 10^{-3}$ |
| 8 | $0.060 \pm 2.9 \times 10^{-3}$ |
| 16 | $0.069 \pm 2.3 \times 10^{-3}$ |

Table 3.2: $I_D/I_G$ ratios of AR-MWCNTs and oxidised MWCNTs.

## 3.3 Interaction of Oxidised MWCNTs with Amino Acids

### 3.3.1 Basic Amino Acids: Arginine & Lysine

An aqueous solution of 0.5 M of the basic amino acids has a pH similar to their pI so their zwitterionic form dominates. It was expected that the negatively charged carboxylate anions on the oxidised MWCNT surface would interact with the positively charged side chain groups of the basic amino acids (Figure 3.16) and increase the dispersibility of the MWCNTs in water.

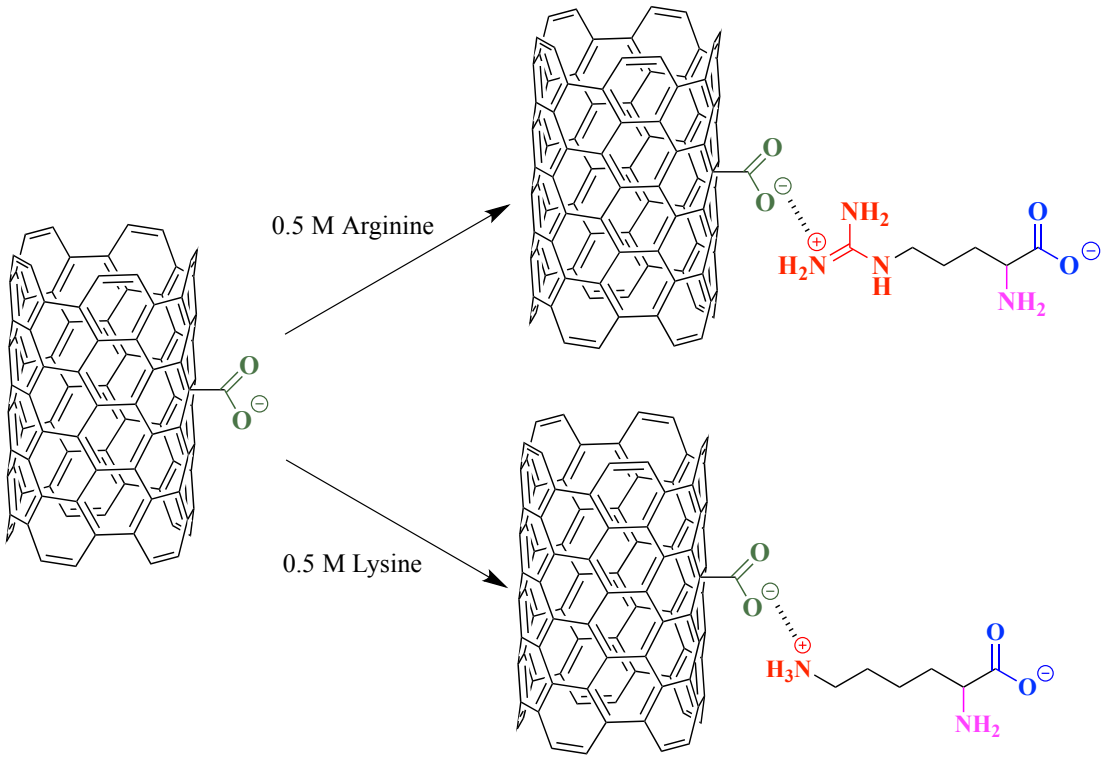


Figure 3.16: Schematic representation of the interaction of arginine and lysine with oxidised MWCNTs.

Ultrasonic sonication of the oxidised MWCNTs in 0.5 M solutions of the basic amino acids resulted in the formation of black dispersions. Dilution of these dispersions by a factor of 30 allows the difference in MWCNT dispersibility between them to be observed (Figure 3.17). The addition of acid to the dispersions was found to cause complete precipitation of the MWCNTs, suggesting that the dispersions are pH dependent (Figure Appendix A.1).

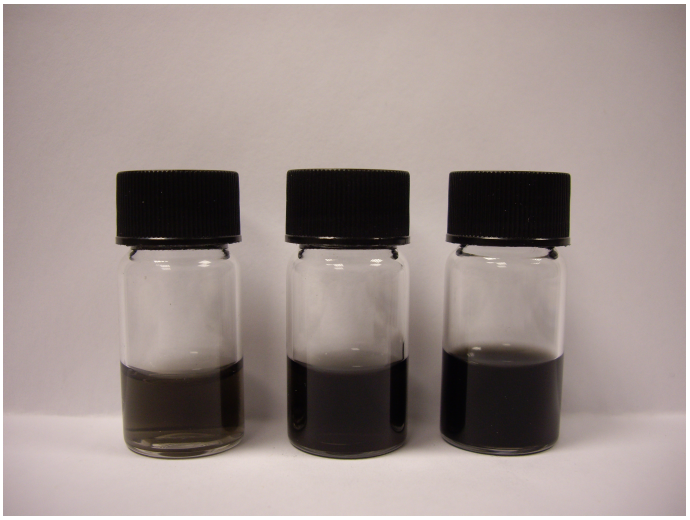

Figure 3.17: Photograph of the stable dispersions of 16 h oxidised MWCNTs in water, 0.5 M lysine and arginine solutions (diluted by a factor of 30) (l-r).

#### 3.3.1.1 UV-vis-NIR Spectroscopy

To determine the dispersibility of the oxidised MWCNTs in the basic amino acid solutions, the UV-vis-NIR spectra of the dispersions were recorded and are shown in Figure 3.18.

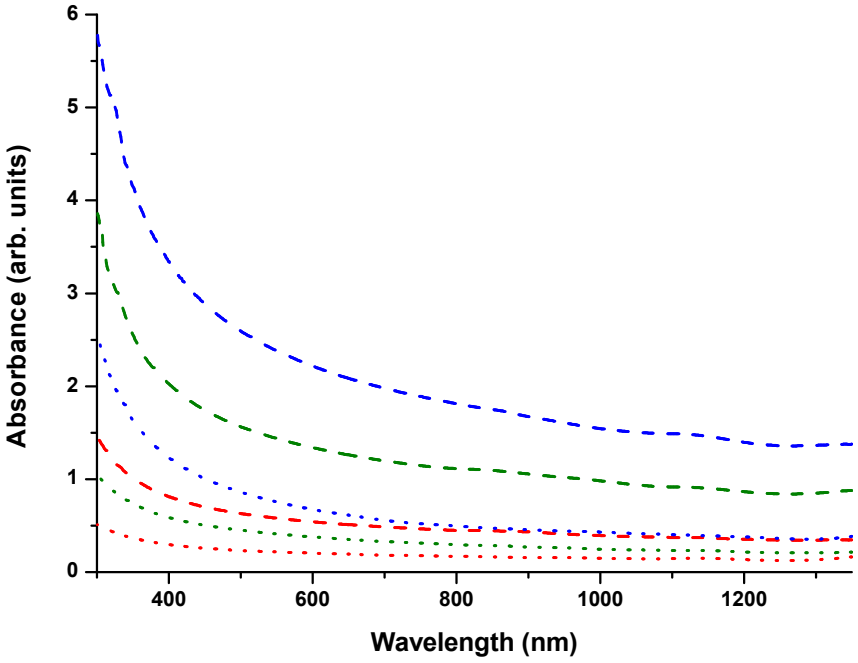


Figure 3.18: UV-vis-NIR spectra of MWCNTs oxidised in 6 M $HNO_3$ for 4 (red), 8 (green) and 16 h (blue) dispersed in 0.5 M arginine (dash) and 0.5 M lysine (dot) (all diluted by a factor of 30 except 16 h arginine diluted by a factor of 100).

The dispersibility of the MWCNTs in the basic amino acid solutions was determined from the absorbance values at 700 nm and by using the extinction coefficient of 28.9 mL $mg^{-1}$ $cm^{-1}$, as outlined in Section 3.2.3, and the results are given in Table 3.3 with those for water for comparison.

| Oxidation Duration (h) | Conc. in Water (mg/mL) | Conc. in 0.5 M Arginine (mg/mL) | Conc. in 0.5 M Lysine (mg/mL) |
|---|---|---|---|
| 0 | 0 | 0 | 0 |
| 4 | 0.11 | 1.01 | 0.38 |
| 8 | 0.23 | 2.48 | 0.69 |
| 16 | 0.35 | 6.79 | 1.15 |

Table 3.3: Concentration (mg/mL) of AR and oxidised MWCNTs in water and 0.5 M arginine and lysine solutions.

### 3.3.2 Neutral Amino Acids: Glycine & Taurine

In aqueous solution the zwitterionic form of the neutral amino acids dominates and it was again expected that the negatively charged carboxylate anions on the oxidised MWCNT surface would interact with the positively charged amine groups of the neutral amino acids to increase the dispersibility of the MWCNTs in water (Figure 3.19).

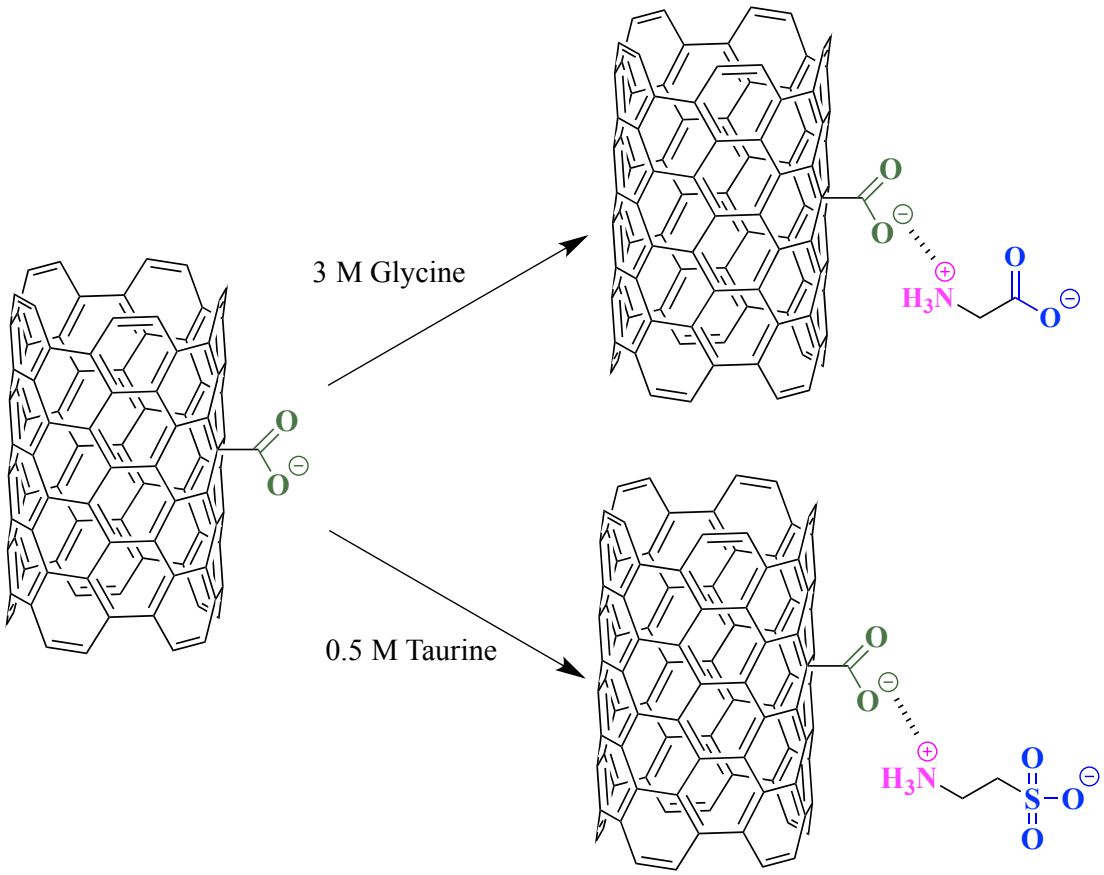


Figure 3.19: Schematic representation of the interaction of glycine and taurine with oxidised MWCNTs.

The UV-vis-NIR spectra (Figure 3.20) of the dispersions were used to determine the concentration of MWCNTs as in Section 3.2.3. The addition of the neutral amino acids improved the dispersibility of the oxidised MWCNTs, with taurine proving more effective than glycine (Table 3.4). The neutral amino acids however were found to be less effective than the basic amino acids at increasing MWCNT dispersibility (Table 3.3). The dispersions were again observed to be pH sensitive as acidification resulted in the precipitation of the MWCNTs.

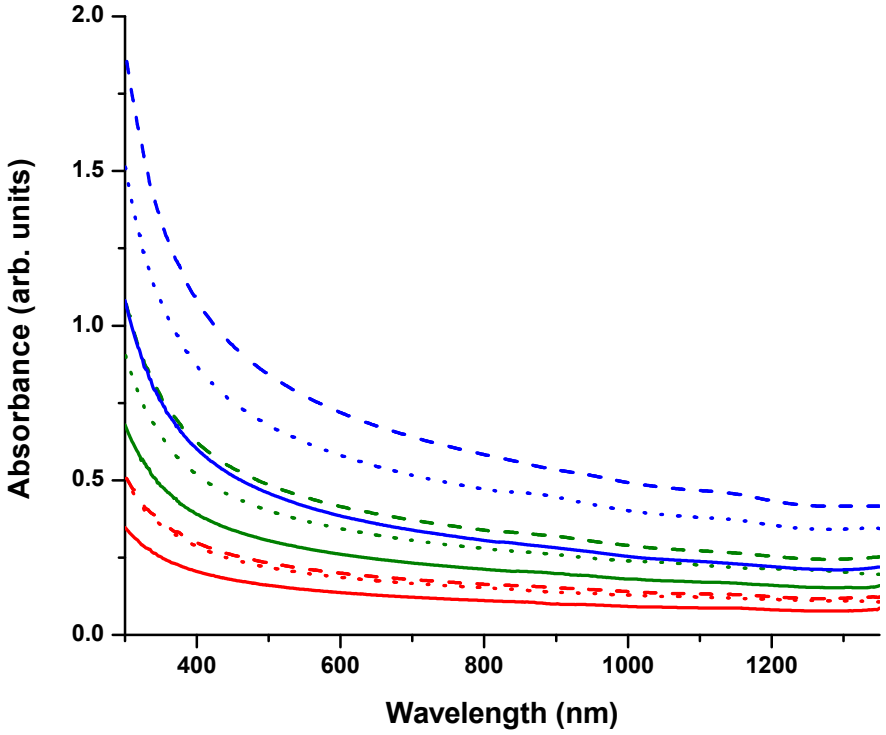


Figure 3.20: UV-vis-NIR spectra of MWCNTs oxidised in 6 M $HNO_3$ for 4 (red), 8 (green) and 16 h (blue) dispersed in water (solid), 3 M glycine (dot) and 0.5 M taurine (dash) (diluted by a factor of 30).

| Oxidation Duration (h) | Conc. in Water (mg/mL) | Conc. in 3 M Glycine (mg/mL) | Conc. in 0.5 M Taurine (mg/mL) |
|---|---|---|---|
| 0 | 0 | 0 | 0 |
| 4 | 0.11 | 0.17 | 0.19 |
| 8 | 0.23 | 0.32 | 0.39 |
| 16 | 0.35 | 0.54 | 0.66 |

Table 3.4: Concentration (mg/mL) of oxidised MWCNTs in water, 3 M glycine and 0.5 M taurine solutions.

### 3.3.3 Acidic Amino Acid: Glutamic Acid

The zwitterionic form of glutamic acid dominates in aqueous solution and so its ability to interact with the negatively charged carboxylate anions on the oxidised MWCNT surface and improve MWCNT dispersibility was investigated (Figure 3.21).

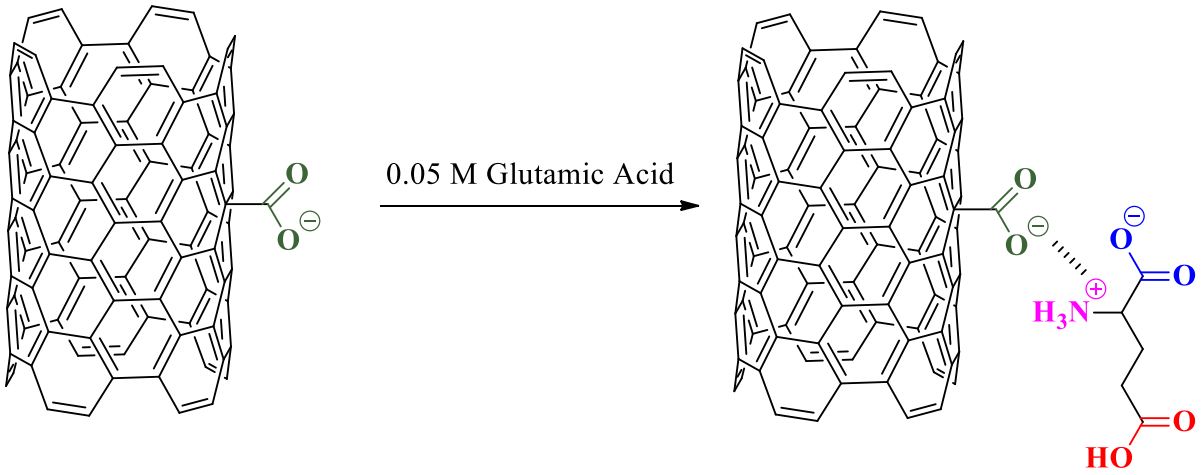


Figure 3.21: Schematic representation of the interaction of glutamic acid with oxidised MWCNTs.

The UV-vis-NIR spectra (Figure 3.22) of the dispersions of the oxidised MWCNTs in glutamic acid showed that the addition of the acidic amino acid resulted in the MWCNTs becoming completely insoluble. This result is presumably due to the acidic nature of the solution which has previously been reported to result in aggregation of oxidised MWCNTs,[295] as protonation occurs at acidic pH, which leads to aggregation due to van der Waals forces.[115]

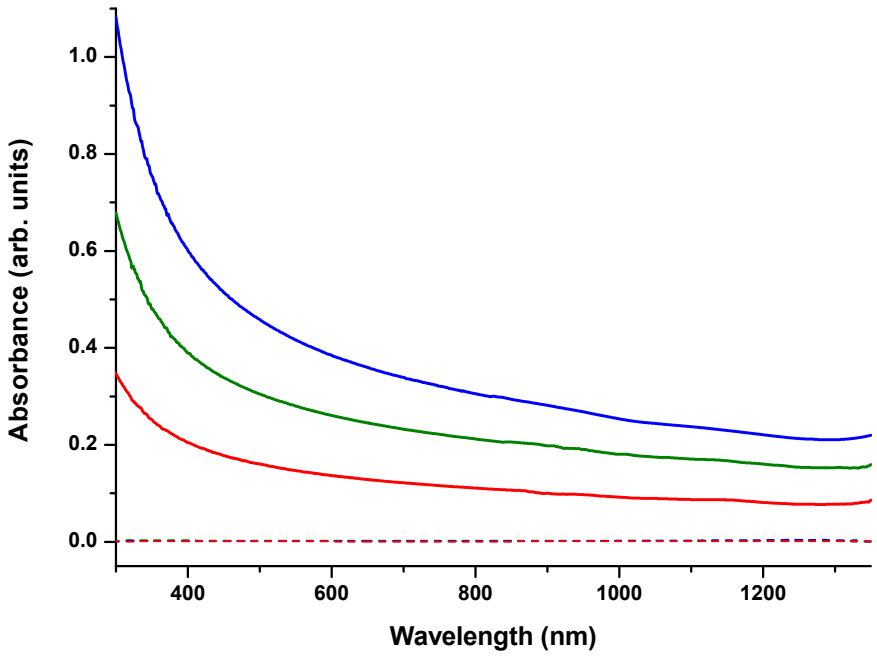


Figure 3.22: UV-vis-NIR spectra of MWCNTs oxidised in 6 M $HNO_3$ for 4 (red), 8 (green) and 16 h (blue) dispersed in water (solid) and in 0.05 M glutamic acid (dash) (diluted by a factor of 30).

## 3.4 Interaction of AR-MWCNTs with Amino Acids

In order to demonstrate the need for the presence of functional groups on the MWCNT surface to interact with the amino acids for the purpose of improving MWCNT dispersibility, a control experiment was performed by dispersing the AR-MWCNTs in solutions of the basic, neutral and acidic amino acids. The resulting dispersions were characterised by UV-vis-NIR spectroscopy (Appendix Figure A.2) which shows that the presence of the amino acids alone does not effect the dispersibility of the MWCNTs when compared to water, as can be clearly seen in Appendix Figure A.3.

## 3.5 Benzoic Acid Functionalised MWCNTs

The covalent modification of MWCNTs using diazonium chemistry has been achieved through many different methods, as discussed in Section 1.7.1. Benzoic acid functional groups were attached to the nanotube surface in this case through reaction of the MWCNTs with a benzoic diazonium salt, which was generated by the addition of isoamyl nitrite to 4-aminobenzoic acid (Figure 3.23).

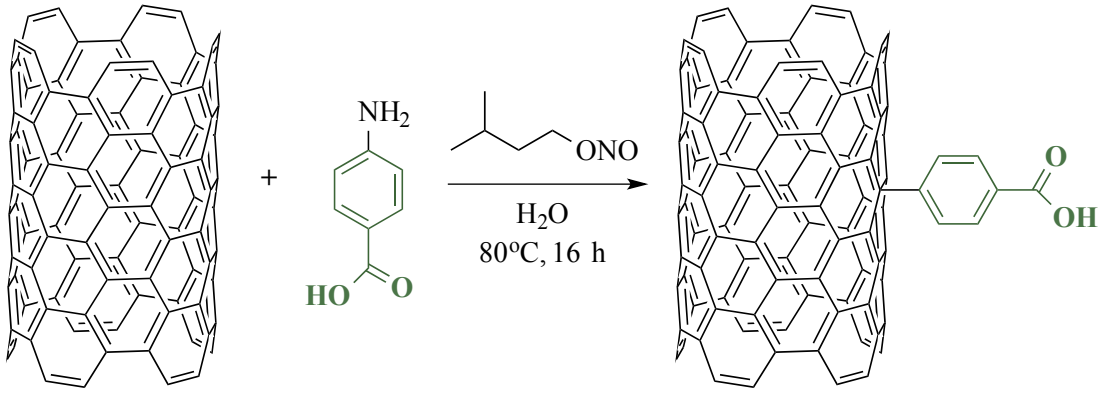


Figure 3.23: Schematic representation of the functionalisation of MWCNTs with benzoic acid.

### 3.5.1 Thermal Analysis

The TGA data of the benzoic acid functionalised MWCNTs (MWCNT-BA) shows an additional weight loss of 14 % at 600 $^{o}$C when compared to the AR-MWCNTs (Figure 3.24), which indicates that functionalisation of the MWCNTs has occurred.

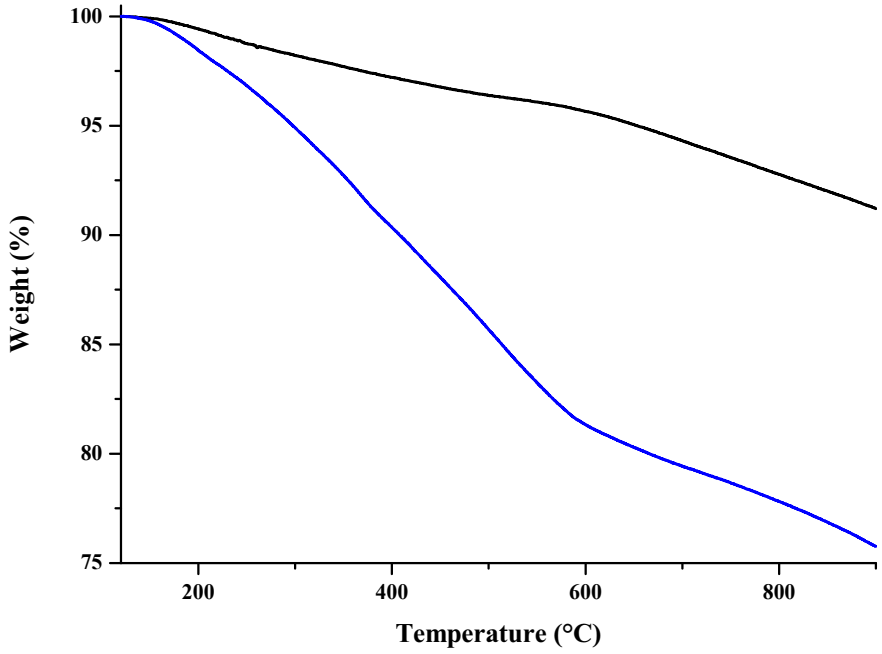


Figure 3.24: TGA results of AR-MWCNTs (black) and benzoic acid functionalised MWCNTs (blue). All the samples were held at 120$^o$C for 30 minutes and then heated at a rate of 10$^o$C min$^{-1}$ to 900$^o$C.

### 3.5.2 UV-vis-NIR Spectroscopy

The functionalisation of MWCNTs with carboxylic acid containing benzoic acid functional groups was expected to facilitate the aqueous dispersion of the MWCNTs. From the UV-vis-NIR spectra (Figure 3.25) and by using the method outlined in Section 3.2.3 it was determined that benzoic acid functionalisation improves MWCNT dispersibility from 0 to 0.13 mg/mL.

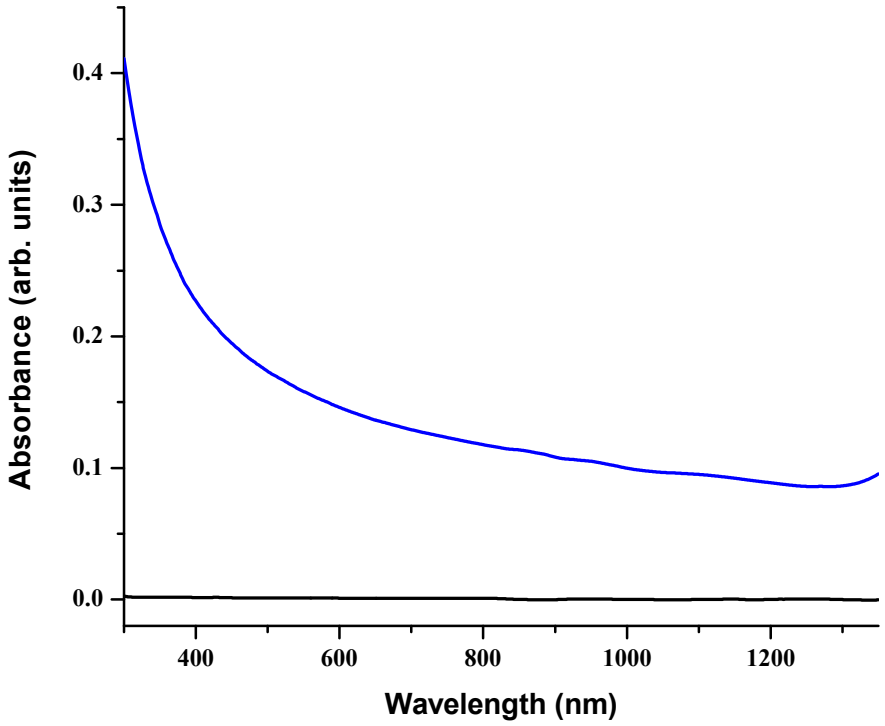


Figure 3.25: UV-vis-NIR spectra of AR-MWCNTs (black) and benzoic acid functionalised MWCNTs in water (blue) (diluted by a factor of 30).

This clear difference in dispersibility, as Figure 3.26 shows, provides further evidence that the functionalisation of the MWCNTs has occurred.

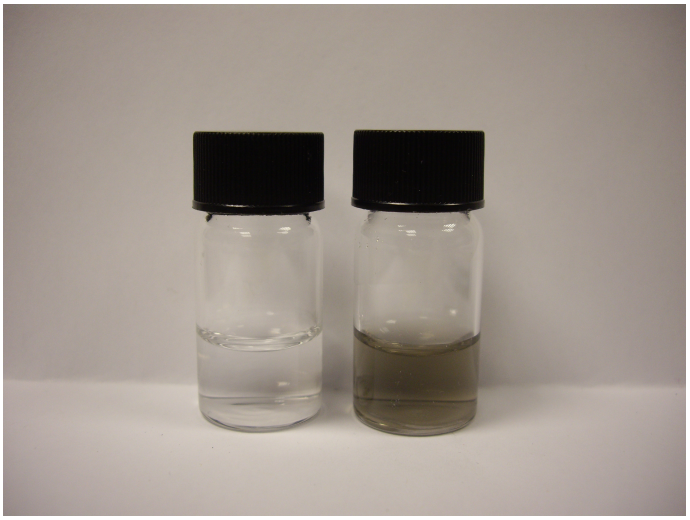

Figure 3.26: Photograph of the stable dispersions of AR-MWCNTs and benzoic acid functionalised MWCNTs in water (l-r) (diluted by a factor of 30).

### 3.5.3 FTIR Spectroscopy

The FTIR spectra of the MWCNTs before and after functionalisation with benzoic acid are shown overlaid in Figure 3.27. The peaks observed at 3200-2800, 1730 and 1220 $cm^{-1}$ after functionalisation are assigned to the OH, C=O and C-O stretches, respectively, of carboxylic acid groups.

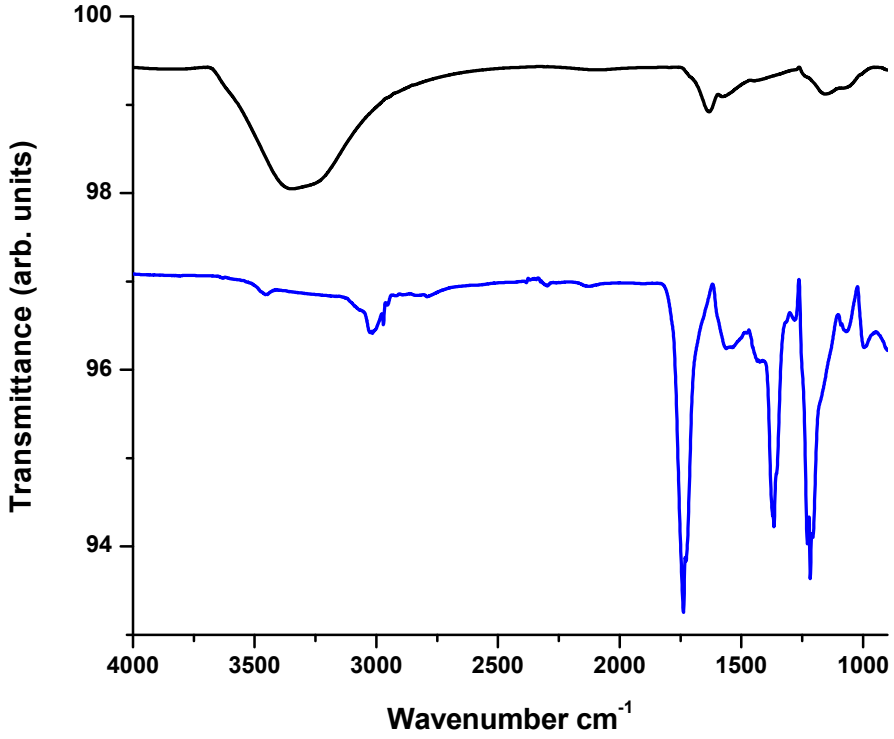


Figure 3.27: FTIR spectra of AR-MWCNTs (black) and benzoic acid functionalised MWCNTs (blue).

### 3.5.4 Raman Spectroscopy

The functionalised MWCNTs show an enhancement in the intensity of the D band at ca. 1350 $cm^{-1}$, as expected, when compared to the spectrum for the AR-MWCNTs (Figure 3.28). MWCNT-BA has a calculated $I_D/I_G$ ratio of 0.050 $\pm$ 3.0 x $10^{-3}$ in comparison to 0.036 $\pm$ 2.1 x $10^{-3}$ for the AR sample, which indicates that the introduction of functional groups to the nanotube surface has occurred.

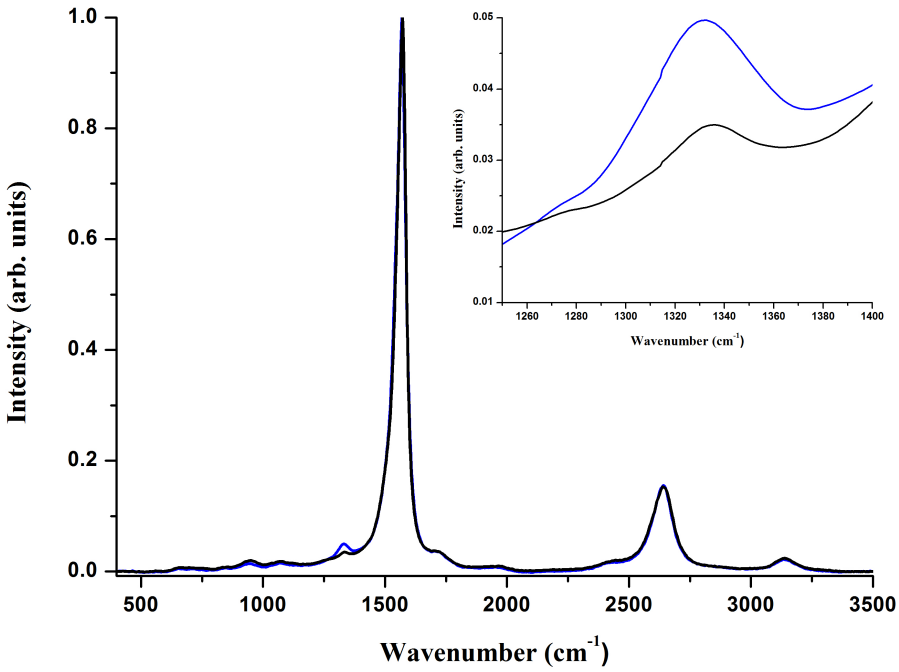


Figure 3.28: Raman spectra (532 nm, 2.33 eV) of AR-MWCNTs (black) and benzoic acid functionalised MWCNTs (blue) normalised at the G band. Inset: the D band.

## 3.6 Interaction of Benzoic Acid Functionalised MWCNTs with Amino Acids

The presence of carboxylic acid groups meant that MWCNT-BA was predicted to interact with the amino acids in an analogous manner to the oxidised MWCNTs. Consequently, it was also expected that the amino acids would effect MWCNT-BA dispersibility in the same way as was observed for oxidised MWCNTs. Figure 3.29 displays the UV-vis-NIR spectra recorded for the dispersions of MWCNT-BA in the amino acid solutions.

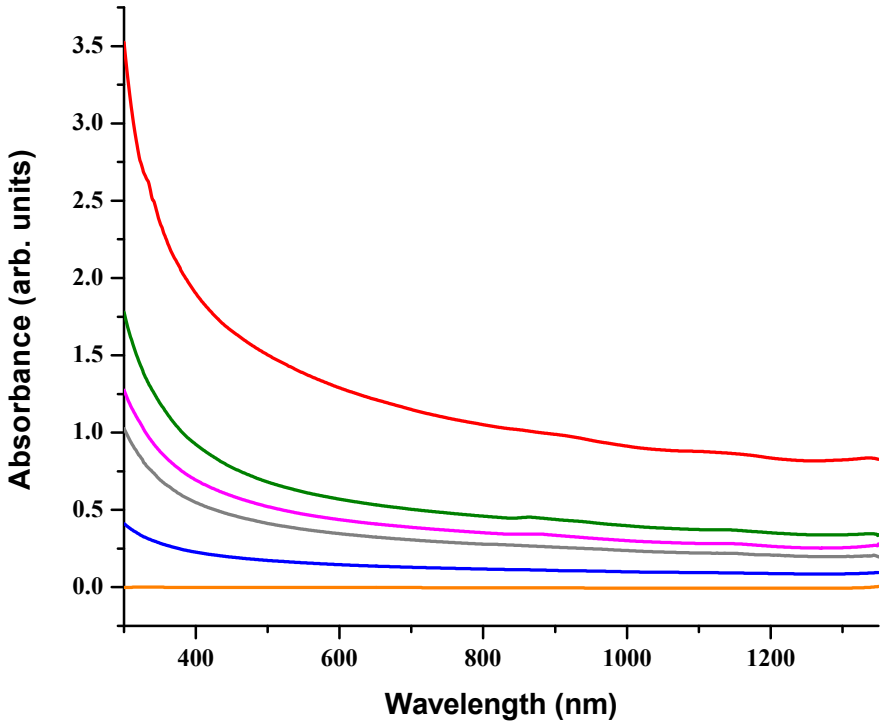


Figure 3.29: UV-vis-NIR spectra of benzoic acid functionalised MWCNTs in water (blue), 0.5 M arginine (red), lysine (green), taurine (magenta), 3 M glycine (grey) and 0.05 M glutamic acid (orange) (diluted by a factor of 30).

The dispersibility of MWCNT-BA in the different amino acid solutions was determined from the UV-vis-NIR spectra, as discussed in Section 3.2.3, and the results are shown in Table 3.5. The dispersibility of MWCNT-BA in the amino acid solutions followed the same trend as that observed for the oxidised MWCNTs, with arginine providing the greatest improvement, while glutamic acid rendered the MWCNTs insoluble. The dispersions using the neutral and basic amino acids were also shown to be pH dependent with the addition of acid leading to complete precipitation of the benzoic acid functionalised MWCNTs, as was found in Sections 3.3.1 and 3.3.2 for the dispersions of the oxidised MWCNTs.

| Amino Acid Solution | Arginine | Lysine | Taurine | Glycine | Glutamic Acid |
|---|---|---|---|---|---|
| Conc. (mg/mL) | 1.2 | 0.52 | 0.40 | 0.32 | 0 |

Table 3.5: Concentration (mg/mL) of benzoic acid functionalised MWCNTs in 0.5 M arginine, lysine and taurine, 3 M glycine and 0.05 M glutamic acid solutions.

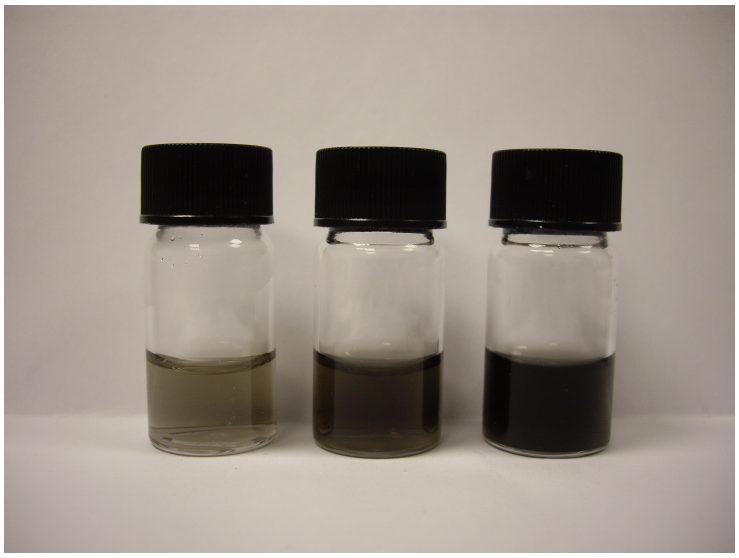

Figure 3.30: Photograph of the stable dispersions of benzoic acid functionalised MWCNTs in water and 0.5 M lysine and arginine solutions (l-r) (diluted by a factor of 30).

## 3.7 *N,N*-Dimethylethylenediaminium Functionalised MWCNTs

Direct coupling of *N,N*-dimethylethylenediamine (DMEN) with the carboxylic acid groups of oxidised MWCNTs through amide bond formation was achieved using 1-[Bis(dimethylamino)methylene]-1H-1,2,3-triazolo[4,5-b]pyridinium 3-oxid hexafluorophosphate (HATU) and *N,N*-diisopropylethylamine (DIPEA) to give MWCNTs functionalised with amine groups. The tertiary amine of the functionalised MWCNTs was then quaternerised using methyl iodide to give MWCNTs functionalised with positively charged functional groups (MWCNT-DMEN$^+$) (Figure 3.31).

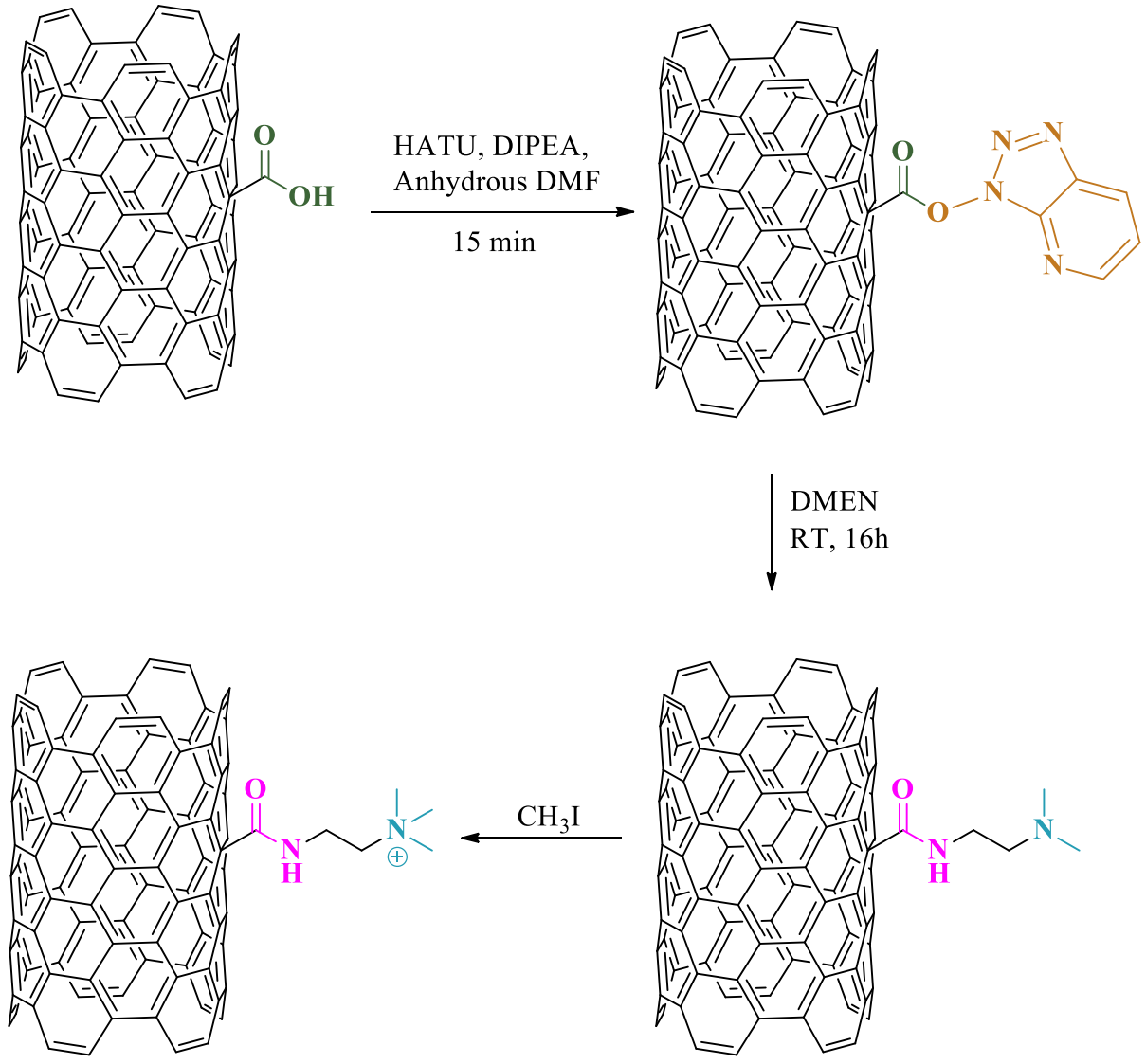


Figure 3.31: Schematic representation of the amidation of oxidised MWCNTs with DMEN and the subsequent quaternisation of the tertiary amine.

### 3.7.1 Thermal Analysis

MWCNT-DMEN$^+$ displays an additional weight loss of 19 % at 600 $^o$C when compared to the starting oxidised material (Figure 3.32), suggesting that further functionalisation of the oxidised MWCNTs has been successful.

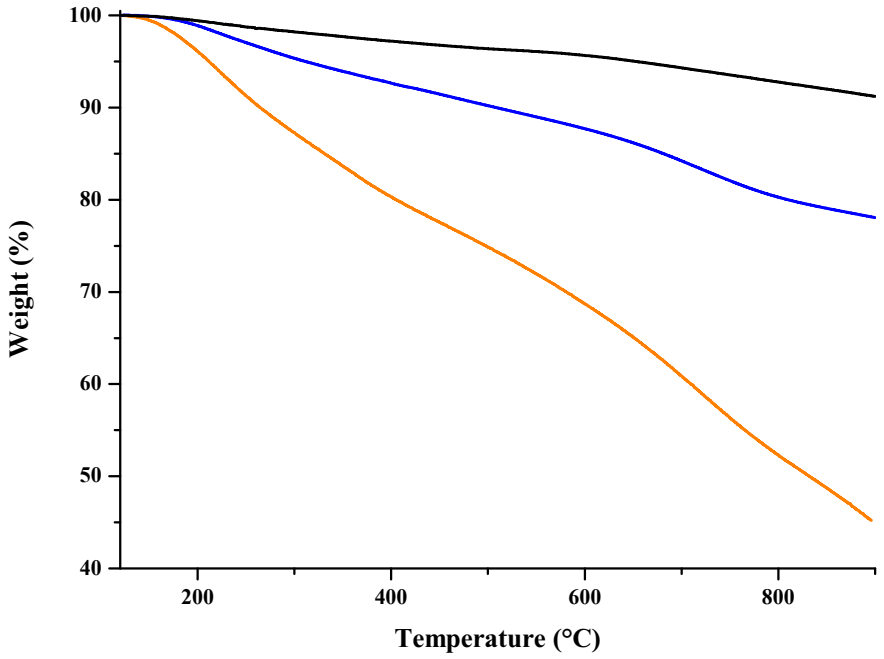


Figure 3.32: TGA results of AR (black), oxidised (blue) and DMEN$^+$ functionalised (orange) MWCNTs. All the samples were held at 120$^o$C for 30 minutes and then heated at a rate of 10$^o$C min$^{-1}$ to 900$^o$C.

### 3.7.2 UV-vis-NIR Spectroscopy

The concentration of the these functionalised MWCNTs in aqueous solution was calculated from Figure 3.33, using the method as outlined in Section 3.2.3. The oxidised MWCNTs used for coupling with DMEN could disperse at a concentration of 0.35 mg/mL, but after functionalisation with DMEN the dispersibility of the MWCNTs decreased to 0.15 mg/mL. The dispersion of MWCNT-DMEN was however observed to be unstable and after two days the majority of the MWCNTs had precipitated out of solution to give a dispersion with a concentration of 5.7x10$^{-3}$ mg/mL. Quaternisation of the tertiary amine with methyl iodide to give MWCNT-DMEN$^+$ resulted in aqueous dispersions of negligible MWCNT concentration.

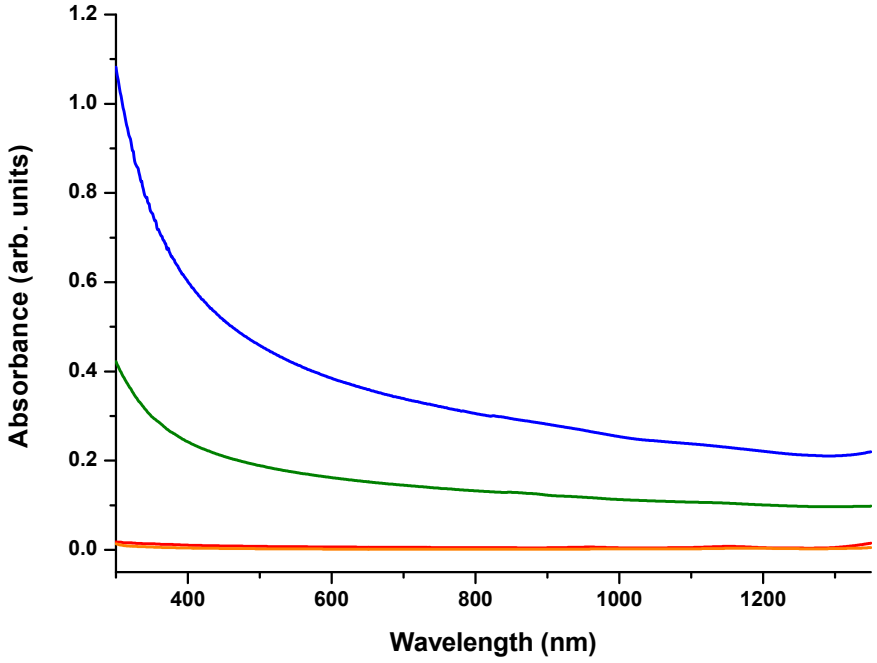


Figure 3.33: UV-vis-NIR spectra of oxidised (blue), DMEN after 1 day (green) and 2 days (red) and $DMEN^+$ (orange) functionalised MWCNTs in water (diluted by a factor of 30).

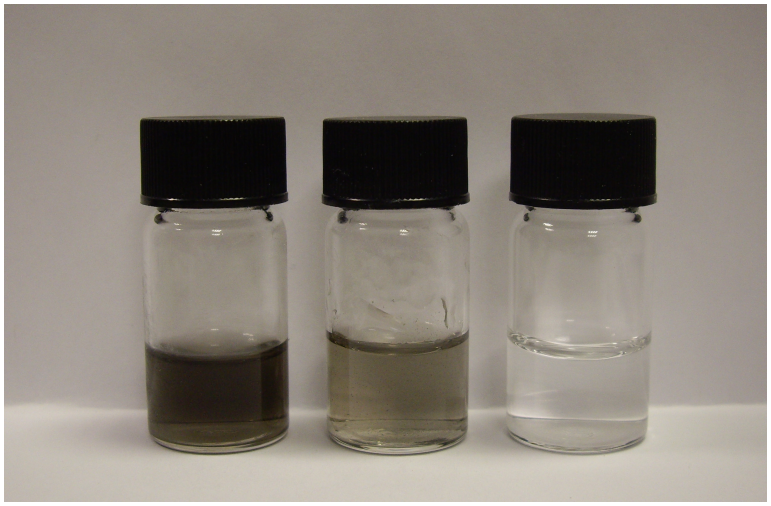

Figure 3.34: Photograph of oxidised, DMEN after one day and $DMEN^+$ functionalised MWCNTs in water (l-r).

### 3.7.3 FTIR Spectroscopy

The FTIR spectra of the oxidised and $DMEN^+$ functionalised MWCNTs are given in Figure 3.35. The peak observed at 1730 $cm^{-1}$ in the spectrum of the oxidised MWCNTs is attributed to the C=O stretch of the carboxylic acid group. In the spectrum of the amide functionalised MWCNTs the peak at 1730 $cm^{-1}$ is absent however the appearance of a peak with lower frequency (1660 $cm^{-1}$) assigned to the amide carbonyl (C=O) stretch is visible. Additionally, the apperance of peaks at 1573 and 1223 $cm^{-1}$, corresponding to N-H in-plane and C-N bond stretching, respectively, further indicates the presence of the amide functional group.

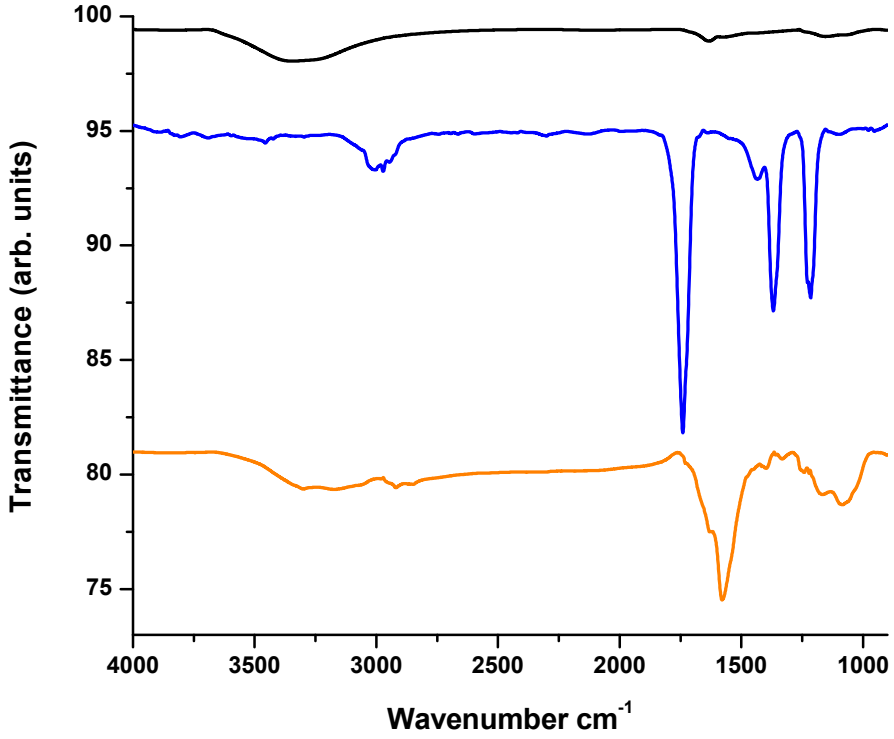


Figure 3.35: FTIR spectra of AR (black), oxidised (blue) and $DMEN^+$ functionalised MWCNTs (orange).

### 3.7.4 Raman Spectroscopy

The Raman spectra of MWCNT-$DMEN^+$ shows no significant change in the intensity of the D band when compared to the spectrum for the oxidised MWCNTs (Figure 3.36). As the D band represents the conversion of MWCNT carbon atoms from a $sp^2$ to a $sp^3$ hybridisation state this result is expected because the reaction is taking place on the carboxylic acid groups. The spectra therefore give comparable $I_D/I_G$ ratios of 0.069 $\pm$ 2.3 x $10^{-3}$ and 0.066 $\pm$ 2.7 x $10^{-3}$ for oxidised MWCNTs and MWCNT-$DMEN^+$ respectively.

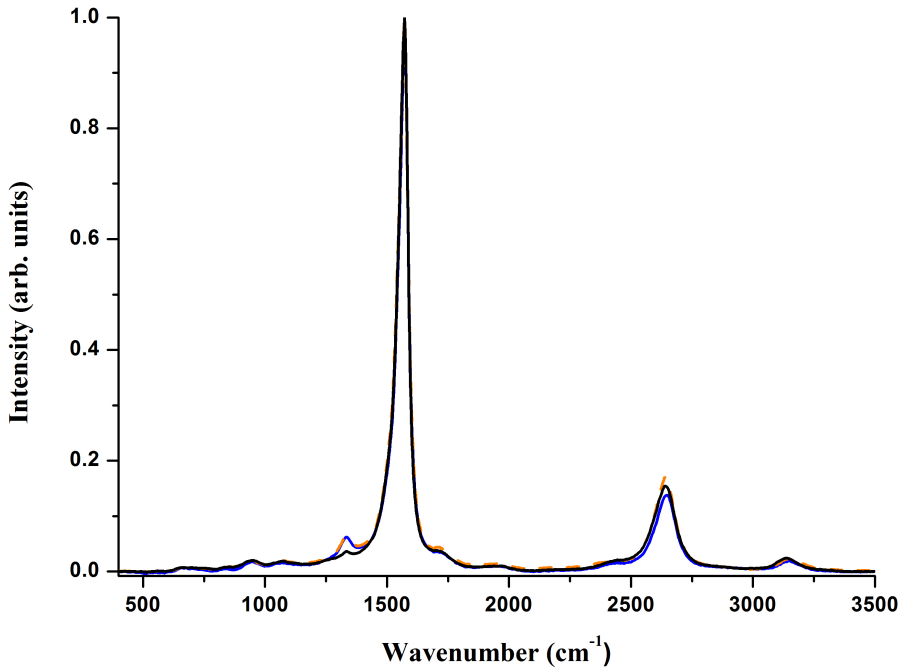


Figure 3.36: Raman spectra (532 nm, 2.33 eV) of AR (black), oxidised (blue) and $DMEN^+$ (orange) functionalised MWCNTs normalised at the G band.

## 3.8 Interaction of Amino Acids with N,N-Dimethylethylenediaminium Functionalised MWCNTs

The positively charged $DMEN^+$ groups on the MWCNTs were expected to interact with the negatively charged groups of the basic, acidic and neutral amino acids that were investigated previously to improve MWCNT dispersibility as shown in Figure 3.37.

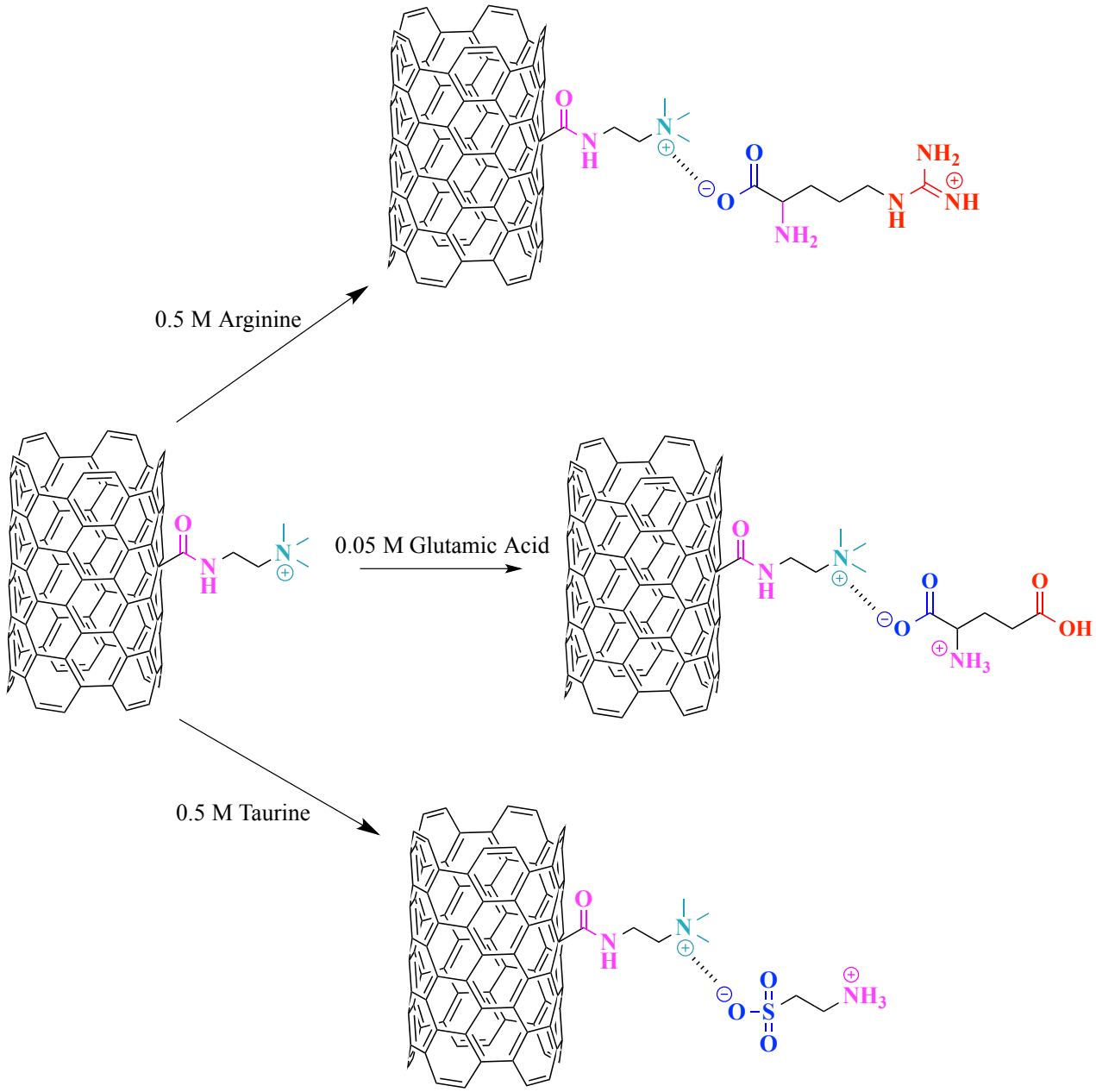


Figure 3.37: Schematic representation of the interaction of basic arginine, acidic glutamic acid and neutral taurine amino acids with MWCNT-DMEN$^+$.

The UV-vis-NIR spectra for the dispersions of MWCNT-DMEN$^+$ in the selected amino acid solutions are given in Figure 3.38. From Figure 3.38 it can be seen that the amino acids did not have any significant effect on the dispersibility of MWCNT-

$DMEN^+$ which remained negligible.

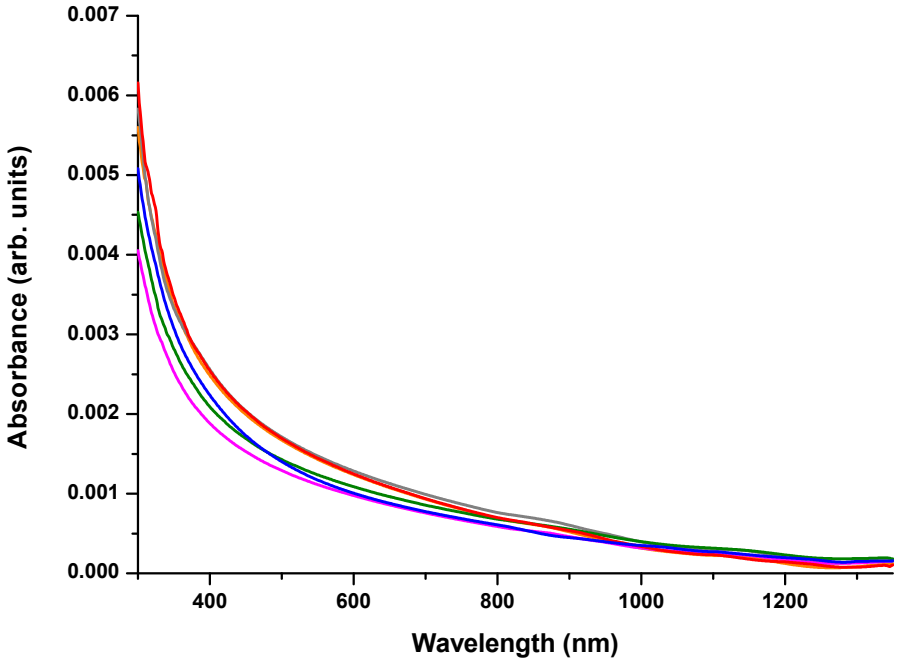


Figure 3.38: UV-vis-NIR spectra of $DMEN^+$ functionalised MWCNTs in water (blue), 0.5 M arginine (red), lysine (green), taurine (magenta), 3 M glycine (grey) and 0.05 M glutamic acid (orange).

## 3.9 MWCNT Thin Films

The observed ability of arginine to create highly exfoliated and stable dispersions of oxidised MWCNTs was investigated for use in the preparation of MWCNT thin films. The thin films were fabricated using the vacuum filtration method, as described in Section 1.9.1. Dispersions of oxidised MWCNTs in water and 0.5 M arginine solution at a concentration of 1 and 2 mg/L with an overall volume of 50 mL were used to give films of 191 and 382 nm thickness, respectively. The conductivity of the thin films is attributed to the formation of a continuous CNT network, and so it was speculated that the sheet resistance of the films fabricated from MWCNTs dispersed in arginine would be less than that measured for water due to a better dispersion of the MWCNTs.

Electrical measurements as outlined in Section 6.2.6 were performed on the thin films produced and the results are given in Table 3.6.

| | Sheet Resistance (Ω/sq) | |
|---|---|---|
| Film Thickness (nm) | Water | Arginine |
| 191 | $(2.1 \pm 0.1) \times 10^3$ | $(2.6 \pm 0.03) \times 10^3$ |
| 382 | $(4.8 \pm 0.2) \times 10^2$ | $(5.4 \pm 0.4) \times 10^2$ |

Table 3.6: Electrical measurements of thin films that have been produced by vacuum filtration of dispersions of oxidised MWCNTs in water and 0.5 M arginine.

From Table 3.6 it can be seen that doubling the concentration of the MWCNTs used decreases the sheet resistance of the films by an order of magnitude in both cases. The use of arginine in the preparation of the MWCNT dispersions however was not observed to result in a decrease of the sheet resistance of the films produced, when compared to water.

## 3.10 Conclusion

Water dispersible CNTs have been obtained previously by the covalent attachment of the amino acids taurine and lysine to carboxylic acid functionalised CNTs.[141, 143] In this chapter, however, the ionic interaction of the amino acids arginine, lysine, glycine, taurine and glutamic acid with MWCNTs functionalised with negatively and positively charged functional groups was investigated in an attempt to increase MWCNT aqueous dispersibility. Oxidative treatment of MWCNTs with 6 M nitric acid was shown to be a mild, yet effective method for introducing carboxylic acid groups to the surface, while a diazonium reaction was successful in functionalising MWCNTs with carboxylic acid containing benzoic acid groups. N,N-dimethylethylenediaminium functionalised MWCNTs were produced by the reaction of *N,N*-dimethylethylenediamine with oxidised MWCNTs and subsequent quarternisation of the amine group using methyl iodide. These MWCNT functional groups were suitably charged in aqueous solution to investigate their ionic interaction with the selected acidic, basic and neutral amino acids. The inability of the amino acids to disperse AR-MWCNTs indicates

that successful dispersion of the MWCNTs with amino acids is dependent on an ionic interaction between the amino acid and the functional groups on the nanotube surface.

The degree to which the amino acids improved functionalised MWCNT dispersibility varied with the number of functional groups present on the MWCNT surface; a greater number of functional groups resulted in more interactions and so a dispersion with a higher MWCNT concentration. Additionally, each amino acid was shown to have a distinct capacity for improving MWCNT dispersibility, as variations in dispersion concentration were found for MWCNTs that were functionalised to the same extent. As the amino acids have the same general structure, this demonstrates the importance of the side chain group in increasing the dispersibility of the functionalised MWCNTs in the case of the basic amino acids and the superiority of the sulfonic acid group over carboxylic acid for the neutral amino acids. Furthermore, it was found that acidification of the basic and neutral amino acid assisted dispersions resulted in the precipitation of the MWCNTs, providing a simple method for removal of the MWCNTs from solution.

Of the amino acids considered in this study arginine was found to provide the greatest improvement in aqueous dispersibility for MWCNTs functionalised with carboxylic acid groups, as shown in Figure 3.39, while no significant change in dispersibility was observed for MWCNT-DMEN$^+$ with any of the amino acids. As a result of the observed exceptional ability of arginine to disperse MWCNTs, it was investigated for use in the preparation of MWCNT dispersions for the fabrication of thin films. Thin films of oxidised CNTs have been made previously, and it was shown that as the level of CNT oxidation increased the electrical conductivity of the films decreased, due to the resulting increase in structural defects.[230, 296] The thin films made in this chapter were prepared using the vacuum filtration method from dispersions of the same concentration of oxidised MWCNTs in both water and 0.5 M arginine solution. It was found that doubling the concentration of MWCNTs decreased the sheet resistance by an order of magnitude in both cases, but the films made from the arginine dispersions did not show a significant decrease in sheet resistance when compared to those made using water.

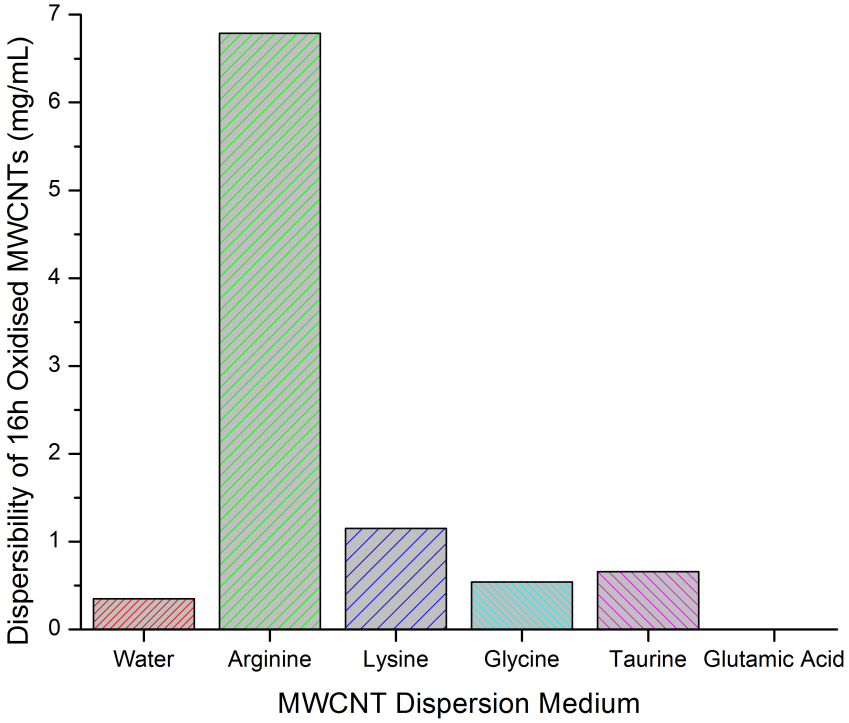


Figure 3.39: The recorded dispersibility (mg/mL) of 16h oxidsed MWCNTs in water and amino acid solutions.

# Chapter 4

# The Covalent Attachment of Amino Acids to MWCNTs

## 4.1 Introduction

This chapter concerns the covalent functionalisation of MWCNTs with the amino acids that were found to improve MWCNT dispersibility through ionic interactions in Chapter 3. The formation of an amide bond between the amine group of the amino acids and the carboxylic acid groups of oxidised MWCNTs was investigated first in order to assess the consequences of the covalent attachment of the amino acids on MWCNT dispersibility.

The basic amino acids, arginine and lysine, have two potential sites of reaction with the oxidised MWCNTs, owing to the presence of the $\alpha$-amine and side chain amine groups. Therefore to specifically form an amide bond using a particular amine group of these amino acids it is necessary to use the commercially available protected forms and remove the required protecting group from the amine before reaction. The neutral amino acids glycine and taurine however have only one amine group through which amide bond formation can occur, meaning protecting groups aren't required and functionalisation with them is more straightforward.

Once it was ascertained which amino acid caused the greatest improvement in the dispersibility of the MWCNTs, further methods to exploit this were investigated. Firstly amine functionalised MWCNTs were synthesised through coupling of ethylene-

diamine to oxidised MWCNTs. The amine functionalised MWCNTs were then further functionalised with mellitic acid, a hexacarboxylic acid, or poly(acrylic acid) (PAA), a carboxylic acid containing polymer, through amide bond formation to give MWCNTs functionalised with many carboxylic acid groups. These carboxylic acid groups were then reacted with the amino acid to attempt to improve MWCNT dispersibility further.

Finally, as non-covalent wrapping of MWCNTs with PAA has previously been shown to facilitate the dispersion of MWCNTs in water,[208, 209] an amino acid modified PAA derivative was prepared, again through amide bond formation, and its effectiveness at dispersing MWCNTs investigated.

## 4.2 Covalent Attachment of Basic Amino Acids to Oxidised MWCNTs

The $\alpha$-amine group of both the arginine and lysine used in this synthesis was protected by the protecting group 9-fluorenylmethyl carbamate (Fmoc), while their side chains were protected using 2,2,4,6,7-pentmethyl-2,3-dihydrobenzofuran-5-sulfonyl (Pbf) and tert-butyloxycarbonyl (BOC) respectively. Fmoc is stable under acidic conditions but is cleaved under mild basic conditions and Pbf and BOC are stable under basic conditions but cleaved under acidic conditions. Basic piperidine, a secondary amine, is a commonly used reagent for Fmoc deprotection and was used to free the $\alpha$-amine group whilst leaving the side chain groups protected (Figure 4.1).

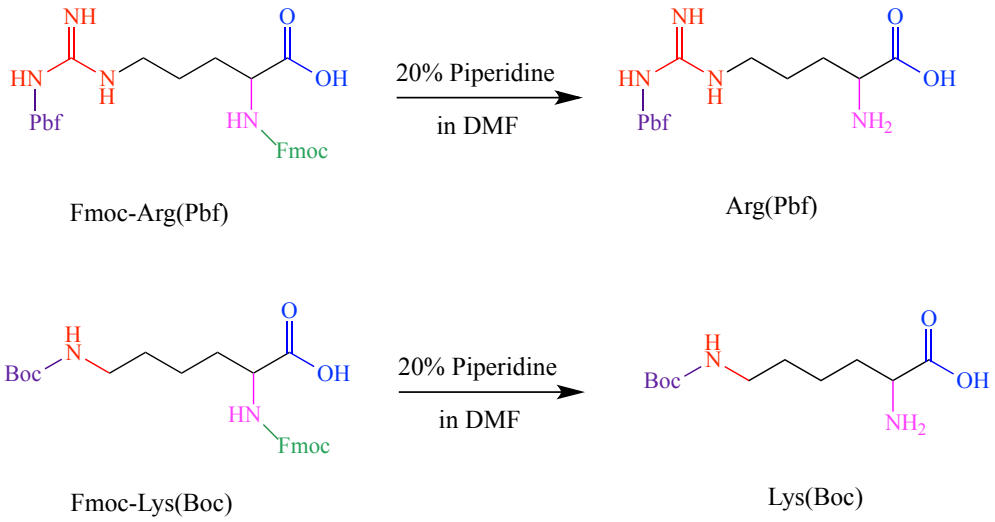


Figure 4.1: Schematic representation of the deprotection of the Fmoc protecting group from arginine (top) and lysine (bottom).

MWCNTs were oxidised for 16h, as outlined in Section 3.2, to form carboxylic acid groups on the MWCNT surface which were then deprotonated using *N,N*-diisopropylethylamine (DIPEA). The resulting carboxylate anions attack 1-[Bis(dimethylamino)methylene]-1H-1,2,3-triazolo[4,5-b]pyridinium 3-oxid hexafluorophosphate (HATU) to form an active ester. This active ester then reacts with the deprotected amine group of the amino acid, which results in the formation of an amide bond between them. After the attachment of the protected amino acid to the MWCNTs the Pbf/Boc protecting groups were removed using trifluoroacetic acid (TFA). Figure 4.2 gives an overview of the covalent attachment reaction to form MWCNT-Arginine**1** and MWCNT-Lysine.

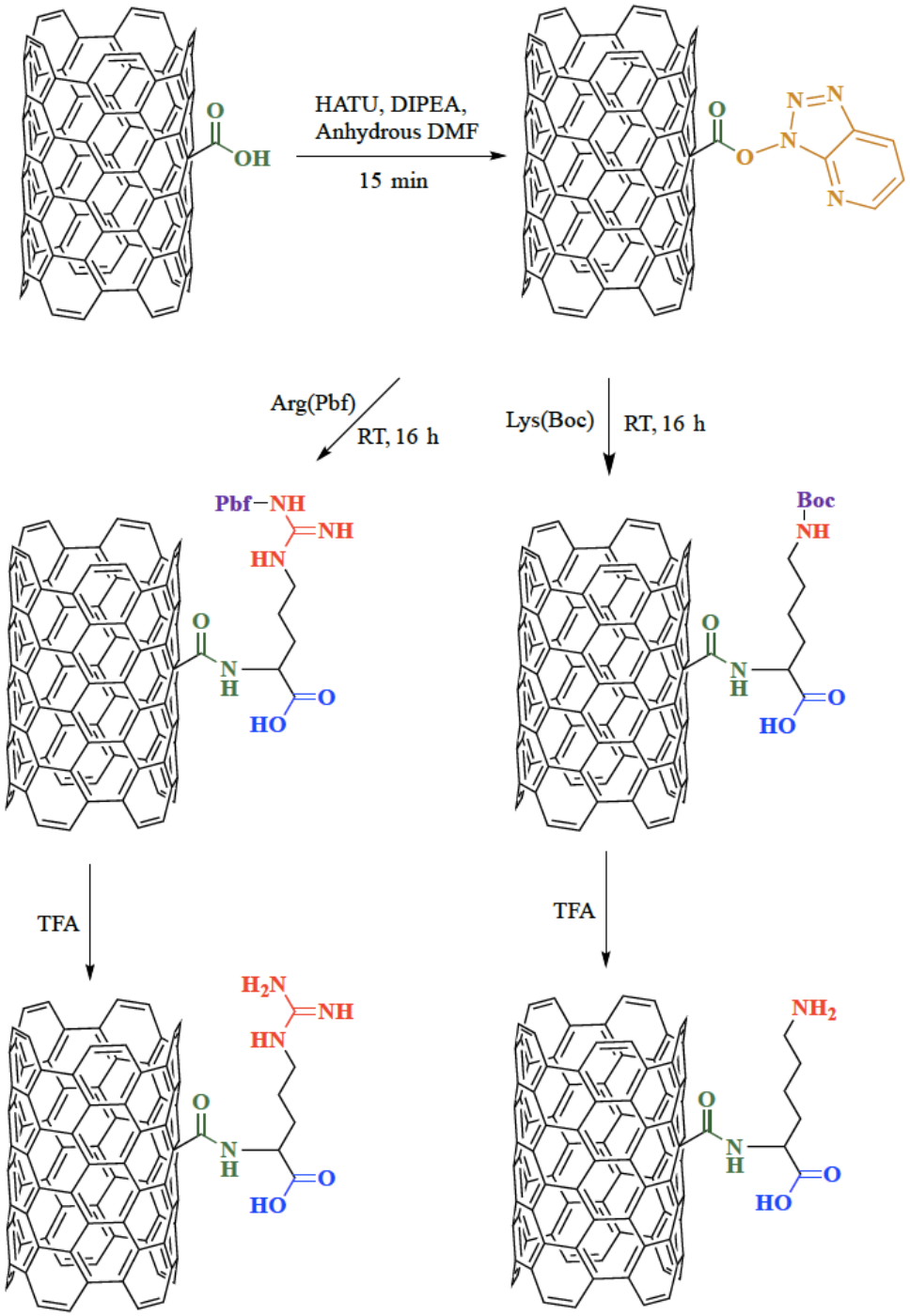


Figure 4.2: Schematic representation of amide bond formation between the $\alpha$-amine group of arginine (l) and lysine (r) to oxidised MWCNTs to give MWCNT-Arginine**1** and MWCNT-Lysine respectively.

Arginine was also covalently attached to oxidised MWCNTs through its side chain guanidinium group by firstly using TFA to remove the Pbf protecting group and then following the same procedure for amide bond formation as described in Section 4.2. Following the attachment of arginine the Fmoc protecting group on the $\alpha$-amine group was removed using piperidine to give MWCNT-Arginine**2** (Figure 4.3).

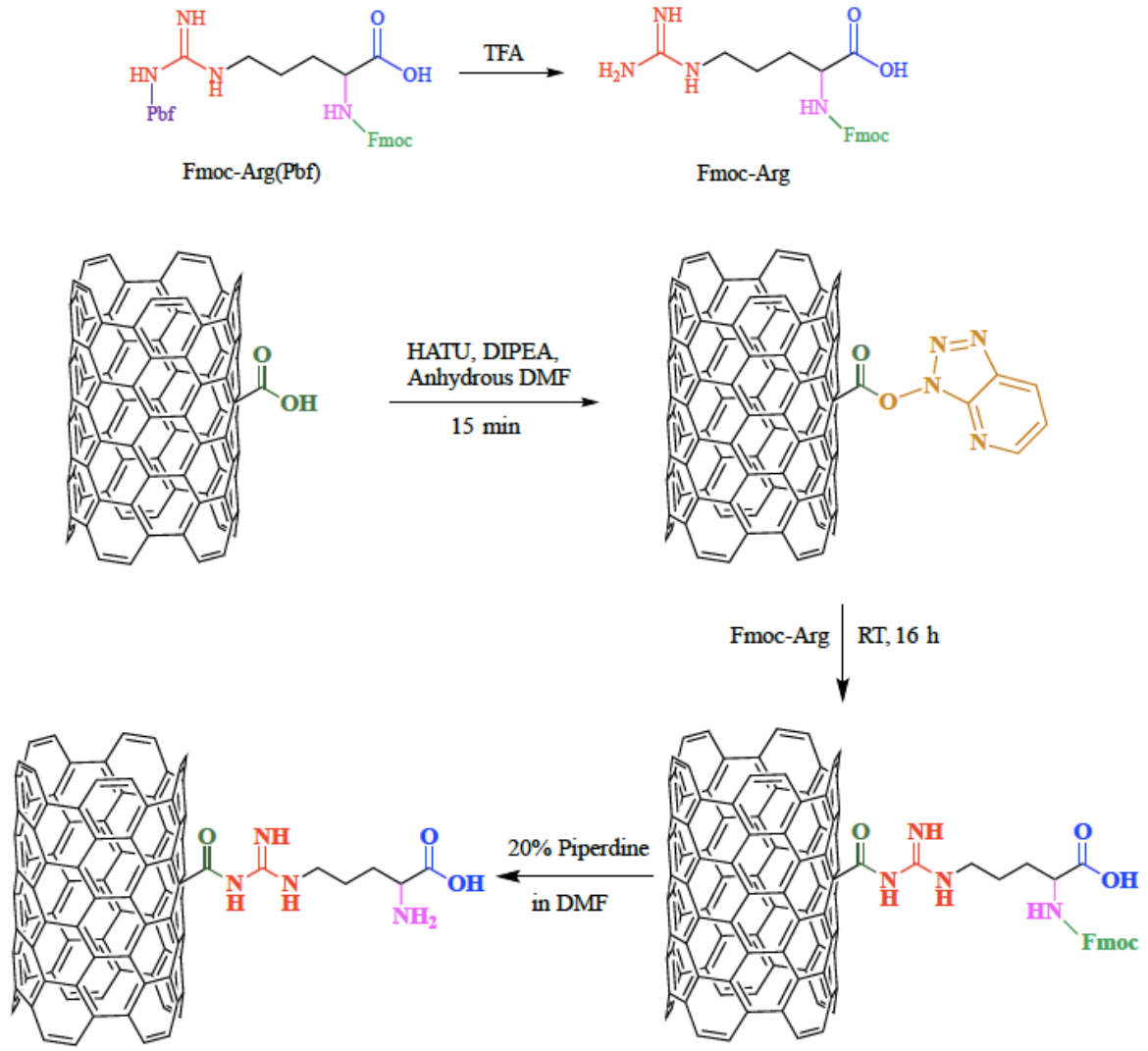


Figure 4.3: Schematic representation of amide bond formation between the guanidinium group of arginine and oxidised MWCNTs to give MWCNT-Arginine**2**.

### 4.2.1 Thermal Analysis

TGA of MWCNT-Arginine**1**, MWCNT-Lysine and MWCNT-Arginine**2** display a further weight loss of 7, 9 and 12 % respectively at 600 $^{o}$C when compared to the oxidised MWCNTs (Figure 4.4). This additional weight loss suggests that the attachment of the amino acids to the carboxylic acid groups present on the MWCNT surface has occurred.

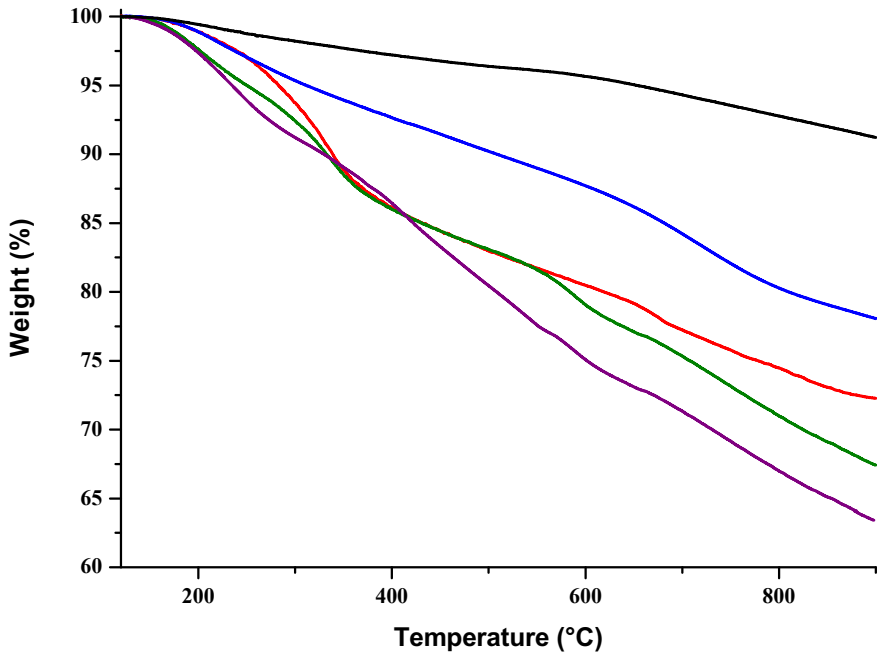


Figure 4.4: TGA results of AR-MWCNTs (black), oxidised MWCNTs (blue), MWCNT-Arginine**1** (red), MWCNT-Lysine (green) and MWCNT-Arginine**2** (purple). All the samples were held at 120$^{o}$C for 30 minutes and then heated at a rate of 10$^{o}$C min$^{-1}$ to 900$^{o}$C.

### 4.2.2 UV-vis-NIR Spectroscopy

As outlined in Section 3.2.3 the aqueous dispersibility of the functionalised MWCNTs can be determined from the UV-vis-NIR spectra (Figure 4.5). The aqueous dispersibility of the oxidised MWCNTs is 0.35 mg/mL, however after functionalisation

with the basic amino acids the concentration of MWCNT-Arginine**1**, MWCNT-Lysine and MWCNT-Arginine**2** decreases to 0 mg/mL in water. Figure 4.6 shows this clear decrease in MWCNT concentration and provides further evidence that the functionalisation of the MWCNTs has occurred. The amino acid functionalised MWCNTs can however be dispersed in basic solution of pH 10, which is similar to the respective isoelectric points of the amino acids (Figure 4.7). MWCNT-Arginine**1** is the most dispersible at 0.24 mg/mL, while MWCNT-Lysine and MWCNT-Arginine**2** disperse at concentrations of 0.089 and 0.099 mg/mL, respectively, as is demonstrated in Figure 4.5, while the dispersibility of the oxidised MWCNTs increases from 0.35 mg/mL to 0.42 mg/mL.

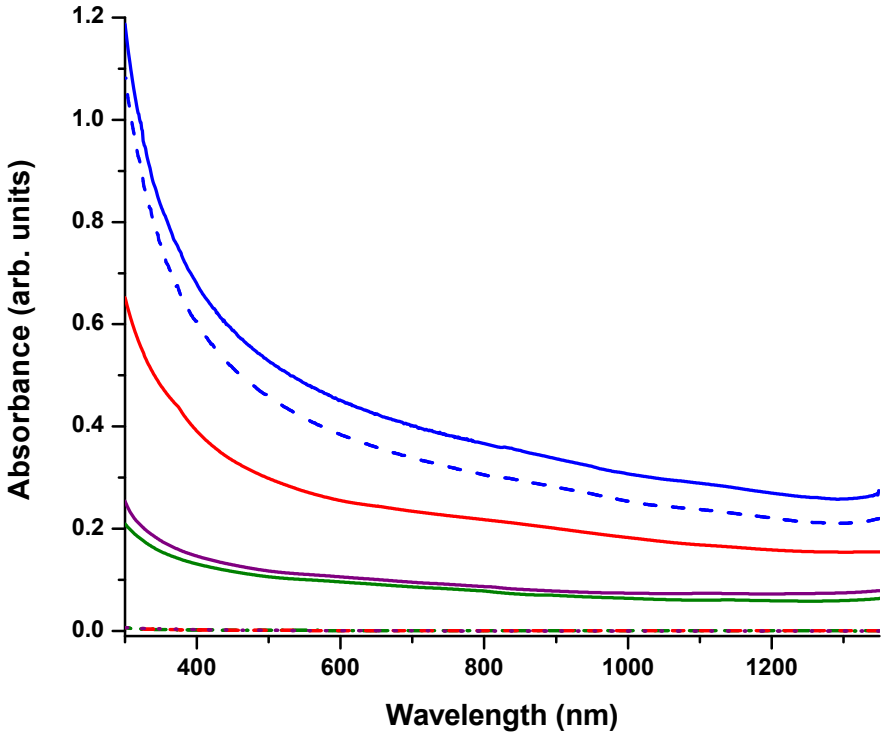


Figure 4.5: UV-vis-NIR spectra of oxidised MWCNTs (blue), MWCNT-Arginine**1** (red), MWCNT-Lysine (green) and MWCNT-Arginine**2** (purple) in water (dashed) and basic solution (solid) (diluted by a factor of 30).

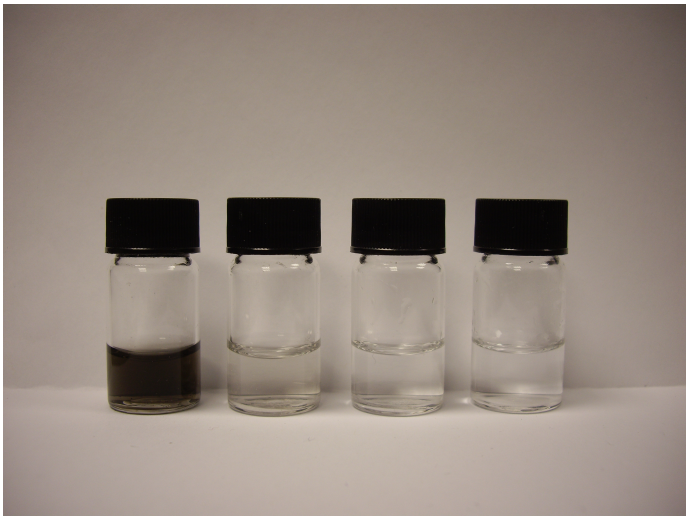

Figure 4.6: Photograph of the dispersions of oxidised MWCNTs, MWCNT-Arginine**1**, MWCNT-Lysine and MWCNT-Arginine**2** in water (diluted by a factor of 30) (l-r).

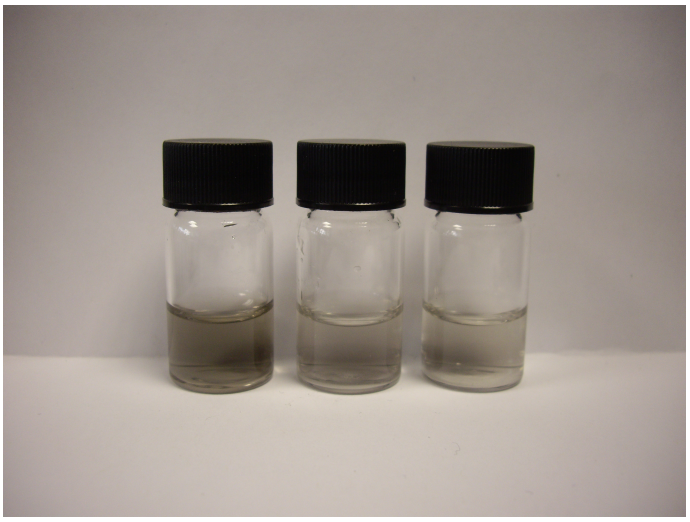

Figure 4.7: Photograph of the dispersions of MWCNT-Arginine**1**, MWCNT-Lysine and MWCNT-Arginine**2** in basic solutions with a pH equal to the respective isoelectric points of the amino acids (diluted by a factor of 30) (l-r).

### 4.2.3 Raman Spectroscopy

The Raman spectra of the amino acid functionalised MWCNTs show no significant change in the intensity of the D band when compared to the spectrum for the oxidised

MWCNTs (Figure 4.8). As the D band represents the conversion of MWCNT carbon atoms from a $sp^2$ to a $sp^3$ hybridisation state this result is expected because further functionalisation is taking place on the carboxylic acid groups already present on the MWCNT surface. The spectra therefore give comparable $I_D/I_G$ ratios of 0.087 ± 2.3 x $10^{-3}$, 0.089 ± 3.1 x $10^{-3}$, 0.087 ± 3.0 x $10^{-3}$ and 0.090 ± 2.3 x $10^{-3}$ for oxidised MWCNTs, MWCNT-Arginine**1**, MWCNT-Lysine and MWCNT-Arginine**2** respectively.

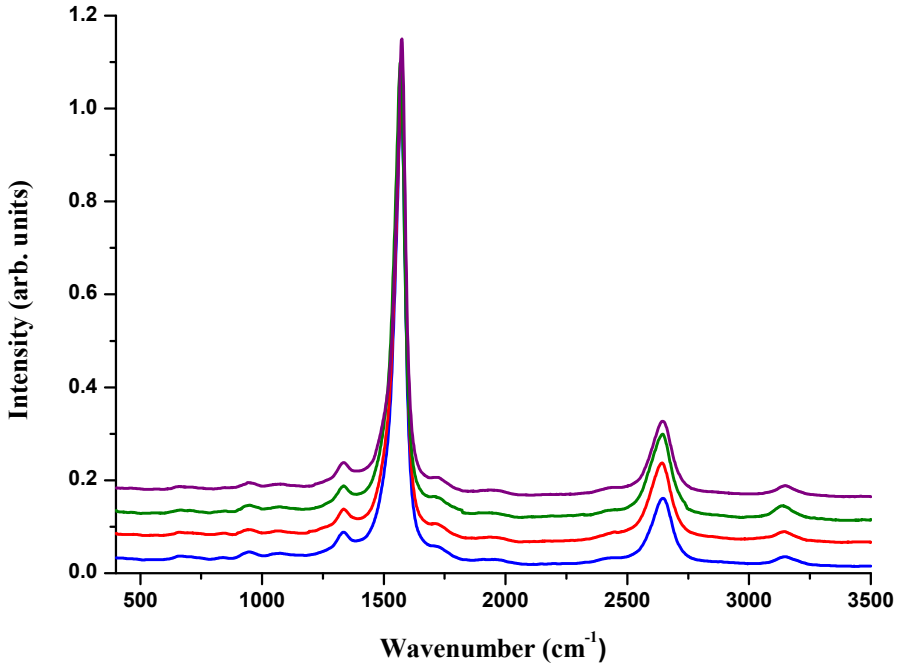


Figure 4.8: Raman spectra (532 nm, 2.33 eV) of oxidised MWCNTs (blue), MWCNT-Arginine**1** (red), MWCNT-Lysine (green) and MWCNT-Arginine**2** (purple) normalised at the G band.

### 4.2.4 Effect of Piperidine and TFA on Oxidised MWCNTs

In order to determine any effects the reagents that were used to deprotect the amino acids could have on the MWCNTs, a control experiment was performed by subjecting the oxidised MWCNTs to the same conditions used in the deprotection steps. The MWCNTs were then isolated using the same procedure given for the amino acid

modified MWCNTs. The resulting material was characterised using thermal anaylsis, Raman and UV-vis-NIR spectroscopy. The Raman and UV-vis-NIR spectra and TGA plot are shown in Appendix C. Overall the data shows that the piperidine and TFA had no effect on the oxidised MWCNTs.

## 4.3 Covalent Attachment of Neutral Amino Acids to Oxidised MWCNTs

The process to attach glycine and taurine to oxidised MWCNTs is more straightforward than for arginine and lysine as these neutral amino acids have only one amine group through which they can form an amide bond with the MWCNTs. The reaction between the amine group of the amino acids and the carboxylic acid groups of oxidised MWCNTs to form an amide bond then occurs as described previously in Section 4.2 (Figure 4.9).

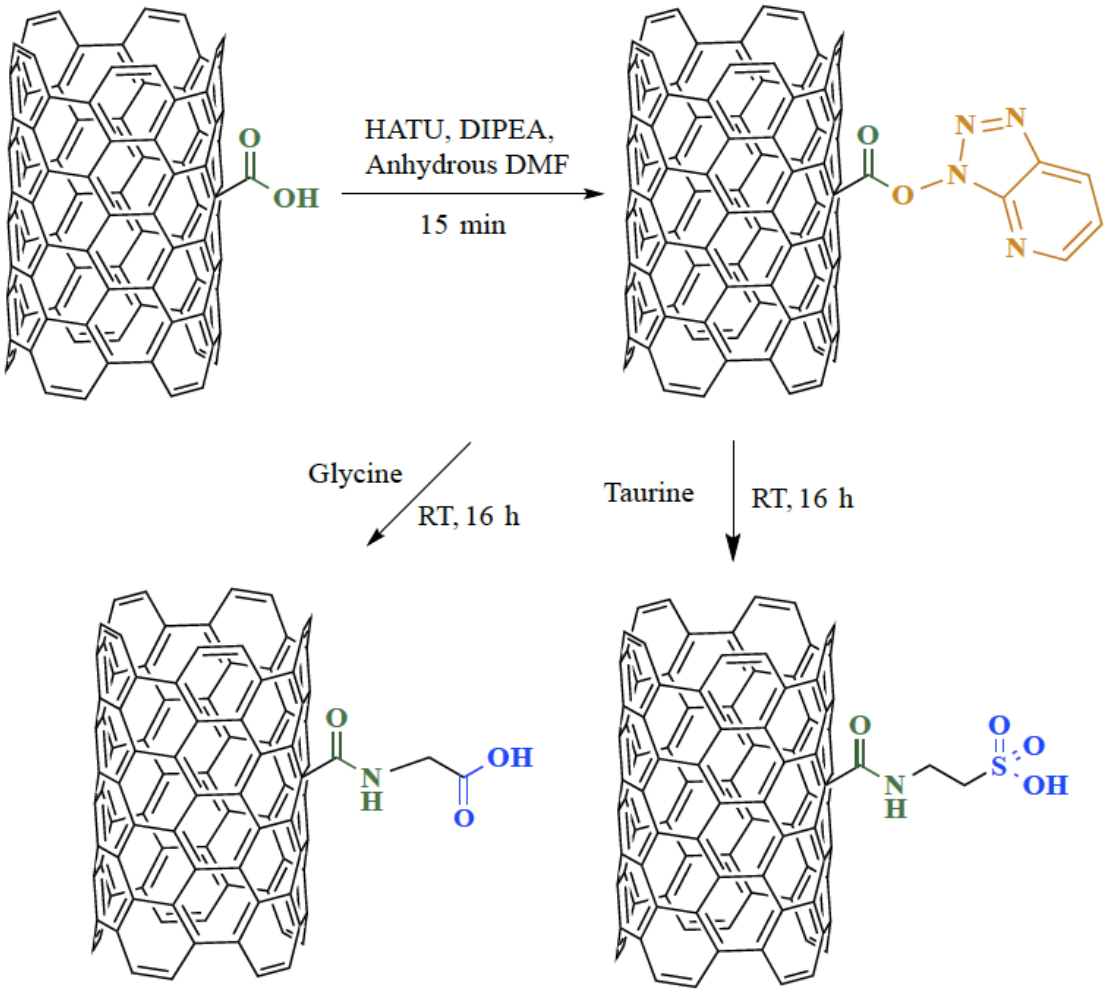


Figure 4.9: Schematic representation of the covalent attachment of glycine (l) and taurine (r) to oxidised MWCNTs through amide bond formation to give MWCNT-Glycine and MWCNT-Taurine respectively.

### 4.3.1 Thermal Analysis

TGA of MWCNT-Glycine and MWCNT-Taurine shows a further weight loss of 10 and 7 % respectively at 600 $^{o}$C when compared to the oxidised MWCNTs. This additional weight loss suggests that the addition of glycine and taurine to the carboxylic acid groups on the MWCNT surface has occurred.

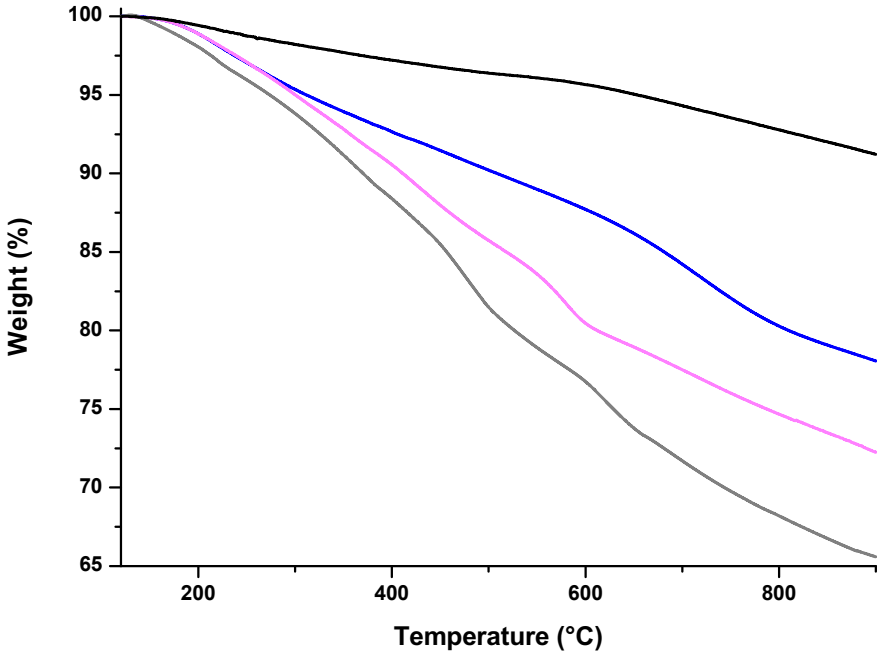


Figure 4.10: TGA results of AR-MWCNTs (black), oxidised MWCNTs (blue), MWCNT-Glycine (grey) and MWCNT-Taurine (magenta). All the samples were held at 120$^o$C for 30 minutes and then heated at a rate of 10$^o$C min$^{-1}$ to 900$^o$C.

### 4.3.2 UV-vis-NIR Spectroscopy

The concentration of functionalised MWCNTs in water was determined from the UV-vis-NIR spectra (Figure 4.11) as outlined in Section 3.2.3. The oxidised MWCNTs could be dispersed at a concentration of 0.35 mg/mL, however after functionalisation with glycine and taurine the aqueous dispersibility of the MWCNTs increased to 0.37 and 0.92 mg/mL, respectively.

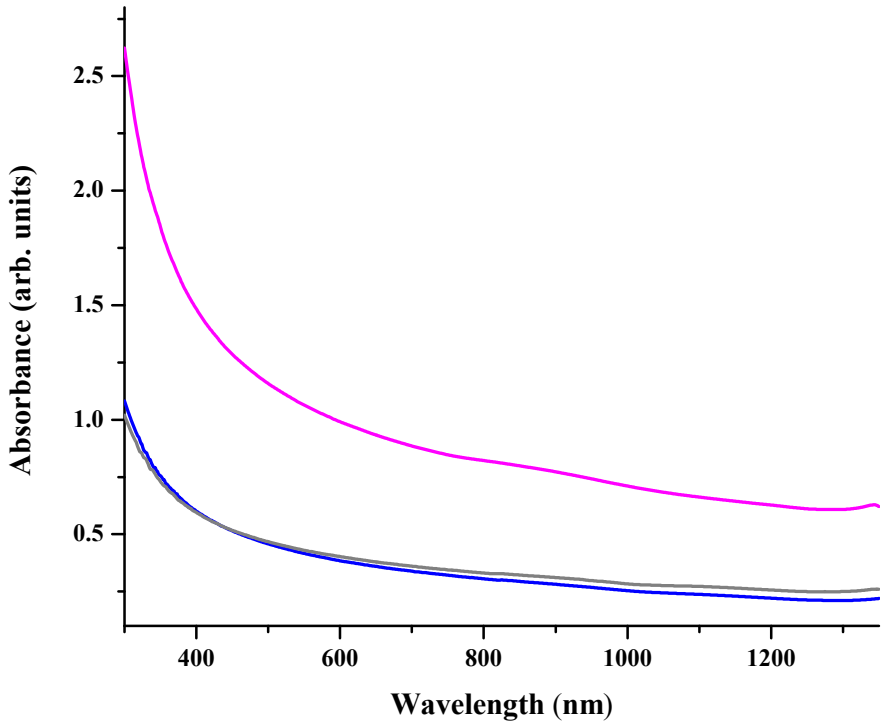


Figure 4.11: UV-vis-NIR spectra in water of oxidised MWCNTs (blue), MWCNT-Glycine (grey) and MWCNT-Taurine (magenta).

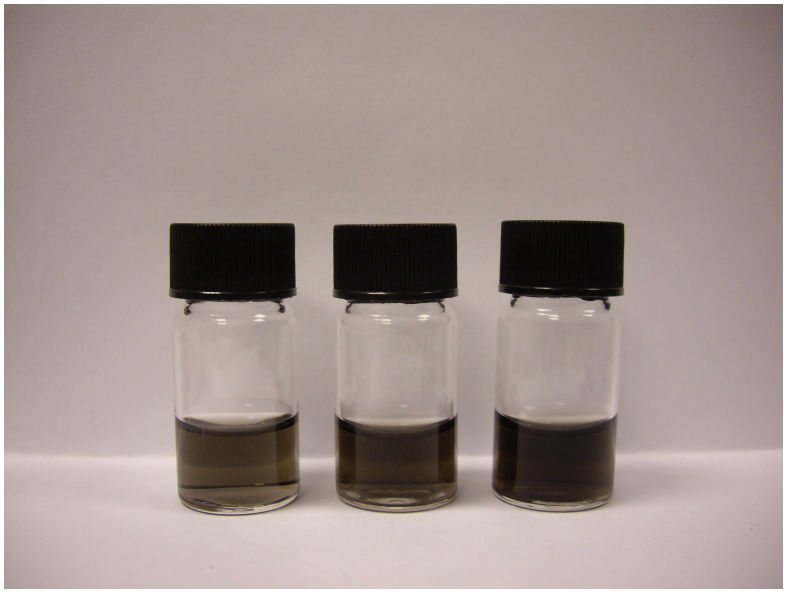

Figure 4.12: Photograph of the dispersions of oxidised MWCNTs, MWCNT-Glycine and MWCNT-Taurine (l-r).

### 4.3.3 Raman Spectroscopy

The Raman spectra of the amino acid functionalised MWCNTs show no significant change in the intensity of the D band when compared to the spectrum for the oxidised MWCNTs (Figure 4.13), and so similar $I_D/I_G$ ratios of 0.087 $\pm$ 2.3 x $10^{-3}$, 0.086 $\pm$ 2.8 x $10^{-3}$ and 0.088 $\pm$ 3.2 x $10^{-3}$ are observed for oxidised MWCNTs, MWCNT-Glycine and MWCNT-Taurine respectively. This outcome is anticipated as the amino acids are attached through the carboxylic acid groups already present on the MWCNTs.

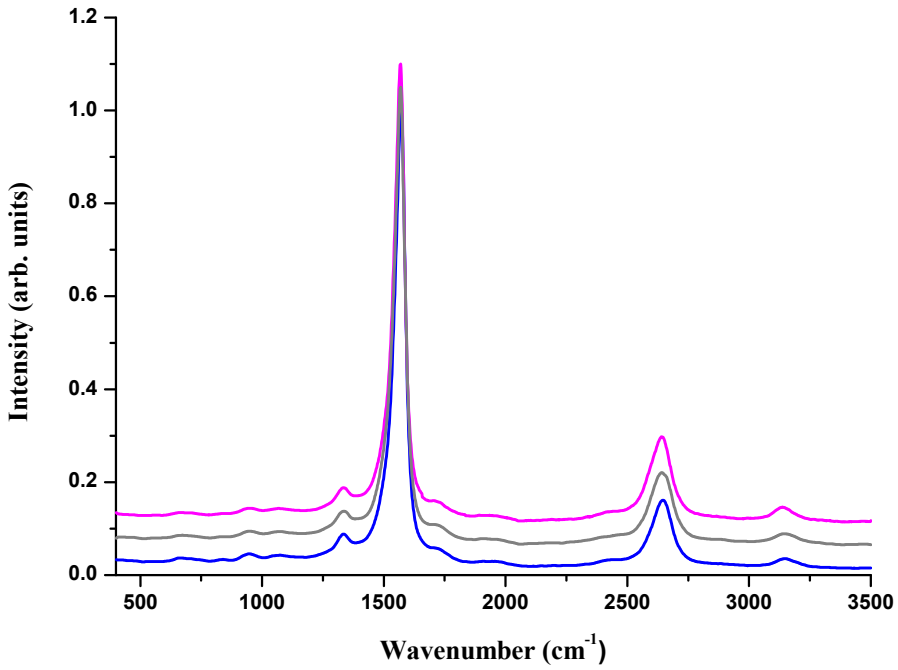


Figure 4.13: Raman spectra (532 nm, 2.33 eV) of oxidised MWCNTs (blue), MWCNT-Glycine (grey) and MWCNT-Taurine (magenta) normalised at the G band.

## 4.4 Covalent Functionalisation of MWCNTs with Mellitic Acid

The approach adopted for the attachment of mellitic acid to MWCNTs initially involved modifying oxidised MWCNTs with amine groups (Figure 4.14). Amine functionalisation was achieved by using HATU to couple the carboxylic acid groups with the simple alkyl chain diamine, ethylenediamine. The formation of an amide bond between the amine-functionalised carbon nanotubes and the carboxyl groups of mellitic acid was again facilitated by HATU and resulted in mellitic acid functionalised MWCNTs (MWCNT-Mellitic). The free carboxyl groups of MWCNT-Mellitic were further modified with taurine by again forming an amide bond between them to give MWCNT-MelliticTaurine.

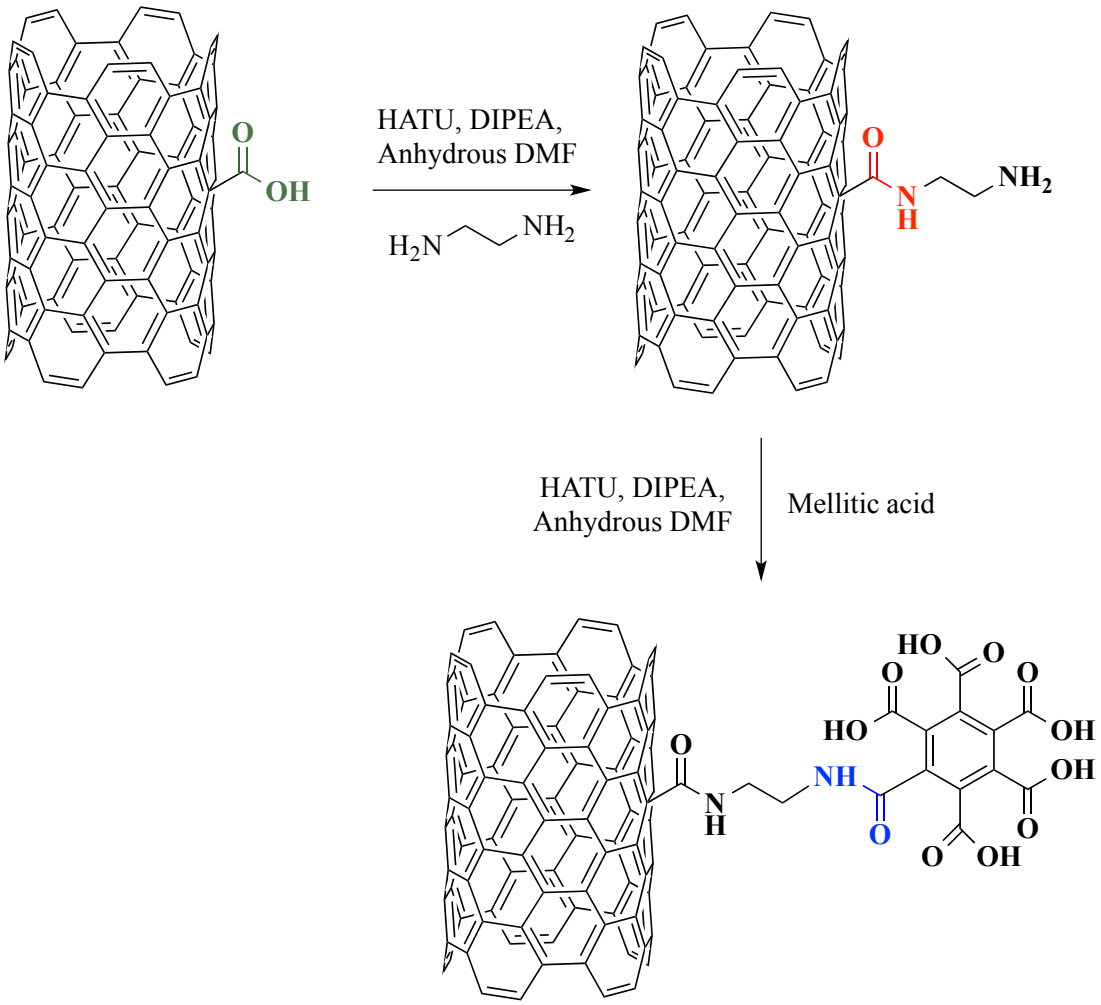


Figure 4.14: Schematic representation of the covalent attachment of mellitic acid to amine functionalised MWCNTs through amide bond formation.

### 4.4.1 Thermal Analysis

The amine functionalised MWCNTs (MWCNT-Amine) display a weight loss of 2 % when compared to the oxidised MWCNTs and MWCNT-Mellitic shows a further weight loss of 9 % at 600 $^{o}$C when compared to MWCNT-Amine (Figure 4.15). This additional weight loss suggests that the attachment of mellitic acid to the amine groups present on the MWCNT surface has occurred. A further weight loss of 3 % at 600 $^{o}$C is shown when MWCNT-MelliticTaurine is compared to MWCNT-Mellitic indicating that modification of the mellitic acid groups with taurine has been successful.

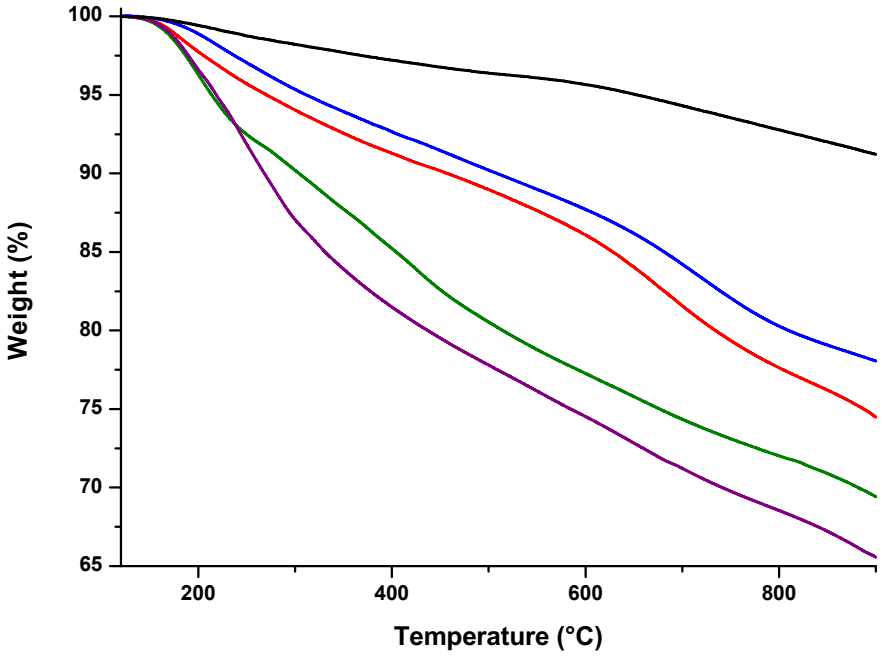


Figure 4.15: TGA results of AR-MWCNTs (black), oxidised MWCNTs (blue), MWCNT-Amine (red), MWCNT-Mellitic (green) and MWCNT-MelliticTaurine (purple). All the samples were held at 120$^o$C for 30 minutes and then heated at a rate of 10$^o$C min$^{-1}$ to 900$^o$C.

### 4.4.2 UV-vis-NIR Spectroscopy

Using the absorbance values at 700 nm from the UV-vis-NIR spectra (Figure 4.16), and the extinction coefficient as described in Section 3.2.3, the functionalisation of the oxidised MWCNTs with amine groups was calculated to decrease their dispersibility from 0.35 to 0.14 mg/mL. However, the reaction of MWCNT-Amine with mellitic acid increases dispersibility to 0.51 mg/mL, and the subsequent functionalisation of MWCNT-Mellitic with taurine improves dispersibility even further to 0.94 mg/mL.

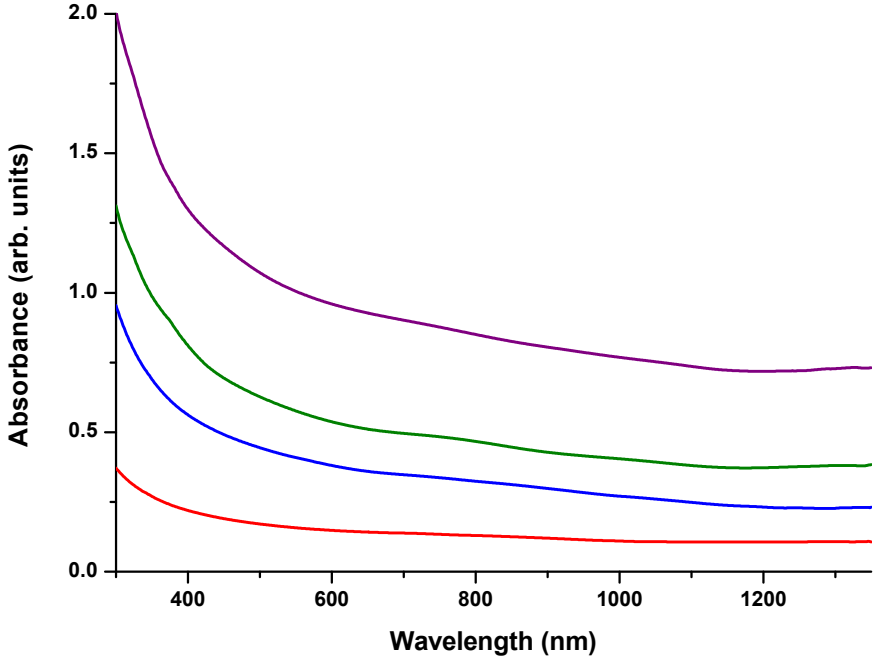


Figure 4.16: UV-vis-NIR spectra in water of oxidised MWCNTs (blue), MWCNT-Amine (red), MWCNT-Mellitic (green) and MWCNT-MelliticTaurine (purple).

### 4.4.3 Raman Spectroscopy

The Raman spectra of the functionalised MWCNTs show no significant change in the intensity of the D band when compared to the spectrum for oxidised MWCNTs (Figure 4.17). As the further reactions required the use of the carboxylic acid groups already present on the MWCNTs this result is anticipated and the spectra give comparable $I_D/I_G$ ratios of 0.087 $\pm$ 2.3 x $10^{-3}$, 0.085 $\pm$ 2.9 x $10^{-3}$, 0.088 $\pm$ 2.1 x $10^{-3}$ and 0.088 $\pm$ 1.9 x $10^{-3}$ for oxidised MWCNTs, MWCNT-Amine, MWCNT-Mellitic and MWCNT-MelliticTaurine respectively.

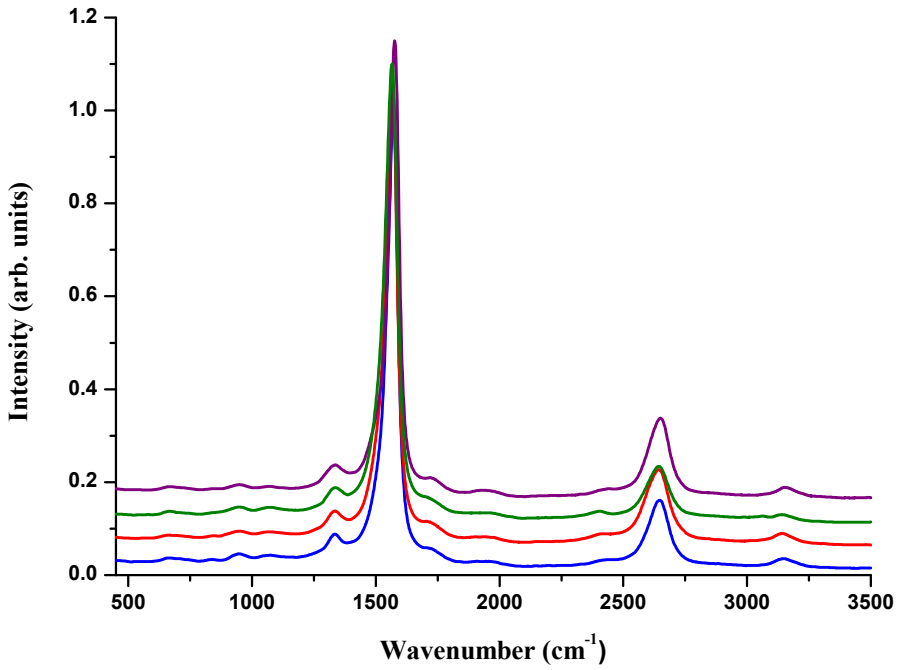


Figure 4.17: Raman spectra (532 nm, 2.33 eV) of oxidised MWCNTs (blue), MWCNT-Amine (red) MWCNT-Mellitic (green) and MWCNT-MelliticTaurine (purple) normalised at the G band.

## 4.5 Functionalisation of MWCNTs with Taurine Modified Poly(acrylic acid)

Functionalisation of MWCNTs with taurine modified PAA was achieved through both covalent and non-covalent means as outlined in Sections 4.5.1 and 4.5.2.

### 4.5.1 Covalent

To covalently functionalise MWCNTs with taurine modified PAA, oxidised MWCNTs were modified with amine groups as described in Section 4.4 and PAA attached through amide bond formation to give MWCNT-PAA (Figure 4.18). Once covalently attached the carboxylic acid groups of PAA were modified with taurine, again through amide

bond formation, resulting in MWCNT-PAATaurine.

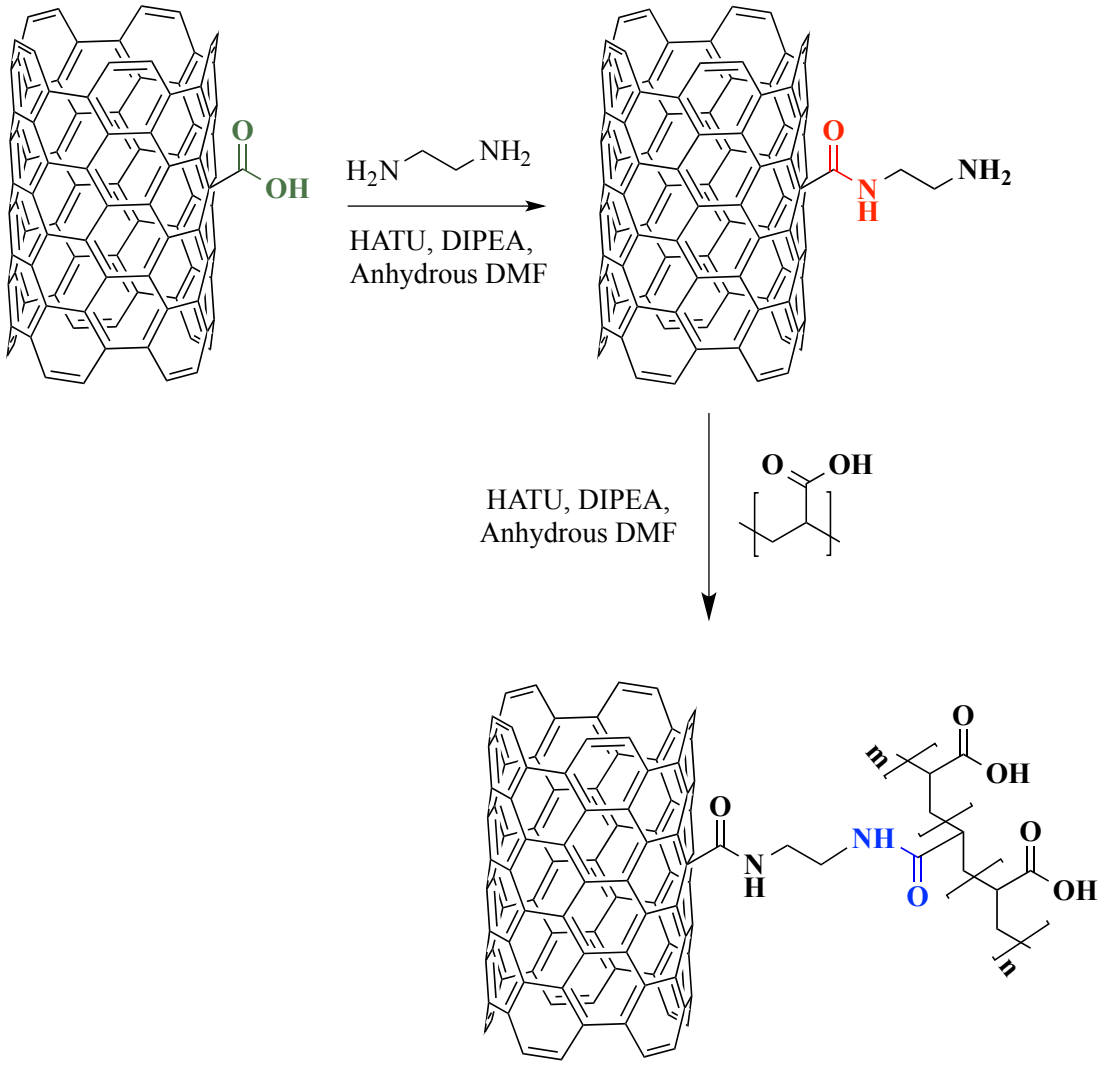


Figure 4.18: Schematic representation of the covalent attachment of PAA to MWCNTs through amide bond formation.

#### 4.5.1.1 Thermal Analysis

TGA of MWCNT-PAA displays a weight loss of 22 % at 600 $^{o}$C when compared to MWCNT-Amine (Figure 4.19). This additional weight loss suggests that the attachment of PAA to the amine groups present on the MWCNT surface has occurred. A further weight loss of 7 % at 600 $^{o}$C is shown when MWCNT-PAATaurine is compared

to MWCNT-PAA indicating that modification of the PAA groups with taurine has been successful.

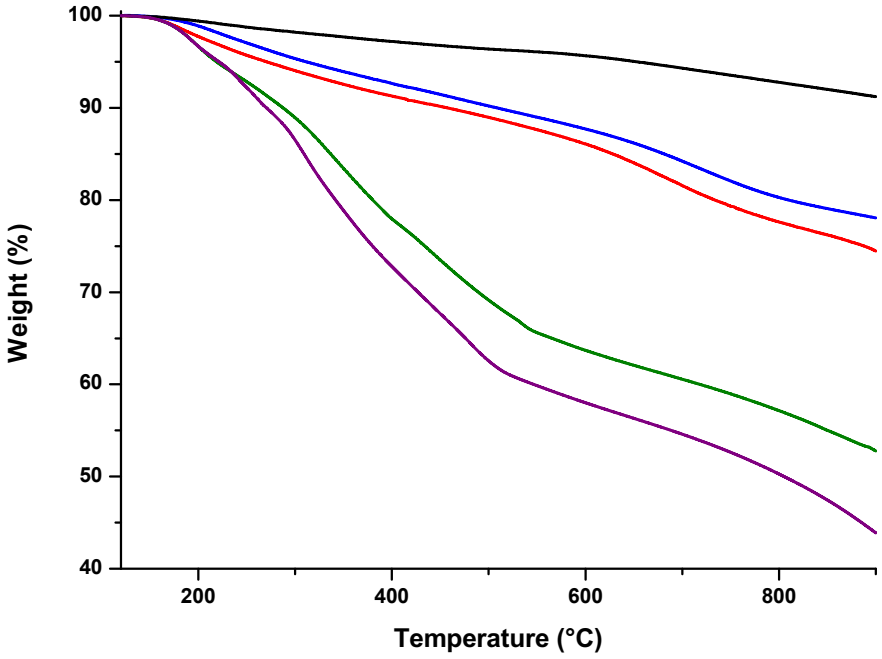


Figure 4.19: TGA results of AR-MWCNTs (black), oxidised MWCNTs (blue), MWCNT-Amine (red), MWCNT-PAA (green) and MWCNT-PAATaurine (purple). All the samples were held at 120$^o$C for 30 minutes and then heated at a rate of 10$^o$C min$^{-1}$ to 900$^o$C.

#### 4.5.1.2 UV-vis-NIR Spectroscopy

Using the same method as described in Section 3.2.3, the aqueous dispersibility of MWCNT-Amine was determined to be 0.14 mg/mL, however after functionalisation with PAA the dispersibility of the MWCNTs increases to 0.82 mg/mL. Further derivatisation of PAA with taurine improves the dispersibility of the MWCNTs to 1.43 mg/mL in water (Figure 4.20).

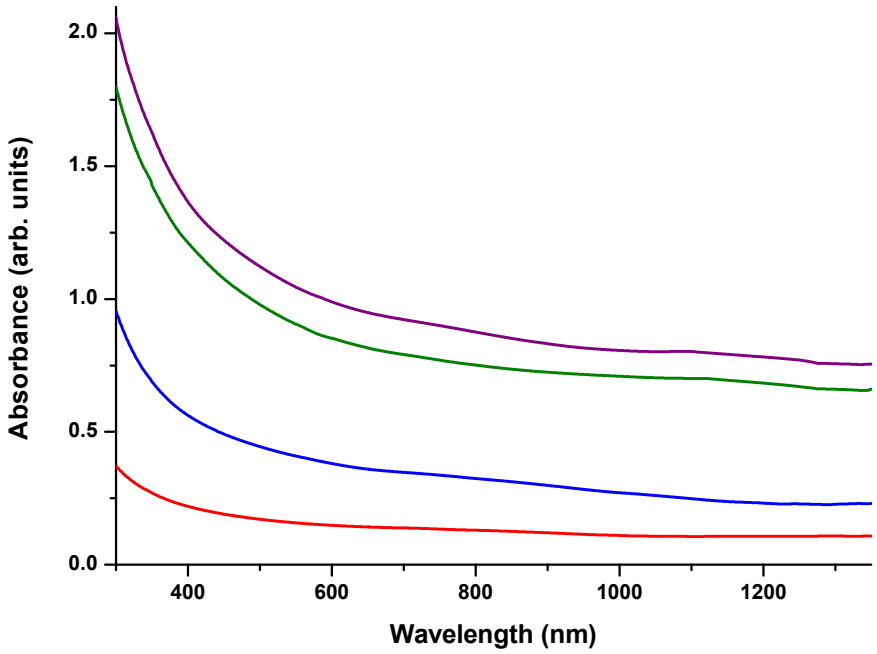


Figure 4.20: UV-vis-NIR spectra in water of oxidised MWCNTs (blue) and MWCNT-Amine (red), MWCNT-PAA (green) and MWCNT-PAATaurine (purple).

#### 4.5.1.3 Raman Spectroscopy

The Raman spectra of the polymer functionalised MWCNTs show no significant change in the intensity of the D band when compared to the spectrum for MWCNT-Amine (Figure 4.21). This result is expected because the additional reactions involve the amine groups already present on the MWCNT surface. The spectra therefore give comparable $I_D/I_G$ ratios of 0.087 $\pm$ 2.3 x $10^{-3}$, 0.085 $\pm$ 2.9 x $10^{-3}$, 0.086 $\pm$ 2.0 x $10^{-3}$ and 0.089 $\pm$ 1.6 x $10^{-3}$ for oxidised MWCNTs, MWCNT-Amine, MWCNT-PAA and MWCNT-PAATaurine respectively.

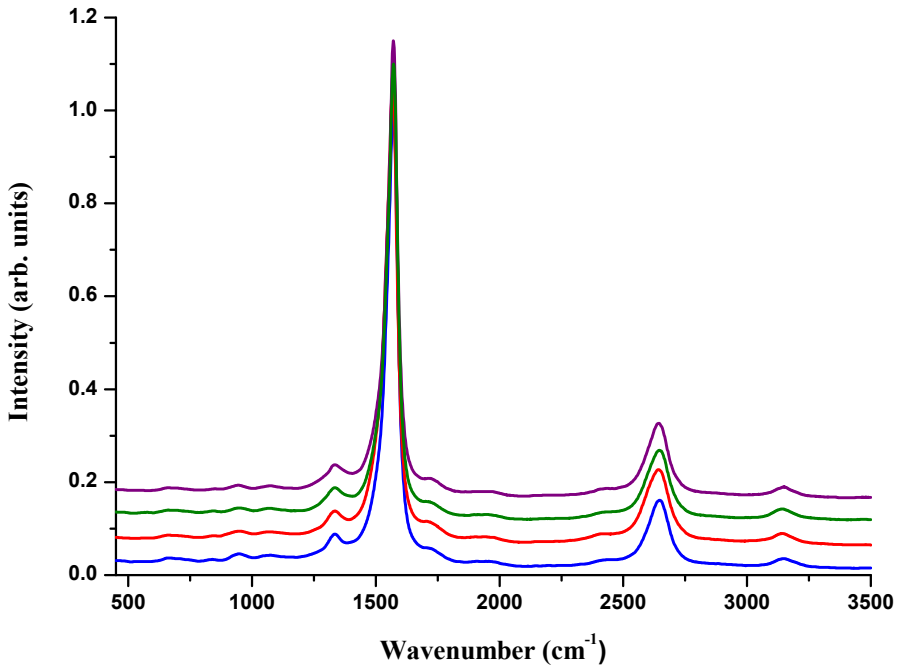


Figure 4.21: Raman spectra (532 nm, 2.33 eV) of oxidised MWCNTs (blue), MWCNT-Amine (red), MWCNT-PAA (green) and MWCNT-PAATaurine (purple) normalised at the G band.

### 4.5.2 Non-Covalent

The carboxylic acid groups of PAA were reacted with taurine in the presence of HATU to give taurine modified PAA (PAA-Taurine) (Figure 4.22). The MWCNTs were then dispersed in a 1 wt% aqueous solution of the modified polymer using an ultrasonic bath for 30 minutes to give MWCNTs non-covalently functionalised with PAA-Taurine.

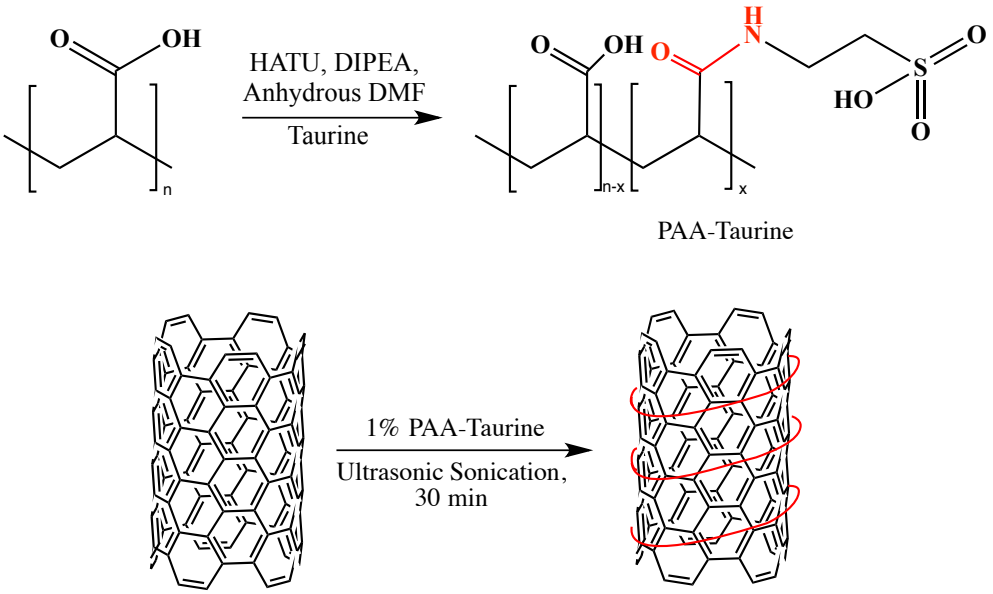


Figure 4.22: Schematic representation of the covalent attachment of taurine to PAA through amide bond formation and the non-covalent functionalisation of MWCNTs with the resulting modified polymer.

#### 4.5.2.1 UV-vis-NIR Spectroscopy

The dispersibility of the MWCNTs in 1 wt% PAA was determined to be 0.04 mg/mL from the UV-vis-NIR spectra (Figure 4.23), by using the method outlined in Section 3.2.3. The dispersion of the MWCNTs in 1 wt% PAA-Taurine however was found to significantly improve MWCNT dispersibility to 0.20 mg/mL. It was also observed that it was not possible to disperse MWCNTs in a 0.5 M aqueous taurine solution that contained 1 wt% PAA, suggesting the covalent modification of PAA with taurine is necessary to improve MWCNT dispersibility.

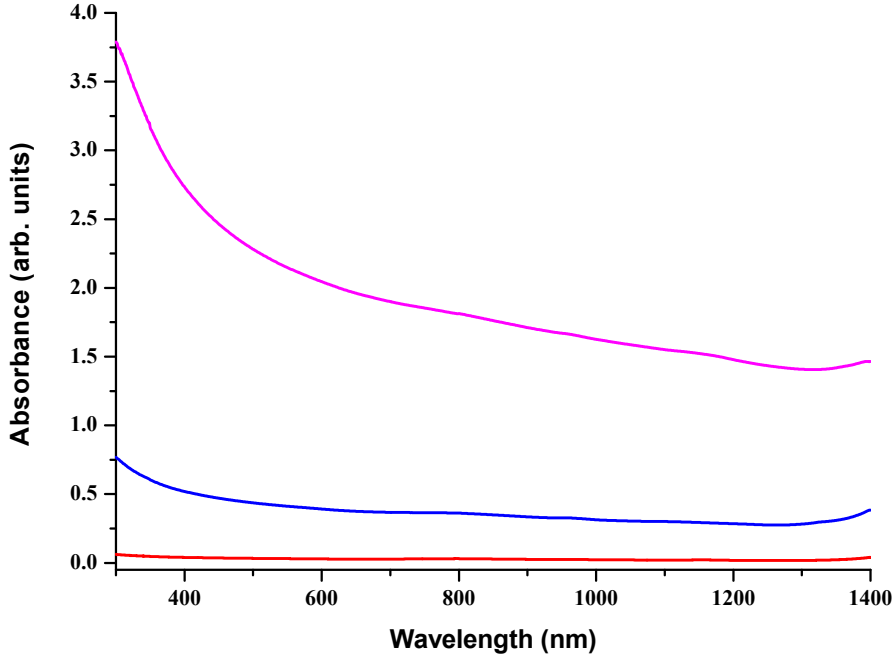


Figure 4.23: UV-vis-NIR spectra of AR-MWCNTs dispersed in 0.5 M taurine/1 wt% PAA solution (red), 1 wt% PAA (blue) and 1 wt% PAA-Taurine (magenta) (diluted by a factor of 3).

The considerable improvement that non-covalent functionalisation with PAA-Taurine has over PAA on MWCNT dispersibility is demonstrated in Figure 4.24 and indicates that the modification of PAA with taurine has been successful.

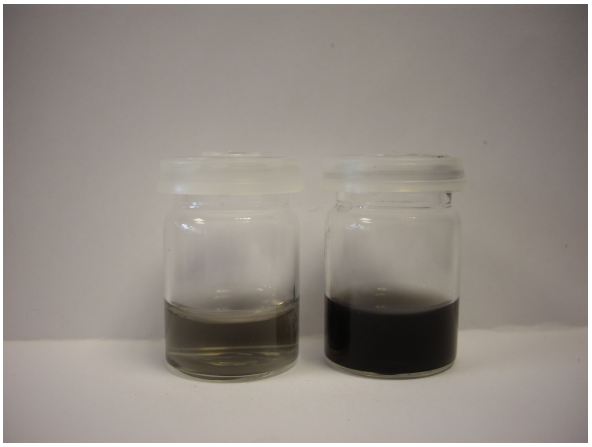

Figure 4.24: Photograph of the dispersion of MWCNTs in 1 wt% PAA (l) and 1 wt% PAA-Taurine (r) (diluted by a factor of 3).

## 4.6 Conclusion

In summary, the covalent attachment of selected basic and neutral amino acids to oxidised MWCNTs has been achieved through amide bond formation. The functionalisation of oxidised MWCNTs with the basic amino acids arginine and lysine however was found to render the MWCNTs insoluble in aqueous solution and significantly decrease the dispersibility of the MWCNTs in basic solution from the level observed for oxidised MWCNTs. This result is in direct contrast to a previous study of lysine functionalised MWCNTs, that were derived from oxidised MWCNTs via the acyl chloride, which could produce stable aqueous concentrations nearly two orders of magnitude higher than the oxidised MWCNTs and were dispersible over the pH range 5-14.[143]

The attachment of the neutral amino acids glycine and taurine on the other hand was found to increase MWCNT aqueous dispersibility beyond that observed simply by oxidation, with the UV-vis-NIR spectra indicating that taurine provided the most significant improvement. The covalent attachment of taurine to oxidsed SWCNTs has previously been reported to increase SWCNT concentration to 1.3 mg/mL in water at pH 7,[141] however glycine functionalised SWCNTs, produced from fluoronanotubes, have previously been found to show no solubility in water across all pH values.[142]

In order to exploit the ability of taurine to improve MWCNT aqueous dispersibility, MWCNTs were covalently functionalised with the carboxylic acid containing com-

pounds mellitic acid and PAA, which were themselves subsequently functionalised with taurine through amide bond formation. The attachment of the carboxylic acid containing compounds was found to improve MWCNT dispersibility beyond that observed by oxidation, while their subsequent modification with taurine improved MWCNT dispersibility even further.

MWCNTs were also non-covalently functionalised with a taurine modified polymer that was sythesised through amide bond formation between PAA and taurine. The dispersion of MWCNTs in a 1 wt% solution of PAA-Taurine resulted in a fivefold increase in MWCNT dispersibility over that achieved with just 1 wt% PAA to 0.20 mg/mL. A previous investigation has however reported that much a higher concentration of 1 mg/mL MWCNTs can be achieved by non-covalent wrapping with unmodified PAA.[207]

# Chapter 5

# The Functionalisation of MWCNTs with Hydroxy Groups

## 5.1 Introduction

This chapter involves the covalent functionalisation of MWCNTs with compounds containing the hydroxy functional group. Alpha-hydroxy acids (AHAs) consist of a carboxylic acid with a hydroxy group on the adjacent carbon. Glycolic and citric acid (Figure 5.1) are common and simple AHAs that have one and three carboxylic acid groups respectively. Amine functionalised MWCNTs were generated from the reaction of oxidised MWCNTs with ethylenediamine and glycolic and citric acid were attached to these amine functionalised MWCNTs through amide bond formation.

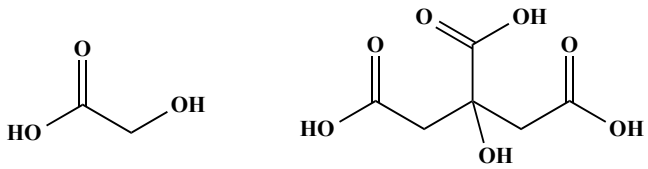


Figure 5.1: Structures of glycolic acid (l) and citric acid (r).

Next the ability of pyridine functionalised MWCNTs to act as the starting point for the covalent attachment of hydroxy group containing compounds was investigated. Pyridine was covalently attached to the carbon nanotube surface through a diazonium reaction, then the nitrogen of pyridine was used to displace bromine from a series of

bromoalcohols. Following the success of these reactions the attachment of the bromo substituted derivatives of the ribonucleosides uridine and adenosine (Figure 5.2) was considered using the same method.

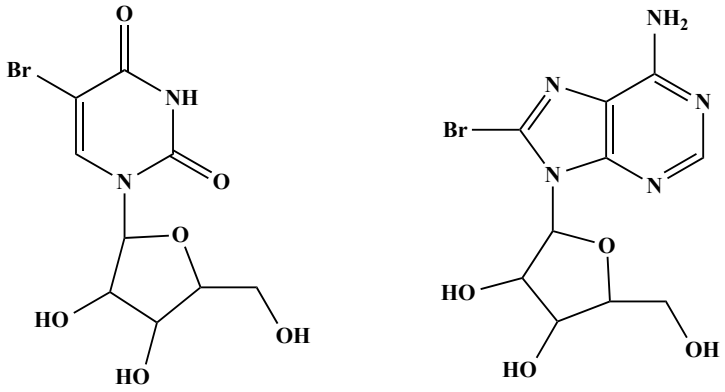


Figure 5.2: Structures of 5-bromouridine (l) and 8-bromoadenosine (r).

The pyridine functionalised MWCNTs were further employed as the basis for the attachment of the simple sugars ribose, fructose and sucrose. This was achieved through the reaction of pyridine with bromoacetyl bromide and then displacement of bromine by the selcted sugar. Finally, the water-soluble polymer poly(ethylene glycol) (PEG), a polymer of ethylene oxide terminated with alcohol groups, was covalently attached to pyridine functionalised MWCNTs in the same manner as the sugars.

## 5.2 Covalent Attachment of Alpha Hydroxy Acids to Oxidised MWCNTs

The AHAs were covalently attached to MWCNTs by the reaction of a carboxylic acid group of the AHAs with amine functionalised MWCNTs as outlined in Figure 5.3. Firstly, the carboxylic groups of oxidised MWCNTs are deprotonated using DIPEA and then activated by HATU. The addition of an excess of ethylenediamine then results in the formation of amine functionalised MWCNTs which can then react with the carboxylic acid group of the AHAs to form an amide bond.

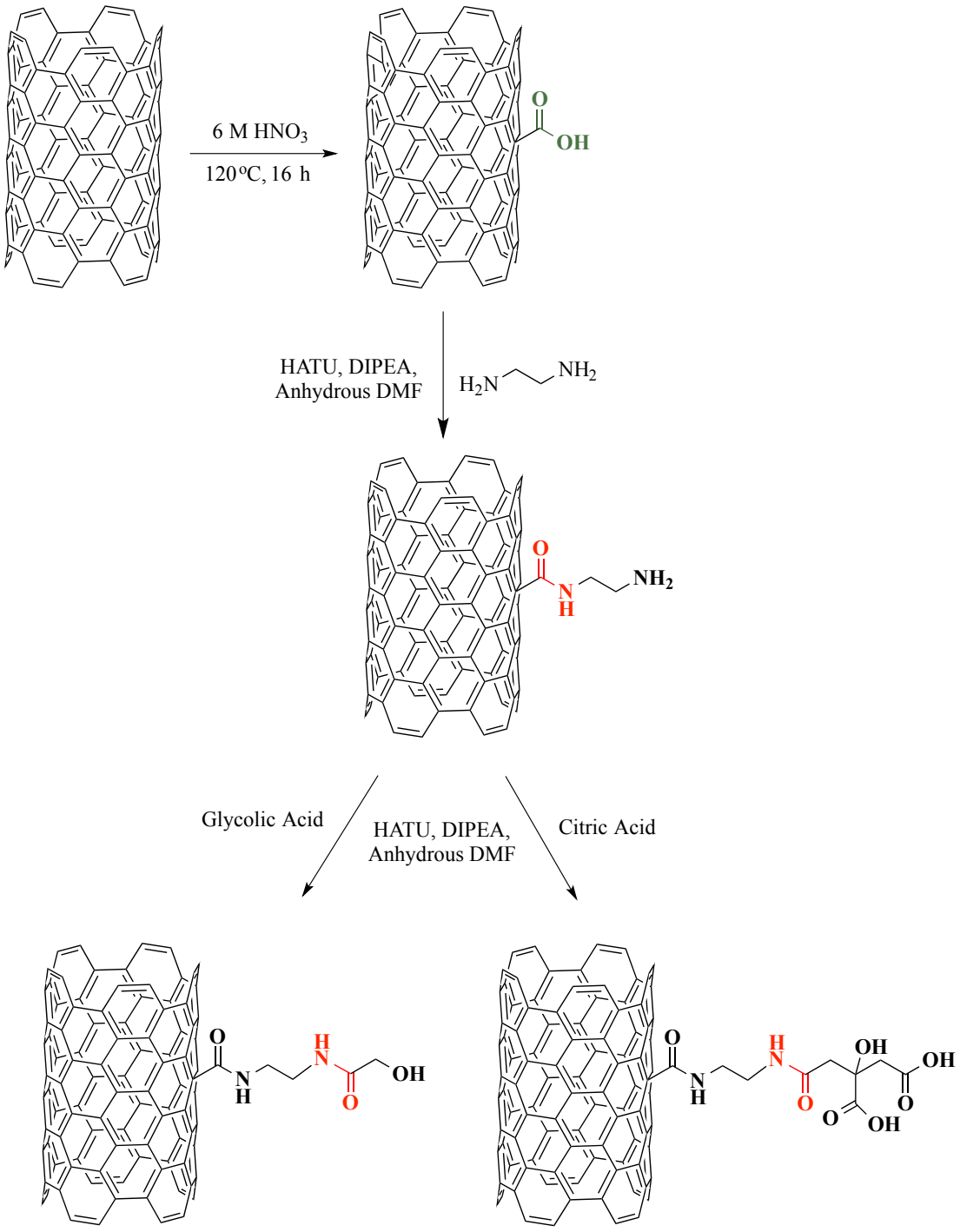


Figure 5.3: Schematic representation of the functionalisation of MWCNTs with glycolic acid and citric acid to give MWCNT-Glycolic (l) and MWCNT-Citric (r).

### 5.2.1 Thermal Analysis

TGA of amine functionalised MWCNTs displays an additional weight loss of 2 % at 600 $^{o}$C when compared to the oxidised MWCNTs (Figure 5.4). This increased weight loss suggests that the attachment of the amine groups to the MWCNTs has occurred. Further weight losses of 2 and 6 % at 600 $^{o}$C are observed when MWCNT-Glycolic and MWCNT-Citric, respectively, are compared to MWCNT-Amine, indicating that the reaction of the amine groups with glycolic and citric acids has been successful.

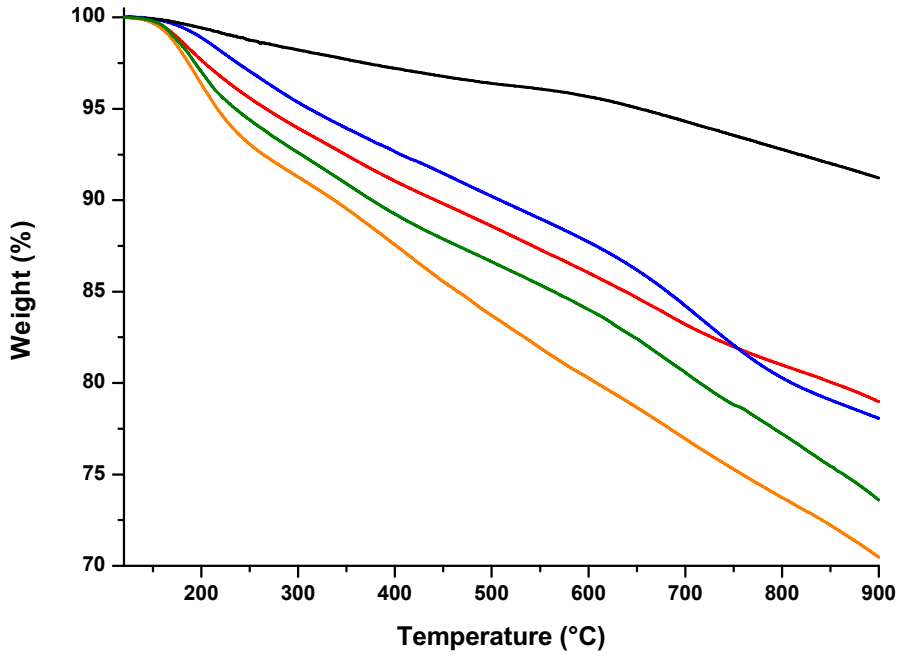


Figure 5.4: TGA results of AR-MWCNTs (black), oxidised MWCNTs (blue), MWCNT-Amine (red), MWCNT-Glycolic (green) and MWCNT-Citric (orange). All the samples were held at 120$^{o}$C for 30 minutes and then heated at a rate of 10$^{o}$C min$^{-1}$ to 900$^{o}$C.

### 5.2.2 UV-vis-NIR Spectroscopy

By applying the Beer Lambert law, as described in Section 3.2.3, the UV-vis-NIR spectra (Figure 5.5) show that the functionalisation of the oxidised MWCNTs with

ethylenediamine was found to result in a significant decrease in MWCNT dispersibility from 0.35 to 0.14 mg/mL. Subsequent functionalisation of MWCNT-Amine with glycolic and citric acid however improved the dispersibility of the MWCNTs to 0.24 and 0.43 mg/mL, respectively, as shown in Figure 5.6.

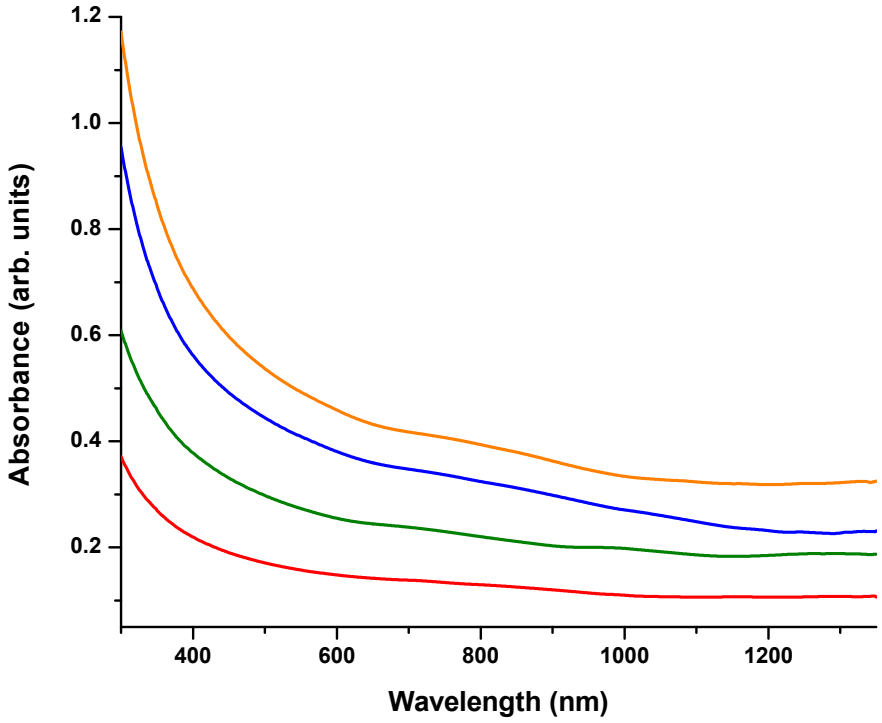


Figure 5.5: UV-vis-NIR spectra in water of oxidised MWCNTs (blue), MWCNT-Amine (red), MWCNT-Glycolic (green) and MWCNT-Citric (orange) (diluted by a factor of 30).

Figure 5.6: Photograph of the dispersions of MWCNT-Glycolic and MWCNT-Citric in water (l-r).

### 5.2.3 Raman Spectroscopy

The Raman spectra of the alpha hydroxy acid functionalised MWCNTs show no significant change in the intensity of the D band when compared to the spectrum for MWCNT-Amine (Figure 5.7). This result is expected because the AHAs are attached to the MWCNTs through the amine groups already present on the MWCNT surface. The spectra therefore give comparable $I_D/I_G$ ratios of 0.087 $\pm$ 2.3 x $10^{-3}$, 0.085 $\pm$ 2.9 x $10^{-3}$, 0.087 $\pm$ 2.8 x $10^{-3}$ and 0.09 $\pm$ 3.2 x $10^{-3}$ for oxidised MWCNTs, MWCNT-Amine, MWCNT-Glycolic and MWCNT-Citric respectively.

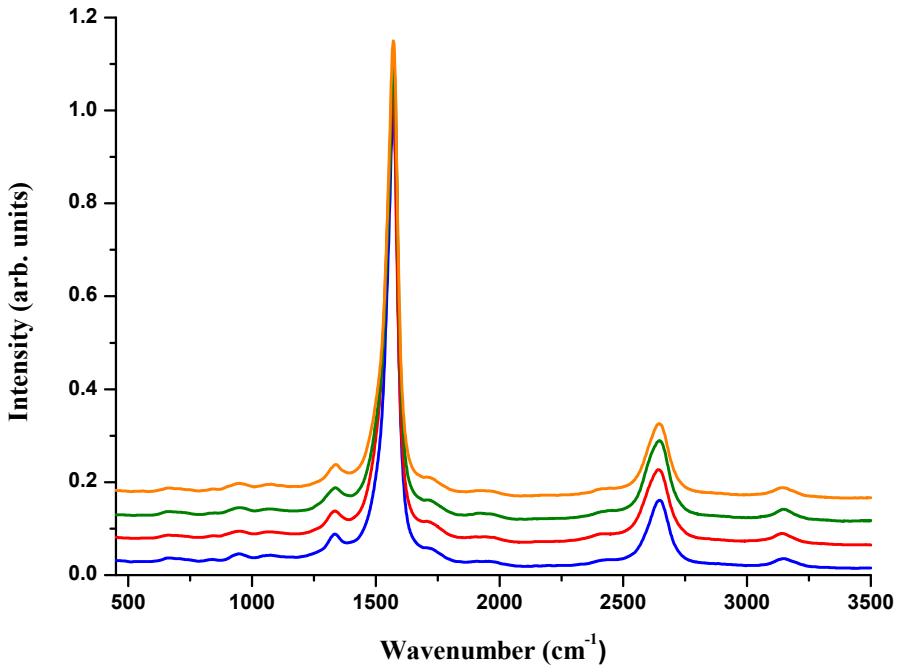


Figure 5.7: Raman spectra (532 nm, 2.33 eV) of oxidised MWCNTs (blue), MWCNT-Amine (red), MWCNT-Glycolic (green) and MWCNT-Citric (orange) normalised at the G band.

## 5.3 Covalent Functionalisation of MWCNTs with Pyridine

Pyridine groups were attached to the nanotube surface by reacting the MWCNTs with a pyridinium diazonium salt, which was prepared by the addition of isoamyl nitrite to 4-aminopyridine in HCl.[51] The acidic conditions of the reaction ensure that the pyridine nitrogen is protonated prior to generation of the diazonium salt, preventing oxidation (Figure 5.8).

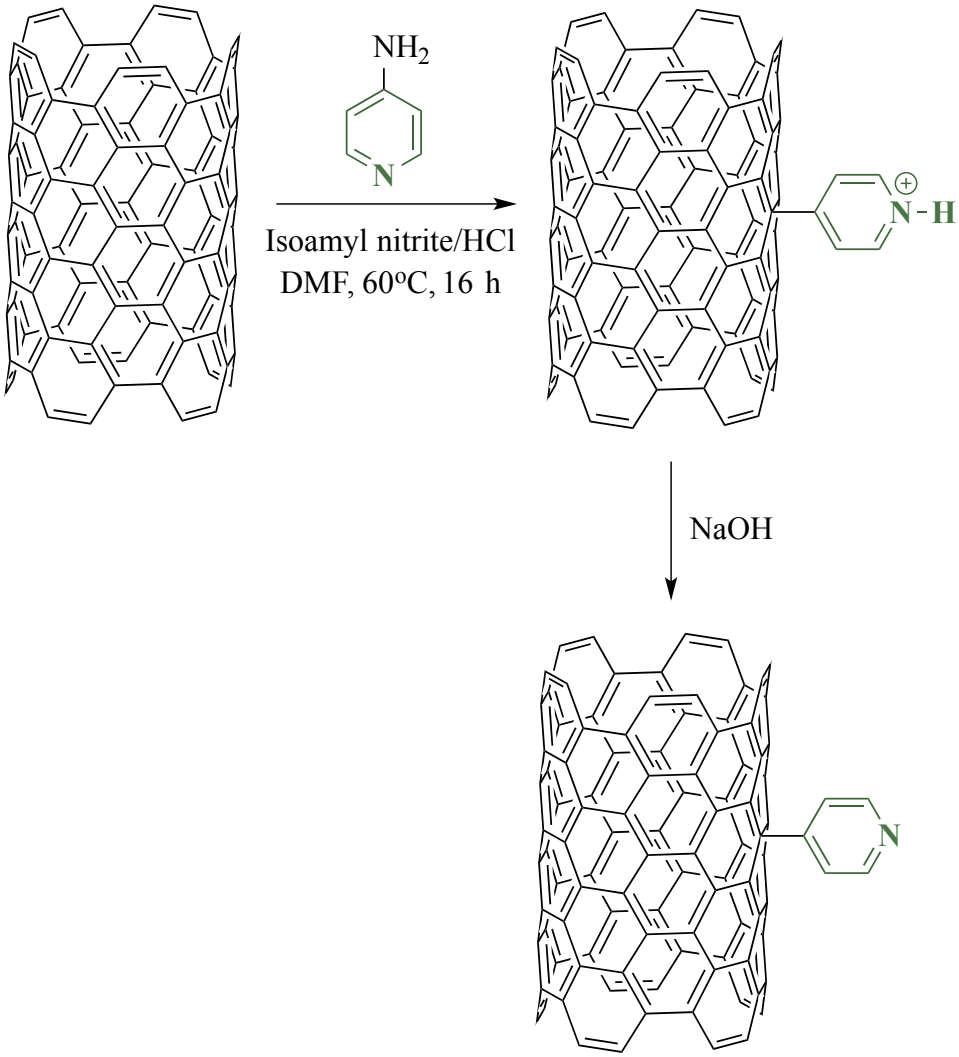


Figure 5.8: Schematic representation of the functionalisation of MWCNTs with pyridine.

### 5.3.1 Thermal Analysis

The TGA data of the pyridine functionalised MWCNTs (MWCNT-Pyridine) shows a further weight loss of 3 % at 600 $^{o}$C when compared to the AR-MWCNTs (Figure 5.9), which corresponds to the presence of 1 functional group per 213 carbon atoms. These values are significantly less than the 18 % weight loss (1 functional group per 30 carbon atoms) reported previously for SWCNTs.[51]

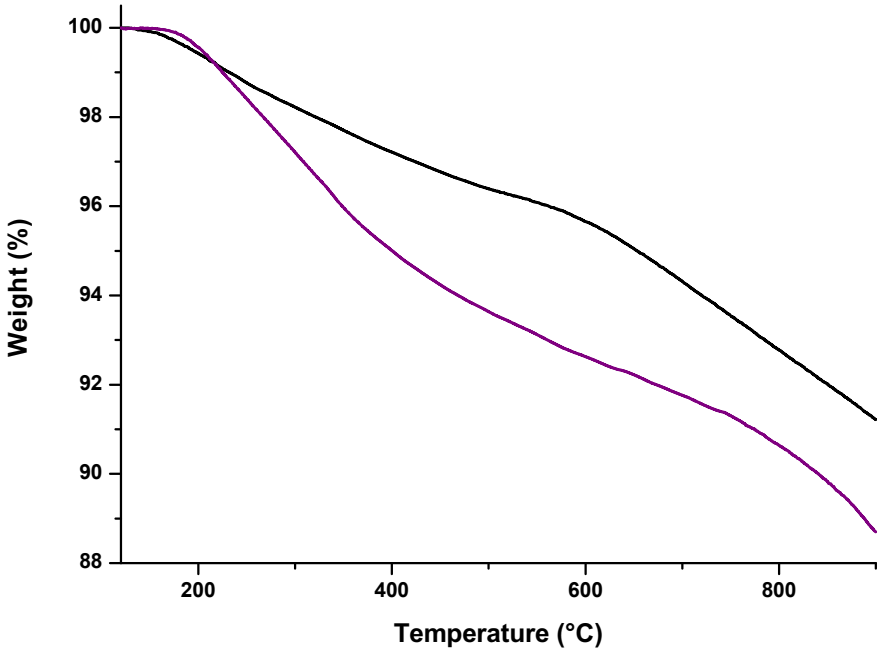


Figure 5.9: TGA results of AR (black) and pyridine functionalised (purple) MWCNTs. All the samples were held at 120$^o$C for 30 minutes and then heated at a rate of 10$^o$C min$^{-1}$ to 900$^o$C.

### 5.3.2 UV-vis-NIR Spectroscopy

The UV-vis-NIR spectra of the AR-MWCNTs and MWCNT-Pyridine are given in Figure 5.10 and by using the absorption values at 700 nm and the extinction coefficient of 28.9 mL mg$^{-1}$ cm$^{-1}$, as outlined in Section 3.2.3, the concentration of MWCNTs in solution can be determined. Functionalisation with pyridine does not facilitate the dispersion of the MWCNTs in water, however an increase in DMF dispersibility from 0 to 1.4 $\mu$g/mL was observed. The observed dispersibility of MWCNT-Pyridine in DMF is however considerably less than the 163 $\mu$g/mL concentration reported before for pyridine functionalised SWCNTs.[51] This improvement in DMF dispersibility can be clearly seen in Figure 5.11 and suggests that the functionalisation of the MWCNTs has been successful.

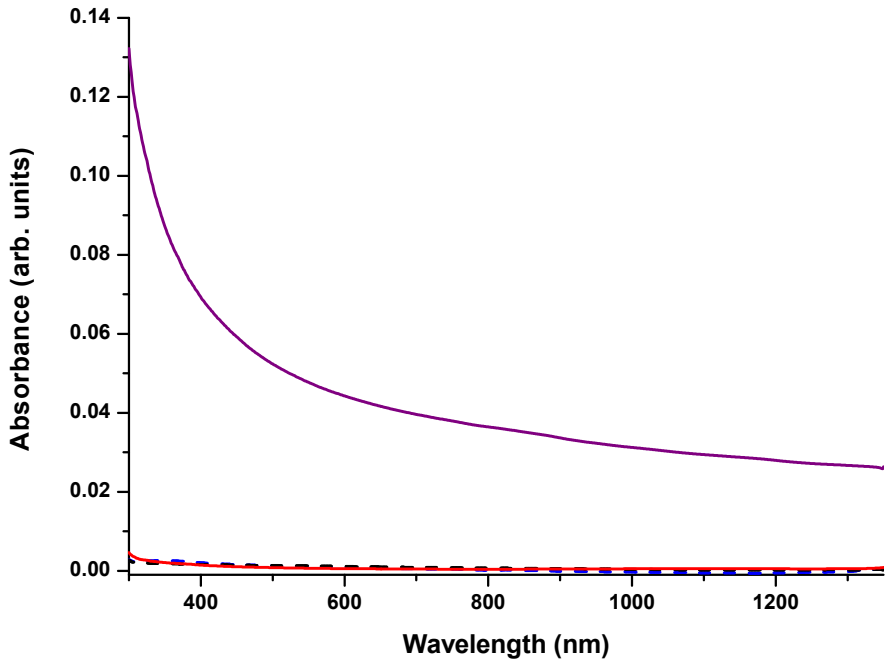


Figure 5.10: UV-vis-NIR spectra of AR-MWCNTs in water (black) and DMF (red) and MWCNT-Pyridine in water (blue) and DMF (purple).

Figure 5.11: Photograph of the dispersion of AR-MWCNTs and MWCNT-Pyridine in DMF (l-r).

### 5.3.3 Raman Spectroscopy

The pyridine functionalised MWCNTs show an enhancement in the intensity of the D band at ca. 1350 $cm^{-1}$ as expected when compared to the spectrum for the AR-MWCNTs (Figure 5.12). MWCNT-Pyridine has a calculated $I_D/I_G$ ratio of 0.045 $\pm$ 1.4 x $10^{-3}$ in comparison to 0.036 $\pm$ 2.1 x $10^{-3}$ for the AR-MWCNTs, which indicates that the introduction of pyridine groups to the nanotube surface has occurred. The $I_D/I_G$ ratios observed for AR-MWCNTs and MWCNT-Pyridine are appreciably lower than the previously reported $I_D/I_G$ ratios of 0.14 and 0.41 for unmodified and pyridine functionalised SWCNTs respectively.[51]

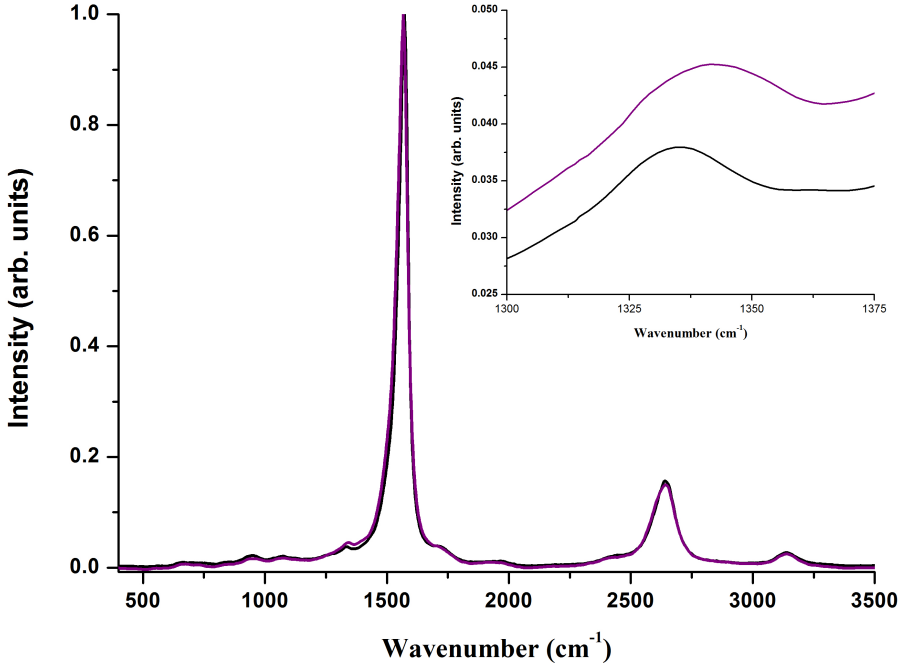


Figure 5.12: Raman spectra (532 nm, 2.33 eV) of AR-MWCNTs (black) and MWCNT-Pyridine (purple) normalised at the G band. Inset: the D band.

## 5.4 Hydroxy Functionalised MWCNTs

Pyridine functionalised MWCNTs were synthesised as described in Section 5.3. The pyridine nitrogen was then used to displace bromine from the bromoalcohols, 2-bromoethanol, 3-bromo-1,2-propanediol and 2-(bromomethyl)-2-(hydroxymethyl)-1,3-propanediol, to give products MWCNT-Hydroxy, MWCNT-Diol and MWCNT-Triol, respectively, as shown in Figure 5.13.

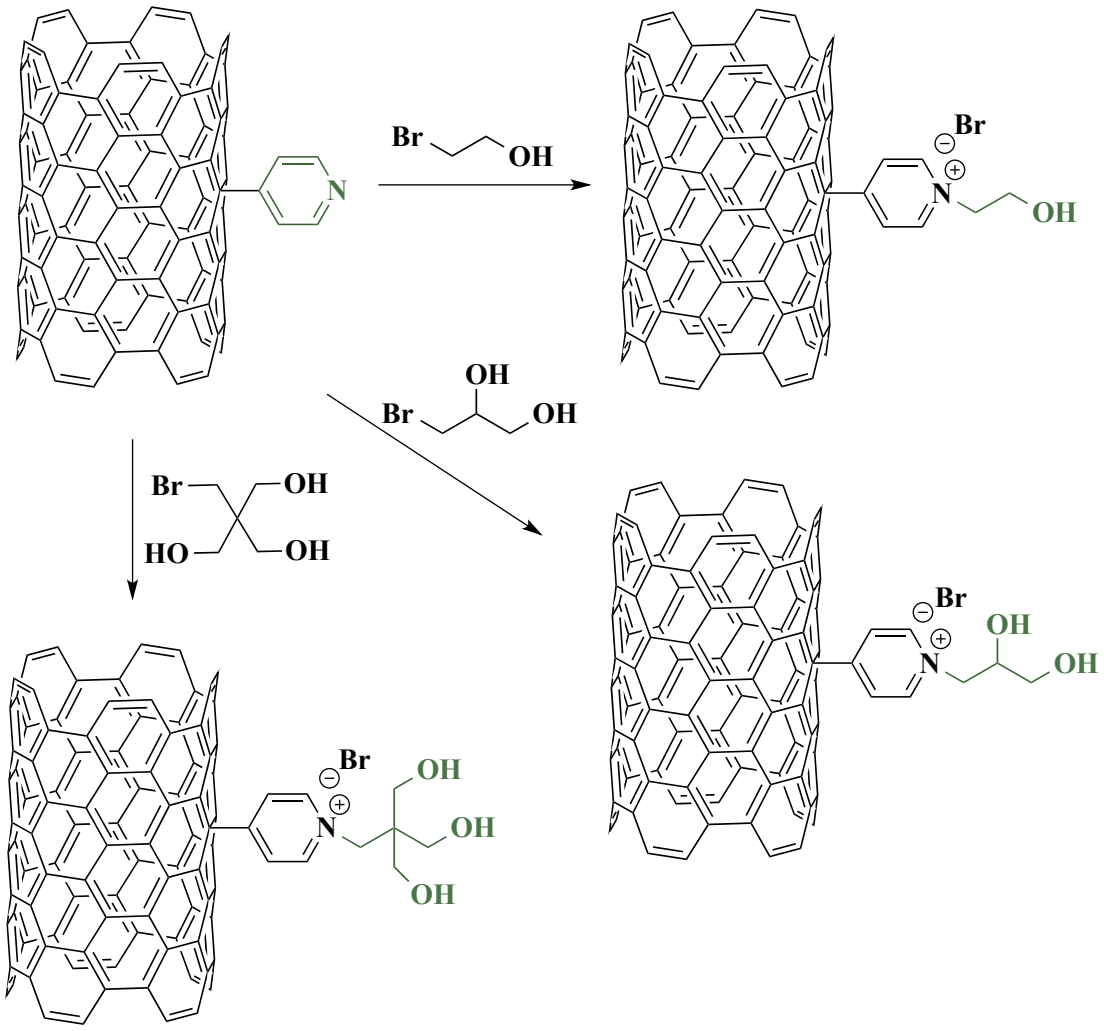


Figure 5.13: Schematic representation of the reaction of 2-bromoethanol, 3-bromo-1,2-propanediol and 2-(bromomethyl)-2-(hydroxymethyl)-1,3-propanediol with MWCNT-Pyridine to give MWCNT-Hydroxy, MWCNT-Diol and MWCNT-Triol, respectively.

### 5.4.1 Thermal Analysis

TGA of MWCNT-Hydroxy, MWCNT-Diol and MWCNT-Triol display a weight loss of 1.7, 2.0 and 2.5 %, respectively, at 600 $^{o}$C when compared to the pyridine functionalised MWCNTs (Figure 5.14). This additional weight loss suggests that the reaction of 2-bromoethanol, 3-bromo-1,2-propanediol and 2-(bromomethyl)-2-(hydroxymethyl)-1,3-

propanediol with the pyridine groups present on the MWCNT surface has occurred.

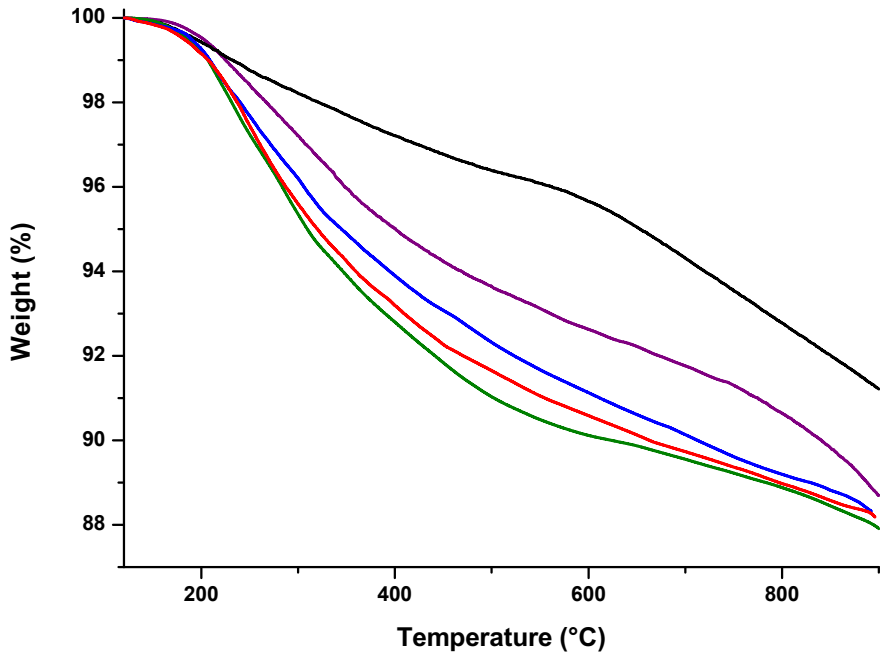


Figure 5.14: TGA results of AR-MWCNTs (black), MWCNT-Pyridine (purple), MWCNT-Hydroxy (blue), MWCNT-Diol (red) and MWCNT-Triol (green). All the samples were held at 120$^o$C for 30 minutes and then heated at a rate of 10$^o$C min$^{-1}$ to 900$^o$C.

### 5.4.2 UV-vis-NIR Spectroscopy

The hydroxy functionalised MWCNTs can be dispered in water through probe sonication, and the UV-vis-NIR spectra of these dispersions are shown in Figure 5.15. The concentration of MWCNT-Pyridine, MWCNT-Hydroxy, MWCNT-Diol and MWCNT-Triol in water after probe sonciation was determined from their UV-vis-NIR spectra, as outlined in Section 3.2.3, and the results are given in Table 5.1. All of the hydroxy functionalised MWCNTs display an improved dispersibility in water, when compared to MWCNT-Pyridine. The highest concetration recorded was for the MWCNT-Triol, which is presumably due to the greater number of hydroxy functional groups present.

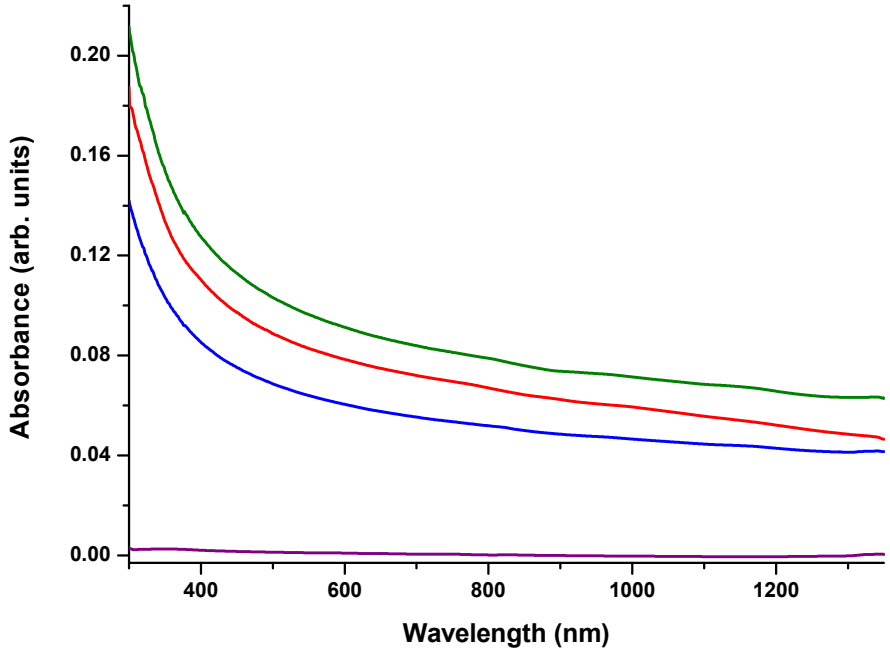


Figure 5.15: UV-vis-NIR spectra of the dispersions of MWCNT-Pyridine (purple), MWCNT-Hydroxy (blue), MWCNT-Diol (red) and MWCNT-Triol (green) in water after probe sonication.

| MWCNT Sample | MWCNT Concentration ($\mu$g/mL) |
|---|---|
| Pyridine | 0 |
| Hydroxy | 1.9 |
| Diol | 2.5 |
| Triol | 2.9 |

Table 5.1: Concentration ($\mu$g/mL) of MWCNT-Pyridine, MWCNT-Hydroxy, MWCNT-Diol and MWCNT-Triol in water after probe sonication.

### 5.4.3 Raman Spectroscopy

The Raman spectra of the series of hydroxy functionalised MWCNTs are shown overlaid for comparison with the spectrum of MWCNT-Pyridine in Figure 5.16. The spectra

show no significant change in the intensity of the D band when compared to the spectrum for MWCNT-Pyridine and so give similar $I_D/I_G$ ratios of 0.063 ± 1.4 x $10^{-3}$, 0.065 ± 2.0 x $10^{-3}$, 0.062 ± 1.9 x $10^{-3}$ and 0.063 ± 2.4 x $10^{-3}$ for MWCNT-Pyridine, MWCNT-Hydroxy, MWCNT-Diol and MWCNT-Triol respectively.

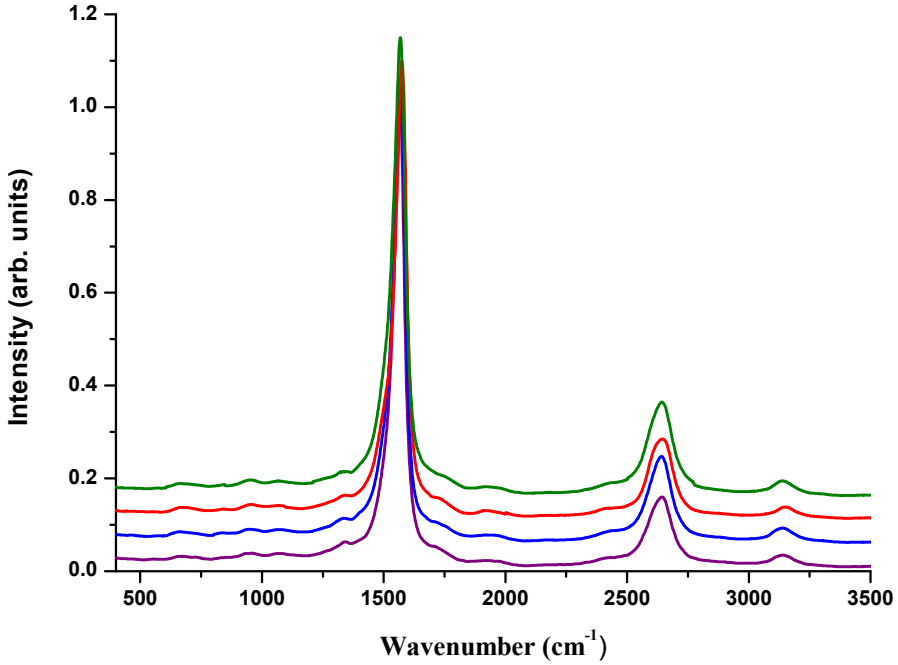


Figure 5.16: Raman spectra (532 nm, 2.33 eV) of MWCNT-Pyridine (purple), MWCNT-Hydroxy (blue), MWCNT-Diol (red) and MWCNT-Triol (green) normalised at the G band.

## 5.5 Ribonucleoside Functionalised MWCNTs

Following on from the successful further functionalisation of MWCNT-Pyridine by using the pyridine nitrogen to displace bromine from a series of bromoalcohols (Section 5.4), the same method was tried with the bromo-substituted ribonucleoside derivatives, 5-bromouridine and 8-bromoadenosine to give MWCNT-Uridine and MWCNT-Adenosine, respectively, as outlined in Figure 5.17.

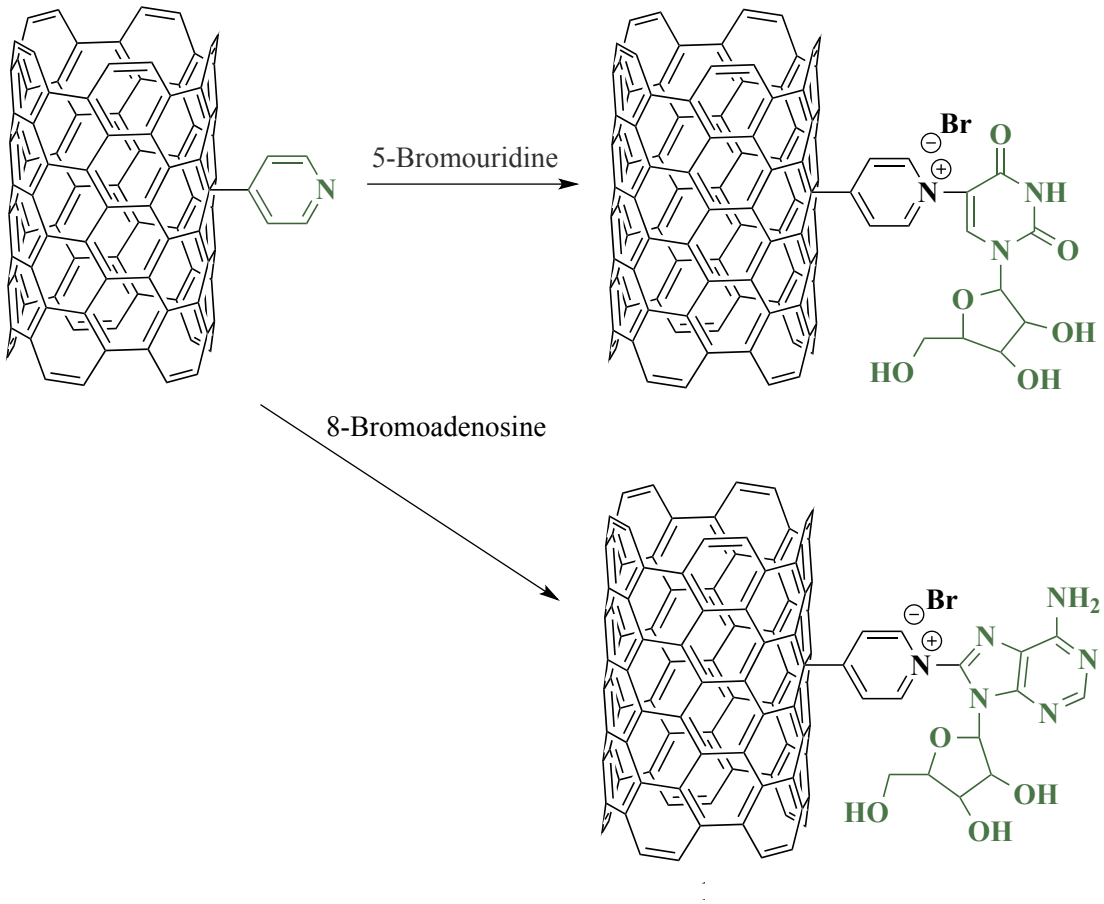


Figure 5.17: Schematic representation of the reaction of 5-bromouridine and 8-bromoadenosine with MWCNT-Pyridine to give MWCNT-Uridine (top) and MWCNT-Adenosine (bottom), respectively.

### 5.5.1 Thermal Analysis

TGA of MWCNT-Uridine and MWCNT-Adenosine both display a further weight loss of 4 % at 600 $^{o}$C when compared to the pyridine functionalised MWCNTs (Figure 5.18). This additional weight loss suggests that the attachment of uridine and adenosine to the pyridine groups present on the MWCNT surface has occurred.

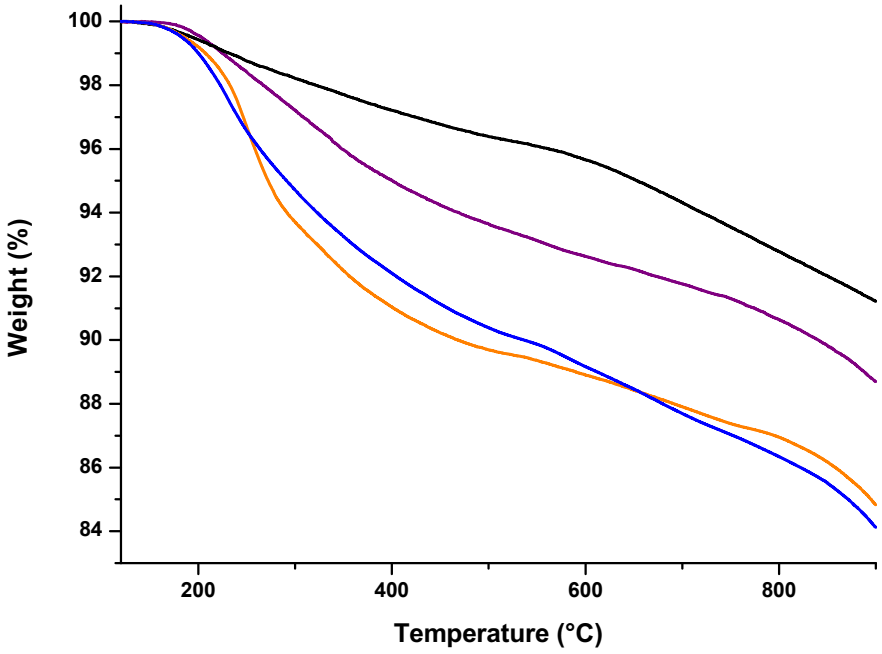


Figure 5.18: TGA results of AR-MWCNTs (black), MWCNT-Pyridine (purple), MWCNT-Uridine (orange) and MWCNT-Adenosine (blue). All the samples were held at 120$^o$C for 30 minutes and then heated at a rate of 10$^o$C min$^{-1}$ to 900$^o$C.

### 5.5.2 UV-vis-NIR Spectroscopy

MWCNT-Pyridine is insoluble in water, however after functionalisation with uridine and adenosine the MWCNTs can be dispersed in water through probe sonication. An MWCNT concentration of 1.5 and 0.4 $\mu$g/mL was determined from the UV-vis-NIR spectra (Figure 5.19), as outlined in Section 3.2.3, for MWCNT-Uridine and MWCNT-Adenosine, respectively.

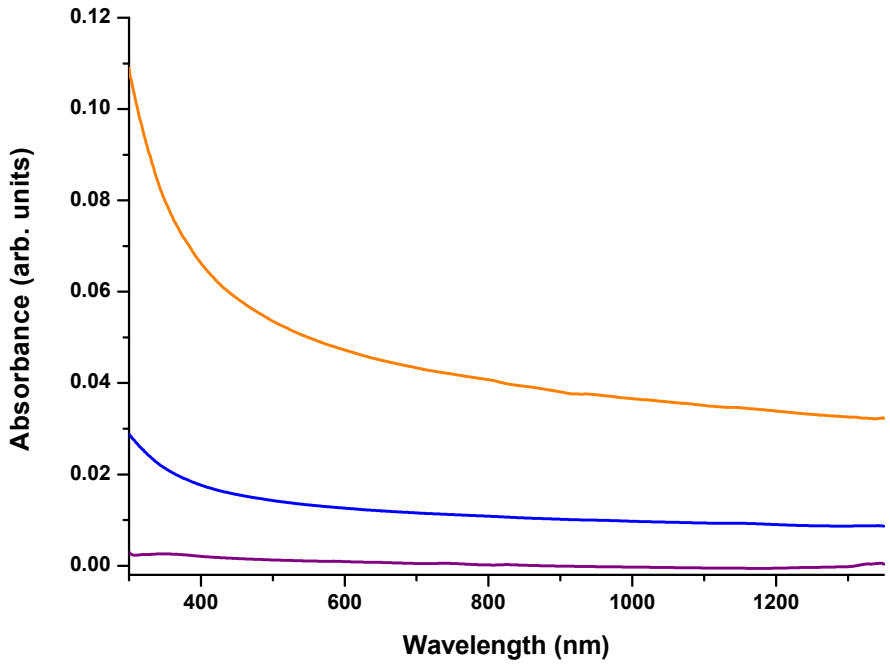


Figure 5.19: UV-vis-NIR spectra of the dispersions of MWCNT-Pyridine (purple), MWCNT-Uridine (orange) and MWCNT-Adenosine (blue) in water after probe sonication.

### 5.5.3 Raman Spectroscopy

The Raman spectra of the nucleoside functionalised MWCNTs do not show a considerable difference in the intensity of the D band when compared to the spectrum for MWCNT-Pyridine (Figure 5.20). Similar $I_D/I_G$ ratios of 0.063 $\pm$ 1.4 x $10^{-3}$, 0.064 $\pm$ 1.4 x $10^{-3}$ and 0.061 $\pm$ 2.3 x $10^{-3}$ for MWCNT-Pyridine, MWCNT-Uridine and MWCNT-Adenosine respectively are observed, as expected, because the ribonucleosides are attached to the MWCNTs through the pyridine groups already present on the MWCNT surface.

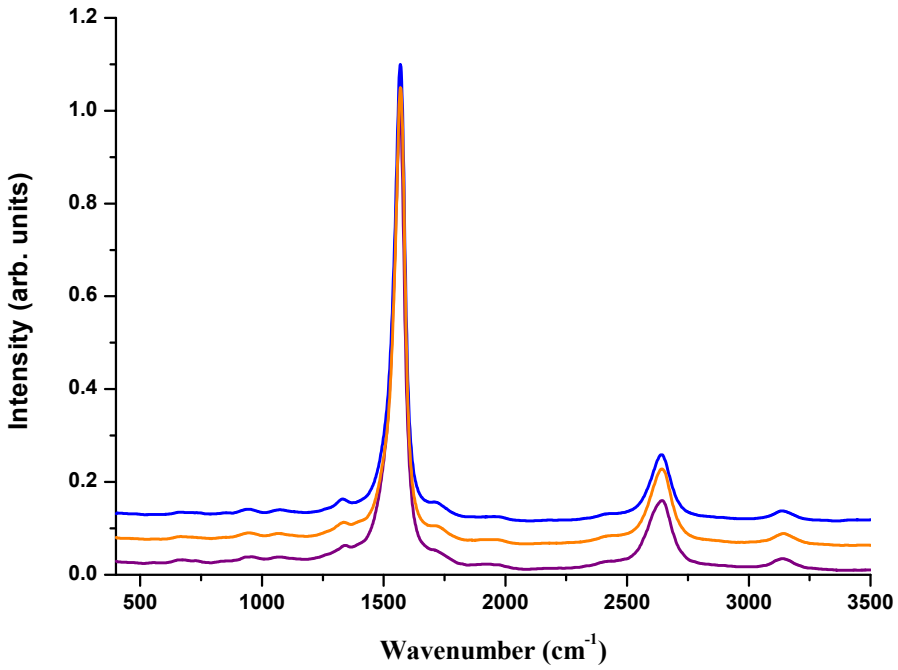


Figure 5.20: Raman spectra (532 nm, 2.33 eV) of MWCNT-Pyridine (purple), MWCNT-Uridine (orange) and MWCNT-Adenosine (blue) normalised at the G band.

## 5.6 Sugar Functionalised MWCNTs

The simple sugars ribose, fructose and sucrose were covalently attached to MWCNT-Pyridine, as outlined in Figure 5.21. The pyridine nitrogen reacted with bromoacetyl bromide to give MWCNT-Bromide which was further reacted with ribose, fructose and sucrose in the presence of the base DIPEA to give products MWCNT-Ribose, MWCNT-Fructose and MWCNT-Sucrose.

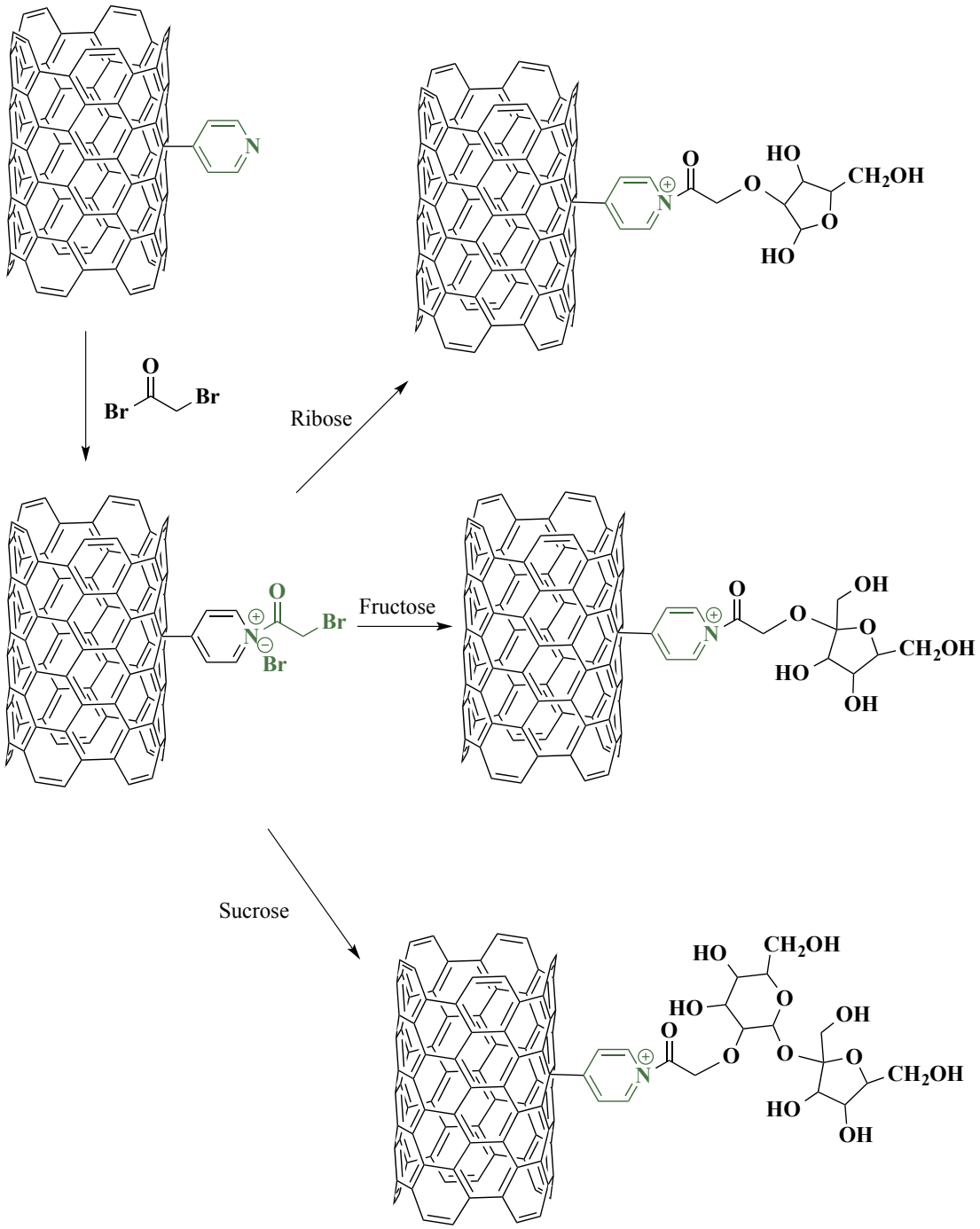


Figure 5.21: Schematic representation of the the covalent attachment of ribose, fructose and sucrose to MWCNT-Pyridine to give MWCNT-Ribose (top), MWCNT-Fructose (middle) and MWCNT-Sucrose (bottom), respectively.

### 5.6.1 Thermal Analysis

At 600 $^{o}$C TGA of CNT-Bromide demonstrates a further weight loss of 1.5 %, when compared to pyridine functionalised MWCNTs (Figure 5.22), which suggests that the reaction of MWCNT-Pyridine with bromoacetyl bromide has occurred. Comparison of the TGA of MWCNT-Ribose, MWCNT-Fructose and MWCNT-Sucrose with MWCNT-Bromide shows an additional weight loss of 5, 7 and 9 %, respectively, indicating that the covalent attachment of the sugars to the MWCNTs has occurred.

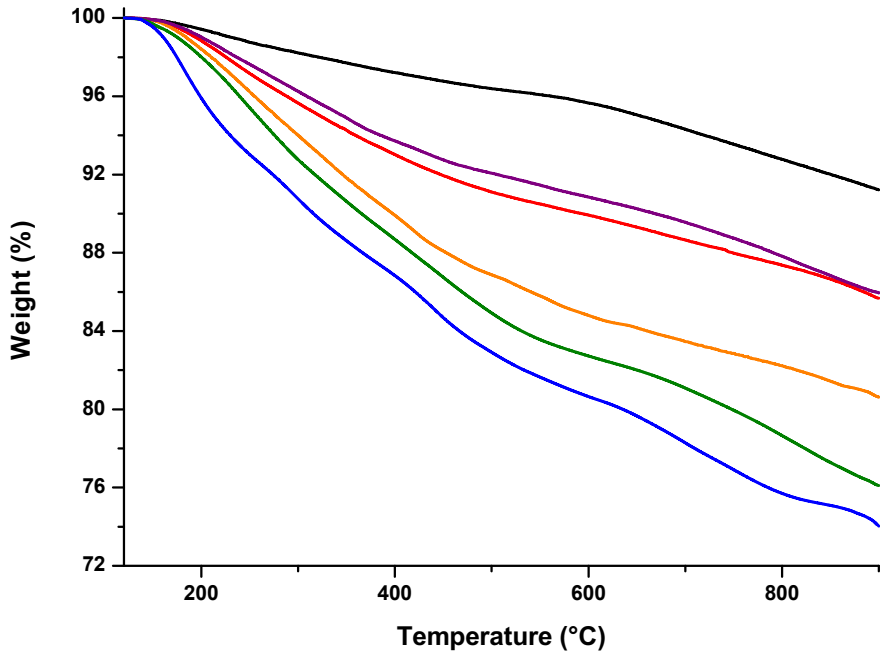


Figure 5.22: TGA results of AR-MWCNTs (black), MWCNT-Pyridine (purple), MWCNT-Bromide (red), MWCNT-Ribose (orange), MWCNT-Fructose (green) and MWCNT-Sucrose (blue). All the samples were held at 120$^{o}$C for 30 minutes and then heated at a rate of 10$^{o}$C min$^{-1}$ to 900$^{o}$C.

### 5.6.2 UV-vis-NIR Spectroscopy

Pyridine functionalised MWCNTs are insoluble in water and after reaction with bromoacetyl bromide the MWCNTs remain insoluble in water (Figure 5.23). However,

functionalisation of MWCNT-Bromide with the selected simple sugars enables the MWCNTs to be dispersed in water using probe sonication, as can be seen in Figure 5.24. The effect of functionalisation with ribose, fructose and sucrose on MWCNT aqueous dispersibility was determined from Figure 5.23, using the method outlined in Section 3.2.3, and the results are shown in Table 5.2.

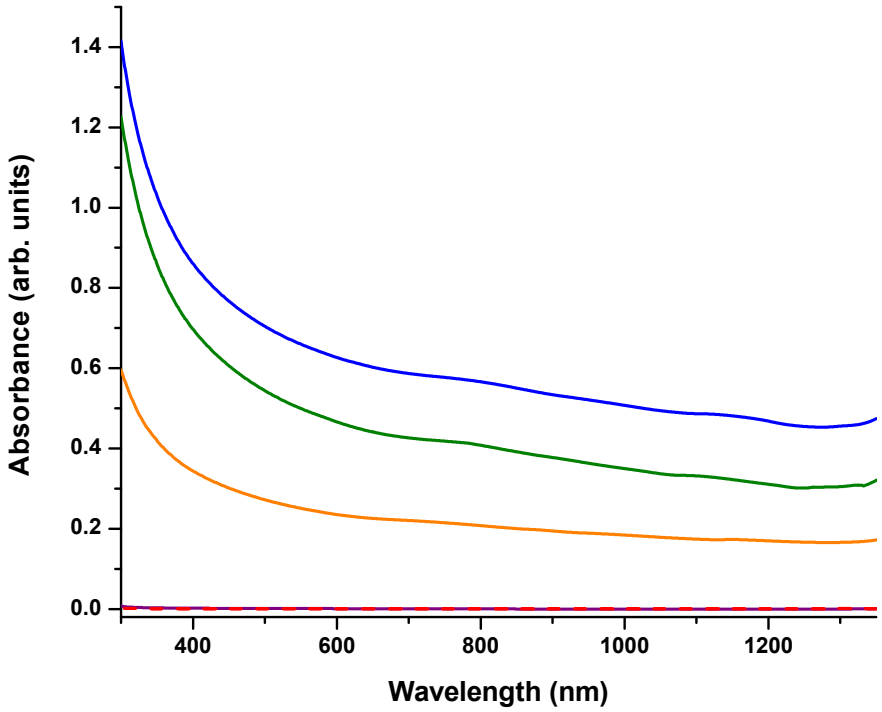


Figure 5.23: UV-vis-NIR spectra of MWCNT-Pyridine (purple), MWCNT-Bromide (red), MWCNT-Ribose (orange), MWCNT-Fructose (green) and MWCNT-Sucrose (blue) normalised at the G band.

Figure 5.24: Photograph of the dispersions of MWCNT-Ribose, MWCNT-Fructose and MWCNT-Sucrose in water (l-r).

| MWCNT Sample | MWCNT Concentration ($\mu$g/mL) |
|---|---|
| Pyridine | 0 |
| Bromide | 0 |
| Ribose | 7.6 |
| Fructose | 15.0 |
| Sucrose | 20.0 |

Table 5.2: Concentration ($\mu$g/mL) of MWCNT-Pyridine, MWCNT-Bromide, MWCNT-Ribose, MWCNT-Fructose and MWCNT-Sucrose in water after probe sonication.

### 5.6.3 Raman Spectroscopy

The Raman spectrum of MWCNT-Pyridine is shown overlaid for comparison with the spectra of MWCNT-Bromide and the sugar functionalised MWCNTs in Figure 5.25. The spectra display comparable $I_D/I_G$ ratios of 0.063 ± 1.4 x $10^{-3}$, 0.064 ± 1.2 x $10^{-3}$, 0.062 ± 3.2 x $10^{-3}$, 0.060 ± 2.8 x $10^{-3}$ and 0.064 ± 1.7 x $10^{-3}$ for MWCNT-Pyridine, **13**, MWCNT-Ribose, MWCNT-Fructose and MWCNT-Sucrose, as expected, because the sugars are attached to the MWCNTs through the pyridine groups already present

on the MWCNT surface.

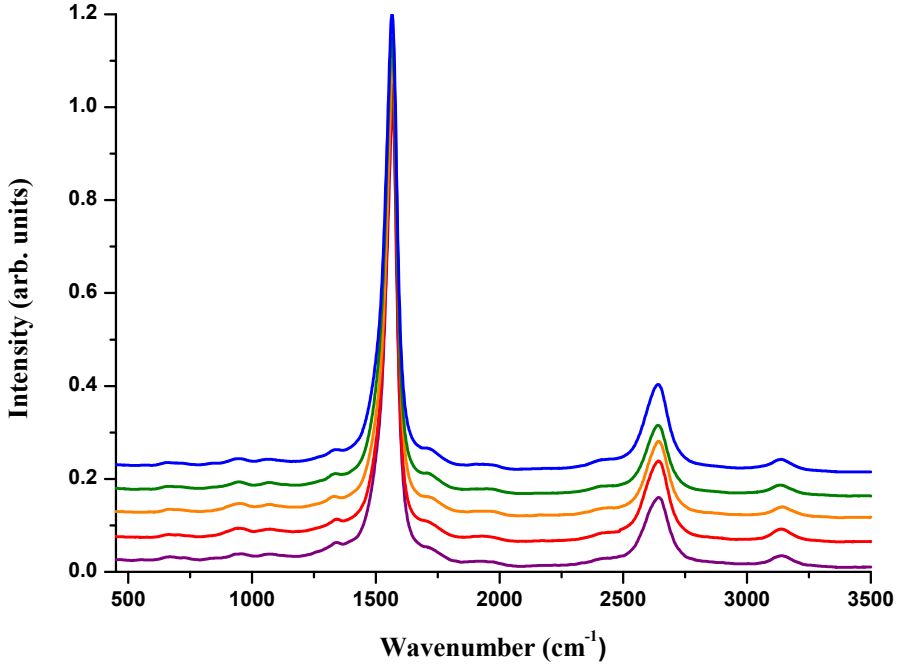


Figure 5.25: Raman spectra (532 nm, 2.33 eV) of MWCNT-Pyridine (purple), MWCNT-Bromide (red), MWCNT-Ribose (orange), MWCNT-Fructose (green) and MWCNT-Sucrose (blue) normalised at the G band.

## 5.7 Covalent Functionalisation of MWCNTs with Poly(ethylene glycol)

The water-soluble polymer poly(ethylene glycol) (PEG) was covalently attached to MWCNT-Pyridine, as shown in Figure 5.26. Pyridine functionalised MWCNTs reacted with bromoacetyl bromide to give MWCNT-Bromide, as in Section 5.6. The hydroxy end groups of $PEG_{400}$ were deprotonated with DIPEA and reacted with MWCNT-Bromide to give PEG functionalised MWCNTs (MWCNT-PEG).

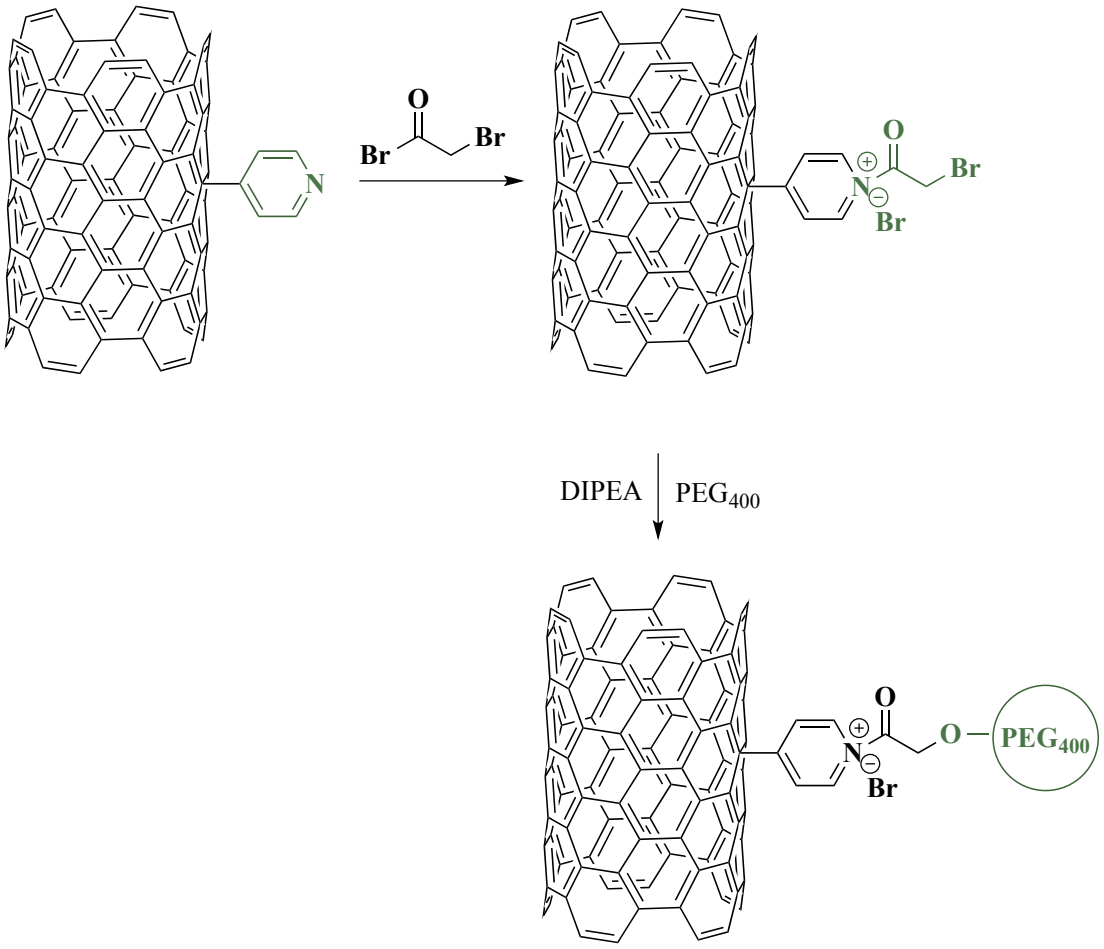


Figure 5.26: Schematic representation of the the covalent attachment of $PEG_{400}$ to CNT-Bromide to give MWCNT-PEG.

### 5.7.1 Thermal Analysis

TGA of MWCNT-Bromide displays a further weight loss of 1.5 % at 600 $^{o}$C when compared to MWCNT-Pyridine (Figure 5.27), suggesting that the reaction of bromoacetyl bromide with the pyridine groups present on the MWCNT surface has occurred. TGA of MWCNT-PEG shows an additional weight loss of 10 % at 600 $^{o}$C when compared to MWCNT-Bromide, which indicates that the attachment of PEG to the MWCNTs has been successful.

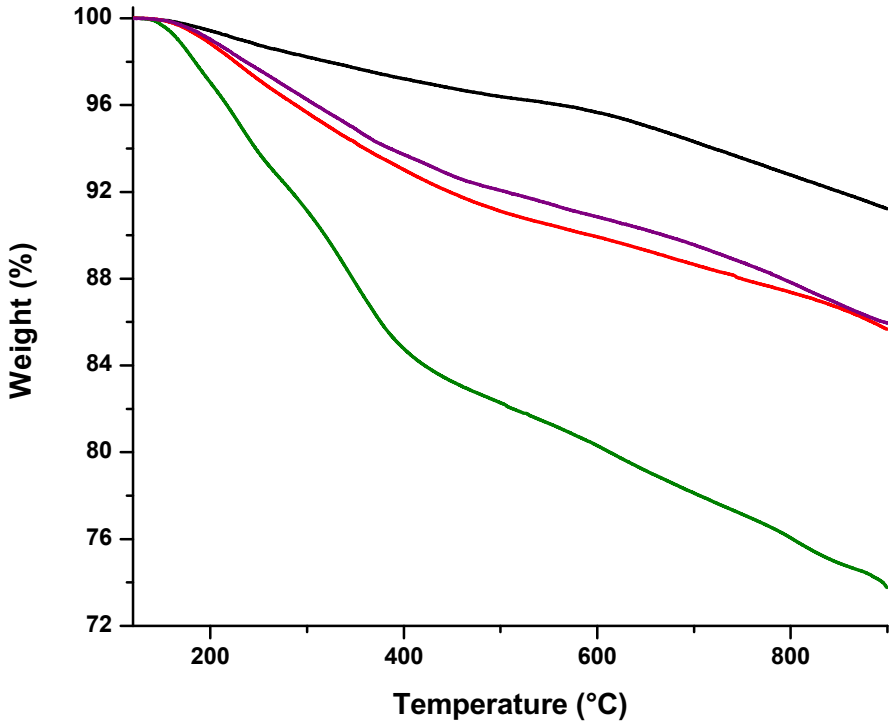


Figure 5.27: TGA results of AR-MWCNTs (black), MWCNT-Pyridine (purple), MWCNT-Bromide (red) and MWCNT-PEG (green). All the samples were held at 120$^o$C for 30 minutes and then heated at a rate of 10$^o$C min$^{-1}$ to 900$^o$C.

### 5.7.2 UV-vis-NIR Spectroscopy

As demonstrated in Section 5.6.2 the dispersibility of the pyridine functionalised MWCNTs in water is 0 $\mu$g/mL, and this remains unchanged after the reaction with bromoacetyl bromide (Figure 5.29). Functionalisation with PEG however facilitates the dispersion of the MWCNTs in water through probe sonication, as shown in Figure 5.28. From the UV-vis-NIR spectrum (Figure 5.29) and by using the method outlined in Section 3.2.3 it was determined that PEG functionalisation improves MWCNT dispersibility to 30 $\mu$g/mL.

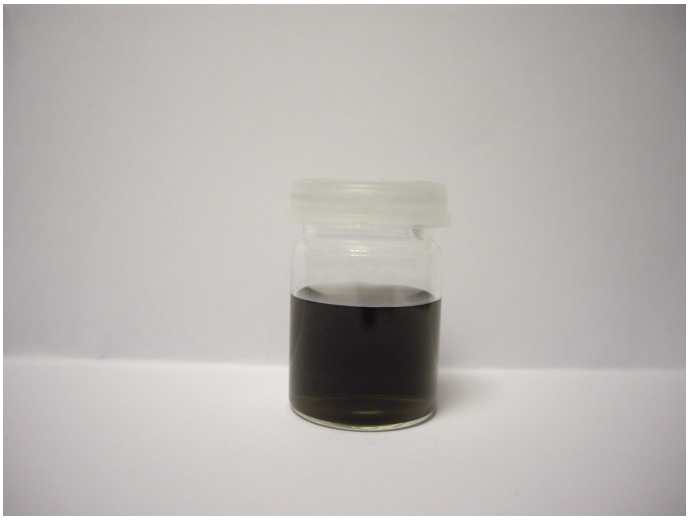

Figure 5.28: Photograph of the dispersion of MWCNT-PEG in water.

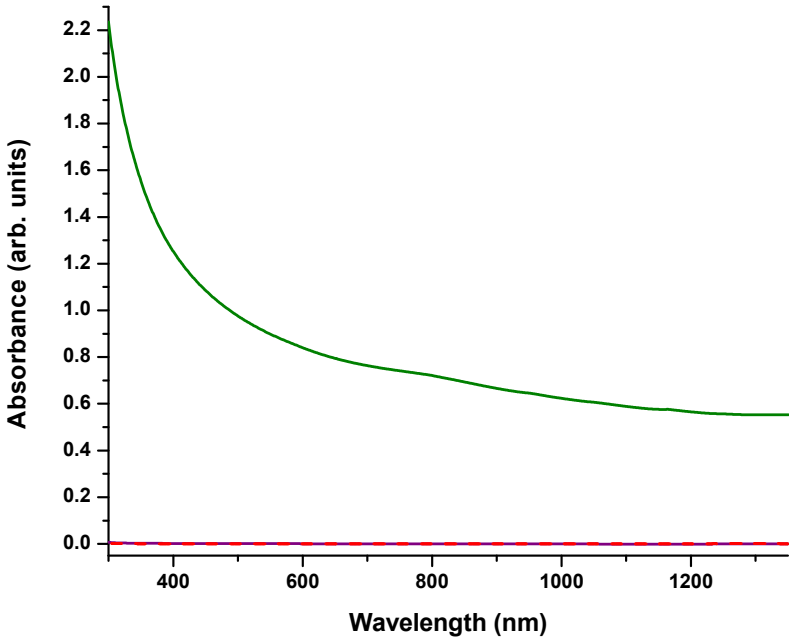


Figure 5.29: UV-vis-NIR spectra of MWCNT-Pyridine (purple), MWCNT-Bromide (red) and MWCNT-PEG (green) in water.

### 5.7.3 Raman Spectroscopy

The Raman spectrum of MWCNT-PEG is shown overlaid with the spectra for MWCNT-Pyridine and MWCNT-Bromide in Figure 5.30. No significant change in the intensity of the D band is expected as PEG is attached to the MWCNTs through the pyridine groups already on the MWCNT surface, and so, as anticipated, the spectra of MWCNT-Pyridine, MWCNT-Bromide and MWCNT-PEG give comparable $I_D/I_G$ ratios of 0.063 ± 1.4 x $10^{-3}$, 0.064 ± 1.2 x $10^{-3}$ and 0.061 ± 2.0 x $10^{-3}$ respectively.

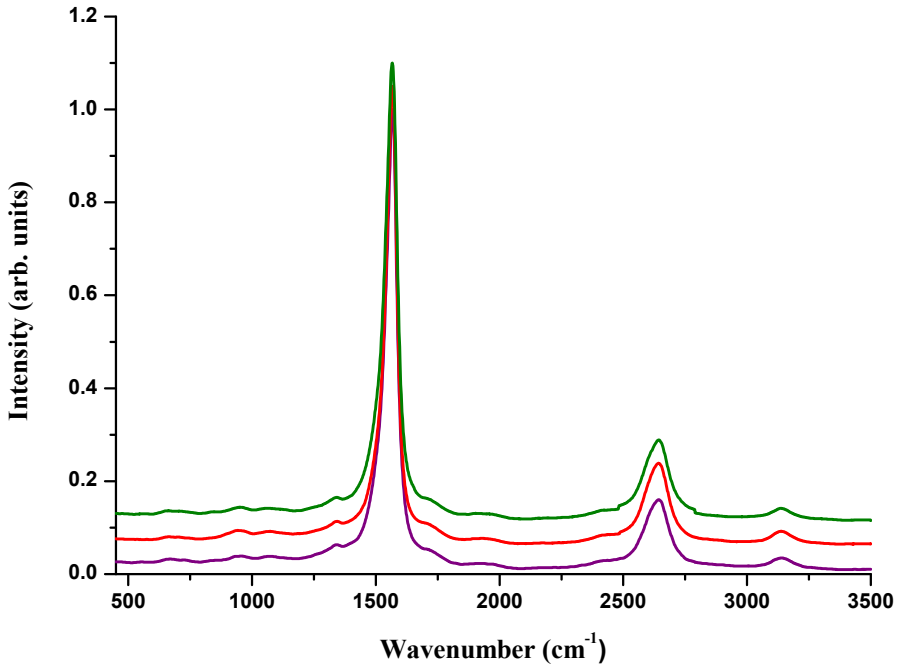


Figure 5.30: Raman spectra (532 nm, 2.33 eV) of MWCNT-Pyridine (purple), MWCNT-Bromide (red) and MWCNT-PEG (green) normalised at the G band.

## 5.8 Conclusion

The attachment of the alpha-hydroxy acids, glycolic and citric acid, to MWCNTs was achieved through amide bond formation with amine functionalised MWCNTs, which had themselves been prepared by the reaction of oxidised MWCNTs with ethylenedi-

amine. The UV-vis-NIR spectra indicated that functionalisation with citric acid had the overall effect of slightly improving the dispersibility of the MWCNTs above the level achieved by just oxidation. On the other hand despite functionalisation with glycolic acid improving MWCNT dispersibility beyond that observed for MWCNT-Amine, the dispersibility was not improved to the extent that could be achieved simply by oxidation.

The attachment of pyridine groups to the surface of SWCNTs through a diazonium reaction has been described previously,[51] and in this chapter pyridine groups were introduced to the MWCNT surface using in situ generated pyridine diazonium salts, which were prepared by the addition of isoamyl nitrite to *p*-aminopyridine in hydrochloric acid. The pyridine functionalised MWCNTs display an improved dispersibility in DMF but remain insoluble in water. The pyridine nitrogen is capable of displacing bromine from a variety of compounds, and so several strategies to further functionalise the MWCNTs using the attached pyridine were developed to try to improve the aqueous dispersibility of the pyridine modified MWCNTs.

Hydroxy functionalised SWCNTs, which display an improved dispersibility in polar solvents, have been produced before through the displacement of fluorine from fluorinated SWCNTs by a series of diols, glycerol and amino alcohols.[121] In this chapter a series of bromoalcohols were used to functionalise MWCNT-Pyridine and of those tried 2-(bromomethyl)-2-(hydroxymethyl)-1,3-propanediol provided the greatest improvement in MWCNT dispersibility, as determined from the UV-vis-NIR spectra, seemingly due to the presence of a greater number of hydroxy functional groups.[121] In the same manner, MWCNT-Pyridine was also covalently functionalised with the bromo-substituted ribonucleosides uridine and adenosine. The UV-vis-NIR spectra indicated that ribonucleosides have a limited dispersion affinity towards the MWCNTs with uridine providing a greater improvement than adenosine, presumably due to the greater aqueous solubility of uridine.

The bromine displacement reaction was then extended to non-brominated compounds by reacting the pyridine groups on the MWCNT surface with bromoacetyl bromide. The three simple sugars ribose, fructose and sucrose were then covalently attached to the MWCNTs by displacement of bromine from the modified pyridine groups on the MWCNTs. Of the sugars used functionalisation with sucrose was found to result in the greatest improvement in MWCNT dispersibility to 20 $\mu$g/mL. This result is

however five times lower than the previously recorded 100 $\mu$g/mL concentration that was reportedly achieved for surcose functionalised SWCNTs which were synthesised through substitution of fluorine from fluorinated SWCNTs by sucrose.[297]

It was also shown that the polymer poly(ethylene glycol) (PEG) could be attached to MWCNT-Pyridine using the same bromine displacement method as used for sugars, which resulted in an even greater improvement in MWCNT dispersibility than was observed through sugar functionalisation. Moderate aqueous dispersibility of SWCNTs functionalised with PEG has been reported before, however in this case amine terminated PEG was used to form an amide bond with oxidised SWCNTs to yield PEG functionalised SWCNTs.[196]

# Chapter 6

# Experimental Details

## 6.1 Materials

The MWCNTs used were received as a wet cake (MWCNT content 3.56 %) from Thomas Swan Ltd (UK), synthesised by the CVD method. All chemicals were purchased from Sigma Aldrich and used without further purification unless otherwise stated.

## 6.2 Analytical Instruments

### 6.2.1 Thermogravimetric Analysis

Thermogravimetric analysis (TGA) data were recorded on 1-2 mg of MWCNT sample using a Perkin-Elmer Pyris I. Data were recorded in flowing He (20 mL $min^{-1}$) at a ramp rate of 10 $^{o}$C $min^{-1}$ to 900 $^{o}$C after being held at 120 $^{o}$C for 30 min to remove any residual solvent.

### 6.2.2 Raman Spectroscopy

Raman spectra were recorded using a HORIBA Jobin Yvon LabRAM HR Evolution spectrometer in a back scattered confocal configuration using Nd:YAG (532 nm, 2.33 eV) laser excitation. All samples were prepared by drop casting onto glass slides and

air drying. All spectra were recorded on the solid samples over five regions and were referenced to the silicon line at 520 $cm^{-1}$ and normalised to the G band.

### 6.2.3 UV-vis-NIR Spectroscopy

The UV-vis-NIR absorption spectra were recorded on a Perkin-Elmer Lambda 900 spectrometer using quartz cells with a 1 cm path length over a wavelength range of 300-1350 nm. The samples were prepared by sonicating the MWCNTs in the appropriate solvent using either an ultrasonic bath (Ultrawave U50, 30-40 kHz) for 30 mins or probe sonication (Cole Parmer Ultrasonic Processor (750 W) for 10 min (30% amplitude, pulse 1 sec on: 1 sec off) with the temperature of the samples during sonication controlled using an external ice bath. The dispersions were then left to settle overnight and filtered through a cotton wool plug to remove particulates. Where necessary the samples were diluted prior to measurement and the absorbance of the original solution was found by multiplying the obtained value by the dilution factor.

### 6.2.4 FTIR Spectroscopy

Infrared spectra were recorded on a Bruker Fourier transform infrared spectrometer (Vector 22 model) working with a globar lamp source, a KBr beam splitter and DTGS/KBr detector. The spectra were recorded in the solid state in KBr pellets in the range 400-4000 $cm^{-1}$ with a resolution of 4 $cm^{-1}$ and employing 32 repetitive scans to obtain a good signal-to-noise ratio. The spectra were first subtracted for the KBr pellet baseline before recording.

### 6.2.5 Transmission Electron Microscopy

Bright-field TEM images were taken using a JEOL 2100F 200 kV FEG-TEM operated at 80 kV. Samples were prepared by dispersing the material in water and pipetting a few drops onto a holey carbon film supported by a copper grid (300 mesh).

### 6.2.6 Electrical Conductivity Measurements

Sheet resistance measurements were recorded using a Keithley 2602 Source Measure Unit (SMU) and a Guardian SRM232-PROBE-625-45-TC-R=10-FH4-point, in-line

probe head. The voltage was swept between -2 to 2 V with a 150 points linear sweep, a compliance of 0.1 A and a sweep delay of 100 ms, and correction factors were applied to correct for the sample geometry.

## 6.3 Experiments

The percentage yields were calculated by dividing the amount of MWCNT product obtained by the amount of MWCNT starting material and then multiplying by 100.

### 6.3.1 Determination of the Extinction Coefficient of MWCNTs in 1% Sodium Dodecyl Sulfate

As received MWCNTs (2.5 mg, 0.2 mmol), that had been dried overnight under vacuum at 60 $^{o}$C, were dispersed in 1% SDS solution (25 mL) using an ultrasonic bath (Ultrawave U50, 30-40 kHz) for 3 min and then probe sonicated (Cole Parmer VC-750 Watt) in an ice bath for a further 30 min (40% amplitude). The resulting dispersion was left to settle for 2 h before removing the supernatant solution and refilling to 25 mL using the stock SDS solution. The procedure was repeated until the MWCNTs no longer precipitated. The supernatant solutions were collected together and made up to 250 mL using the stock SDS solution.

### 6.3.2 Oxidation of MWCNTs

As received MWCNTs (2 g (3.56% MWCNT content) = 71.2 mg, 6 mmol) were added to 6 M nitric acid (140 mL) in a round-bottomed flask. The solution was heated to 120 $^{o}$C and refluxed for 4, 8 or 16 h, after which time it was diluted with high purity water and filtered through a polycarbonate membrane (0.2 $\mu$m, Whatman). The functionalised MWCNTs were then washed with a copious amount of water until pH neutral and dried overnight under vacuum at 60 $^{o}$C. Yield; 4h: 58 mg, 81%; 8h: 45 mg, 63%; 16h: 34 mg, 48%.

### 6.3.3 Base Washing of Oxidised MWCNTs

The oxidised MWCNTs (30 mg, 2.5 mmol) were washed with 0.01 M sodium hydroxide (50 mL). The base wash initially produced a yellow/brown filtrate and was repeated until the filtrate ran clear. The MWCNTs were then washed with high purity water until the filtrate reached a neutral pH. Finally, the MWCNTs were washed with 0.01 M HCl and once again returned to neutrality with high purity water and then dried overnight under vacuum at 60 $^{o}$C. Yield; 4h: 26 mg, 87%; 8h: 24 mg, 80%; 16h: 23 mg, 77%

### 6.3.4 Dispersion of Functionalised MWCNTs in Aqueous Amino Acid Solutions

Functionalised MWCNTs (10 mg, 0.8 mmol) were dispersed in the stated concentration of the required amino acid solution (1 mL) using an ultrasonic bath (Ultrawave U50, 30-40 kHz) for 30 min with the temperature of the samples controlled using an external ice bath. The resulting dispersions were left to settle overnight and then filtered through a cotton wool plug.

### 6.3.5 Synthesis of MWCNT-Benzoic Acid

As received MWCNTs (2 g (3.56% MWCNT content) = 71.2 mg, 6 mmol) were added to high purity water (60 mL) in a round-bottomed flask and the contents sonicated using an ultrasonic bath (Ultrawave U50, 30-40 kHz) for 15 min, after which time the reaction flask was heated to 60 $^{o}$C in an oil bath. 4-aminobenzoic acid (0.92 g, 6.7 mmol) and isoamyl nitrite (0.9 mL, 6.7 mmol) were then added to the reaction flask and a condenser attached. The resulting mixture was stirred at 60 $^{o}$C for 16 h. The contents were allowed to cool for 1 h and were then filtered through a polycarbonate membrane (0.2 $\mu$m, Whatman). The filter cake was washed with high purity water and acetone until the filtrate ran clear. The product was then stirred for 10 min in DMF (30 mL) and collected by filtration using a nylon membrane (0.2 $\mu$m, Whatman), rinsed with acetone and dried overnight under vacuum at 60 $^{o}$C. Yield; 54 mg, 76%

### 6.3.6 Synthesis of *N,N*-Dimethylethylenediamine Functionalised MWCNTs

As received MWCNTs (2 g (3.56% CNT content) = 71.2 mg, 6 mmol) were oxidised for 16 h as in Section 6.3.2 and washed with base as in Section 6.3.3. The oxidised MWCNTs (20 mg, 1.67 mmol) were dispersed in DMEN (60 mL) and DIPEA (1 mL). To this dipsersion was added HATU (10 mg) and the mixture stirred for 16 h at room temperature. The product was then diluted with methanol (300 mL), isolated by filtration over a nylon membrane (0.2 $\mu$m, Whatman) and washed extensively with excess methanol and then water. The functionalised MWCNTs were then dried overnight in a vacuum oven at 60 $^{o}$C. Yield; 15 mg, 75%

### 6.3.7 Quaternisation of *N,N*-Dimethylethylenediamine Functionalised MWCNTs

The DMEN functionalised MWCNTs (15 mg, 1.25 mmol) were stirred in methyl iodide (10 mL) for 16 h to give the ammonium salt. The resulting mixture was filtered through a nylon membrane (0.2 $\mu$m, Whatman), washed with acetone and dried at room temperature. Yield; 11 mg, 73%

### 6.3.8 Fabrication of MWCNT Thin Films

Oxidised MWCNTs (0.05 or 1 mg) were dispersed in either water (50 mL) or 0.5 M arginine (50 mL) to give dispersions with a MWCNT concentration of either 1 mg/L or 2 mg/L. The thin films of the oxidised MWCNTs (16 mm diameter) were prepared by vacuum filtration of these dispersions through a polycarbonate membrane (0.2 $\mu$m, Whatman). The resulting films were washed with water (3 x 25mL) and left to air dry for 1 week.

### 6.3.9 Removal of the Fmoc Protecting Group from Fmoc-Arg(Pbf)-OH and Fmoc-Lys(Boc)-OH

The Fmoc groups of Fmoc-Arg(Pbf)-OH (2.5 g) and Fmoc-Lys(Boc)-OH (2.5 g) were removed by stirring in 20 % piperidine in DMF (v/v). After 1 h the product was

precipitated in cold diethyl ether and washed with excess cold diethyl ether. Yield; Arginine: 1.3 g, 52%; Lysine: 1.0 g, 40%

### 6.3.10 Covalent Attachment of Basic Amino Acids through their $\alpha$ Amine Group to Oxidised MWCNTs

As received MWCNTs (2 g (3.56% MWCNT content) = 71.2 mg, 6 mmol) were oxidised for 16 h as in Section 6.3.2 and washed with base as in Section 6.3.3. The oxidised MWCNTs (20 mg, 1.7 mmol) were added to HATU (10 mg) and DIPEA (1 mL) in anhydrous DMF (50 mL). After sonication using an ultrasonic bath (Ultrawave U50, 30-40 kHz) for 30 min, the Fmoc deprotected amino acid (0.5 g) was added and the resulting mixture was stirred for 16 h at room temperature. The product was then diluted with methanol (300 mL), isolated by filtration over a nylon membrane (0.2 $\mu$m, Whatman) and washed extensively with excess methanol. Trifluoroacetic acid/triisopropylsilane/$H_2O$, 95:2.5:2.5 v/v) was used for deprotection of Pbf and BOC groups from the respective amino acids (stir for 3 h at room temperature). The functionalised MWCNTs were washed with excess ether and dried overnight in a vacuum oven at 60 $^o$C. Yield; CNT-Arginine: 13 mg, 65%; CNT-Lysine: 12 mg, 60%

### 6.3.11 Removal of the Pbf Protecting Group from Fmoc-Arg(Pbf)-OH

The Pbf groups of Fmoc-Arg(Pbf)-OH (2.5 g) were removed by stirring in trifluoroacetic acid/triisopropylsilane/$H_2O$, 95:2.5:2.5 v/v) for 3 h at room temperature. The deprotected amino acid was precipitated in cold diethyl ether and washed with excess cold diethyl ether. Yield; Arginine: 1.1 g, 44%

### 6.3.12 Covalent Attachment of Arginine through the Guanidinium Group to Oxidised MWCNTs

As received MWCNTs (2 g (3.56% MWCNT content) = 71.2 mg, 6 mmol) were oxidised for 16 h as in Section 6.3.2 and washed with base as in Section 6.3.3. The oxidised MWCNTs (20 mg, 1.7 mmol) were added to HATU (10 mg) and DIPEA (1 mL) in

anhydrous DMF (50 mL). After sonication using an ultrasonic bath (Ultrawave U50, 30-40 kHz) for 30 min, Pbf deprotected arginine (0.5 g) was added and the resulting mixture was stirred for 16 h at room temperature. The product was then diluted with methanol (300 mL), isolated by filtration over a nylon membrane (0.05 $\mu$m, Whatman) and washed extensively with excess methanol. The Fmoc protecting groups of arginine where then removed by stirring the functionalised MWCNTs in 20 % piperidine in DMF (v/v) for 1 h. The resulting MWCNTs was washed with excess ether and dried overnight in a vacuum oven at 60 $^o$C. Yield; 14 mg, 70%

### 6.3.13 Covalent Attachment of Neutral Amino Acids to Oxidised MWCNTs

As received MWCNTs (2 g (3.56% MWCNT content) = 71.2 mg, 6 mmol) were oxidised for 16 h as in Section 6.3.2 and washed with base as in Section 6.3.3. The oxidised MWCNTs (20 mg, 1.7 mmol) were added to HATU (10 mg) and DIPEA (1 mL) in anhydrous DMF (50 mL). After sonication using an ultrasonic bath (Ultrawave U50, 30-40 kHz) for 30 min, the amino acid (0.5 g) was added and the resulting mixture was stirred for 16 h at room temperature. The product was then diluted with methanol (300 mL), isolated by filtration over a nylon membrane (0.2 $\mu$m, Whatman) and washed extensively with excess methanol. The functionalised MWCNTs were then dried overnight in a vacuum oven at 60 $^o$C. Yield; Glycine: 14 mg, 70%; Taurine 16 mg, 80%

### 6.3.14 Synthesis of Amine Functionalised MWCNTs

As received MWCNTs (2 g (3.56% MWCNT content) = 71.2 mg, 6 mmol) were oxidised for 16 h as in Section 6.3.2 and washed with base as in Section 6.3.3. The oxidised MWCNTs (20 mg, 1.7 mmol) were dispersed in ethylenediamine (60 mL) using an ultrasonic bath (Ultrawave U50, 30-40 kHz) for 30 min. HATU (10 mg) and DIPEA (1 mL) was then added and the dispersion stirred at room temperature for 16 h. The product was then diluted with 300 ml of methanol, isolated by filtration over a nylon membrane (0.2 $\mu$m, Whatman) and washed extensively with excess methanol. The functionalised MWCNTs were then dried in a vacuum oven at 60 $^o$C overnight. Yield;

17 mg, 85%

### 6.3.15 Functionalisation of MWCNT-Amine with Mellitic Acid/PAA

Oxidised MWCNTs were functionalised with amine groups as in Section 6.3.14. Amine functionalised MWCNTs (15 mg, 1.25 mmol) were added to HATU (10 mg) and DIPEA (1 mL) in anhydrous DMF (75 mL). After sonication using an ultrasonic bath (Ultrawave U50, 30-40 kHz) for 30 min, mellitic acid (0.5 g, 1.46 mmol) or PAA (3 g, 0.007 mmol) was added and the resulting mixture was stirred for 16 h at room temperature. The product was then diluted with methanol (300 mL), isolated by filtration over a nylon membrane (0.2 $\mu$m, Whatman) and washed extensively with excess methanol. The functionalised MWCNTs were then dried overnight in a vacuum oven at 60 $^{o}$C. Yield; CNT-Mellitic: 13 mg, 87%; CNT-PAA: 11 mg, 73%

### 6.3.16 Covalent Attachment of Taurine to Mellitic Acid and PAA Functionalised MWCNTs

The mellitic acid/PAA functionalised MWCNTs (10 mg, 0.8 mmol) were added to HATU (10 mg) and DIPEA (1 mL) in anhydrous DMF (50 mL). After sonication using an ultrasonic bath (Ultrawave U50, 30-40 kHz) for 30 min, taurine (0.5 g, 4 mmol) was added and the resulting mixture was stirred for 16 h at room temperature. The product was then diluted with methanol (300 mL), isolated by filtration over a nylon membrane (0.2 $\mu$m, Whatman) and washed extensively with excess methanol. The functionalised MWCNTs were then dried overnight in a vacuum oven at 60 $^{o}$C. Yield; CNT-MelliticTau: 8 mg, 80%; CNT-PAATau: 9 mg, 90%

### 6.3.17 Synthesis of PAA-Taurine

PAA (3 g, 0.007 mmol), HATU (10 mg) and DIPEA (1 mL) were dissolved in anhydrous DMF using an ultrasonic bath (Ultrawave U50, 30-40 kHz). After 15 min, taurine (0.5 g, 4 mmol) was added and the resulting mixture was stirred for 16 h at room temperature. The product was precipitated in cold diethyl ether and washed with excess ether. The product was then solubilised in water and dialysed against high

purity water overnight. The final product was collected after freeze-drying, yielding a white powder. Yield; 1.4 g, 47%

### 6.3.18 Functionalisation of MWCNT-Amine with $\alpha$-Hydroxy Acids

Oxidised MWCNTs were functionionalised with amine groups as in Section 6.3.14. The amine functionalised MWCNTs (15 mg, 1.25 mmol) were added to HATU (10 mg) and DIPEA (1 mL) in anhydrous DMF (50 mL). After sonication using an ultrasonic bath (Ultrawave U50, 30-40 kHz) for 30 min, glycolic acid (0.4 g, 5.2 mmol) or citric acid (1 g, 5.2 mmol) was added and the resulting mixture was stirred for 16 h at room temperature. The product was then diluted with methanol (300 mL), isolated by filtration over a nylon membrane (0.05 $\mu$m, Whatman) and washed extensively with excess methanol. The functionalised MWCNTs were then dried overnight in a vacuum oven at 60 $^o$C. Yield; CNT-Glycolic: 9 mg, 60%; CNT-Citric: 11 mg, 15%

### 6.3.19 Synthesis of MWCNT-Pyridine

MWCNTs (20 mg, 1.7 mmol) were added to DMF (60 mL) in a round-bottomed flask and the contents sonicated using an ultrasonic bath (Ultrawave U50, 30-40 kHz) for 30 min, after which time the reaction flask was heated to 60 $^o$C in an oil bath. 4-aminopyridine (0.63 g, 6.7 mmol, Alfa Aesar) dissolved in 4M HCl (5 mL) and isoamyl nitrite (0.9 mL, 6.7 mmol) were then added to the reaction flask and a condenser attached. The resulting mixture was stirred at 60 $^o$C for 16 h. The contents were allowed to cool for 1 h and were then filtered through a nylon membrane (0.2 $\mu$m, Whatman). The filter cake was washed with high purity water and acetone until the filtrate ran clear. The product was then stirred for 10 min in DMF (30 mL) and collected by filtration using a nylon membrane (0.2 $\mu$m, Whatman), rinsed with acetone and dried overnight under vacuum at 60 $^o$C. Yield; 17 mg, 85%

### 6.3.20 Synthesis of Hydroxy Functionalised MWCNTs

Pyridine functionalised MWCNTs (15 mg, 1.25 mmol) were dispersed in DMF (20 mL) using an ultrasonic bath (Ultrawave U50, 30-40 kHz) for 15 min. Either 2-bromoethanol

(0.35 mL, 5 mmol), 3-bromo-1,2-propanediol (0.44 mL, 5 mmol) or 2-(bromomethyl)-2-(hydroxymethyl)-1,3-propanediol (0.1 g, 5 mmol, Acros Organics) was then added to the reaction flask and the mixture stirred for 16 h at room temperature. The MWCNTs were then filtered through a nylon membrane (0.2 $\mu$m pore, Whatman) and washed extensively with DMF then water and dried overnight under vacuum at 60 $^{o}$C. Yield; MWCNT-Hydroxy: 8 mg, 53%; MWCNT-Diol: 11 mg, 73%; and MWCNT-Triol: 10 mg, 67%

### 6.3.21 Synthesis of Nucleoside Functionalised MWCNTs

Pyridine functionalised MWCNTs (15 mg, 1.25 mmol) were dispersed in DMF (20 mL) using an ultrasonic bath (Ultrawave U50, 30-40 kHz) for 15 min. 5-bromouridine (0.13 g, 0.4 mmol) or 8-bromoadenosine (0.14 g, 0.4 mmol) was then added and the reaction mixture stirred for 16 h at room temperature. The MWCNTs were filtered through a nylon membrane (0.2 $\mu$m pore, Whatman) and washed extensively with DMF then water and dried overnight under vacuum at 60 $^{o}$C. Yield; MWCNT-Uridine: 12 mg, 80%; MWCNT-Adenosine: 10 mg, 67%

### 6.3.22 Functionalisation of MWCNT-Pyridine with Bromoacetyl Bromide

Pyridine functionalised MWCNTs (15 mg, 1.25 mmol) were dispersed in anhydrous $CH_2Cl_2$ (30 mL) using an ultrasonic bath (Ultrawave U50, 30-40 kHz) for 15 min and the dispersion cooled to 0 $^{o}$C. At 0 $^{o}$C bromoacetyl bromide (1 mL, 11.5 mmol) was added dropwise to the MWCNT dispersion and stirred at room temperature for 16 h. The mixture was filtered through a membrane (0.2 $\mu$, Whatman), washed with water and dried under vacuum overnight at 60 $^{o}$C. Yield; 14 mg, 93%

### 6.3.23 Synthesis of Sugar Functionalised MWCNTs

Bromoacetyl bromide modified MWCNT-Pyridine (12 mg, 1 mmol) was dispersed in DMF (20 mL) using an ultrasonic bath (Ultrawave U50, 30-40 kHz) for 15 min. DIPEA (0.44 mL, 2.5 mmol) and either ribose (0.38 g, 2.5 mmol), fructose (0.45g, 2.5 mmol) or sucrose (0.86 g, 2.5 mmol) was then added and the reaction mixture stirred for 16

h at room temperature. The MWCNTs were filtered through a nylon membrane (0.2 $\mu$m pore, Whatman) and washed with acetone (2 x 30 mL) and dried overnight at 60 $^{o}$C. Yield; MWCNT-Ribose: 8 mg, 67%; MWCNT-Fructose: 8 mg, 67%; MWCNT-Sucrose: 10 mg, 83%

### 6.3.24 Synthesis of PEG Functionalised MWCNTs

Bromoacetyl bromide modified MWCNT-Pyridine (12 mg, 1.25 mmol) was dispersed in DMF (20 mL) using an ultrasonic bath (Ultrawave U50, 30-40 kHz) for 15 min. $PEG_{400}$ (1 g, 2.5 mmol) and DIPEA (0.44 mL, 2.5 mmol) were then added and the reaction mixture stirred for 16 h at room temperature. The MWCNTs were filtered through a nylon membrane (0.2 $\mu$m pore, Whatman) and washed with acetone (2 x 30 mL) and dried overnight at 60 $^{o}$C. Yield; 10 mg, 83%

# Chapter 7

# Appendix

## 7.1 Appendix A: Supporting Information for Chapter 3

### 7.1.1 Photograph of the pH Effect on Carboxylic Acid Functionalised MWCNT/Amino Acid Dispersions

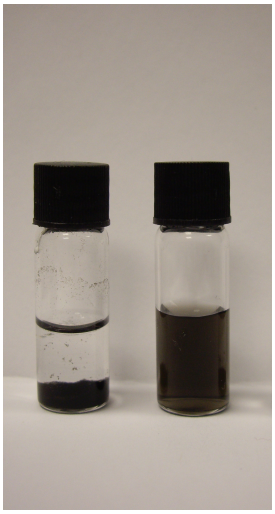

Figure A.1: Photograph of the dispersions of oxidised MWCNTs in 0.5 M arginine at pH 6 and 11 (l-r).

### 7.1.2 UV-vis-NIR Spectra of AR-MWCNTs in Aqueous Amino Acid Solutions

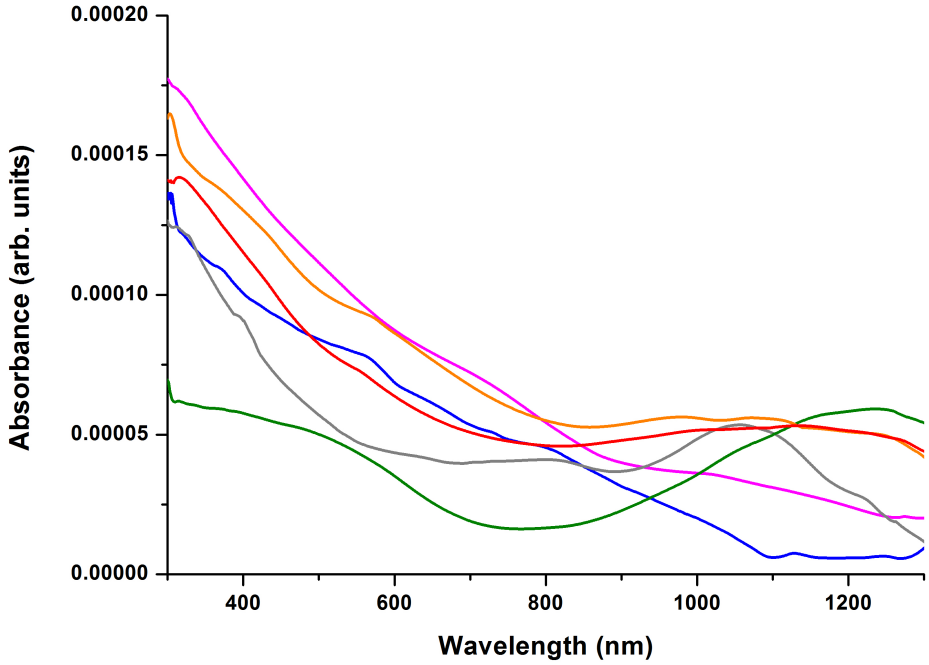


Figure A.2: UV-vis-NIR spectra of AR-MWCNTs water (blue), 0.5 M arginine (red), 0.5 M lysine (green), 3 M glycine (grey), 0.5 M taurine (magenta) and 0.05 M glutamic acid solutions (orange) (The absorbance at 700 nm is effectively 0 for all amino acids).

### 7.1.3 Photograph of the Dispersion of AR-MWCNTs in Aqueous Amino Acid Solutions

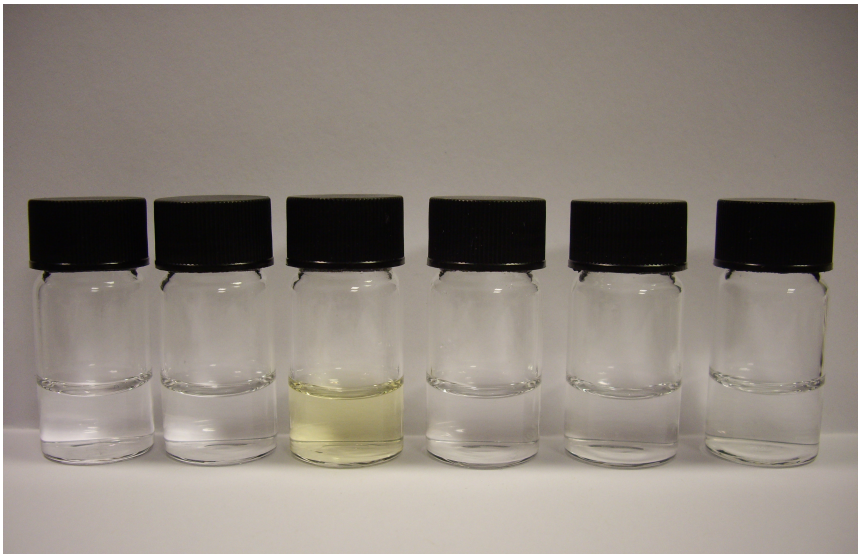

Figure A.3: Photograph of the dispersion of AR-MWCNTs in water, 0.5 M arginine, 0.5 M lysine, 3 M glycine, 0.5 M taurine and 0.05 M glutamic acid solutions (l-r).

## 7.2 Appendix B: Supporting Information for Chapter 4

### 7.2.1 TGA of Piperidine and TFA Treated Oxidised MWCNTs

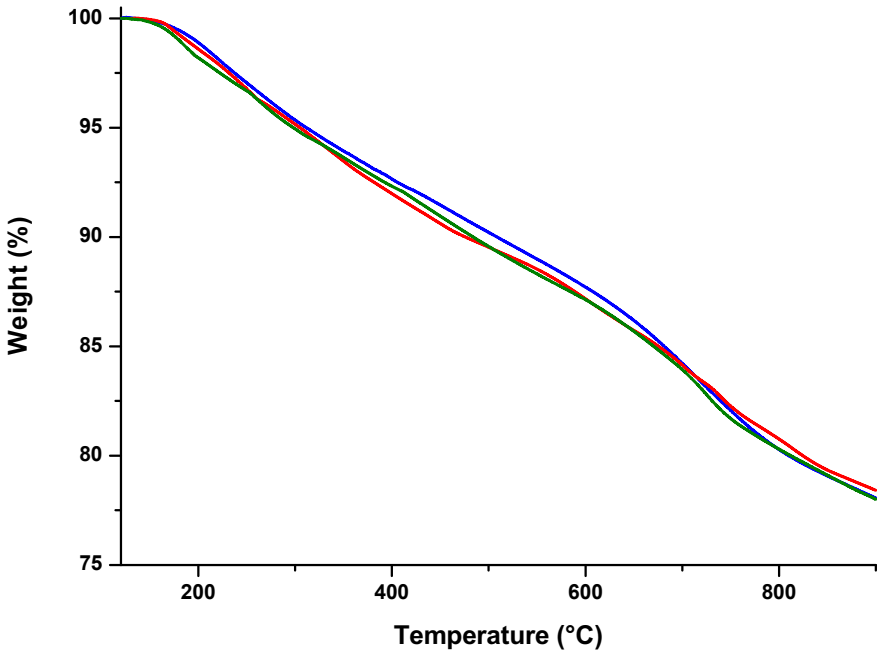


Figure B.1: TGA results of oxidised MWCNTs (blue) treated with piperidine (red) and TFA (green).

### 7.2.2 UV-vis-NIR Spectra of Piperidine and TFA Treated Oxidised MWCNTs

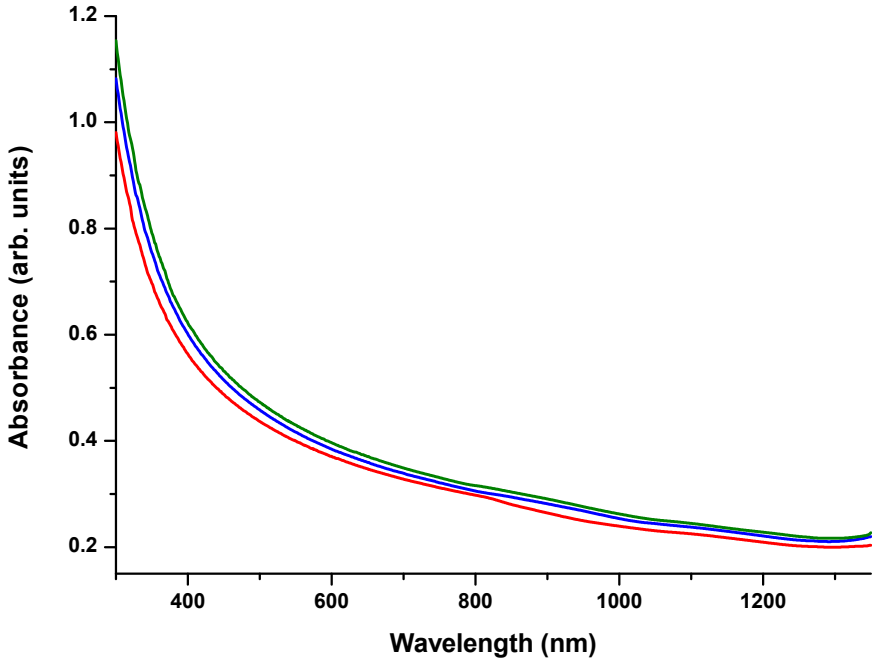


Figure B.2: UV-vis-NIR spectra in water of oxidised MWCNTs (blue) treated with piperidine (red) and TFA (green).

### 7.2.3 Raman Spectra of Piperidine and TFA Treated Oxidised MWCNTs

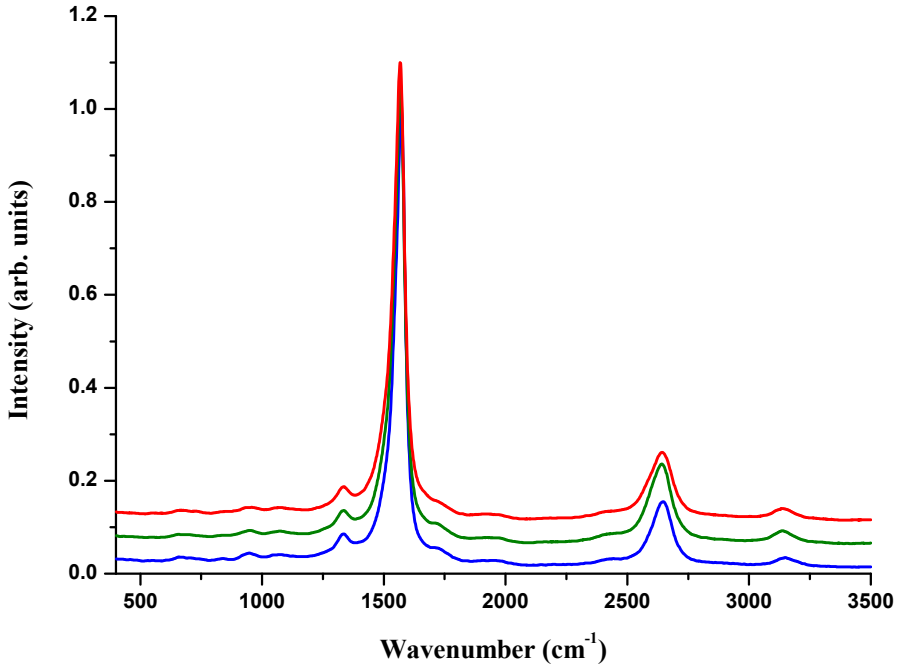


Figure B.3: Raman spectra (532 nm, 2.33 eV) of oxidised MWCNTs (blue) treated with piperidine (red) and TFA (green) normalised at the G band.

# References


[1] Meyyappan, M. *Carbon Nanotubes: Science and Applications*; CRC Press, 2004.

[2] Zheng, L. X.; O'Connell, M. J.; Doorn, S. K.; Liao, X. Z.; Zhao, Y. H.; Akhadov, E. A.; Hoffbauer, M. A.; Roop, B. J.; Jia, Q. X.; Dye, R. C.; Peterson, D. E.; Huang, S. M.; Liu, J.; Zhu, Y. T. *Nat. Mater.* **2004**, *3*, 673.

[3] Wang, X.; Li, Q.; Xie, J.; Jin, Z.; Wang, J.; Li, Y.; Jiang, K.; Fan, S. *Nano Lett.* **2009**, *9*, 3137.

[4] Ajayan, P. M. *Chem. Rev.* **1999**, *99*, 1787–1799.

[5] Vajtai, R. *Springer Handbook of Nanomaterials*; Springer, 2013.

[6] Shen, C.; Brozena, A. H.; Wang, Y. *Nanoscale* **2011**, *3*, 503.

[7] Dresselhaus, M. S.; Dresselhaus, G.; Avouris, P. In *Carbon Nanotubes: Synthesis, Structure, Properties, and Applications*; Dresselhaus, M. S., Dresselhaus, G., Avouris, P., Eds.; Springer, 2001.

[8] Terrones, M. *Annual Review of Materials Research* **2003**, *33*, 419–501.

[9] Iijima, S. *Nature* **1991**, *354*, 56.

[10] Iijima, S.; Ichihashi, T. *Nature* **1993**, *363*, 603.

[11] Bethune, D. S.; Klang, C. H.; de Vries, M. S.; Gorman, G.; Savoy, R.; Vazquez, J.; Beyers, R. *Nature* **1993**, *363*, 605.

[12] Ebbesen, T. W.; Ajayan, P. M. *Nature* **1992**, *358*, 220.

[13] Guo, T.; Nikolaev, P.; Thess, A.; Colbert, D. T.; Smalley, R. E. *Chem. Phys. Lett.* **1995**, *2614*, 49.

[14] Prasek, J.; Drbohlavova, J.; Chomoucka, J.; Hubalek, J.; Jasek, O.; Adam, V.; Kizek, R. *J. Mater. Chem.* **2011**, *21*, 15872.

[15] Rao, C. N. R.; Voggu, R.; Govindaraj, A. *Nanoscale* **2009**, *1*, 96–105.

[16] Park, T.-J.; Banerjee, S.; Hemraj-Benny, T.; Wong, S. S. *J. Mater. Chem.* **2006**, *16*, 141.

[17] Chattopadhyay, D.; Lastella, S.; Kim, S.; Papadimitrakopoulos, F. *J. Am. Chem. Soc.* **2002**, *124*, 728–9.

[18] Bandow, S.; Rao, A. M.; Williams, K. A.; Thess, A.; Smalley, R. E.; Eklund, P. C. *J. Phys. Chem. B* **1997**, *5647*, 8839–8842.

[19] Shelimov, K. B.; Esenaliev, R. O.; Rinzler, A. G.; Huffman, C. B.; Smalley, R. E. *Chem. Phys. Lett.* **1998**, *282*, 429–434.

[20] Moon, J.-M.; An, K. H.; Lee, Y. H.; Park, Y. S.; Bae, D. J.; Park, G.-S. *J. Phys. Chem. B* **2001**, *105*, 5677–5681.

[21] Chiang, I. W.; Brinson, B. E.; Huang, A. Y.; Willis, P. A.; Bronikowski, M. J.; Margrave, J. L.; Smalley, R. E.; Hauge, R. H. *J. Phys. Chem. B* **2001**, *105*, 8297.

[22] Strong, K. L.; Anderson, D. P.; Lafdi, K.; Kuhn, J. N. *Carbon* **2003**, *41*, 1477–1488.

[23] Rinzler, A. G.; Liu, J.; Dai, H.; Nikolaev, P.; Huffman, C. B.; Rodríguez-Macías, F. J.; Boul, P. J.; Lu, A.; Heymann, D.; Colbert, D.; Lee, R.; Fischer, J.; Rao, A.; Eklund, P.; Smalley, R. *Appl. Phys. A Mater. Sci. Process.* **1998**, *67*, 29–37.

[24] Dillon, A. C.; Gennett, T.; Jones, K. M.; Alleman, J. L.; Parilla, P. A.; Heben, M. J. *Adv. Mater.* **1999**, *11*, 1354–1358.

[25] Stobinski, L.; Lesiak, B.; Kövér, L.; Tóth, J.; Biniak, S.; Trykowski, G.; Judek, J. *J. Alloys Compd.* **2010**, *501*, 77–84.

[26] Tchoul, M. N.; Ford, W. T.; Lolli, G.; Resasco, D. E.; Arepalli, S. *Chem. Mater.* **2007**, *19*, 5765–5772.

[27] Lee, G.-W.; Kim, J.; Yoon, J.; Bae, J.-S.; Shin, B. C.; Kim, I. S.; Oh, W.; Ree, M. *Thin Solid Films* **2008**, *516*, 5781–5784.

[28] Avilés, F.; Cauich-Rodríguez, J.; Moo-Tah, L.; May-Pat, A.; Vargas-Coronado, R. *Carbon* **2009**, *47*, 2970–2975.

[29] Kahn, M. G. C.; Banerjee, S.; Wong, S. S. *Nano Lett.* **2002**, *2*, 1215–1218.

[30] Hamon, M. A.; Hui, H.; Bhowmik, P.; Itkis, H. M. E.; Haddon, R. C. *Appl. Phys. A Mater. Sci. Process.* **2002**, *74*, 333–338.

[31] Zhao, C.; Ji, L.; Liu, H.; Hu, G.; Zhang, S.; Yang, M.; Yang, Z. *Journal of Solid State Chemistry* **2004**, *177*, 4394–4398.

[32] Ramanathan, T.; Fisher, F. T.; Ruoff, R. S.; Brinson, L. C. *Chem. Mater.* **2005**, *17*, 1290–1295.

[33] Yao, Z.; Kane, C. L.; Dekker, C. *Phys. Rev. Lett.* **2000**, *84*, 2941–4.

[34] Robertson, J. *Mater. Today* **2007**, *10*, 36–43.

[35] Saito, R.; Fujita, M.; Dresselhaus, G.; Dresselhaus, M. S. *Appl. Phys. Lett.* **1992**, *60*, 2204–2206.

[36] Charlier, J.-C. *Acc. Chem. Res.* **2002**, *35*, 1063–9.

[37] Hassanien, A.; Tokumoto, M.; Ohshima, S.; Kuriki, Y.; Ikazaki, F.; Uchida, K.; Yumura, M. *Appl. Phys. Lett.* **1999**, *75*, 2755.

[38] Treacy, M. M. J.; Ebbesen, T. W.; Gibson, J. M. *Nature* **1996**, *381*, 678.

[39] Wong, E. W. *Science* **1997**, *277*, 1971–1975.

[40] Krishnan, A.; Dujardin, E.; Ebbesen, T. W.; Yianilos, P. N.; Treacy, M. M. J. *Phys. Rev. B.* **1998**, *58*, 13–19.

[41] Yu, M.-F.; Files, B. S.; Arepalli, S.; Ruoff, R. S. *Phys. Rev. Lett.* **2000**, *84*, 5552–5.

[42] Yu, M. *Science* **2000**, *287*, 637–640.

[43] Sinnott, S. B.; Shenderova, O. A.; White, C. T.; Brenner, D. W. *Carbon* **1998**, *36*, 1.

[44] Coleman, J. N.; Khan, U.; Blau, W. J.; Gun'ko, Y. K. *Carbon* **2006**, *44*, 1624–1652.

[45] Iijima, S.; Brabec, C.; Maiti, A.; Bernholc, J. *J. Chem. Phys.* **1996**, *104*, 2089.

[46] Andrews, R.; Weisenberger, M. C. *Curr. Opin. Solid State Mater. Sci.* **2004**, *8*, 31–37.

[47] Wilson, N. R.; Macpherson, J. V. *Nat. Nanotechnol.* **2009**, *4*, 483–91.

[48] Niyogi, S.; Hamon, M. A.; Hu, H.; Zhao, B.; Bhowmik, P.; Sen, R.; Itkis, M. E.; Haddon, R. C. *Acc. Chem. Res.* **2002**, *35*, 1105–1113.

[49] Hodge, S. A.; Bayazit, M. K.; Coleman, K. S.; Shaffer, M. S. P. *Chem. Soc. Rev.* **2012**, *41*, 4409.

[50] Strano, M. S.; Dyke, C. A.; Usrey, M. L.; Barone, P. W.; Allen, M. J.; Shan, H.; Kittrell, C.; Hauge, R. H.; Tour, J. M.; Smalley, R. E. *Science* **2003**, *301*, 1519.

[51] Bayazit, M. K.; Clarke, L. S.; Coleman, K. S.; Clarke, N. *J. Am. Chem. Soc.* **2010**, *132*, 15814.

[52] Yang, C.-M.; Park, J. S.; An, K. H.; Lim, S. C.; Seo, K.; Kim, B.; Park, K. A.; Han, S.; Park, C. Y.; Lee, Y. H. *The Journal of Physical Chemistry B* **2005**, *109*, 19242.

[53] Miyata, Y.; Maniwa, Y.; Kataura, H. *J. Phys. Chem. B* **2006**, *110*, 25.

[54] Bayazit, M. K.; Coleman, K. S. *J. Am. Chem. Soc.* **2009**, *131*, 10670.

[55] Lu, X.; Chen, Z.; Schleyer, P. V. R. *J. Am. Chem. Soc.* **2005**, *127*, 20–1.

[56] Hirsch, A. *Angew. Chem. Int. Ed.* **2002**, *41*, 1853.

[57] Charlier, J.; Ebbesen, T. W.; Lambin, P. *Phys. Rev. B.* **1996**, *53*, 11108–11113.

[58] Chico, L.; Crespi, V. H.; Benedict, L. X.; Louie, S. G.; Cohen, M. L. *Phys. Rev. Lett.* **1996**, *76*, 971–974.

[59] Girifalco, L. A.; Hodak, M.; Lee, R. S. *Phys. Rev. B.* **2000**, *62*, 13104.

[60] Lu, K. L.; Lago, R. M.; Chen, Y. K.; Green, M. L. H.; Harris, P. J. F.; Tsang, S. C. *Carbon* **1996**, *34*, 814–816.

[61] Bahr, J. L.; Tour, J. M. *J. Mater. Chem.* **2002**, *12*, 1952–1958.

[62] Tasis, D.; Tagmatarchis, N.; Bianco, A.; Prato, M. *Chem. Rev.* **2006**, *106*, 1105–36.

[63] Karousis, N.; Tagmatarchis, N.; Tasis, D. *Chem. Rev.* **2010**, *110*, 5366–97.

[64] Cai, L.; Bahr, L.; Y, Y.; James, M. T. *Chem. Mater.* **2002**, *14*, 4235–4241.

[65] Zhang, J.; Zou, H.; Qing, Q.; Yang, Y.; Li, Q.; Liu, Z. *J. Phys. Chem. B* **2003**, *107*, 3712–3718.

[66] Ziegler, K. J.; Gu, Z.; Peng, H.; Flor, E. L.; Hauge, R. H.; Smalley, R. E. *J. Am. Chem. Soc.* **2005**, *127*, 1541–7.

[67] Tsang, S. C.; Harris, P. J. F.; Green, M. L. H. *Nature* **1993**, *362*, 520–522.

[68] Xia, W.; Jin, C.; Kundu, S.; Muhler, M. *Carbon* **2009**, *47*, 919–922.

[69] Xing, Y.; Li, L.; Chusuei, C. C.; Hull, R. V. *Langmuir* **2005**, *21*, 4185–90.

[70] Yoon, S.-M.; Kim, S. J.; Shin, H.-J.; Benayad, A.; Choi, S. J.; Kim, K. K.; Kim, S. M.; Park, Y. J.; Kim, G.; Choi, J.-Y.; Lee, Y. H. *J. Am. Chem. Soc.* **2008**, *130*, 2610–6.

[71] Miyata, Y.; Maniwa, Y.; Kataura, H. *J. Phys. Chem. B* **2006**, *110*, 25–9.

[72] Wang, Y. B.; Iqbal, Z.; Mitra, S. *J. Am. Chem. Soc.* **2006**, *128*, 95–99.

[73] Zhou, J.; Wang, C.; Qian, Z.; Chen, C.; Ma, J.; Du, G.; Chen, J.; Feng, H. *J. Mater. Chem.* **2012**, *22*, 11912.

[74] Salzmann, C. G.; Llewellyn, S. A.; Tobias, G.; Ward, M. A. H.; Huh, Y.; Green, M. L. H. *Adv. Mater.* **2007**, *19*, 883–887.

[75] Shao, L.; Tobias, G.; Salzmann, C. G.; Ballesteros, B.; Hong, S. Y.; Crossley, A.; Davis, B. G.; Green, M. L. H. *Chem. Commun.* **2007**, *1*, 5090–2.

[76] Verdejo, R.; Lamoriniere, S.; Cottam, B.; Bismarck, A.; Shaffer, M. *Chem. Commun.* **2007**, 513.

[77] Fogden, S.; Verdejo, R.; Cottam, B.; Shaffer, M. *Chem. Phys. Lett.* **2008**, *460*, 162–167.

[78] Worsley, K. A.; Kalinina, I.; Bekyarova, E.; Haddon, R. C. *J. Am. Chem. Soc.* **2009**, *131*, 18153–8.

[79] Del Canto, E.; Flavin, K.; Movia, D.; Navio, C.; Bittencourt, C.; Giordani, S. *Chem. Mater.* **2011**, *23*, 67–74.

[80] Hudson, J. L.; Jian, H.; Leonard, A. D.; Stephenson, J. J.; Tour, J. M. *Chem. Mater.* **2006**, *18*, 2766–2770.

[81] Bahr, J. L.; Yang, J.; Kosynkin, D. V.; Bronikowski, M. J.; Smalley, R. E.; Tour, J. M. *J. Am. Chem. Soc.* **2001**, *123*, 6536.

[82] Dyke, C. A.; Tour, J. M. *Nano Lett.* **2003**, *3*, 1215–1218.

[83] Price, B. K.; Hudson, J. L.; Tour, J. M. *J. Am. Chem. Soc.* **2005**, *127*, 14867–70.

[84] Strano, M. S. *J. Am. Chem. Soc.* **2003**, *125*, 16148–53.

[85] Schmidt, G.; Gallon, S.; Esnouf, S.; Bourgoin, J.-P.; Chenevier, P. *Chemistry* **2009**, *15*, 2101–10.

[86] Bahr, J. L.; Tour, J. M. *Chem. Mater.* **2001**, *13*, 3823.

[87] Price, B. K.; Tour, J. M. *J. Am. Chem. Soc.* **2006**, *128*, 12899–12904.

[88] Doyle, C. D.; Tour, J. M. *Carbon* **2009**, *47*, 3215–3218.

[89] Dyke, C. A.; Tour, J. M. *J. Am. Chem. Soc.* **2003**, *125*, 1156–7.

[90] Georgakilas, V.; Kordatos, K.; Prato, M.; Guldi, D. M.; Holzinger, M.; Hirsch, A. *J. Am. Chem. Soc.* **2002**, *124*, 760–1.

[91] Tagmatarchis, N.; Prato, M. *J. Mater. Chem.* **2004**, *14*, 437–439.

[92] Brunetti, F. G.; Herrero, M. A.; Muñoz, J. D. M.; Giordani, S.; Díaz-Ortiz, A.; Filippone, S.; Ruaro, G.; Meneghetti, M.; Prato, M.; Vázquez, E. *J. Am. Chem. Soc.* **2007**, *129*, 14580–1.

[93] Banerjee, S.; Wong, S. S. *J. Phys. Chem. B* **2002**, *106*, 12144.

[94] Alvaro, M.; Atienzar, P.; de la Cruz, P.; Delgado, J. L.; Garcia, H.; Langa, F. *J. Phys. Chem. B* **2004**, *108*, 12691–12697.

[95] Alvaro, M.; Atienzar, P.; de la Cruz, P.; Delgado, J. L.; Troiani, V.; Garcia, H.; Langa, F.; Palkar, A.; Echegoyen, L. *J. Am. Chem. Soc.* **2006**, *128*, 6626–35.

[96] Holzinger, M.; Vostrowsky, O.; Hirsch, A.; Hennrich, F.; Kappes, M.; Weiss, R. *Angew. Chem. Int. Ed.* **2001**, *40*, 4002–4005.

[97] Holzinger, M.; Steinmetz, J.; Samaille, D.; Glerup, M.; Paillet, M.; Bernier, P.; Ley, L.; Graupner, R. *Carbon* **2004**, *42*, 941–947.

[98] Coleman, K. S.; Bailey, S. R.; Fogden, S.; Green, M. L. H. *J. Am. Chem. Soc.* **2003**, *125*, 8722–3.

[99] Mickelson, E. T.; Huffman, C. B. *Chem. Phys. Lett.* **1998**, *296*, 188–194.

[100] Khabashesku, V. N.; Billups, W.; Margrave, J. L. *Acc. Chem. Res.* **2002**, *35*, 1087–95.

[101] Saini, R. K.; Chiang, I. W.; Peng, H.; Smalley, R. E.; Billups, W. E.; Hauge, R. H.; Margrave, J. L. *J. Am. Chem. Soc.* **2003**, *125*, 3617–21.

[102] Maiti, J.; Kakati, N.; Lee, S. H.; Yoon, Y. S. *J. Fluorine Chem.* **2012**, *135*, 362–366.

[103] Vaisman, L.; Wagner, H. D.; Marom, G. *Adv. Colloid Interface Sci.* **2006**, *128-130*, 37–46.

[104] Zhao, Y.-L.; Stoddart, J. F. *Acc. Chem. Res.* **2009**, *42*, 1161–71.

[105] Bilalis, P.; Katsigiannopoulos, D.; Avgeropoulos, A.; Sakellariou, G. *RSC Advances* **2014**, *4*, 2911.

[106] Nakashima, N.; Tomonari, Y.; Murakami, H. *Chem. Lett.* **2002**, 638–639.

[107] Detriche, S.; Devillers, S.; Seffer, J.-F.; Nagy, J.; Mekhalif, Z.; Delhalle, J. *Carbon* **2011**, *49*, 2935–2943.

[108] Li, H.; Zhou, B.; Lin, Y.; Gu, L.; Wang, W.; Fernando, K. A. S.; Kumar, S.; F. Allard, L.; Sun, Y.-P. *J. Am. Chem. Soc.* **2004**, *126*, 1014–1015.

[109] Chen, J. Y.; Collier, C. P. *J. Phys. Chem. B* **2005**, *109*, 7605–7609.

[110] Fujigaya, T.; Nakashima, N. *Sci. Tech. Adv. Mater.* **2015**, *16*, 024802.

[111] Matarredona, O.; Rhoads, H.; Li, Z. R.; Harwell, J. H.; Balzano, L.; Resasco, D. E. *J. Phys. Chem. B* **2003**, *107*, 13357–13367.

[112] Bomboi, F.; Bonincontro, A.; La Mesa, C.; Tardani, F. *J. Colloid Interface Sci.* **2011**, *355*, 342–7.

[113] Horn, D. W.; Tracy, K.; Easley, C. J.; Davis, V. A. *J. Phys. Chem. C* **2012**, *116*, 10341–10348.

[114] Chen, Z. Y.; Kobashi, K.; Rauwald, U.; Booker, R.; Fan, H.; Hwang, W. F.; Tour, J. M. *J. Am. Chem. Soc.* **2006**, *128*, 10568–10571.

[115] Zhao, W.; Song, C. H.; Pehrsson, P. E. *J. Am. Chem. Soc.* **2002**, *124*, 12418–12419.

[116] Brozena, A. H.; Moskowitz, J.; Shao, B. Y.; Deng, S. L.; Liao, H. W.; Gaskell, K. J.; Wang, Y. H. *J. Am. Chem. Soc.* **2010**, *132*, 3932–3938.

[117] Rosca, I. D.; Watari, F.; Uo, M.; Akasaka, T. *Carbon* **2005**, *43*, 3124–3131.

[118] Marsh, D. H.; Rance, G. A.; Zaka, M. H.; Whitby, R. J.; Khlobystov, A. N. *Phys. Chem. Chem. Phys.* **2007**, *9*, 5490–6.

[119] Zhang, T.; Xu, M.; He, L.; Xi, K.; Gu, M.; Jiang, Z. *Carbon* **2008**, *46*, 1782–1791.

[120] Chen, S.; Shen, W.; Wu, G.; Chen, D.; Jiang, M. *Chem. Phys. Lett.* **2005**, *402*, 312–317.

[121] Zhang, L.; Kiny, V. U.; Peng, H.; Zhu, J.; Lobo, R. F. M.; Margrave, J. L.; Khabashesku, V. N. *Chem. Mater.* **2004**, *16*, 2055–2061.

[122] Hudson, J. L.; Casavant, M. J.; Tour, J. M. *J. Am. Chem. Soc.* **2004**, *126*, 11158–11159.

[123] Liang, F.; Beach, J. M.; Rai, P. K.; Guo, W. H.; Hauge, R. H.; Pasquali, M.; Smalley, R. E.; Billups, W. E. *Chem. Mater.* **2006**, *18*, 1520–1524.

[124] Stephenson, J. J.; Sadana, A. K.; Higginbotham, A. L.; Tour, J. M. *Chem. Mater.* **2006**, *18*, 4658–4661.

[125] Simmons, T. J.; Bult, J.; Hashim, D. P.; Linhardt, R. J.; Ajayan, P. M. *ACS nano* **2009**, *3*, 865–70.

[126] Ding, Y.; Chen, S.; Xu, H.; Wang, Z.; Zhang, X.; Ngo, T. H.; Smet, M. *Langmuir* **2010**, *26*, 16667–16671.

[127] Tomonari, Y.; Murakami, H.; Nakashima, N. *Chem. Eur. J.* **2006**, *12*, 4027–34.

[128] Paloniemi, H.; Aaritalo, T.; Laiho, T.; Liuke, H.; Kocharova, N.; Haapakka, K.; Terzi, F.; Seeber, R.; Lukkari, J. *J. Phys. Chem. B* **2005**, *109*, 8634–8642.

[129] Li, P.; Liu, H.; Ding, Y.; Wang, Y.; Chen, Y.; Zhou, Y.; Tang, Y.; Wei, H.; Cai, C.; Lu, T. *J. Mater. Chem.* **2012**, *22*, 15370–15378.

[130] Backes, C.; Schmidt, C. D.; Hauke, F.; Böttcher, C.; Hirsch, A. *J. Am. Chem. Soc.* **2009**, *131*, 2172–84.

[131] Backes, C.; Mundloch, U.; Schmidt, C. D.; Coleman, J. N.; Wohlleben, W.; Hauke, F.; Hirsch, A. *Chemistry* **2010**, *16*, 13185–92.

[132] Backes, C.; Schmidt, C. D.; Rosenlehner, K.; Hauke, F.; Coleman, J. N.; Hirsch, A. *Adv. Mater.* **2010**, *22*, 788–802.

[133] Backes, C.; Schunk, T.; Hauke, F.; Hirsch, A. *J. Mater. Chem.* **2011**, *21*, 3554–3557.

[134] Zu, S.-Z.; Sun, X.-X.; Zhou, D.; Han, B.-H. *Carbon* **2011**, *49*, 5339–5347.

[135] Liu, C.-H.; Li, J.-J.; Zhang, H.-L.; Li, B.-R.; Guo, Y. *Colloids and Surfaces A: Physicochemical and Engineering Aspects* **2008**, *313-314*, 9–12.

[136] Ramli, M. M.; Zhang, W.; Silva, S. R. P.; Henley, S. J. *AIP Adv.* **2012**, *2*, 032165.

[137] Hu, C. G.; Chen, Z. L.; Shen, A. G.; Shen, X. C.; Li, H.; Hu, S. S. *Carbon* **2006**, *44*, 428–434.

[138] Zhang, C.; Ren, L.; Wang, X.; Liu, T. *J. Phys. Chem. C* **2010**, *35*, 11435–11440.

[139] Cousins, B. G.; Das, A. K.; Sharma, R.; Li, Y.; McNamara, J. P.; Hillier, I. H.; Kinloch, I. A.; Ulijn, R. V. *Small* **2009**, *5*, 587–90.

[140] Georgakilas, V.; Tagmatarchis, N.; Pantarotto, D.; Bianco, A.; Briand, J. P.; Prato, M. *Chem. Commun.* **2002**, 3050–3051.

[141] Li, B.; Shi, Z.; Lian, Y.; Gu, Z. *Chem. Lett.* **2001**, *30*, 598–599.

[142] Zeng, L. L.; Zhang, L.; Barron, A. R. *Nano Lett.* **2005**, *5*, 2001–2004.

[143] Hu, N.; Dang, G.; Zhou, H.; Jing, J.; Chen, C. *Mater. Lett.* **2007**, *61*, 5285–5287.

[144] Wang, D.; Chen, L. *Nano Lett.* **2007**, *7*, 1480–4.

[145] Wang, T.; Zhao, G.-C.; Wei, X.-W. *Chem. Lett.* **2005**, *34*, 518–519.

[146] Dieckmann, G. R.; Dalton, A. B.; Johnson, P. A.; Razal, J.; Chen, J.; Giordano, G. M.; Muñoz, E.; Musselman, I. H.; Baughman, R. H.; Draper, R. K. *J. Am. Chem. Soc.* **2003**, *125*, 1770–7.

[147] Zorbas, V.; Ortiz-Acevedo, A.; Dalton, A. B.; Yoshida, M. M.; Dieckmann, G. R.; Draper, R. K.; Baughman, R. H.; Jose-Yacaman, M.; Musselman, I. H. *J. Am. Chem. Soc.* **2004**, *126*, 7222–7.

[148] Zorbas, V.; Smith, A. L.; Xie, H.; Ortiz-acevedo, A.; Dalton, A. B.; Dieckmann, G. R.; Draper, R. K.; Baughman, R. H.; Musselman, I. H. *J. Am. Chem. Soc.* **2005**, *127*, 12323–12328.

[149] Arnold, M. S.; Guler, M. O.; Hersam, M. C.; Stupp, S. I. *Langmuir* **2005**, *21*, 4705–9.

[150] Ortiz-Acevedo, A.; Xie, H.; Zorbas, V.; Sampson, W. M.; Dalton, A. B.; Baughman, R. H.; Draper, R. K.; Musselman, I. H.; Dieckmann, G. R. *J. Am. Chem. Soc.* **2005**, *127*, 9512–7.

[151] Asuri, P.; Karajanagi, S. S.; Sellitto, E.; Kim, D.-Y.; Kane, R. S.; Dordick, J. S. *Biotechnol. Bioeng.* **2006**, *95*, 804–811.

[152] Asuri, P.; Bale, S. S.; Pangule, R. C.; Shah, D. A.; Kane, R. S.; Dordick, J. S. *Langmuir* **2007**, *23*, 12318–12321.

[153] Nie, H.; Wang, H.; Cao, A.; Shi, Z.; Yang, S.-T.; Yuan, Y.; Liu, Y. *Nanoscale* **2011**, *3*, 970.

[154] Nepal, D.; Geckeler, K. E. *Small* **2006**, *125*, 406–12.

[155] Huang, W.; Taylor, S.; Fu, K.; Lin, Y.; Zhang, D.; Hanks, T. W.; Rao, A. M.; Sun, Y.-P. *Nano Lett.* **2002**, *2*, 311–314.

[156] Kim, H.-S.; Yoon, S.-H.; Kwon, S.-M.; Jin, H.-J. *Biomacromolecules* **2009**, *10*, 82–6.

[157] Pompeo, F.; Resasco, D. E. *Nano Lett.* **2002**, *2*, 369–373.

[158] Gu, L.; Luo, P. G.; Wang, H.; Meziani, M. J.; Lin, Y.; Veca, L. M.; Cao, L.; Lu, F.; Wang, X.; Quinn, R. A.; Wang, W.; Zhang, P.; Lacher, S.; Sun, Y.-P. *Biomacromolecules* **2008**, *9*, 2408–18.

[159] Leinonen, H.; Pettersson, M.; Lajunen, M. *Carbon* **2011**, *49*, 1299–1304.

[160] Dodziuk, H.; Ejchart, A.; Anczewski, W.; Ueda, H.; Krinichnaya, E.; Dolgonos, G.; Kutner, W. *Chem. Commun.* **2003**, 986–987.

[161] Ikeda, A.; Hayashi, K.; Konishi, T.; Kikuchi, J.-I. *Chem. Commun.* **2004**, 1334–1335.

[162] Ogoshi, T.; Yamagishi, T.-A.; Nakamoto, Y.; Harada, A. *Chem. Lett.* **2007**, *36*, 1026–1027.

[163] Ogoshi, T.; Ikeya, M.; Yamagishi, T.; Nakamoto, Y.; Harada, A. *J. Phys. Chem. C* **2008**, *112*, 13079–13083.

[164] Dohi, H.; Kikuchi, S.; Kuwahara, S.; Sugai, T.; Shinohara, H. *Chem. Phys. Lett.* **2006**, *428*, 98–101.

[165] Adsul, M. G.; Rey, D. A.; Gokhale, D. V. *J. Mater. Chem.* **2011**, *21*, 2054–2056.

[166] Yang, Q.; Shuai, L.; Zhou, J.; Lu, F.; Pan, X. *J. Phys. Chem. B* **2008**, *112*, 12934–9.

[167] Takahashi, T.; Tsunoda, K.; Yajima, H.; Ishii, T. *Jpn. J. Appl. Phys.* **2004**, *43*, 3636–3639.

[168] Minami, N.; Kim, Y.; Miyashita, K.; Kazaoui, S.; Nalini, B. *Appl. Phys. Lett.* **2006**, *88*, 093123.

[169] Iamsamai, C.; Hannongbua, S.; Ruktanonchai, U.; Soottitantawat, A.; Dubas, S. T. *Carbon* **2010**, *48*, 25–30.

[170] Yang, H.; Wang, S. C.; Mercier, P.; Akins, D. L. *Chem. Commun.* **2006**, 1425–7.

[171] Takahashi, T.; Luculescu, C. R.; Uchida, K.; Ishii, T.; Yajima, H. *Chem. Lett.* **2005**, *34*, 1516–1517.

[172] Yang, Q.; Shuai, L.; Pan, X. *Biomacromolecules* **2008**, *9*, 3422–6.

[173] Wu, Z.; Feng, W.; Feng, Y.; Liu, Q.; Xu, X.; Sekino, T.; Fujii, A.; Ozaki, M. *Carbon* **2007**, *45*, 1212–1218.

[174] Ke, G.; Guan, W.; Tang, C.; Zeng, D.; Deng, F. *Biomacromolecules* **2007**, *8*, 322–6.

[175] Yan, L. Y.; Poon, Y. F.; Chan-Park, M. B.; Chen, Y.; Zhang, Q. *J. Phys. Chem. C* **2008**, *112*, 7579–7587.

[176] Yan, L. Y.; Li, W.; Mesgari, S.; Leong, S. S. J.; Chen, Y.; Loo, L. S.; Mu, Y.; Chan-Park, M. B. *Small* **2011**, *7*, 2758–2768.

[177] Moulton, S. E.; Maugey, M.; Poulin, P.; Wallace, G. G. *J. Am. Chem. Soc.* **2007**, *129*, 9452–7.

[178] Liu, Y.; Liang, P.; Zhang, H.-Y.; Guo, D.-S. *Small* **2006**, *2*, 874–8.

[179] Bandyopadhyaya, R.; Nativ-Roth, E.; Regev, O.; Yerushalmi-Rozen, R. *Nano Lett.* **2002**, *2*, 25–28.

[180] Numata, M.; Asai, M.; Kaneko, K.; Bae, A.-H.; Hasegawa, T.; Sakurai, K.; Shinkai, S. *J. Am. Chem. Soc.* **2005**, *127*, 5875–84.

[181] Star, A.; Steuerman, D. W.; Heath, J. R.; Stoddart, J. F. *Angew. Chem. Int. Ed.* **2002**, *41*, 2508–2512.

[182] Ikeda, A.; Hamano, T.; Hayashi, K.; Kikuchi, J.-I. *Org. Lett.* **2006**, *8*, 1153–1156.

[183] Nakashima, N.; Okuzono, S.; Murakami, H.; Nakai, T.; Yoshikawa, K. *Chem. Lett.* **2003**, *32*, 456–457.

[184] Zheng, M.; Jagota, A.; Semke, E. D.; Diner, B. A.; McLean, R. S.; Lustig, S. R.; Richardson, R. E.; Tassi, N. G. *Nat. Mater.* **2003**, *2*, 338–42.

[185] Zheng, M.; Jagota, A.; Strano, M. S.; Santos, A. P.; Barone, P.; Chou, S. G.; Diner, B. A.; Dresselhaus, M. S.; McLean, R. S.; Onoa, G. B.; Samsonidze, G. G.; Semke, E. D.; Usrey, M.; Walls, D. J. *Science* **2003**, *302*, 1545–8.

[186] Kim, J. H.; Kataoka, M.; Shimamoto, D.; Muramatsu, H.; Jung, Y. C.; Tojo, T.; Hayashi, T.; Kim, Y. A.; Endo, M.; Terrones, M.; Dresselhaus, M. S. *ChemPhysChem* **2009**, *10*, 2414–7.

[187] Tasis, D. *Carbon Nanotube-Polymer Composites*; Royal Society of Chemistry, 2013.

[188] Zhang, H.; Li, H. X.; Cheng, H. M. *J. Phys. Chem. B* **2006**, *110*, 9095–9099.

[189] Qin, S.; Qin, D.; Ford, W. T.; Herrera, J. E.; Resasco, D. E.; Bachilo, S. M.; Weisman, R. B. *Macromolecules* **2004**, *37*, 3965–3967.

[190] Yang, D.; Hu, J.; Wang, C. *Carbon* **2006**, *44*, 3161–3167.

[191] Li, H.; Adronov, A. *Carbon* **2007**, *45*, 984–990.

[192] Sun, Y.-P.; Huang, W.; Lin, Y.; Fu, K.; Kitaygorodskiy, A.; Riddle, L. A.; Yu, Y. J.; Carroll, D. L. *Chem. Mater.* **2001**, *13*, 2864–2869.

[193] Huang, W.; Fernando, S.; Allard, L. F.; Sun, Y.-P. *Nano Lett.* **2003**, *3*, 565–568.

[194] Fernando, K. A. S.; Lin, Y.; Sun, Y.-P. *Langmuir* **2004**, *20*, 4777–4778.

[195] Sano, M.; Kamino, A.; Okamura, J.; Shinkai, S. *Langmuir* **2001**, *17*, 5125–5128.

[196] Chattopadhyay, J.; de Jesus Cortez, F.; Chakraborty, S.; Slater, N. K. H.; Billups, W. E. *Chem. Mater.* **2006**, *18*, 5864–5868.

[197] Zhao, B.; Hu, H.; Haddon, R. C. *Adv. Funct. Mater.* **2004**, *14*, 71–76.

[198] Zhao, B.; Hu, H.; Yu, A. P.; Perea, D.; Haddon, R. C. *J. Am. Chem. Soc.* **2005**, *127*, 8197–8203.

[199] Narain, R.; Housni, A.; Lane, L. *J. Polym. Sci. A Polym. Chem.* **2006**, *44*, 6558–6568.

[200] Hong, C.-Y.; You, Y.-Z.; Pan, C.-Y. *Chem. Mater.* **2005**, *17*, 2247–2254.

[201] Soll, S.; Antonietti, M.; Yuan, J. *ACS Macro Lett.* **2012**, *1*, 84–87.

[202] Etika, K. C.; Jochum, F. D.; Theato, P.; Grunlan, J. C. *J. Am. Chem. Soc.* **2009**, *131*, 13598–13599.

[203] Etika, K. C.; Jochum, F. D.; Cox, M. A.; Schattling, P.; Theato, P.; Grunlan, J. C. *Macromol. Rapid Commun.* **2010**, *31*, 1368–72.

[204] Yang, D.; Zhang, X.; Wang, C.; Tang, Y.; Li, J.; Hu, J. *Prog. Nat. Sci.* **2009**, *19*, 991–996.

[205] O'Connell, M. J.; Boul, P.; Ericson, L. M.; Huffman, C.; Wang, Y.; Haroz, E.; Kuper, C.; Tour, J.; Ausman, K. D.; Smalley, R. E. *Chem. Phys. Lett.* **2001**, *342*, 265–271.

[206] Kang, Y. K.; Lee, O.-S.; Deria, P.; Kim, S. H.; Park, T.-H.; Bonnell, D. A.; Saven, J. G.; Therien, M. J. *Nano Lett.* **2009**, *9*, 1414–8.

[207] Liu, A.; Watanabe, T.; Honma, I.; Wang, J.; Zhou, H. *Biosens. Bioelectron.* **2006**, *22*, 694–9.

[208] Saint-Aubin, K.; Poulin, P.; Saadaoui, H.; Maugey, M.; Zakri, C. *Langmuir* **2009**, *25*, 13206–11.

[209] Grunlan, J. C.; Liu, L.; Kim, Y. S. *Nano Lett.* **2006**, *6*, 911–5.

[210] Etika, K. C.; Cox, M. A.; Grunlan, J. C. *Polymer* **2010**, *51*, 1761–1770.

[211] Meyer, F.; Minoia, A.; Raquez, J. M.; Spasova, M.; Lazzaroni, R.; Dubois, P. *J. Mater. Chem.* **2010**, *20*, 6873.

[212] Liu, Y. Q.; Gao, L.; Zheng, S.; Wang, Y.; Sun, J.; Kajiura, H.; Li, Y.; Noda, K. *Nanotechnology* **2007**, *18*.

[213] Wang, R.; Cherukuri, P.; Duque, J. G.; Leeuw, T. K.; Lackey, M. K.; Moran, C. H.; Moore, V. C.; Conyers, J. L.; Smalley, R. E.; Schmidt, H. K.; Weisman, R. B.; Engel, P. S. *Carbon* **2007**, *45*, 2388–2393.

[214] Lee, J. U.; Huh, J.; Kim, K. H.; Park, C.; Jo, W. H. *Carbon* **2007**, *45*, 1051–1057.

[215] Xue, C. H.; Shi, M. M.; Yan, Q. X.; Shao, Z.; Gao, Y.; Wu, G.; Zhang, X. B.; Yang, Y.; Chen, H. Z.; Wang, M. *Nanotechnology* **2008**, *19*, 115605.

[216] Xue, C. H.; Zhou, R. J.; Shi, M. M.; Gao, Y.; Wu, G.; Zhang, X. B.; Chen, H. Z.; Wang, M. *Nanotechnology* **2008**, *19*, 215604.

[217] Goak, J. C.; Lee, S. H.; Han, J. H.; Jang, S. H.; Kim, K. B.; Seo, Y.; Seo, Y.-S.; Lee, N. *Carbon* **2011**, *49*, 4301–4313.

[218] Randhawa, P.; Park, J.-S.; Sharma, S.; Kumar, P.; Shin, M.-S.; Sekhon, S. S. *J. Nanoelectron. and Optoe.* **2012**, *7*, 279–286.

[219] Wang, H. *Current Opinion in Colloid & Interface Science* **2009**, *14*, 364–371.

[220] O'Connell, M. J.; Bachilo, S. M.; Huffman, C. B.; Moore, V. C.; Strano, M. S.; Haroz, E. H.; Rialon, K. L.; Boul, P. J.; Noon, W. H.; Kittrell, C.; Ma, J.; Hauge, R. H.; Weisman, R. B.; Smalley, R. E. *Science* **2002**, *297*, 593–6.

[221] Richard, C.; Balavoine, F.; Schultz, P.; Ebbesen, T. W.; Mioskowski, C. *Science* **2003**, *300*, 775–8.

[222] Islam, M. F.; Rojas, E.; Bergey, D. M.; Johnson, A. T.; Yodh, A. G. *Nano Lett.* **2003**, *3*, 269–273.

[223] Yurekli, K.; Mitchell, C. A.; Krishnamoorti, R. *J. Am. Chem. Soc.* **2004**, *126*, 9902–3.

[224] Moore, V. C.; Strano, M. S.; Haroz, E. H.; Hauge, R. H.; Smalley, R. E.; Schmidt, J.; Talmon, Y. *Nano Lett.* **2003**, *3*, 1379–1382.

[225] Paredes, J. I.; Burghard, M. *Langmuir* **2004**, *20*, 5149–5152.

[226] Rastogi, R.; Kaushal, R.; Tripathi, S. K.; Sharma, A. L.; Kaur, I.; Bharadwaj, L. M. *J. Colloid Interface Sci.* **2008**, *328*, 421–428.

[227] Clark, M. D.; Subramanian, S.; Krishnamoorti, R. *J. Colloid Interface Sci.* **2011**, *354*, 144–151.

[228] Kördel, C.; Setaro, A.; Bluemmel, P.; Popeney, C. S.; Reich, S.; Haag, R. *Nanoscale* **2012**, *4*, 3029–31.

[229] Baughman, R. H.; Zakhidov, A. a.; de Heer, W. a. *Science* **2002**, *297*, 787–92.

[230] Hennrich, F.; Lebedkin, S.; Malik, S.; Tracy, J.; Barczewski, M.; Rösner, H.; Kappes, M. *Phys. Chem. Chem. Phys.* **2002**, *4*, 2273–2277.

[231] Bianco, A.; Kostarelos, K.; Partidos, C. D.; Prato, M. *Chemical communications (Cambridge, England)* **2005**, 571–577.

[232] Shaffer, M. S. P.; Windle, A. H. *Macromolecules* **1999**, *32*, 6864–6866.

[233] Liu, L.; Barber, A. H.; Nuriel, S.; Wagner, H. D. *Adv. Funct. Mater.* **2005**, *15*, 975–980.

[234] Ma, P.-C.; Siddiqui, N. A.; Marom, G.; Kim, J.-K. *Composites Part A: Applied Science and Manufacturing* **2010**, *41*, 1345–1367.

[235] Okay, O. In *Hydrogel Sensors and Actuators: Engineering and Technology*; Urban, G., Ed.; Springer, 2009.

[236] Barbucci, R. In *Hydrogels: Biological Properties and Applications*, 1st ed.; Barbucci, R., Ed.; Springer-Verlag Mailand, 2009; p 197.

[237] Ogoshi, T.; Takashima, Y.; Yamaguchi, H.; Harada, A. *J. Am. Chem. Soc.* **2007**, *129*, 4878–9.

[238] Wang, Z.; Chen, Y. *Macromolecules* **2007**, *40*, 3402–3407.

[239] Bhattacharyya, S.; Guillot, S.; Dabboue, H.; Tranchant, J.-F.; Salvetat, J.-P. *Biomacromolecules* **2008**, *9*, 505–9.

[240] Yan, L. Y.; Chen, H.; Li, P.; Kim, D.-H.; Chan-Park, M. B. *ACS applied materials & interfaces* **2012**, *4*, 4610–5.

[241] Wager, J. F. *Science* **2003**, *300*, 1245.

[242] Cao, Q.; Rogers, J. A. *Adv. Mater.* **2009**, *21*, 29–53.

[243] Sreekumar, T. V.; Liu, T.; Kumar, S.; Ericson, L. M.; Hauge, R. H.; Smalley, R. E. *Chem. Mater.* **2003**, *15*, 175–178.

[244] in het Panhuis, M.; Heurtematte, A.; Small, W. R.; Paunov, V. N. *Soft Matter* **2007**, *3*, 840.

[245] Kim, Y.; Minami, N.; Zhu, W.; Kazaoui, S.; Azumi, R.; Matsumoto, M. *Jpn. J. Appl. Phys.* **2003**, *42*, 7629–7634.

[246] Zhou, Y.; Hu, L.; Gruner, G. *Appl. Phys. Lett.* **2006**, *88*, 123109.

[247] Unalan, H. E.; Fanchini, G.; Kanwal, A.; Du Pasquier, A.; Chhowalla, M. *Nano Lett.* **2006**, *6*, 677–82.

[248] Geng, H.-Z.; Kim, K. K.; So, K. P.; Lee, Y. S.; Chang, Y.; Lee, Y. H. *J. Am. Chem. Soc.* **2007**, *129*, 7758–9.

[249] Ng, M. H. A.; Hartadi, L. T.; Tan, H.; Poa, C. H. P. *Nanotechnology* **2008**, *19*, 205703.

[250] Saran, N.; Parikh, K.; Suh, D.-S.; Muñoz, E.; Kolla, H.; Manohar, S. K. *J. Am. Chem. Soc.* **2004**, *126*, 4462–3.

[251] Zhang, X.; Sreekumar, T. V.; Liu, T.; Kumar, S. *J. Phys. Chem. B* **2004**, *108*, 16435–16440.

[252] Chiang, I. W.; Brinson, B. E.; Smalley, R. E.; Margrave, J. L.; Hauge, R. H. *J. Phys. Chem. B* **2001**, *105*, 1157.

[253] Bom, D.; Andrews, R.; Jacques, D.; Anthony, J.; Chen, B.; Meier, M. S.; Selegue, J. P. *Nano Lett.* **2002**, *2*, 615–619.

[254] Arepalli, S.; Nikolaev, P.; Gorelik, O.; Hadjiev, V. G.; Holmes, W.; Files, B.; Yowell, L. *Carbon* **2004**, *42*, 1783–1791.

[255] Pekker, S.; Salvetat, J.-P.; Jakab, E.; Bonard, J.-M.; Forró, L. *J. Phys. Chem. B* **2001**, *105*, 7938–7943.

[256] Gebhardt, B.; Syrgiannis, Z.; Backes, C.; Graupner, R.; Hauke, F.; Hirsch, A. *J. Am. Chem. Soc.* **2011**, *133*, 7985.

[257] Itkis, M. E.; Niyogi, S.; Meng, M. E.; Hamon, M. A.; Hu, H.; Haddon, R. C. *Nano Lett.* **2002**, *2*, 155.

[258] Wunderlich, D.; Hauke, F.; Hirsch, A. *J. Mater. Chem.* **2008**, *18*, 1493.

[259] Rance, G. A.; Marsh, D. H.; Nicholas, R. J.; Khlobystov, A. N. *Chem. Phys. Lett.* **2010**, *493*, 19–23.

[260] Evans, G. P.; Buckley, D. J.; Skipper, N. T.; Parkin, I. P. *RSC Adv.* **2014**, *4*, 51395–51403.

[261] Mickelson, E. T.; Chiang, I. W.; Zimmerman, J. L.; Boul, P. J.; Lozano, J.; Liu, J.; Smalley, R. E.; Hauge, R. H.; Margrave, J. L. *J. Phys. Chem. B* **1999**, *103*, 4318.

[262] Bahr, J. L.; Mickelson, E. T.; Bronikowski, M. J.; Smalley, R.; Tour, J. M. *Chem. Commun.* **2001**, 193.

[263] Landi, B. J.; Ruf, H. J.; Worman, J. J.; Raffaelle, R. P. *J. Phys. Chem. B* **2004**, *108*, 17089.

[264] Dresselhaus, M. S.; Dresselhaus, G.; Saito, R.; Jorio, A. *Phys. Rep.* **2005**, *409*, 47.

[265] Matthews, M. J.; Pimenta, M. A.; Dresselhaus, G.; Dresselhaus, M. S.; Endo, M. *Phys. Rev. B.* **1999**, *59*, R6585.

[266] Dresselhaus, M. S.; Eklund, P. C. *Adv. Phys.* **2000**, *49*, 705.

[267] Jorio, A.; Pimenta, M. A.; Filho, A. G. S.; Saito, R.; Dresselhaus, G.; Dresselhaus, M. *New J. Phys.* **2003**, *5*, 139.

[268] Ying, Y.; Saini, R. K.; Liang, F.; Sadana, A.; Billups, W. E. *Org. Lett.* **2003**, *5*, 1471.

[269] Nelson, D. J.; Rhoads, H.; Brammer, C. *J. Phys. Chem. C* **2007**, *111*, 17872–17878.

[270] Kukovecz, A.; Kramberger, C.; Holzinger, M.; Kuzmany, H.; Schalko, J.; Mannsberger, M.; Hirsch, A. *J. Phys. Chem. B* **2002**, *106*, 6374–6380.

[271] Martinez, M. T.; Callejas, M. A.; Benito, A. M.; Cochet, M.; Seeger, T.; Anson, A.; Schreiber, J.; Gordon, C.; Marhic, C.; Chuavet, O.; Fierro, J. L. G.; Maser, W. K. *Carbon* **2003**, *41*, 2247–2256.

[272] Mukherjee, A.; Combs, R.; Chattopadhyay, J.; Abmayr, D. W.; Engel, P. S.; Billups, W. E. *Chem. Mater.* **2008**, *20*, 7339–7343.

[273] Itkis, M. E.; Haddon, R. C. *Chem. Phys. Lett.* **2001**, *347*, 8–10.

[274] Hu, H.; Zhao, B.; Hamon, M. A.; Kamaras, K.; Itkis, M. E.; Haddon, R. C. *J. Am. Chem. Soc.* **2003**, *125*, 14893–14900.

[275] Osswald, S.; Havel, M.; Gogotsi, Y. *J. Raman Spectrosc.* **2007**, *38*, 728–736.

[276] Vinayan, B. P.; Nagar, R.; Raman, V.; Rajalakshmi, N.; Dhathathreyan, K. S.; Ramaprabhu, S. *J. Mater. Chem.* **2012**, *22*, 9949.

[277] Trigueiro, J. P. C.; Silva, G. G.; Lavall, R. L.; Furtado, C. A.; Oliveira, S.; Ferlauto, A. S.; Lacerda, R. G.; Ladeira, L. O.; Liu, J.-W.; Frost, R. L.; George, G. A. *J. Nanosci. Nanotechnol.* **2007**, *7*, 3477–3486.

[278] Lehman, J. H.; Terrones, M.; Mansfield, E.; Hurst, K. E.; Meunier, V. *Carbon* **2011**, *49*, 2581–2602.

[279] Branca, C.; Frusteri, F.; Magazù, V.; Mangione, A. *J. Phys. Chem. B* **2004**, *108*, 3469–3473.

[280] Kiang, C.-H.; Endo, M.; Ajayan, P. M.; Dresselhaus, G.; Dresselhaus, M. S. *Phys. Rev. Lett.* **1998**, *81*, 1869.

[281] Wepasnick, K. A.; Smith, B. A.; Bitter, J. L.; Fairbrother, D. H. *Anal. Bioanal. Chem.* **2010**, *396*, 1003–1014.

[282] Smith, B. W.; Luzzi, D. E. *J. Appl. Phys.* **2001**, *90*, 3509–3515.

[283] Hu, H.; Zhao, B.; Itkis, M. E.; Haddon, R. C. *J. Phys. Chem. B* **2003**, *107*, 13838–13842.

[284] Datsyuk, V.; Kalyva, M.; Papagelis, K.; Parthenios, J.; Tasis, D.; Siokou, A.; Kallitsis, I.; Galiotis, C. *Carbon* **2008**, *46*, 833–840.

[285] Chen, J.; Rao, A. M.; Lyuksyutov, S.; Itkis, M. E.; Hamon, M. A.; Hu, H.; Cohn, R. W.; Eklund, P. C.; Colbert, D. T.; Smalley, R. E.; Haddon, R. C. *J. Phys. Chem. B* **2001**, *105*, 2525–2528.

[286] Wang, Z.; Korobeinyk, A.; Whitby, R. L. D.; Meikle, S. T.; Mikhalovsky, S. V.; Acquah, S. F. A.; Kroto, H. W. *Carbon* **2010**, *48*, 916–918.

[287] Stephenson, J. J.; Hudson, J. L.; Azad, S.; Tour, J. M. *Chem. Mater.* **2006**, *18*, 374–377.

[288] Hirano, A.; Kameda, T.; Arakawa, T.; Shiraki, K. *J. Phys. Chem. B* **2010**, *114*, 13455–13462.

[289] Ariki, R.; Hirano, A.; Arakawa, T.; Shiraki, K. *J. Biochem.* **2011**, *149*, 389–394.

[290] Arakawa, T.; Kita, Y.; Koyama, A. H. *Int. J. Pharm.* **2008**, *355*, 220–223.

[291] Hirano, A.; Arakawa, T.; Shiraki, K. *J. Biochem.* **2008**, *144*, 363–369.

[292] Shiraki, K.; Kudou, M.; Fujiwara, S.; Imanaka, T.; Takagi, M. *J. Biochem.* **2002**, *132*, 591–595.

[293] Arakawa, T.; Tsumoto, K. *Biochem. Biophys. Res. Commun.* **2003**, *304*, 148–152.

[294] McMurry, J. *Fundamentals of Organic Chemistry*; Cengage Learning, 2010; pp 506–507.

[295] Arrais, A.; Diana, E.; Pezzini, D.; Rossetti, R.; Boccaleri, E. *Carbon* **2006**, *44*, 587–590.

[296] Zhang, X.; Sreekumar, T. V.; Liu, T.; Kumar, S. *J. Phys. Chem. B* **2004**, *108*, 16435–16440.

[297] Kuznetsov, O. V.; Pulikkathara, M. X.; Lobo, R. F. M.; Khabashesku, V. N. *Russ. Chem. Bull.* **2010**, *59*, 1495–1505.